Influence of Lecithin on Structure and Stability of Parenteral Fat Emulsions

Den Naturwissenschaftlichen Fakultäten
der Friedrich-Alexander-Universität Erlangen-Nürnberg
zur
Erlangung des Doktorgrades

vorgelegt von

Christoph Wabel

aus Frankfurt am Main

Als Dissertation genehmigt von den Naturwissenschaftlichen Fakultäten der Friedrich-Alexander-Universität Erlangen-Nürnberg

Tag der mündlichen Prüfung:	30.07.1998
Vorsitzender der Promotionskommission:	Prof. Dr. D. Kölzow
Erstberichterstatter:	Prof. Dr. G. Lee
Zweitberichterstatter:	Prof. Dr. E. Nürnberg

To my parents

and Andrea

Knowledge comes,

but wisdom lingers

(Lord Alfred Tennyson, 1842)

Acknowledgements

For contribution to this work I am indebted to:

Prof. Geoffrey Lee who made this work possible, gave me encouraging and constructive discussions and supported me in my efforts to improve my approaches to this field.

Prof. Dr. Eberhard Nuernberg for being co-referee and his helpful hints on pharmacopeial issues.
All the colleagues at the Department for a comfortable and friendly working atmosphere.
Dr. Detlef Schenk for his efforts concerning the thermoanalytical equipment.

Prof. Dr. Manige Fartasch, Institute of Dermatology, University of Erlangen for the opportunity to use the TEM.
Prof. Dr. Karl-Ernst Wirth, Department of Mechanical Engineering, University of Erlangen for his permission to carry out the measurements on the Zetasizer 3000.
Prof. Dr. Martin Stratmann and Dipl. Ing. Elke Hornung, Institute of Material Sciences, University of Erlangen for the opportunity to use the film balance.

Outside the University of Erlangen I want to express my sincere thanks to the following persons:
Prof. Michael Groves, Institute for Tuberculosis Research, University of Illinois at Chicago for inspiring this work, helpful suggestions and for his support ‘through the wire’.
Prof. Dr. Werner Maentele, University of Frankfurt/Main, for his help in obtaining and evaluating the FT-IR thin film cuvette.
Prof. Dr. Christel Mueller-Goymann and Carmen Groechtemeier, Institute of Pharmaceutics, University of Braunschweig for permitting and performing preparation of freeze-fracture specimen.
Prof. Dr. Rolf Schubert and Margret Froehlich, Department of Pharmaceutics, University of Freiburg for their kind support and help in conducting the Cryo-TEM experiments.
Prof. Dr. Ingfried Zimmermann, Department of Pharmaceutics, University of Wuerzburg for the opportunity to repeatedly undertake measurements with the LS230.
Prof. Dr. Achim Goepferich, Department of Pharmaceutics, now University of Regensburg, for helpful advice and the opportunity to use the flying-spot densitometer.
All the people at the Department of Biochemistry and Molecular Biology, University of

Murcia, especially Prof. Dr. José Villalaín Boullón, now University of Elche, for the invitation to stay at the Department, his invaluable help and advice concerning the ^{31}P-NMR measurements and for introducing me to the ‘tapas murcianas’. Gracias a todos !
DAAD and ‘acciónes integradas’ are acknowledged for the grant for my stay in Murcia as well as Dr. Christoph Johann, Wyatt Deutschland, for realising the AFFF measurements.

For generously providing me with all kinds of materials and support I want to thank the companies BASF AG, Henkel KG, B.Braun Melsungen AG, Fresenius AG, Lipoid KG and Pharmacia & Upjohn GmbH. Especially Franz Kachler and Gabriela Wolf, Pharmacia & Upjohn, Erlangen and Dres. Zirkel and Waibel, Lipoid KG, Ludwigshafen have to be given thanks for their continued support, valuable information and fruitful discussions.

Last but not least I wish to thank everybody else at the Department who made the time there so memorable: Winfried Bauer for his skills in repairing, improving or even inventing all kinds of parts. Christiane Blaha is given thanks for supplying me with materials in due time, Waltrud Klenk and Petra Neubarth for being helpful in ever renewing paperwork and Luise Schedl for preparation of slides.

Finally, special thanks go to Anette Brunner for the great comradeship in our lab, Michael Adler for some great nine years of mutual profit, compassion and encouragement, all the colleagues who shared the students’ practical courses with me and the ‘human interface’ crew at the universities’ computing centre who helped me in overcoming all the imperfections of software, hardware and the user and supported me in keeping the network up ;-).

All those, who could not be mentioned here, please be sure of my gratefulness and sympathy.

Table of Contents

List of Abbreviations

AFFF	**Asymmetrical Flow Field-Flow Fractionation**
ATR	**Attenuated Total Reflection**
CMC	**Critical Micelle-Forming Concentration**
CPP	**Critical Packing Parameter**
Cryo-TEM	**Cryo-Transmission Electron Microscopy**
DPPC	**Di-Palmitoyl-Phosphatidylcholine**
DSC	**Differential Scanning Calorimetry**
FFA	**Free Fatty Acid(s)**
FFF	**Field Flow Fractionation**
FF-TEM	**Freeze-Fracture Transmission Electron Microscopy**
FT-IR	**Fourier-Transform Infrared Spectroscopy**
HPLC	**High-Performance Liquid Chromatography**
HPTLC	**High-Performance Thin-Layer Chromatography**
LCT	**Long Chain Triglycerides**
LD	**Laser Diffractometry**
LDA	**Laser Doppler Anemometry**
LIPOID E75®	**Commercial Egg Yolk Lecithin**
LIPOID E80®	**Commercial Egg Yolk Lecithin**
LIPOID ELPC®	**Commercial Lyso-Phosphatidylcholine from Egg Yolk**
LIPOID EPC®	**Commercial Phosphatidylcholine from Egg Yolk**
LPC	**Lysophosphatidylcholine**
LPE	**Lysophosphatidylethanolamine**
LUV	**Large Unilamellar Vesicle (Liposome)**
MCT	**Middle Chain Triglycerides**
MLV	**Multilamellar Vesicle (Liposome)**
n.a.	**not available**
n.d.	**not determined**

PA	**Phosphatidic Acid**
PC	**Phosphatidylcholine**
PCS	**Photon-Correlation Spectrometry**
PE	**Phosphatidylethanolamine**
PG	**Phosphatidylglycerol**
PI	**Phosphatidylinositol**
PIDS	**Polarisation Intensity Differential Scattering**
PLM	**Polarised-Light Microscopy**
^{31}P-NMR	**^{31}Phosphorous-Nuclear Magnetic Resonance Spectroscopy**
PS	**Phosphatidylserine**
rpm	**Rounds Per Minute**
SLN	**Solid Lipid Nanoparticles**
SPM	**Sphingomyelin**
SUV	**Small Unilamellar Vesicle (Liposome)**
WAXD	**Wide-Angle X-Ray Diffractometry**

Chapter 1 – Introduction

1.1 Lecithin - an Emulsifier for Parenteral Use

Only a limited number of emulsifiers is commonly regarded as safe to use for parenteral administration, of which the most important are Pluronic F68® (Poloxamer 188), Tween 80® (Polysorbate 80) and lecithin. Compared with its synthetic alternatives, lecithin can be totally biodegraded and metabolised, since it is an integral part of biological membranes, making it virtually non-toxic. Other emulsifiers can only be excreted via the kidneys, and Pluronic F68®, owing to impurities contained, even has been reported to be the cause of endogenous pyrogen release [Huth et al., 1967]. The natural origin of lecithin produces, however, a rather complex composition, although in pharmacy in general well-defined singular excipients are favoured. The Ph.Eur. 1997 does not contain a monograph on lecithin, however, a monograph on soya lecithin will be contained in Ph.Eur. 1998, and USP23/NF18 [1995] only describes it as 'a complex mixture of acetone-insoluble phosphatides', but also does not specify content limits concerning its intended use. Nevertheless, lecithin is regarded as a well tolerated and non-toxic compound (which is also expressed by its *GRAS-status ['Generally Recognised As Safe']* approved by the FDA), making it suitable for long-term and large-dose infusion. As an emulsifier of intravenously administered fat emulsions, its composition and behaviour determine the structure and stability of the emulsion in a decisive way. Although extensive research in this field has been done, there is still disagreement about emulsion structure and the influence of the emulsifier. It is essential to understand the behaviour of lecithin in order to understand the behaviour of emulsions stabilised with it.

'Lecithin' is usually used as synonym for phosphatidylcholine (PC), which is the major component of a phosphatide fraction which is frequently isolated from either egg yolk (Greek 'λέκιθος'), or soya beans and is commercially available in high purity. Isolation and purification of lecithins from different sources are described in Kuksis [1985] and Prosise [1985]. PC is a mixture of differently substituted sn-glycerol-3-phosphatidylcholine backbones. As can be seen from Tab. 1, the structure of PC is variable and dependent on fatty acid substitution. In the sn-1-position, saturated acyl-groups, and in sn-2-position, unsaturated species are more common [Kuksis, 1985]. By dietetic means the fatty acid substitution of egg phospholipids can be altered in the sn-2-position [Hanahan, 1960]. Fatty acids of mainly 16-20 C in chain length dominate in egg PC. The sn-1-chain typically shows an average of 16 C, whereas the sn-2-chain shows an average of 18 C. Naturally occurring unsaturated fatty acids are almost entirely of all-cis-conformation [Gennis, 1989].

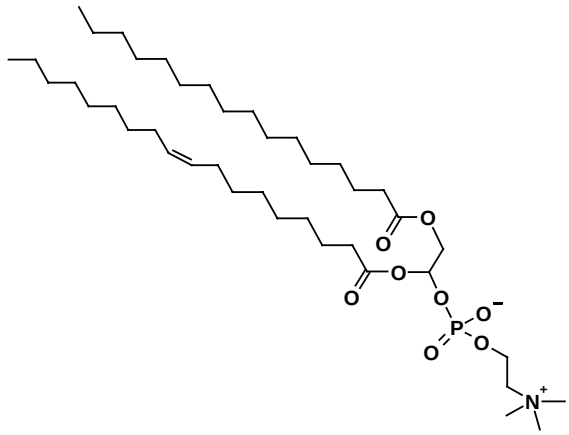	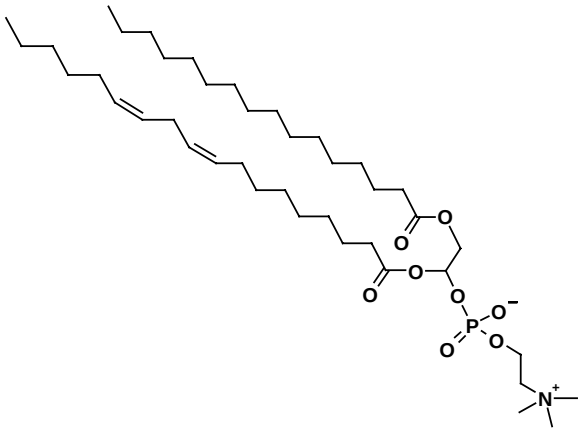
Palmitoyl/Oleoyl [16:0/18:1]-PC **(POPC)** 38.2% in Egg PC	Palmitoyl/Linoleoyl [16:0/18:2]-PC **(PLPC)** 21.8% in Egg PC
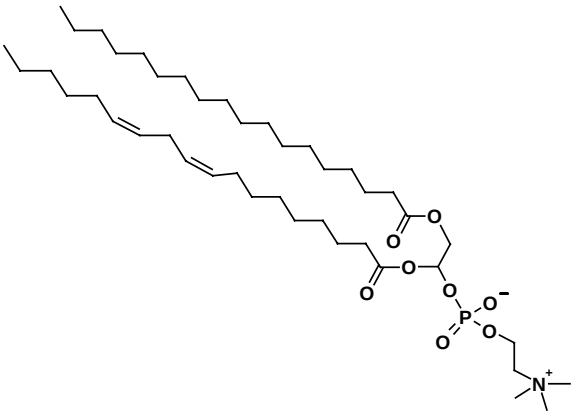	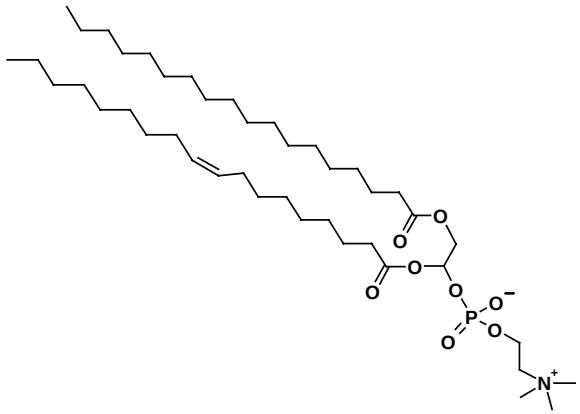
Stearoyl/Linoleoyl [18:0/18:2]-PC **(SLPC)** 11.22% in Egg PC	Stearoyl/Oleoyl [18:0/18:1]-PC **(SOPC)** 9.3% in Egg PC
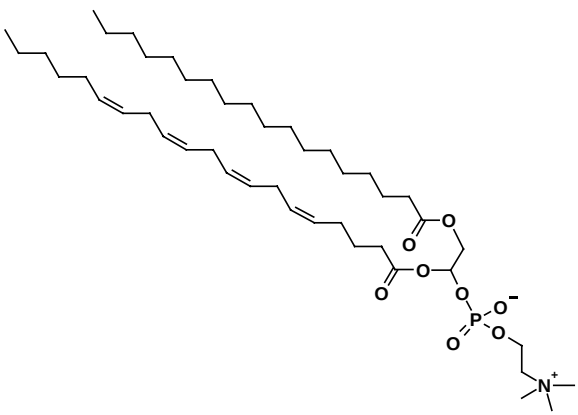	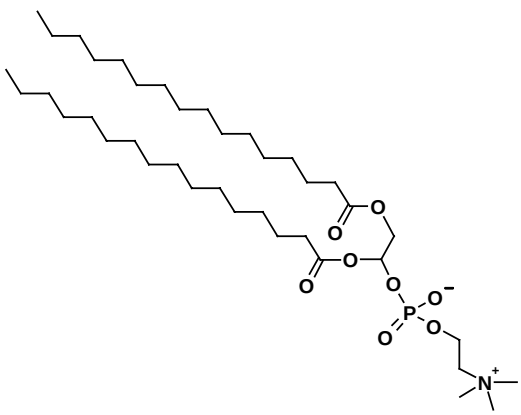
Stearoyl/Arachidoyl [18:0/20:4]-PC **(SAPC)** 3.36% in Egg PC	Di-Palmitoyl [16:0/16:0]-PC **(DPPC)** 0.72% in Egg PC

Tab. 1 Different species of PC and their natural occurrence in egg yolk lecithin (mol/mol) (values after Kuksis [1985])

1.1.1 Properties of Amphiphilic Lipids

Amphiphilic lipids consist of a rather polar 'head group' and comparably apolar residues. In the solid state, the molecules tend to orientate in a distinct way, which is that lipophilic tails and hydrophilic head groups take a separate, packed arrangement. The state of order and the length of the lipophilic tail depends on the conformation of the carbon chains which preferably will be 'all-trans' in the case of saturated acyl-chains, since in this case a potential energy minimum occurs. Thus, the carbon chains become extended to a maximum, whereas in the case of a carbon-carbon bond taking on the gauche-conformation, a kink in the chain occurs. A similar displacement can be observed if a cis-double-bond is located in the hydrocarbon chain (Fig. 1).

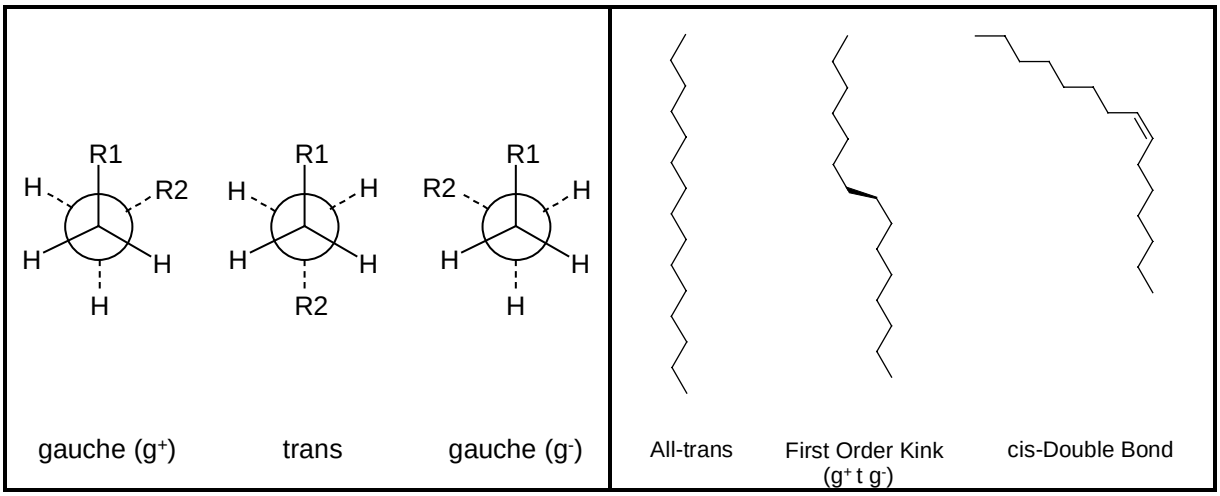

Fig. 1 Newman projections of the rotation about a carbon-carbon bond in an alkyl chain **(left)** and several C15-alkyl chain configurations **(right)**
(adapted from Gennis [1989])

The shrinking of chain elongation owing to kinks or insertion of double bonds notably also increases the cross sectional area covered by each chain ('Σ' in Fig. 4). Amphiphilic lipids typically often do not exhibit abrupt transitions from the solid to the liquid state, but do undergo 'intermediate' states, where properties of solid crystals and of liquids can be observed, as well [Lee, 1977]. This is why these 'intermediate' states are also known as 'mesophases' or 'liquid crystals'. This so-called mesomorphic behaviour can be attributed either to temperature changes when e.g. heating causes 'chain melting' which means transformation of the alkyl chains into a less ordered state owing to increased occurrence of thermodynamically unfavourable chain kinks and consequently increased chain space requirement ('thermotropic phase transition'), or changes in hydration state owing to the fact that only the polar head groups bind to water and become hydrated, which increases their respective space requirements and eventually results in changes in molecule packing ('lyotropic phase change').

The resulting mesophases are usually named according to IUPAC nomenclature using the following abbreviations which describe long-range and short-range orders in lipid-water phases:

Abbreviation	Phase
Long-range order	
L	Lamellar (one-dimensional)
H	Hexagonal (two-dimensional)
P	Oblique or Centred (two-dimensional)
Q	Cubic (named also 'viscous isotropic')
R	Rhombohedral
C	Crystalline (three-dimensional)
M	Micellar (disordered)
Short-range order	
α	Disordered (fluid)
β	Partly ordered, untilted (gel-state)
β'	Partly ordered, tilted
δ	Partly ordered, helical
I	Paraffin-in-Water Type
II	Water-in-Paraffin Type

Tab. 2 IUPAC nomenclature of lipid-water phases (after Marsh [1990])

The following phases are most commonly encountered in lipid-water systems:

a) Lamellar liquid crystalline phase (L_α)

Molecules are located in a two-dimensional order, but acyl chain-regions show considerable disordered (fluid) state. This phase represents the most common arrangement of phospholipids in biological membranes.

b) Lamellar gel phase (L_β)

At lower temperatures the molecules become more tightly packed and the acyl chains become more ordered (all-trans). In lipids with larger 'head groups', acyl chains are found in tilted positions which is indicated by a prime (like in $L_{\beta'}$).

The density and the bilayer thickness of gel phases are slightly larger compared to the liquid crystalline state.

c) Hexagonal I phase (H_I)

Lipids are organised in the form of cylinders with the polar 'head groups' outside, facing the water. The cylinders themselves are packed in a hexagonal array.

d) Hexagonal II phase (H_{II})

In this case the acyl chains face the outer side of the cylindrical shapes, whereas on the inside the polar groups are located facing a continuous area of water.

e) Cubic I phase (Q_I)

Discontinuous phase consisting of spherical micelles with head groups facing a continuous phase of water at the outside.

f) Cubic II phase (Q_{II})

Bicontinuous phase representing an intermediate state between lamellar and hexagonal phase.

The interdependence of lyotropic and thermotropic phase transitions of lipid-water systems can be summarised in the following fashion:

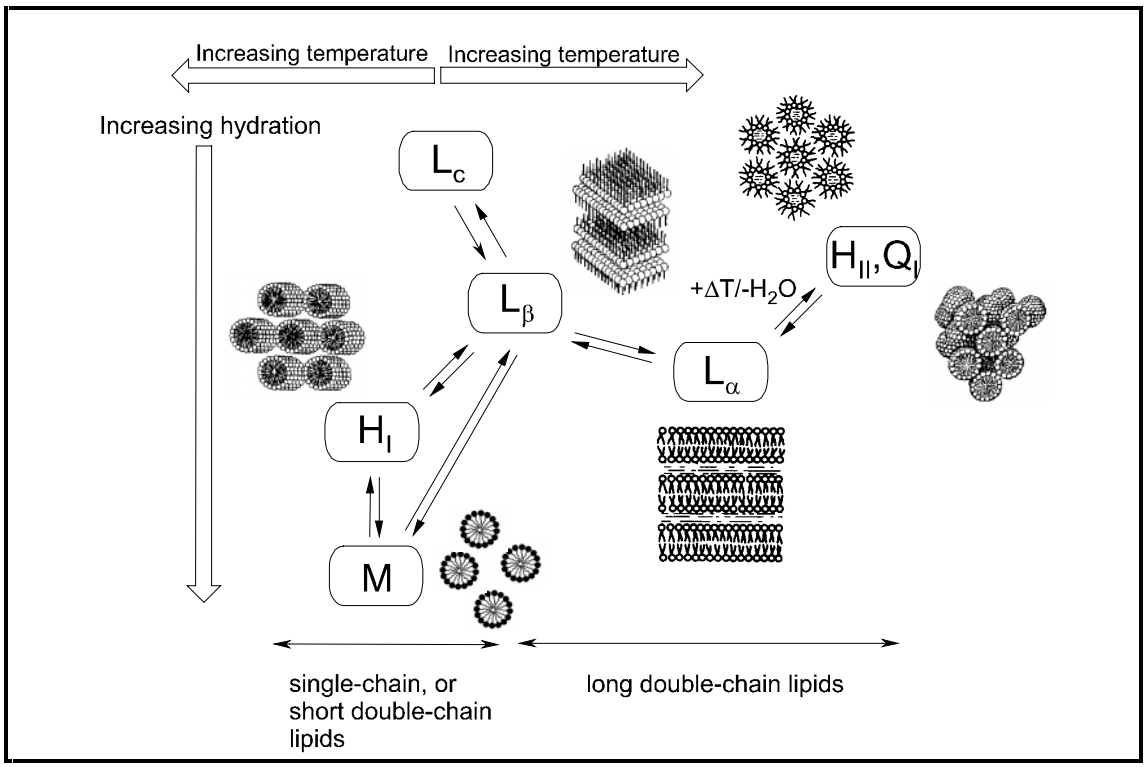

Fig. 2 Dependence of phase transitions of lipid-water mixtures on hydration and temperature (adapted from Brown and Wolker [1979], Gennis [1989] and Marsh [1990])

Lamellar phases (L_α/L_β), Hexagonal phases (H_I/H_{II}), Cubic phase (Q_I) and Micellar solution (M)

Fig. 2 shows that certain preferences in phase behaviour according to substitution and temperature exist, which in most cases are reversible. It must also be stressed, however, that the thermal 'history' of the lipid plays also an important role at which phase changes occur. Similarly, in the case of phospholipid-water mixtures, occurrence of thermotropic or lyotropic phase changes is also well known. To have an idea which phases occur in a lecithin-stabilised O/W emulsion system, one has to start by looking at the phase diagram of lecithin alone.

1.1.2 Properties of Phospholipids

At low water contents of egg lecithin, a variety of phases are observable (Fig. 3). The surface area per molecule ('S' in Fig. 4) at 21°C has been determined as 59.3 $Å^2$. With increasing water content, molecular area increases to about 71.7 $Å^2$, and lamellar structures (L_α) become predominant. At 21°C and 40-44 wt% water content, excess water forms a second phase, in which the L_α phase is dispersed. Temperature increase leads only to melting of the L_α phase to an isotropic liquid at about 220°C [Small, 1986].

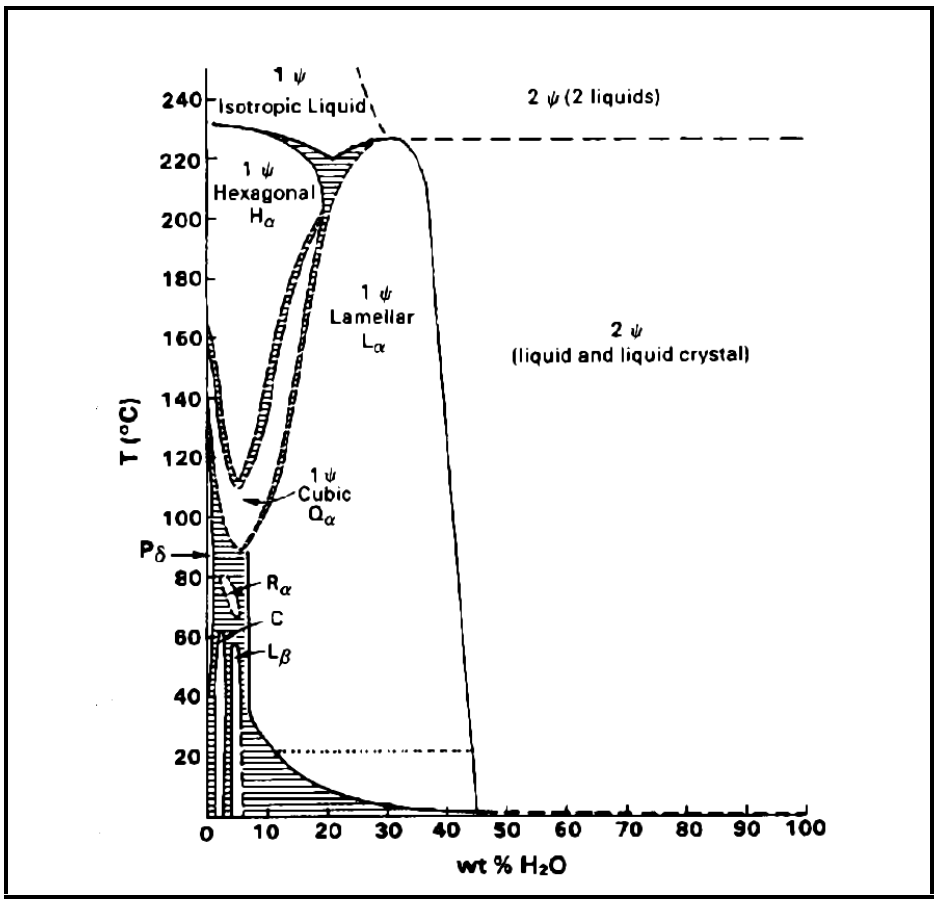

Fig. 3 Influence of temperature and water content on phases of egg lecithin (modified after Small [1986])

C = Crystalline / H_α = Hexagonal liquid crystalline / L_α = Lamellar liquid crystalline / L_β = Lamellar gel / Q_α = Cubic disordered / R_α = Rhombohedral disordered

Depending on its intended use, lecithin is purified to different degrees. Yeadon et al. [1958], Hansrani [1980] and Rydhag and Wilton [1981] noted that the emulsifying properties of pure PC were by far inferior to mixtures of PC with its naturally occurring byproducts, e.g. phosphatidylethanolamine (PE). This is one of many different other compounds (often referred to as 'minor components') typically associated with PC (a selection is given below in Tab. 3 in which fatty acid substituents are abbreviated [R1, R2]). By way of comparison two commercial egg lecithins are also given, showing that composition is largely dependent on lecithin-source and degree of purification. The commercially used egg yolk lecithins designed for parenteral use (Lipoid E80® or egg phosphatide for Intralipid®) are enriched in PC at the expense of PE, compared with the crude product. In contrast to PC, which carries a zwitterionic charge in its head group, a few components are negatively charged (PA, PS) or uncharged at neutral pH values [Szoka and Papahadjopoulos, 1980]. This structural difference causes different hydration behaviour of the head groups, which is in turn responsible for different molecular head group space requirement and packing behaviour. Rydhag [1979] reported increased swelling of lamellar arrangements on incorporation of negatively charged components. Additionally, Hansrani [1980] found that various minor lecithin components like PA, PI, PS and especially the lysophospholipids were able to contribute to enhanced emulsion stability.

The so-called lysophospholipids are derived from hydrolytic cleavage of a fatty acid (where the sn-2 position appears to be preferred). Herman and Groves [1992] have shown that this process occurs according to first-order Arrhenius kinetics with different activation energies for PC and PE, whereas Håkansson [1966] reported that formation of free fatty acids was accelerated at acidic conditions where catalysis by hydronium ions occurred. Herman [1992] also pointed out that hydrolysis appears at the same rates for sn-1 and sn-2 positions and that subsequent intramolecular acyl migration may let the hydrolysis appear to have taken place at the sn-2 position. Ongoing hydrolysis results in cleavage of the second fatty acid residue, eventually yielding a molecule of the respective glycerophosphorylic compound, GPC or GPE.

Soya lecithins contain more PA and PI than egg lecithin, and are also reported to show excellent emulsifying properties [Rydhag, 1979], which led to development of various parenteral emulsions containing fractionated lecithin from soybean (see Tab. 5). Some reports on adverse reactions after parenteral application of soya lecithin-stabilised emulsions [Schuberth and Wretlind, 1961] were assigned to its higher PI content [Wretlind, 1976]. These emulsions successively vanished from the market, although other authors claimed that these toxic effects might be circumvented by further purification of soya lecithin [Mueller and Iacono, 1967]. Nevertheless egg lecithin has become the preferred lecithin type for parenteral use today.

Component	Formula	(%) in crude Soya lecithin	(%) in crude Egg lecithin	(%) in Lipoid E80®	(%) in Intralipid® lecithin
Phosphatidylcholine **(PC)**	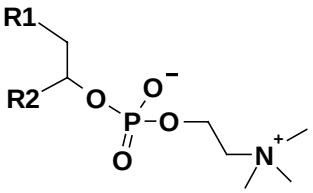	33.0	66 – 76	77.7 (77 - 82)	87.1
Phosphatidylethanol-amine **(PE)**	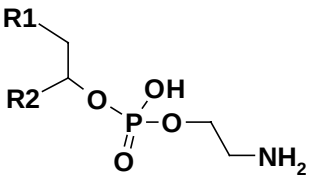	14.1	15 – 24	7.8 (7.0 - 9.5)	7.8
Phosphatidylserine **(PS)**	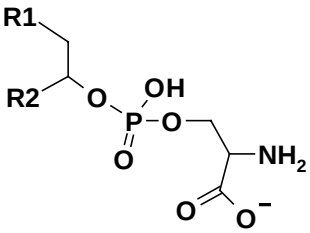	0.4	1	n.a.	n.a.
Phosphatidylinositol **(PI)**	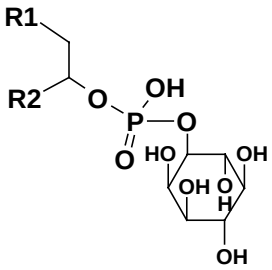	16.8	n.a.	n.a.	n.a.

Tab. 3a Distribution of selected phosphatides and lipids in crude and commercial lecithins (values for Lipoid E80® batch 19890-8 and tolerated ranges in brackets are given after product analysis sheet by the manufacturer, values for Intralipid® lecithin and egg lecithin [Kuksis, 1985], for soybean lecithin [Weber, 1985])

Component	Formula	(%) in crude Soya lecithin	(%) in crude Egg lecithin	(%) in Lipoid E80®	(%) in Intralipid® lecithin
Phosphatidic Acid **(PA)**	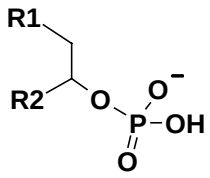	6.4	n.a.	n.a.	n.a.
Lyso-Phosphatidylcholine **(LPC)**	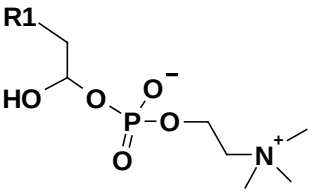	0.9	3 - 6	2.5 (max. 3)	2.5
Lyso-Phosphatidylethanol-amine **(LPE)**	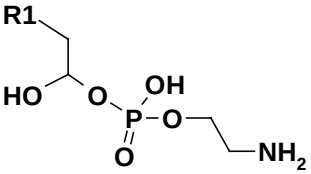	0.2		< 0.5 (< 0.5)	
Sphingomyelin **(SPM)**	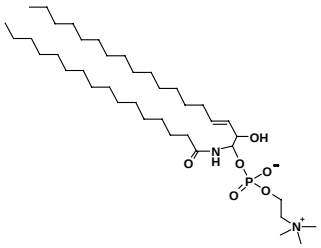	n.a.	3 - 6	3.0 (2 - 3)	2.5

Tab. 3b Distribution of selected phosphatides and lipids in crude and commercial lecithins (values for Lipoid E80® batch 19890-8 and tolerated ranges in brackets are given after product analysis sheet by the manufacturer, values for Intralipid® lecithin and egg lecithin [Kuksis, 1985], for soybean lecithin [Weber, 1985])

The mesomorphic behaviour of lecithins depends on lecithin composition, ionic strength and pH. This points to the influence of charge and hydration on molecular packing orientation and phase shapes. The orientation of a PC molecule towards an interface is shown in Fig. 4. The acyl chains show a distinct tilt from the interface normal, because the polar region extends

as far as the second C-atom of the sn-2 acyl chain and forces this part into parallel orientation to the interface. This molecular geometry favours orientation into lamellar phases (compare with Tab. 4). For each unsaturated site, the partitioning of both acyl chains increases, as chain displacement and consequently increased space requirements occur. Thus a less tighter packing, better mobility and lower melting of the fatty acid chains and of packed molecules can be observed. Accordingly, it is desirable to determine the fatty acid composition of a phospholipid fraction. Soybean lecithin, for example, carries more unsaturated fatty acids than the egg species [Rydhag, 1979 / Fiedler, 1996]. Furthermore, the space covered by the hydrated 'head groups' has strong influence on molecular orientation in organised arrangements (see Fig. 6 and Tab. 4). For the lecithin mixtures examined in this work, phase behaviour proves to be more complex than that described, for example, in liposome research literature, where exactly defined lipids are used.

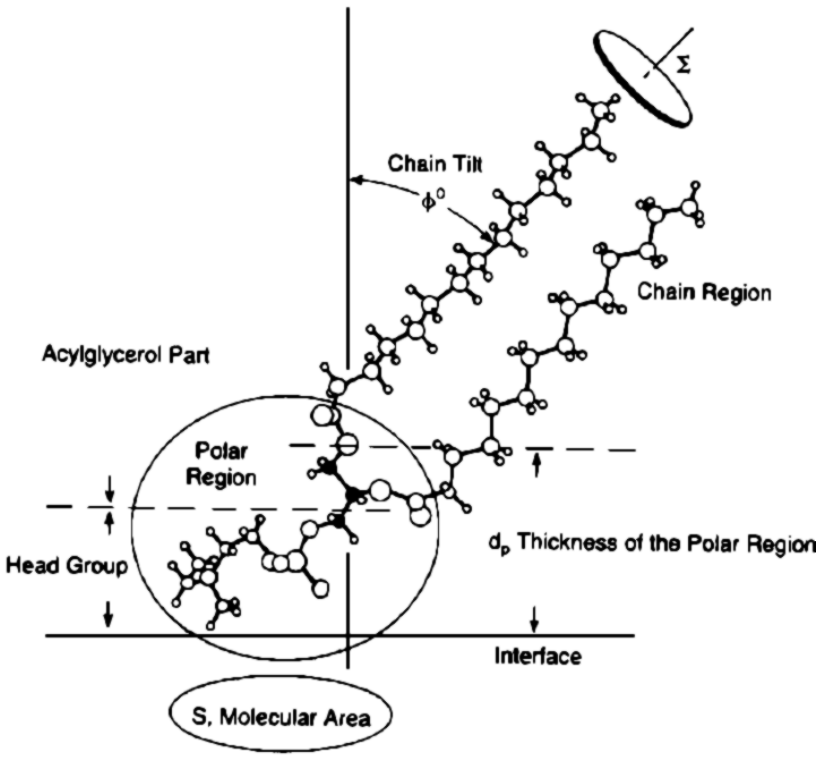

Fig. 4 Schematic of PC showing its various regions and molecular orientation at an interface (from Gennis [1989])

The influence of the head group on molecular arrangement is illustrated by comparing PC with PE, the latter having a smaller head group [Gennis, 1989]. Thermotropic phase changes from and into lamellar phases are markedly different for both species (see Fig. 6). Also, packing adaptations are different: PE allows closer packing (Fig. 5a), whereas the more

bulky head group of PC brings about different packing adaptations (Fig. 5b+c). Accordingly, the relation between the cross sectional area of the head group and the chains leads to different packing adaptations (see Tab. 4).

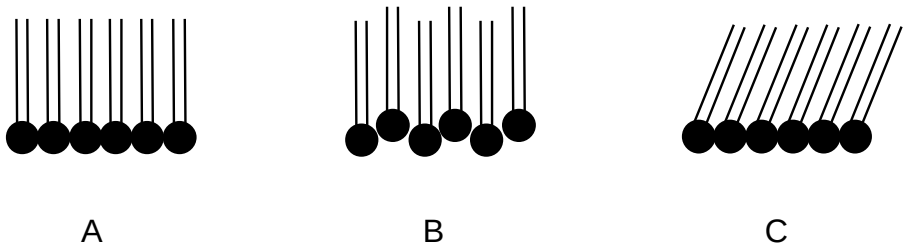

Fig. 5 Different packing adaptations in lamellar mesophases (after Gennis [1989]):
(A) Space requirement of 'head group' and chains are the same
(B) Head group requires more space than chains
(C) Tilted arrangement of chains allowing tighter packing

In Fig. 6, for PC a 'ripple phase' is observed as an intermediate state of transition from L_β to L_α. With PE, the ordered arrangement appears to melt directly into the liquid crystalline state. Different molecular shapes can be assigned to phospholipid molecules, explaining these preferential packing geometries and phases.

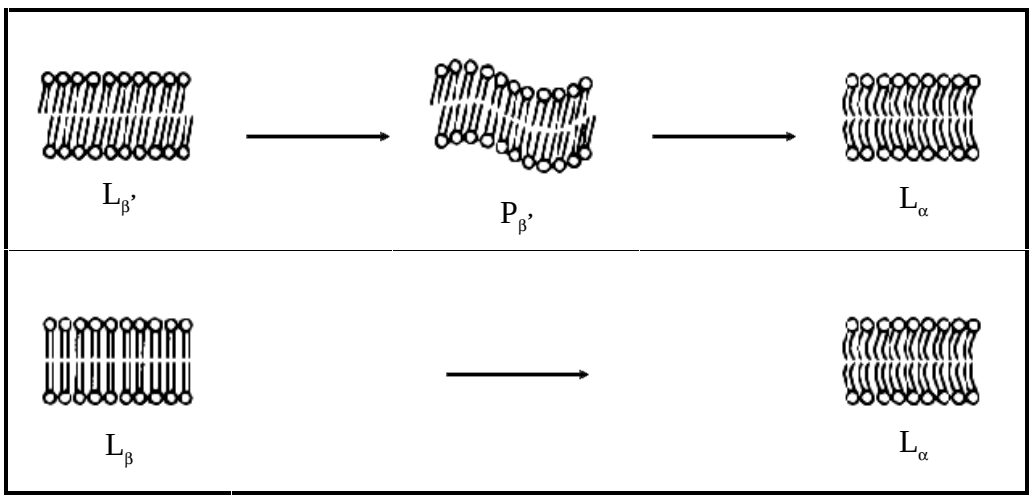

Fig. 6 Phase transitions of PC with intermediate 'ripple phase' **(above)** and of PE **(below)** caused by heating (after Gennis [1989])

Typical packing adaptations are explained by means of the 'critical packing parameter' (CPP), which is the ratio of effective volume v, head group area S_0 and chain length l_c (CPP = $v/S_0 \cdot l_c$). The CPP determines the preferred association structures assumed for each molecular shape.

How the properties of phospholipid-water mixtures and, accordingly, their phase behaviour vary, is summarised in Tab. 4, where examples of typical molecular shapes, phase arrangements and CPPs are shown for the most prominent phospholipids.

Critical packing shape	Critical packing parameter	Phase formed	Lipid examples
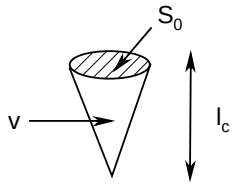 Cone	< 1/3 (spheres) 1/3 – 1/2 (rods)	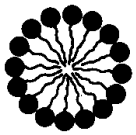	Lysophospholipids (e.g. LPC, LPE, etc.), free fatty acids (e.g. oleate, stearate, etc.)
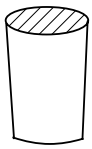 Truncated cone	1/2 – 1 (lamellar, vesicles)	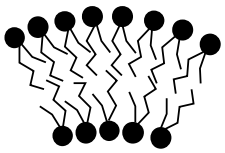	Double-chained lipids with large head group areas and fluid chains: PC, PS, PG, PI, PA, SPM
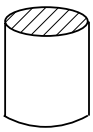 Cylinder	~ 1 (lamellar, planar bilayers)	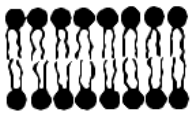	Double-chained lipids with small head group areas, anionic lipids and saturated chains: PE, PS + Ca^{2+}
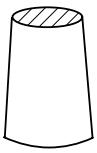 Inverted truncated cone	> 1 (hexagonal H_{II})	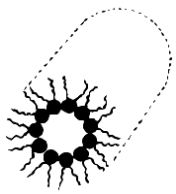	Double-chained lipids with small head group areas, non-ionic lipids and polyunsat. chains: PE (unsat.), PA + Ca^{2+}, PS (pH<4)

Tab. 4 Molecular shapes and association structures of phospholipids (modified after Cevc and Marsh [1987] and Gennis [1989])

Lamellar lecithin phases show increasing inter-bilayer spacing on uptake of water ('swelling') to form myelins, which on further dilution form closed bilayer vesicles. These so called 'liposomes' show diverse size and number of bilayers (lamellae) [New, 1990]. Curvature of the phospholipid bilayers, which is *inter alia* determined by packing geometries, limits the smallest possible size of the bilayer and is also the reason for different distribution of the phospholipid molecules in the inner and outer bilayers [Vance and Vance, 1991]. Typical vesicular structures formed by phospholipids that favour lamellar phases are depicted in Fig. 7.

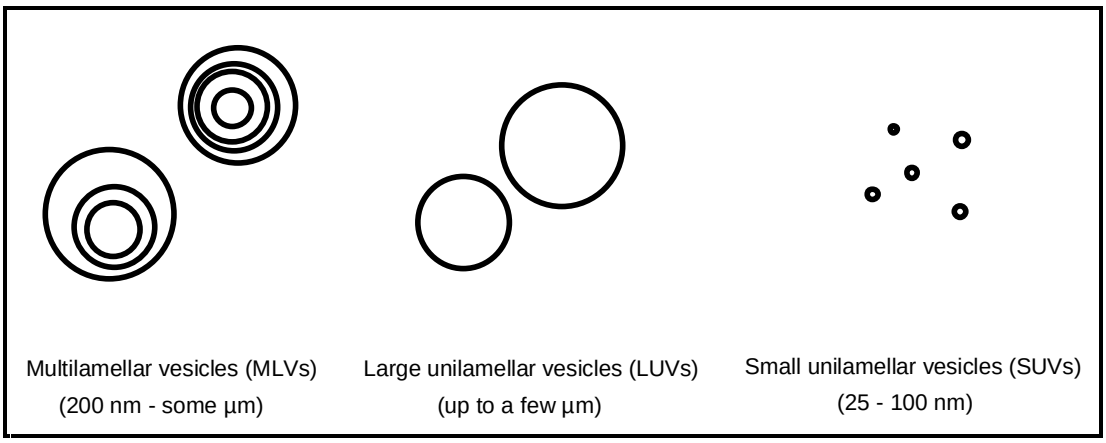

Fig. 7 Different vesicular structures (liposomes) formed by lamellar lecithin phases (adapted from New [1990])

PC and its minor components exhibit preferentially micellar, lamellar or hexagonal phases depending on e.g. head group type, fatty acid substitution, pH, temperature and hydration [Cullis et al., 1991]. For the various lipids contained in lecithin-stabilised emulsions, one would expect lamellar (vesicular) and micellar phases, as well as monolayers at the oil/water-interface. Chapman [1975] stressed that in mixed PC/PE systems not a single phase but rather separation of phospholipids into different phases can occur (lateral phase separation), which could be proven by thermal analysis and electron microscopy [Cevc and Marsh, 1987]. Owing to the complexity of commercial lecithin composition, analytical data (e.g. thermoanalytical data) only yield limited, imprecise information, and it still remains a challenge to determine phases exhibited in lecithin-stabilised emulsions. Possible resulting influences on emulsion structure and stability are discussed in Section 1.2.3.

More detailed information and data on phase equilibria and transitions of phospholipids are available in Marsh [1990], Gennis [1989], Small [1986] and Cevc and Marsh [1987].

1.2 Parenteral Fat Emulsions

Intravenously-administered oil-in-water emulsions containing triglycerides as the dispersed phase and egg lecithin as the preferred emulsifier, are common in modern intensive care medicine. Containing essential, unsaturated fatty acids, such emulsions provide calories for patients which cannot be nourished orally. It is assumed that owing to their similar particle sizes and composition, parenteral fat emulsion droplets behave like chylomicra, which are natural-borne fat-globules circulating in the blood stream after oral intake of fat [Schoefl, 1968 / Thompson, 1974]. Accordingly, clearance from the blood is believed to be comparable with chylomicra in vivo. Parenteral emulsions are not only used as nutrients, but also as potential carriers or controlled delivery systems for poorly water-soluble, oil-soluble drugs [Jeppsson,

1976 / Prankerd and Stella, 1990 / Yamaguchi et al., 1995b]. Furthermore, reduced adsorption of drugs on infusion sets, reduction of local toxicity on infusion [Davis et al., 1985] or reduced drug hydrolysis [Repta, 1981] by incorporation of drugs into parenteral fat emulsions was reported. Renewed interest has emerged recently for the well-tolerated application of Amphotericin-B, an anti-fungal drug, using a liposomal formulation, which is commercially available as Ambisome®. Some promising attempts to incorporate this drug into commercial parenteral fat emulsions and thus also lower relatively high nephro-toxicity compared with solubilised drug were reported [Lipp et al., 1993]. However other reports could not confirm these findings [Schoeffski et al., 1996]. Other applications of lecithin-stabilised parenteral emulsions comprise x-ray [Vermess et al., 1977] and ultrasonic [Lanza et al., 1996] contrast-emulsions, as well as perfluorocarbon-emulsions as possible blood-substitutes [Magdassi et al., 1991 / Pelura et al., 1992 / Ni et al., 1996].

Kleinberger and Pamperl [1983] identified four generations of fat emulsions for parenteral nutrition (Tab. 5), to which a fifth was added a few years ago. The first parenteral fat emulsions used various emulsifiers, the first of which was egg lecithin in the late 1920s contained in Yanol® [Nomura, 1929]. After severe side effects had been reported, the emulsion was withdrawn by the end of the 1930s [Thompson, 1974]. McKibbin et al. [1943] examined lecithins from egg and soya and stated that combination with synthetic emulsifiers yielded the most stable emulsions. Lipomul® / Infonutrol® represents the second generation of parenteral fat emulsions now containing purified soya lecithins in combination with a synthetic emulsifier and the oil phase used consisted of cottonseed oil (Tab. 5). Again, pharmacological issues necessitated development of a new formula, since long-term administration of cottonseed-emulsions led to toxic side effects owing to gossypol contamination [LeVeen et al., 1961]. Soya oil and safflower oil therefore became the new triglyceride sources of choice (contained in Intralipid® and Abbolipid®) [Wretlind, 1964]. These products were produced with fractionated egg lecithin as the sole emulsifier, since the toxic behaviour of long-term Pluronic-administration was, and still remains, unclear (Tab. 5). The introduction of Intralipid® in the early 1960s thus marked the third generation, and many emulsions with similar composition (soybean oil, egg lecithin) have since been introduced. Other formulations used soybean phosphatides and other polyalcohols as isotonicity agents (see Tab. 5). But as soybean lecithin was reported to be more toxic than egg lecithin (refer to Section 1.1.2), this is now not used in commercial products, and glycerol is the only isotonicity agent.

Generation	Proprietary name	Oil phase (w/v)	Emulsifier (w/v)	Other excipients (w/v)
I	**Yanol®**	Castor oil (3%)	Egg Lecithin	-
II	**Lipophysan®**	Cottonseed oil (10%)	Soya Phospholipids (2.0%)	Glycerol (2.5%), Tocopherol
II	**Lipomul® / Infonutrol®**	Cottonseed oil (20%)	Soya Phospholipids (1.2%) + Poloxamer 188 (0.3%)	Glucose (4.0%)
III	**Intralipid®**	Soya oil (10%/20%)	3-sn-PC from egg yolk (0.6%/1.2%)	Glycerol (2.2%)
IV	**Lipofundin S 10®**	Soya oil (10%)	Soya Phospholipids (0.75%)	Xylitol (5.0%)

Tab. 5 Composition of parenteral fat emulsions
(modified after Kleinberger and Pamperl [1983] and Thompson [1974])

In the late 1980s a new approach was made using as the oil phase a combination of middle-chain triglycerides (MCT) derived from coconut oil and possessing C8-10 chains, together with conventional long-chain triglycerides (LCT). Eckart et al. [1980] and Guisard and Debry [1972] claim MCT to have the advantage over LCT triglycerides of better availability owing to faster metabolisation and faster clearing. The side effects related to an 'overloading' of the reticulo-endothelial system (RES) in the liver with fat droplets observed with earlier products [Thompson, 1974 / Darby and Wallin, 1978], therefore, could be diminished [Bach et al., 1989]. Pure MCT oils were found to be less well tolerated, however [Bach et al., 1989]. The first emulsions of this kind to be marketed were Lipofundin® MCT, where conventional LCT and MCT were used in equal proportions. Fig. 8 shows typical fatty acid compositions of a conventional soybean emulsion (Intralipid®, LCT) and Lipofundin® MCT (MCT/LCT). There is no reported data on how these different triglyceride fractions effect emulsion structure and stability. It seems desirable to expand our knowledge of how different oil sources could effect the interfacial behaviour of lecithin, especially since the quest to improve tolerability and therapeutic effects has already led to new formulations containing further refined triglyceride sources. Omegaven-Fresenius® (containing ω-3-fatty-acids [fish oil] in the triglyceride-phase) and Structolipid® (containing randomly re-esterified MCT/LCT mixtures) are currently being introduced to the market or under clinical trials, respectively.

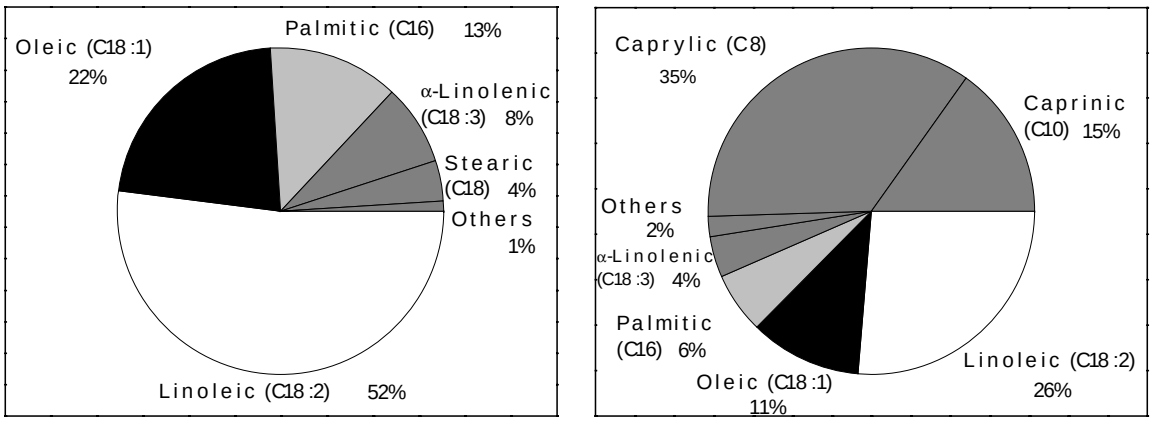

Fig. 8 Fatty acid composition of parenteral fat emulsions: Intralipid® **(LCT, left)** and Lipofundin® MCT **(LCT/MCT mixture, right)**, MCTs being C8 and C10 fractions. (after Pharmacia&Upjohn [1997] and Bell et al. [1991])

ω-3-fatty-acids given intravenously were shown *inter alia* to lead to improved blood circulation [Pscheidl et al., 1992] and reduced occurrence of undesirable prostaglandin-related side-effects. This improved tolerability of parenteral emulsions compared with those having typical fatty acid composition [Bell et al., 1991 / Carpentier et al., 1997]. Structolipid® contains LCT and MCT enzymatically cleaved and randomly re-esterified instead of using physical mixtures of LCT/MCT. By doing so, improved metabolism of triglycerides and their fatty acids and overall better tolerability was reported, making them particularly useful in critically ill patients [Bell et al., 1991 / Sandström et al., 1993 / Dahn, 1995 / Hyltander et al., 1995 / Pscheidl et al., 1995].

Tab. 6 gives the formulations of current parenteral emulsions. Frequently, only 3-sn-phosphatidylcholine (PC) is quoted as the emulsifier, with variable PC contents, and minor components (see Tab. 3) are not referred to. Emulsifier composition has been demonstrated to change constantly owing to degradation during production and storage [Herman,1992], which has to be taken into account when speaking of 'the emulsifier'. In most cases soya oil is used as the oil phase, sometimes admixed with MCT or safflower oil. In all cases, glycerol is the isotonicity agent, and sodium hydroxide or sodium oleate are employed to adjust pH to values between 7-8 (according to declaration by some manufacturers) as is desired for large-dose parenterals [Ph.Eur.1997, 1997]. In the case of drug-loaded emulsions, lipophilic drugs, especially narcotics or tranquillisers dominate.

Proprietary name	Oil phase (w/v)	Emulsifier (w/v)	Active ingredients	Other excipients (w/v)
Abbolipid® 10% / 20%	Soya oil + Safflower oil (5% / 10% each)	3-sn-PC from egg (0.74% / 1.2%)	-	Glycerol (2.5%), Sodium Hydroxide
Deltalipid® 10% / 20%	Soya oil (10% / 20%)	Egg phospholipids (70-83% 3-sn-PC) (1.2% / 1.2%)	-	Glycerol (2.5%), Sodium Hydroxide, Oleic Acid (0.03%)
Intralipid® 10 / 20	Soya oil (10% / 20%)	3-sn-PC from egg yolk (0.6% / 1.2%)	-	Glycerol (2.2%), Sodium Hydroxide
Lipofundin® N 10% / 20%	Soya oil (fract.) (10% / 20%)	Egg phospholipids (min. 68% 3-sn-PC) (0.8% / 1.2%)	-	Glycerol (2.5%), Sodium Oleate, α-Tocopherol
Lipofundin MCT® 10% / 20%	Soya oil + Middle chain triglycerides (5% / 10% each)	Egg phospholipids (min. 68% 3-sn-PC) (0.8% / 1.2%)	-	Glycerol (2.5%), Sodium Hydrox., Sod. Oleate, α-Toc.
Lipovenoes® 10% PLR / 20%	Soya oil (10% / 20%)	Egg phospholipids (min.75-81% 3-sn-PC) (0.6% / 1.2%)	-	Glycerol (2.5%), Sodium Hydrox., Sodium Oleate
Lipovenoes® MCT 10% / 20%	Soya oil + Middle chain triglycerides (5% / 10% each)	Egg phospholipids (min.75-81% 3-sn-PC) (0.6% / 1.2%)	-	Glycerol (2.5%), Sodium Hydrox., Sodium Oleate
Salvilipid® 10 / 20	Soya oil (10% / 20%)	3-sn-PC from egg yolk (60%) (1.2% / 1.2%)	-	Glycerol (2.5%), Sodium Hydroxide, Sod. Oleate (0.03%)
Intralipid® 30	Soya oil (30%)	3-sn-PC from egg yolk (1.2%)	-	Glycerol (1.67%), Sodium Hydroxide
Diazepam Lipuro® 1% / 2%	Soya oil + Middle chain triglycerides	Egg lecithin	Diazepam (5%)	Glycerol, Sodium Oleate (for pH adjustment)
Disoprivan® 1% / 2%	Soya oil	3-sn-PC	Propofol (1% / 2%)	Glycerol, Sodium Hydroxide
Etomidat Lipuro®	Soya oil + Middle chain triglycerides	Egg lecithin	Etomidate (2%)	Glycerol, Sodium Oleate (for pH adjustment)
Lipotalon®	Soya oil (10%)	Egg phospholipids (1.2%)	Dexamethasone-21-palmitate (0.4%)	Glycerol
Propofol Abbot 1%	Soya oil	Egg lecithin	Propofol (1%)	Glycerol, Sodium Hydroxide
Propofol 1% Parke-Davis®	Soya oil	3-sn-PC	Propofol (1%)	Glycerol, Sodium Hydroxide, Oleic Acid
Stesolid®	Soya oil	Phospholipids from egg yolk	Diazepam (5%)	Glycerol, Acetylated Monoglycerides, Sodium Hydroxide

Tab. 6 A selection of presently marketed parenteral emulsions in Germany [Rote Liste, 1998]

Early Intralipid® emulsions and its generics were produced using 1.2% w/v emulsifier regardless of the oil content of the emulsions. It was assumed that this amount was necessary to stabilise 10% w/v of soybean oil and according to Ishii et al. [1990], it appeared to be the optimal concentration. Groves et al. [1985] proposed from calculations and experimental data that excess emulsifier was present and remained as multi-lamellar liposomes (MLVs) in the finished product. It could be shown that emulsions containing 10% inner phase held a substantial excess of lecithin [Hajri et al., 1990 / Férézou et al., 1994] forming separate phases besides emulsion droplets. This excess was suggested to be the reason for unfavourable dislipidemias found on long-term infusion [Lutz et al., 1990]. Deviation from the chylomicron-like behaviour, and thus a different metabolic fate than that of lecithin-coated oil droplets, was presumed. This excess was again suspected to consist of liposomes which caused enhanced formation of abnormal 'Lipoprotein-X', increased cholesterol release and other dislipidemic effects [Bach et al., 1996]. Consequently, most commercially available 10% emulsions that formerly contained 1.2% emulsifier, were reformulated and the lecithin concentration reduced to 0.6% w/v. In Intralipid 30® even threefold quantities of oil (30%) are incorporated using 1.2% lecithin, as further reduction of the lecithin/triglyceride ratio was sought.

Thus the historical changes in parenteral fat emulsion formulation were necessary for pharmacological reasons, not because of stability issues. Parenteral emulsions are often administered admixed with different amino acid, carbohydrate or electrolyte solutions, which is termed as 'Total Parenteral Nutrition (TPN)' and frequently causes incompatibilities. In the case of Intralipid 10® and Lipofundin®10% and 20%, admixtures are explicitly forbidden by the manufacturer, whereas for Intralipid 20® or Lipovenoes 20%® these are regarded as being possible taking due care. Emulsion formulation and its 'stability' is evidently still a sensitive issue and a matter not yet fully understood. All commercial lecithin-stabilised emulsions also show high, unexpected stability against steam-sterilisation which also may be related to their structure [Herman and Groves, 1992]. Instability problems during production or storage of lecithin-stabilised O/W emulsions do, however, occur [Magdassi et al., 1991 / Krafft et al., 1991 / Chaturvedi et al., 1992 / Lucks, 1993]. Differences in raw materials, equipment and preparation might, however, have been underestimated here. In the following sections, therefore, a brief overview of the decisive steps in parenteral emulsion production are given.

1.2.1 Preparation of Parenteral Fat Emulsions

The properties of the final emulsion are largely dependent on the preparation techniques applied. Schurr [1969] gives an introduction to large batch and Pscherer [1981] to industrial manufacturing of parenteral fat emulsions.

1.2.1.1 Preparation of Coarse Emulsions

To reduce the bioburden and possible pyrogens, both oil and water phases are filtered before they are mixed together to form the pre-dispersion [Pscherer, 1981]. Water-soluble components like glycerol or sodium hydroxide can directly be dissolved into the Water for Injection. Lecithin is practically insoluble in either oil or in water. By applying elevated temperatures (70-80°C), lecithin dissolves into the oil, which allows filtration of all of the components prior to premixing. High shear mixers (e.g. colloid-mill) or rotor-stator mixers are subsequently used to form pre-emulsions of rather wide particle size distribution of preferably ≤ 20 µm [Bock, 1994].

In lab-scale setups, rotor-stator mixers like the ultra turrax have frequently been used [Washington and Davis, 1987 / Bock et al., 1994]. However, magnetic stirrers [Rabiner et al., 1986] or high-shear mixers [Ishii et al., 1990] have also been used. Various methods of incorporation of lecithin into pre-dispersions were reported. Hansrani [1980], Rabiner et al. [1986], Washington and Davis [1987], Herman [1992] and Chaturvedi et al. [1992] used the lecithin dispersed in the (heated) water phase, whereas e.g. Ishii et al. [1990] and Bock et al. [1994] used the heated oil phase as a vehicle for the emulsifier. Bock [1994] assumed that lowered pH values during pre-emulsification were caused by incipient hydrolysis of the emulsifier, which he related to decreasing stability of the system. He stated that the phase-inversion method led to a markedly shorter pre-emulsification step and, therefore, to reduced hydrolysis. However, neither of the authors examined particle size after the pre-emulsification step, presumably because the subsequent homogenisation step was considered to be the more crucial process.

1.2.1.2 High-Pressure Homogenisation

Homogenisation involves concurrent reduction of particle size and narrowing of particle size distribution [Walstra, 1983]. This is of twofold importance. Injectables must avoid capillary blockage (see Section 1.2.2) and additionally are more stable against creaming when droplets are uniformly small and only subject to Brownian movement (see Section 1.2.2.4). To produce such emulsions of submicron particle size, size reduction must be highly effective. During emulsification, droplets are disrupted when they are deformed beyond a critical value for

longer than a critical time. High energy input provides the tension necessary to break up a droplet by overcoming the Laplace pressure and interfacial tension.
The energy density (E_V, [J/m^3]) applied by the homogenising equipment can be described as:

$$E_V = \overline{P_V} \cdot \bar{t}_{res} = \frac{P}{\dot{V}}$$

Eq. 1 The Energy Density

where $\overline{P_V}$ is the mean power density [W/m^3] and $\bar{t}_{res}$ the mean residence time [s] in the dissipation zone of the homogeniser. This could also be rewritten as P (power input) [W] divided by $\dot{V}$ (volume flow rate) [m^3/s] [Schubert, 1997]. The resulting mean droplet diameter can be assumed to be a function of the energy density applied [Karbstein, 1994]. Effective droplet disruption could be achieved by exposing the droplets to high laminar or turbulent flow or shear stress of high energy density. High-pressure homogenisers have successfully been used for this purpose. They provide high P_V and produce effective particle size reduction, especially in low viscosity dispersions [Karbstein, 1994], which can directly be related to the homogenisation pressure. Conventional valve homogenisers disrupt droplets by both shear forces existing adjacent to energy-bearing eddies in turbulent flow, and cavitation (owing to high local pressure fluctuations) which causes solvent vapour bubbles to form and collapse which in turn shatters the droplets [Walstra, 1983]. In submerged jet homogenisers, such as the 'Microfluidizer®' or the 'Nanojet®', turbulent flow more than shear or cavitation cause droplet disruption [Karbstein, 1994 / Schubert, 1997].

Particle sizes of homogenised emulsions are dependent on four key factors [Karbstein, 1994 / Schubert, 1997]:

1) ratio of emulsifier to dispersed phase
2) adsorption kinetics of the emulsifier on newly-created interface
3) viscosity of the dispersed phase (can be reduced by elevating temperature)
4) power density P_V (determined by homogenisation pressure, flow rate)

Excess pressure or prolonged homogenisation can, however, lead to overprocessed emulsions, where droplet diameter increases [Pscherer, 1981 / Karbstein, 1994]. This coalescence is not a result of enhanced particle collision rates, since collision times in homogenisers are too short to allow film drainage between approaching droplets [Chesters, 1991]. It is rather a matter of insufficient emulsifier concentration at the oil-water-interface (discussed in Section 1.2.2.1). A plateau in particle size reduction with time is reached, where neither increasing temperature nor homogenising pressure lead to further droplet size reduction [Washington and Davis, 1987

/ Lidgate et al., 1989 / Ishii et al., 1990]. The same authors report that reprocessing of the emulsion for several homogenisation cycles narrows particle size distributions further, but that major particle size reduction is already achieved after 2-3 cycles. Since heating during homogenisation may not alter only disruption and 'recoalescence' mechanisms but also enhance chemical degradation, temperature should be controlled carefully [Washington and Davis, 1987 / Bock et al., 1994].

1.2.1.3 Sterilisation by Autoclaving

As other sterilisation techniques are not applicable to emulsions, steam-sterilisation is favoured. Emulsions are sterilised according to pharmacopeial requirements (e.g. 121°C, 2 bar for at least 15 min). Thermal stress might, however, change the physical and chemical stability of the emulsions unfavourably. To minimise physical changes, rotating autoclaves are used to avoid unequal heat-distribution in the emulsions. To prevent excess thermal stress and to avoid refluxing on the upper surface of the bottles, readjustment to atmospheric conditions can be accelerated by spraying iced water onto the bottles in the autoclave [Schurr, 1969].

1.2.2 Stability of Parenteral Fat Emulsions

Stability of a parenteral emulsion is mainly used in terms of maintaining of its main physical property, namely the dispersed phase particle size distribution. Safety of application is to a high degree dependent on the particle size distribution of the oil phase, since particles larger than 5 µm given intravenously can lead to emboli in vivo [Hadfield, 1966 / Davis, 1974]. Therefore, USP23/NF18 [1995] limits particulate matter in parenterals to ≤ 25 µm and Ph.Eur.1997 [1997] states 'controlling particle size range within suitable limits according to its intended use'. For injectables, this alludes to the diameter of the smallest capillaries of the body (~5 µm). The shelf life of commercial parenteral emulsions lies in a range of 2 years, although physical stability can be maintained for longer periods [Mueller et al., 1992 / Schuhmann, 1995]. Despite this, chemical and microbiological properties must also be controlled for toxicological reasons; one has to consider that these emulsions are often given to critically-ill patients for long periods.

According to the IUPAC definition, emulsions are disperse systems of two immiscible liquids or liquid crystals [International Union of Pure and Applied Chemistry, 1972]. They are, therefore, thermodynamically unstable ($\Delta G \neq 0$) and droplets tend to decrease their interfacial area by coalescence, leading to coarsening of droplet size and finally irreversible separation of the phases ('coalescence', 'cracking'). Prevention of coalescence is thus used as a synonym for stabilisation of an emulsion. This can be achieved by use of an emulsifier to reduce the

interfacial tension (γ) and interfacial free energy (G) which are equivalent to tendency to coalesce [Hiemenz, 1986 / Stricker, 1987]. Although ΔG can be seen as the driving force for coalescence, droplet approach is governed by other factors like steric hindrance [Fisher and Parker, 1988], electrostatic attraction and repulsion according to DLVO-theory [Derjaguin, 1989], hydration forces [LeNeveu et al., 1976] and emulsifier film viscoelasticity [Boyd et al., 1974]. This is also true for the interfacial barrier of lecithin-stabilised O/W emulsions [Hansrani, 1980 / Davis and Hansrani, 1985 / Fisher and Parker, 1988], where various aspects of stability need to be considered.

1.2.2.1 Stability against Recoalescence

During homogenisation of an emulsion, the dispersity of the internal phase is increased by breaking up its structure by means of high shear forces, cavitation impact, turbulence, etc. . Depending on the conditions existing, the droplets formed in situ will instantaneously start to 'recoalesce', if maintenance of this state of dispersion cannot be achieved [Dickinson and Stainsby, 1988], which is illustrated in Fig. 9. Only dissolved, molecularly dispersed emulsifier molecules are capable of stabilising the newly-created interface. If a high energy input during homogenisation creates too large an oil-water-interface to be either stabilised by this limited amount of free emulsifier or by too slow adsorption of emulsifier at the interface, recoalescence will occur. Low molecular weight emulsifiers (e.g. < 500) are transported more rapidly to the interface by diffusion and conduction, and can thus prevent coalescence on a time scale of milliseconds to a few minutes [Das and Kinsella, 1991 / Schubert, 1997]. Emulsifiers of higher molecular weight, e.g. proteins or polymeric emulsifiers, exhibit slower transport rates and thus less effective short time range coverage of a newly-created interface [Schubert, 1997 / Stang and Schubert, 1997]. According to Gibbs' adsorption isotherm (Eq. 2), the emulsifier concentrations at an interface and in bulk solution at equilibrium are related via the interfacial tension:

$$\Gamma = -\frac{1}{R \cdot T} \cdot \frac{d\gamma}{d \ln c}$$

Eq. 2 The Gibbs' adsorption isotherm

Γ [mol/m^2] gives the excess concentration of the emulsifier at the interface, c [mol/l] its concentration in the bulk solution, γ [N/m] is the interfacial tension, R the gas constant and T the absolute temperature [K]. γ is approx. 25 mNm^{-1} for a pure triglyceride-water-interface [Fisher and Parker, 1988]. PC, as the major component of lecithin, has a very low aqueous

solubility (Small [1986] quotes $4.6 \cdot 10^{-10}$ mol/l for DPPC). Additionally, a second lecithin phase exists in aqueous dispersions in the form of liposomes. Eq. 2 predicts that now equilibrium between lecithin concentration at the O/W interface and in bulk solution as monomers lies greatly in favour of the interface, i.e. Γ is large. Convective transport of lecithin in the form of liposomes to freshly-created interface during homogenisation appears intuitively more probable than passive diffusion processes.

Accordingly, stability refers to a short-time stability during homogenisation, where creaming becomes negligible. An emulsifier suitable for long-term stabilisation of larger droplets, therefore, will not necessarily be sufficient for production of small particle size. Owing to this fact, co-emulsifiers are frequently used for this purpose, which either enhance the initial effect of the main emulsifier, or often also show complementary effects regarding stabilising mechanisms (see Section 1.2.2.4).

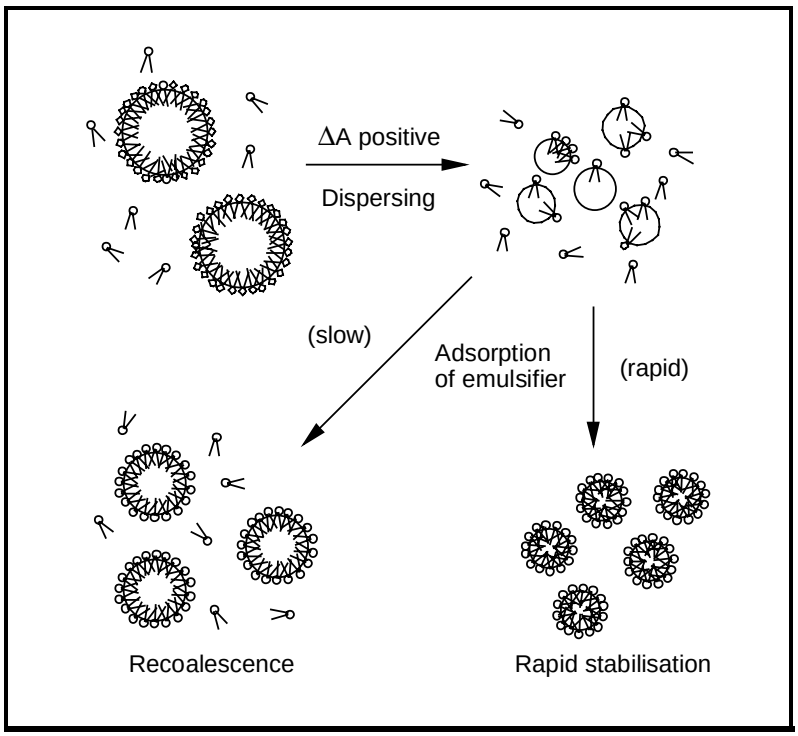

Fig. 9 Influence of free emulsifier adsorption kinetics during homogenisation on dispersity

Karbstein [1994] reported that increasing the fraction of the dispersed phase, Φ, does not increase rate of recoalescence during homogenisation, although droplet collision events are increased, provided the emulsifier stabilises the newly-created interfaces sufficiently fast. This is also true for high Φ, since now higher viscosity and less collision events are expected. Fisher and Parker [1988] suggested that although droplet break-up may be improved by higher temperatures, a more rigid emulsifier film allows better stabilisation and can be obtained by cooling the sample during homogenisation.

1.2.2.2 Stability during Autoclaving

Emulsions are readily destabilised and coalesce when stress (viz heat, freeze-thawing or shaking) is applied upon them [Becher, 1965]. Parenteral fat emulsions exhibit, however, a remarkable resistance against heat-stress during terminal heat-sterilisation, where 121°C is maintained for ≥ 15 min. This has been related to their structure, suggesting either the existence of a liquid-crystalline mesophase at the oil-water-interface [Groves et al., 1985 / Groves and Herman, 1993], which was suggested to prevent droplet coalescence by increasing the emulsifier film viscoelasticity. Washington and Davis [1987] stressed the importance of free fatty acids, since these would increase electrostatic repulsion between droplets.

Since heat-sterilisation is unavoidable in parenteral emulsion production, instability in this state must be circumvented. This necessitates avoiding coalescence and its various stages over a short time range, and also enhanced chemical degradation, where physical and toxicological properties are concerned. Effects observed at elevated temperature are accelerated chemical and physical degradation reactions, which appear to be interdependent [Herman and Groves, 1992].

1.2.2.3 Stability against Chemical Degradation

Possible chemical degradation within parenteral fat emulsions includes oxidation of unsaturated fatty acid residues in the triglyceride or lecithin molecules [Kemps and Crommelin, 1988] and hydrolysis of phospholipids [Grit et al., 1989 / Herman, 1992].

Oxidation of double bonds within the lecithin may influence the nature of the O/W interfacial film. As a possible mechanism, Magdassi et al. [1991] proposed that despite oxidation, polymerisation of molecules could also take place and subsequently desorption from the interfacial layer. The detection of initial formation of conjugated dienes is reported by New [1990] using UV absorption at 230 nm. Magdassi et al. quote that oxidation level could be determined by monitoring the ratio of UV absorption at 233 nm and 215 nm, whereas other authors use the ratio of the absorptions at 234 nm and 270 nm to follow oxidation of unsaturated fatty acids [Belitz and Grosch, 1982]. Despite trace amounts of the natural antioxidant tocopherol contained in soy bean oil, all production steps must be carried out under inert gas purging.

Hydrolysis of phospholipids leads to formation of free fatty acids, lyso-phospholipids and glycerophosphorylic compounds (Fig. 10). Grit et al. [1989] and Herman and Groves [1992] determined hydrolysis rates of PC and PE in aqueous media at various temperatures, which were lowest at pH 6.5. However, different hydrolysis rates were determined, according

to the concentration of additional phospholipid components [Grit et al., 1991]. The degradation products are more water-soluble than the original phospholipids, which may influence emulsifier distribution at the O/W interface, and also promote further degradation as they cause lowering of pH [Boberg and Håkansson, 1964 / Kawilarang et al., 1980 / Herman and Groves, 1992]. Accordingly, adjustment of pH of an emulsion before autoclaving provides physiological pH in the finished product, but also allows less hydrolysis to occur in the final product during storage, where pH is about 6-8.

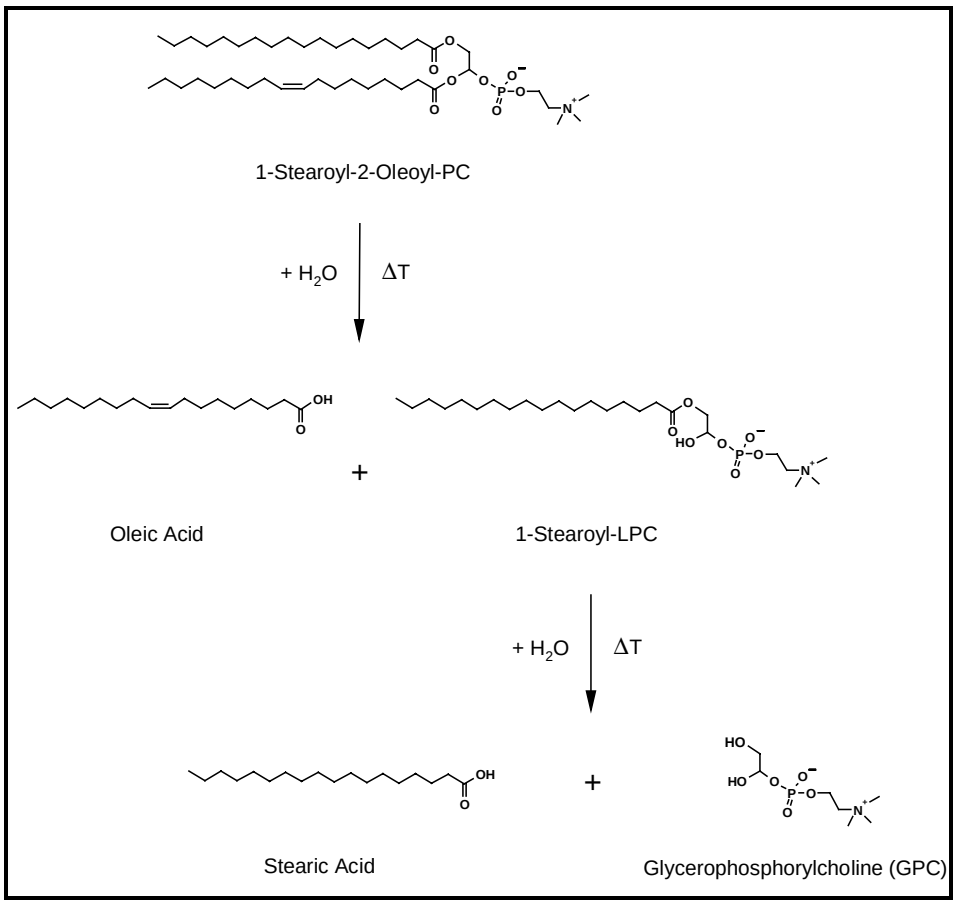

Fig. 10 Pathways of phospholipid hydrolysis for the example of SOPC

Hydrolysis products need to be minimised since lyso-phospholipids exhibit haemolytic effects in vitro and have, therefore, to be regarded as toxic [Saunders, 1957 / Weltzien, 1979]. It has been demonstrated, however, that LPC has a stabilising effect on PC vesicles by adhering to the bilayer [Kumar et al., 1989]. This could reduce the concentration of free lyso-compounds in the emulsion, thus explaining why toxicity in vivo does not occur despite up to 8% lyso-compound concentration [Muehlebach et al., 1987], or 8.2% LPC and 3% LPE [Herman, 1992] have been reported. Hansrani [1980] also reported a stabilising effect of LPC on lecithin-stabilised emulsions from admixing experiments using a droplet-surface coalescence model.

Hydrolysis of triglycerides to fatty acids and di- or mono-glycerides is also theoretically possible in these emulsions. The resulting hydrolysis products again would be surface active, with possible changes in emulsifier film properties and an influence on pH of the bulk water phase.

1.2.2.4 Stability against Physical Degradation

Emulsions are inherently unstable. Comprehensive discussions of the physical stability of emulsions are available elsewhere [Becher, 1988 / Dickinson and Stainsby, 1988 / Friberg and Larsson, 1997], and only the major processes involved are summarised in Fig. 11. The driving force of coalescence is always the reduction in Gibbs free energy (ΔG), achieved by reducing the size of the O/W interface (A) of tension (γ), despite the associated decrease in entropy, ($T \cdot \Delta S$).

$$\Delta G = \gamma \cdot \Delta A - T \cdot \Delta S$$

Eq. 3 The Gibbs free energy

Disruption of a continuous soya oil phase into droplets of 300 nm within water increases the interfacial area by approx. 10^5-fold, whereas the presence of 0.5% w/v lecithin reduces γ only approx. 68-fold [Mueller and Heinemann, 1993]. Therefore, additional factors affecting the mechanisms of coalescence must be considered for lecithin-stabilised soya oil-in-water emulsions. Droplet coalescence irreversibly changes the quality of dispersion and is a first-order process [Cockbain and McRoberts, 1953 / Van den Tempel, 1953], where the rate-determining steps are either the drainage of the continuous liquid film between two approaching droplets to its rupture thickness, or the probability of film collapse occurring as a consequence of mechanical distortion when equilibrium thickness has been reached [Fisher and Parker, 1988]. At surfactant concentrations well above the CMC (which is certainly the case in lecithin-stabilised emulsions), the rate of film drainage, $-dD/dt$, follows approx. the Reynolds equation (Eq. 4) for two rigid discs spaced by the interfacial film [Fisher and Parker, 1988].

$$-\frac{dD}{dt} = \frac{2FD^3}{3\pi\eta R_c^4}$$

Eq. 4 The Reynolds equation for liquid flow between rigid discs

F is the net interdroplet attraction force, η is the viscosity of the continuous phase, and R_c is the radius of the discs. The processes which counteract film drainage and thus inhibit coalescence are:

1) The *Gibbs-Marangoni effect*: interfacial surfactant resists displacement from the thinning area, where a surfactant concentration gradient already exists. This leads to osmotic retention of liquid from the continuous phase [Ewers and Sutherland, 1952].

2) *Viscoelastic properties*: viscoelastic behaviour of the adsorbed emulsifier film resists mechanical 'rupture' [Boyd et al., 1974].

3) *Born hydration repulsion*: this becomes effective when emulsifier (e.g. PC) head groups surrounded by a solvation layer approach each other to distances ≤ than the thickness of the layer (~3 nm). The solvation layer has to be dispersed to allow closer contact, which is counteracted by the hydration energy. Though of considerable magnitude, this repulsion is not capable of avoiding long-distance interactions like *flocculation* [LeNeveu et al., 1976].

4) *Steric repulsion*: occurs when the size and geometric extension of molecules in the adsorbed film prevent droplets from approaching each other [Napper, 1983].

5) *Electrostatic repulsion*: According to the DLVO theory, which describes the balance between attractive (Van-der-Waals-) and repulsive (electrostatic) forces, droplet approach and *flocculation* can be diminished [Verwey and Overbeek, 1948].

Coalescence is accompanied by *flocculation* and sometimes also *creaming*. The first describes the adhesion of dispersed droplets, which yet remain single bodies. The latter describes the movement of the less dense phase (in the case of O/W emulsions i.e. triglycerides) to the upper region of the container. In both cases the droplet number and their size distribution remain unchanged, and although distribution of the droplets becomes inhomogeneous, this can often readily be reversed by gentle agitation. Fisher and Parker [1988] stated that interfacial multilayers of surfactant may enhance *flocculation*, but allow easy redispersion since multilayers are sensitive to shear force. This could cause enhanced mechanical stabilisation against coalescence during droplet collision. However, formation of larger aggregates may be facilitated, which in turn promotes faster creaming and may thus facilitate *coalescence*. This is

especially true for highly polydisperse systems where different *creaming* rates produce enhanced droplet encounter rates [Dickinson and Stainsby, 1988]. Small particles, which remain in Brownian dispersion, are therefore separated from the larger particles.

The contribution of negative surface charge (*Zeta potential*) of lecithin-stabilised emulsion droplets to their ability to withstand *flocculation* or *coalescence* has been frequently investigated. There is substantial agreement that increasing *Zeta potential* gives rise to enhanced stability against various stress factors as predicted by DLVO-theory [Kawilarang et al., 1980 / Washington and Davis, 1987 / Washington et al., 1989 / Ishii et al., 1990 / Rubino, 1990 / Chaturvedi et al., 1992]. However, enhanced stability was not reported in all cases; sometimes coalescence was enhanced or flocculation increased after addition of electrolytes or charged lipids [Rubino, 1990 and Muchtar et al., 1991]. Davis et al. [1985] and Mueller and Heinemann [1993] stressed that also the mechanical barrier functions of the lecithin film have to be taken into account in order to estimate stability of an emulsion.

Phase inversion and *Ostwald ripening* are considered to be of no importance for parenteral fat emulsions. In the latter case a pronounced solubilisation of the oil phase in surfactant micelles in the aqueous phase would be required to allow migration of oil through the aqueous phase [Dickinson and Stainsby, 1988]. This is clearly not possible owing to PC's extremely low solubility in water.

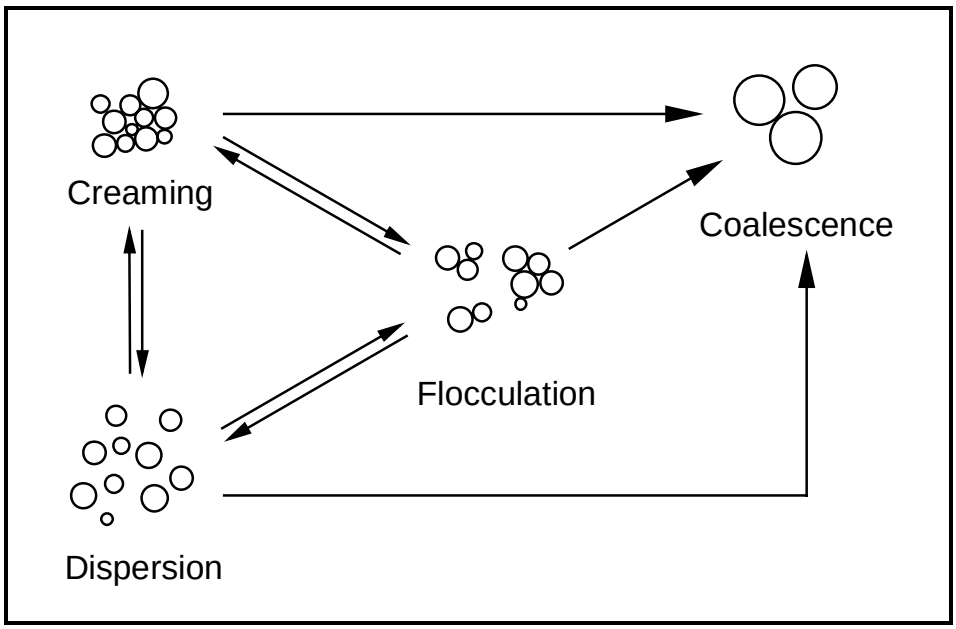

Fig. 11 Major mechanisms of physical instability in emulsions

1.2.2.5 Stability against Microbiological Degradation

Microbiological contamination always has to be considered when water is the continuous phase of an emulsion and is, of course, completely unacceptable for intravenous application. Since preservatives are not allowed as additives in parenteral emulsions [Ph.Eur.1997, 1997], even refrigerated storage of opened containers will not suffice to prevent microbiological degradation. Only manufacture under aseptic conditions with terminal steam-sterilisation can ensure the product's sterility.

1.2.2.6 Stability against Admixing

Parenteral emulsions are often admixed with other injectable solutions to yield smaller total volumes for total parenteral nutrition (TPN) regimes. However, undesirable physical destabilisation is unpredictable, and prevents commercial pre-production of such TPN-regimes. Interactions of admixed components with parenteral emulsions have been discussed by Dawes and Groves [1978], Whateley et al. [1984], Davis et al. [1985], Washington et al. [1990], Washington et al. [1991], Washington [1992] and Mueller and Heinemann [1994]. It is important to consider compatibility with various amounts and kinds of admixed parenterals like carbohydrates, amino acids and ionic solutes, which can be regarded as an additional stress towards the emulsion. Since it still remains unclear, whether surplus emulsifier acts as a 'buffer' that enhances stability of emulsion droplets against degrading factors like ionic admixtures, the newly marketed 10% formulations (like e.g. Intralipid 10®) which contain reduced emulsifier excess, are believed not to be suitable for use in such mixed formulations as the respective 20% emulsions.

1.2.3 Model Theories of Parenteral Emulsion Structure

According to IUPAC, emulsions are dispersions of immiscible liquids and/or liquid crystals in other liquids [International Union of Pure and Applied Chemistry, 1972]. Boyd et al. [1974] reported the marked improvement in stability of an emulsion owing to the pronounced viscoelastic properties of liquid-crystalline mesophases as the interfacial film. Friberg et al. [1976], Rydhag [1979] and Rydhag and Wilton [1981] have all reported that phospholipids that form liquid crystalline phases, show lamellar layers at the oil-water interface which enhance emulsion stability. Rydhag [1979] showed that negatively-charged lipids increased the swelling of liquid-crystalline phases and related this finding to the enhancement of emulsion stability by using lecithins containing more negatively-charged components (PI, PS, PA). Groves and Herman [1993] postulated that reversible formation of viscous cubic phases could

account for the emulsion's stability against autoclaving. The systems reported by Rydhag [1979] and Rydhag and Wilton [1981] had, however, larger droplet size than typical for parenteral fat emulsions, which would result in a smaller O/W interfacial area. This causes a large emulsifier excess, which now forms the extensive liquid-crystalline structures reported [Westesen and Wehler, 1992].

Several authors have reported excess lecithin in parenteral emulsions, which could form liposomes beside the emulsion droplets [Groves et al., 1985 and Rotenberg et al., 1991]. Westesen and Wehler [1992] found that the dispersed phase consisted of ideal emulsion droplets covered by monolayers of the emulsifier. Groves and co-workers [1985] showed micrographs of multilamellar structures contained in the emulsions, whereas the latter authors reported the presence of unilamellar vesicles. However, Westesen and Wehler [1992] drew their conclusions from model systems containing higher lecithin/oil-ratios than in commercial systems. Groves and co-workers [1985] and Rotenberg et al. [1991] investigated centrifuged Intralipid® 10 samples, which possibly were changed in some way by centrifugation. Indeed, the mesophase which may form in the aqueous phase of an O/W emulsion and which theoretically may be able to adsorb on the interface as a multilayer, is not necessarily of the same composition as an interfacial mesophase, since the surface material may change over time [Fisher and Parker, 1988].

However, it still remains uncertain whether surplus lecithin (assuming an interfacial monolayer) contributes to the stability of the emulsions. If this were the case, it would thereby counteract the pharmacological demand for reduction of excess lecithin [Hajri et al., 1990]. This has been suggested by Groves et al. [1985], but contradicted by the reports of Chiba and Tada [1990] and Krafft et al. [1991], who claimed that excess lecithin may even destabilise emulsions. It has not been possible to clarify whether such excess emulsifier was inherent to lecithin-stabilised emulsions, or if it could be avoided. Although theoretically possible, the presence of micelles formed by lyso-compounds or free fatty acids in emulsions, has not been confirmed (e.g. [Westesen and Wehler, 1992]).

It is astounding that six decades of research in this field have resulted in substantial disagreement about the behaviour of the lecithin in emulsified structures and those not related with the interface. It is also not yet completely understood to which degree possible stabilisation mechanisms contribute to the stability of lecithin-stabilised O/W-emulsions during autoclaving.

1.3 Objectives of this Work

This work is intended to contribute a better understanding and a more precise definition of the ill-defined term 'stability' of parenteral fat emulsions. A combination of experimental methods was used here to give a more detailed insight into the structure of these 'simple' emulsions with their paradoxically 'complex' behaviour, which, undoubtedly is mostly due to the nature of the emulsifier.

Today's knowledge of parenteral fat emulsions is derived from two sources: studies of commercial emulsions and experimental data from model emulsions. Even in the commercial systems different compositions and manufacturing procedures are used, making comparisons difficult. This is certainly the reason why previous work does not give a complete image of the structures present and how these influence stability and therapeutic efficacy. All studies on commercial samples reported here were undertaken with the respective up-to-date formulations (e.g. lecithin-reduced 10% formulations). Model systems made from 'outdated' composition were also investigated to confirm older reports, which dealt with former commercial formulations. As Westesen and Wehler [1992] stressed, lecithin-stabilised parenteral fat emulsions cannot be seen as mere monomodal oil-in-water-dispersions, since pharmacological (e.g. lipoprotein-x-like particles, hypercholesterolemia) and physical phenomena (e.g. ability to tolerate admixtures of drugs or i.v. solutions) are related to the existence of possible additional structures. Innovations such as admixture of amphiphilic or lipophilic drugs or incorporation of new fat components are new challenges to the developer, since emulsion structure and stability in these cases cannot necessarily be compared with conventional emulsions [Hamilton et al., 1996].

In this thesis, an elucidation of the structure of egg lecithin-stabilised fat emulsions is presented. The following questions define the objectives of this work:

1. Which structures occur within parenteral fat emulsions ?
2. Which changes occur during autoclaving ?
3. Does excess lecithin influence the structure and stability of the emulsions ?
4. How best to determine and control the amount of excess lecithin ?

To these ends ^{31}*P-Nuclear Magnetic Resonance Spectroscopy, X-ray analysis, Freeze-Fracture- and Cryo-Transmission Electron Microscopy* were used together with *Fourier-Transform-Infrared-Spectroscopy* and *Differential Scanning Calorimetry* to characterise various emulsifier compositions as well as emulsions and separated phases. *Asymmetrical Flow Field-Flow Fractionation* helped to separate the systems and elucidate structure of liposome dispersions and model emulsions. To examine their physical stability, particle sizing using

Photon Correlation Spectroscopy, *Laser Diffractometry with and without PIDS* and other techniques were used and judged regarding their advantages and disadvantages. *Chromatographic analyses* of the emulsifier composition together with *Zeta Potential Measurements* were used to follow chemical stability and its impact on the physical properties of the emulsions. The addition of minor components and their effect on interfacial properties using droplet/interface coalescence kinetics was investigated. Furthermore, emulsions of known properties were creamed and resuspended in different aqueous media to examine the influence of the latter on the stability of the dispersions.

Chapter 2 - Materials and Methods

2.1 Materials

2.1.1 Emulsifiers

Proprietary name	Supplier	Lot	Composition
Lipoid E75®	Lipoid KG, Ludwigshafen, Germany	193123-1	72.6% PC, 13.5% PE, 2.6% LPC, 2.3% SPM
Lipoid E80®	Lipoid KG, Ludwigshafen, Germany	19890-8	77.7% PC, 7.8% PE, 2.5% LPC, 3.0% SPM
Lipoid EPC®	Lipoid KG, Ludwigshafen, Germany	T 12085-1	98.0% PC, < 0.2% LPC
Lipoid ELPC®	Lipoid KG, Ludwigshafen, Germany	T 22014	0.3% PC, 99.0% LPC
LPC (1-Palmitoyl-LPC)	Avanti Polar Lipids, Alabaster, AL,USA	(used for ^{31}P-NMR experiments)	> 99 % LPC
Egg-Phosphatidyl-ethanolamine Type III P7943	Sigma Chemicals GmbH, Deisenhofen, Germany	0016H8359	> 99 % PE
Egg-Lysophospha-tidylcholine Type I L4129	Sigma Chemicals GmbH, Deisenhofen, Germany	0085H8365	> 99% LPC
DPPC	Lipoid KG, Ludwigshafen, Germany	n.a.	Di-Palmitoyl-PC
Lutrol (Pluronic) F 68®	BASF AG, Ludwigshafen, Germany	52-0791	Poloxamer 188
Texapon K 12®-96C	Henkel KGaA, Duesseldorf, Germany	63182	Sodium lauryl-sulphate
Sodium Oleate	Aldrich Chemicals, Deisenhofen, Germany	Q631-96	≥ 98% Sodium cis-9-Octadecenoate

(PC = phosphatidylcholine; PE = phosphatidylethanolamine; LPC = lyso-PC; SPM = sphingomyelin)

All lecithins and sodium oleate were stored under N_2 and at -20°C. Pluronic® and Texapon® were stored tightly closed at room temperature. Composition is given according to the manufacturer's declaration.

2.1.2 Oils and waxes

Proprietary name	Supplier	Lot	Composition
Soybean Oil S7381	Sigma Chemicals GmbH, Deisenhofen, Germany	003H1127	(Complied with USP and BP requirements)
Paraffin viscous, USP, Ph.Eur.	Merck KGaA, Darmstadt, Germany	9026K214-09460_516	$\eta_{dyn}^{20°C}$: 110-230 mPas
Paraffin liquid, USP, Ph.Eur.	BP Oiltech, Hamburg, Germany	Enerpar M002	$\eta_{dyn}^{20°C}$: 26.2 mPas
Cutina CP®	Henkel KgaA, Duesseldorf, Germany	50635310/410	Hexadecanoic acid hexadecyl ester

Soybean oil was stored away from light under N_2 at room temperature. Cutina® and paraffins were stored tightly closed at room temperature. Composition is given according to the manufacturer's declaration.

2.1.3 Additives

Proprietary name	Supplier	Lot	Composition
Glycerol, Ph.Eur.	Carl Roth GmbH&Co, Karlsruhe, Germany	35420112	Glycerol, double-distilled, 98%
Sodium hydroxide purum, p.a. grade	Fluka Chemie AG, Deisenhofen, Germany	347308/1 396	> 98% NaOH
Palmitic acid	Sigma Chemicals GmbH, Deisenhofen, Germany	n.a.	≥ 99% Hexadecanoic acid
Oleic acid O3879	Sigma Chemicals GmbH, Deisenhofen, Germany	0038F8468	Ca. 99% Cis-9-Octadecenoic acid

Fatty acids were stored under N_2 at -20°C. Glycerol was stored tightly closed under N_2 at room temperature. Sodium hydroxide was stored tightly closed; solutions were prepared freshly and stored at room temperature. Composition is given according to the manufacturer's declaration.

2.1.4 Parenteral Fat Emulsions

Proprietary name	Supplier	Lot	Expiry
Intralipid® 10 / 20 / 30	Pharmacia&Upjohn GmbH, Erlangen, Germany	68460-51 & 87535-51 **(10%)** 70178-51 & 85375-51 **(20%)** 88555-71 & 87537-51 **(30%)**	3/97 & 1/99 **(10%)** 5/97 & 8/98 **(20%)** 3/99 & 1/99 **(30%)**
Lipofundin® 10% N / 20% N	B.Braun Melsungen AG, Melsungen, Germany	5471A81 **(10%)** 6071A81 **(20%)**	10/97 **(10%)** 1/98 **(20%)**
Lipofundin MCT® (aka Medialipide®, Vasolipid®) 10% / 20 %	B.Braun Melsungen AG, Melsungen, Germany	6023A81 **(10%)** 6031A81 **(20%)**	12/97 **(10%)** 12/97 **(20%)**
Lipovenoes® LCT 10 PLR / 20	Fresenius AG, Bad Homburg v.d.H., Germany	FG 1013P **(10%PLR)** FK 1005 **(20%)**	1/97 **(10%PLR)** 10/97 **(20%)**

Original emulsion bottles were stored away from light at room temperature.

2.1.5 Reagents

Proprietary name	Supplier	Lot	Composition
Copper sulphate, anhydrous	Fluka Chemie AG, Deisenhofen, Germany	n.a.	$CuSO_4$
Potassium chloride, extra pure	Merck KGaA, Darmstadt, Germany	023 TA 839135	KCl
Sulphuric acid, purum p.a. grade	Fluka Chemie AG, Deisenhofen, Germany	3523 90/1 1295	95-97% H_2SO_4
Phosphoric acid, extra pure	Merck KGaA, Darmstadt, Germany	810 K040 186 63	85% ortho-H_3PO_4-solution
Hydrochloric acid, purum p.a. grade	Fluka Chemie AG, Deisenhofen, Germany	3585 33/1 34596	37% HCl-solution

2.1.6 Solvents

Proprietary name	Supplier	Lot	Composition
2-Propanol, gradient grade (LiChrosolv®)	Merck KgaA, Darmstadt, Germany	I 732340 723	≥ 99.8% 2-Propanol
n-Hexane, HPLC grade (LiChrosolv®)	Merck KGaA, Darmstadt, Germany	I 757591 740	≥ 97% n-Hexane
Water for HPLC	-	Freshly prepared in a Destamat Bi 18 T, (Heraeus, Germany)	Double-distilled water 0.22 µm-vacuum-filtered
Glycerol/Water for Particle Sizing Dilution	-	Kept in stock after autoclaving	2.25% (w/w) Glycerol/Water 0.22µm-filtered
Water for Langmuir Film Balance	-	Freshly prepared in a Seralpur DELTA UV, (Seral, Germany)	Ultra-pure water 0.2 µm-filtered (Supor DCF filter)
Methanol, p.a. ACS grade (Rotipuran®)	Carl Roth GmbH&Co, Karlsruhe, Germany	21731794	≥ 99.8% Methanol
Chloroform, p.a. (Rotipuran®)	Carl Roth GmbH&Co, Karlsruhe, Germany	20730746	≥ 99% Trichloromethane
Chloroform, spectroscopy grade (Uvasol®)	Merck KGaA, Darmstadt, Germany	I 375547	≥ 98% purity, 0.0005% residue on evaporation
Ammonia solution, extra pure	Merck KGaA, Darmstadt, Germany	B826826607	32% NH_3-solution

2.2 Methods

2.2.1 Investigation of Emulsifying Properties

2.2.1.1 Measurement of Droplet Coalescence Times with Coalescence Cell

A droplet-to-planar-surface coalescence model was used to study survival times of oil droplets released to coalesce at a soybean oil-water interface as a function of addition of phospholipids. The coalescence cell consisted of a double-walled glass apparatus connected to a Haake FE 2 thermostatting device (Fig. 12). A micrometer-controlled CR-700-200 type Hamilton® syringe equipped with a customised, curved needle (end-to-end length: 10 cm, ∅: 0.4 mm) with repeated-action function was fitted through an acrylic glass lid, which covered the cell and also kept the syringe fixed in position. To adapt droplet ejection speed to the viscosity of the oil phase, a different spring was used in the syringe. Thus, for each ejection oil was drawn from the upper phase and released, yielding uniform, single droplets of 20 µl. Before each experiment the syringe and the glass apparatus were thoroughly rinsed with 2-propanol, double-distilled water followed by sulfurochromic acid and again double-distilled water. The oil-phase (10 g soya oil) containing the emulsifier was layered on the water phase (90 g) and 100 droplets counted. Each experiment was repeated at least once.

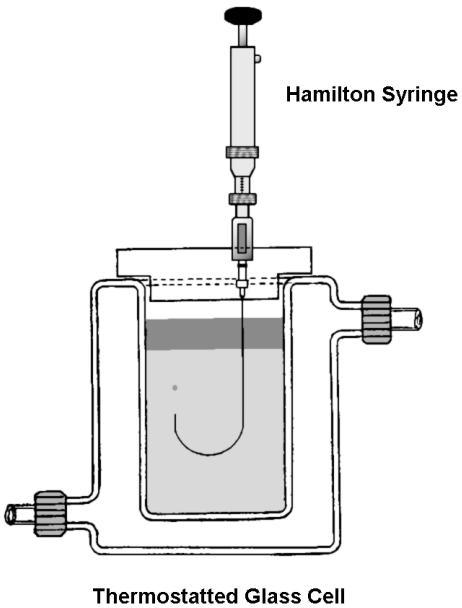

Fig. 12 Thermostatted coalescence cell equipped with a repeated-action Hamilton® syringe

2.2.1.2 Determination of Emulsifier Film Compressibility with Langmuir Film Balance

Recording of film pressure-molecular area (π-A) isotherms was carried out with an FW-2 type Langmuir film balance (Lauda GmbH&Co KG, Lauda-Koenigshofen, Germany) connected to a thermostatting bath (RC20CP, Lauda GmbH&Co KG) which allowed measurements at 0°C - 55°C ± 0.1°C. Fig. 13 shows the principle of film pressure measurement by a Langmuir film balance of insoluble films from amphiphilic molecules at the air-liquid interface.

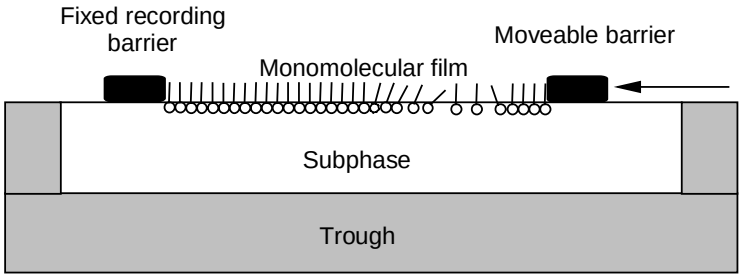

Fig. 13 Principle of film pressure measurement with a Langmuir film balance

Monomolecular Langmuir-Blodgett films of amphiphilic compounds at air-water interfaces, are prepared by dissolving the amphiphile into a suitable solvent which by rapid evaporation leaves a two-dimensional film of the amphiphile when the solution is spread across the surface of a second liquid, which must be immiscible with the solution. Typical solvents used for preparation of such films are e.g. hexane or chloroform [Gaines, 1966], which are also suitable for the case of lecithin. Solvents should be of high purity, since any remnants after evaporation capable of film-formation would lead to erroneous results. Best results were found for 2 mM chloroformic solutions, which were spread at various points of the subphase and allowed to evaporate. Film pressure-area dependence can be measured with either a Langmuir film balance or a Wilhelmy-plate [Gaines, 1966]. Both methods use either Teflon or glass troughs containing the subphase, a moveable barrier which allows compression (or expansion) of the film floating on top of the subphase, and an assembly to record the forces transduced by the film [Shaw, 1983 / Ulman, 1991]. In the case of the Langmuir film balance used in this study, a fixed barrier float is employed to continuously record the film pressure π [mN/m] of the monolayer against the barrier when being compressed by the moveable barrier.

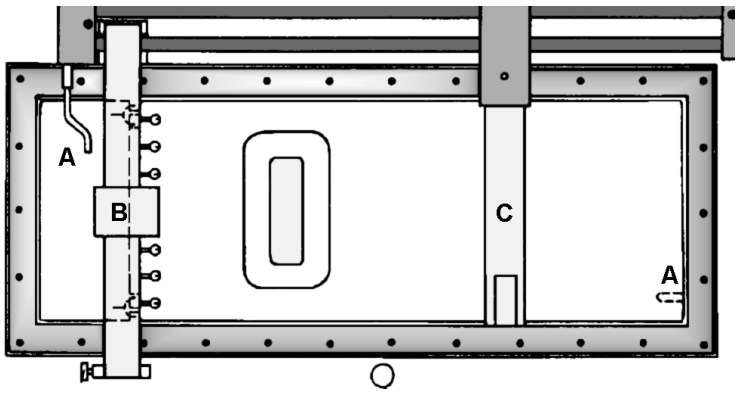

Fig. 14 Top view of the FW-2 Langmuir film balance: Temperature sensors **(A)**, recording barrier float attached to force transducer bridge **(B)** and moveable barrier **(C)**

Calibration of area and pressure was carried out automatically by the film balance before each measurement. Monolayers were spread on the cleaned subphase consisting of high-purity water (see Materials), which was verified by measurement of two consecutive zero-isotherms before each run. Each measurement was carried out in triplicate using 25 µl of solution metered by a Hamilton syringe. Before starting compression, chloroform was allowed to evaporate for 10 min. The complete isotherm measurement was preset to take 40 min in order to allow careful compression of the film (approx. 225 mm^2/min). At the end of each measurement the compressed film was drawn from the surface by means of six aspiration nozzles located at the fixed barrier and connected to a vacuum pump, and highly purified water was refilled from behind the moveable barrier.

2.2.2 Preparation of Emulsions, Solid Lipid Nanoparticles (SLN) and Liposomes

For preparation of pre-emulsions, phospholipid pre-dispersions and solutions two JKAMAG RET type magnetic stirrers/heaters were employed equipped with a JKA-TRON® ETS-D thermostatting control unit (JKA, Staufen, Germany) to maintain preset temperature values. Stirring speed was approx. 700 rpm. Unless stated otherwise, lecithin was dispersed, or Pluronic® or sodium oleate were dissolved in double-distilled water which had been heated to 60°C, then glycerol was added. Subsequently, in the case of emulsions and SLNs, the oil or melted wax heated to 60°C was slowly incorporated into the lecithin dispersion. After about 15 min of stirring, the final weight was adjusted with double-distilled water. A typical emulsion formulation consisted of:

1)	Oil phase (e.g. soya oil)		5 / 10 / 20 or 30 g
2)	Emulsifier (e.g. lecithin)		0.6 or 1.2 g
3)	Sodium oleate		0.03 g (only where indicated)
4)	Glycerol		2.25 g
5)	Double-distilled water	to	100.0 g

Liposomal dispersions were of the same formulation by omitting addition of the oil.

2.2.2.1 Customised Evacuable Ultra-Turrax® Mixer

Increase in state of dispersion of the pre-emulsions or liposome dispersions was achieved using a customised high-speed stirrer. An JKA Ultra-Turrax® TP 18/10 stirrer with an 18K type vacuum homogenising rotor coupled to a Thyristor JKA TR50 for speed control (JKA, Staufen, Germany) was fitted into an evacuable steel jacket with a glass window for visual control (Fig. 15). Approx. 5000 rpm was applied for approx. 5 min to homogenise the samples in a glass beaker placed inside the jacket. High-speed stirring always leads to incorporation of air bubbles which deplete the emulsion of emulsifier and, furthermore, necessitates additional nitrogen flushing to prevent fast oxidation of unsaturated components by incorporated oxygen. By evacuating the jacket by a RD-2 Vacuubrand® vacuum pump (R. Brand, Wertheim, Germany) to approx. $3 \cdot 10^{-2}$ mbar, incorporation of gas during stirring could be avoided. Additionally, rise in temperature owing to vigorous stirring was also counteracted.

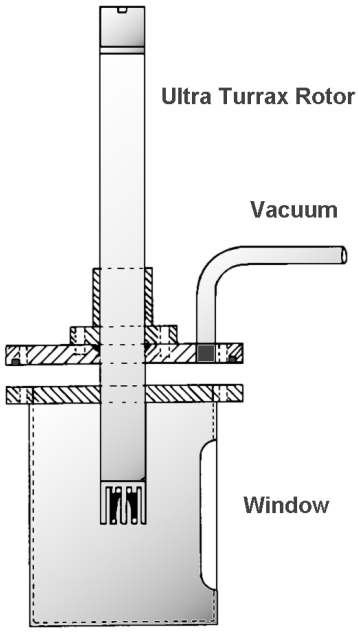

Fig. 15 Evacuable Ultra-Turrax® high-speed stirrer

2.2.2.2 High-Pressure Homogenisation by Microfluidizer®

For production of fine emulsions, a Microfluidizer® 110S high-pressure homogeniser (Microfluidics International Corp., MA-Newton, USA) was used, similar to those already described by Washington and Davis [1988], Lidgate et al. [1989] and Chaturvedi et al. [1992]. A preset pressure of up to 5 bar (≅ 75 psi) is amplified via a hydraulic assembly by a factor of 243 up to 1200 bar (≅ 18000 psi) hydrostatic pressure in the fluid circuit. The disruption of the samples is a result of the characteristic flow profiles of partitioned fluid streams that are reunited under high pressure and speed in the so-called 'interaction chamber'. The disperse phase is disrupted by the high turbulence, shear and cavitation action occurring there [Schubert, 1997]. The dispersity obtained is directly dependent on flow velocity and thus homogenisation pressure applied. The homogeniser allows recycling of the samples for repeated dispersing action. To prevent excess heating of the sample during homogenisation, the liquid was driven through a heat exchange coil immersed in an ice bath, before re-entering the interaction chamber. Sample temperatures were thus maintained at about 30°C. No backpressure chamber (auxiliary processing module) was used with this model, as has been described elsewhere [Lidgate et al., 1989]. Nevertheless, dispersing results were reproducible and similar to those already reported. Fig. 16 shows a cross-section of the dispersion zone of the Microfluidizer 110S®. As recommended for processing of low viscosity samples [Microfluidics International Corp., 1996], the 'F12Y' type interaction chamber, which possesses a flow channel with a diameter of 75 µm at the narrowest site, was used. The chamber was made of an aluminium oxide type ceramic, which showed no abrasion throughout the experiments.

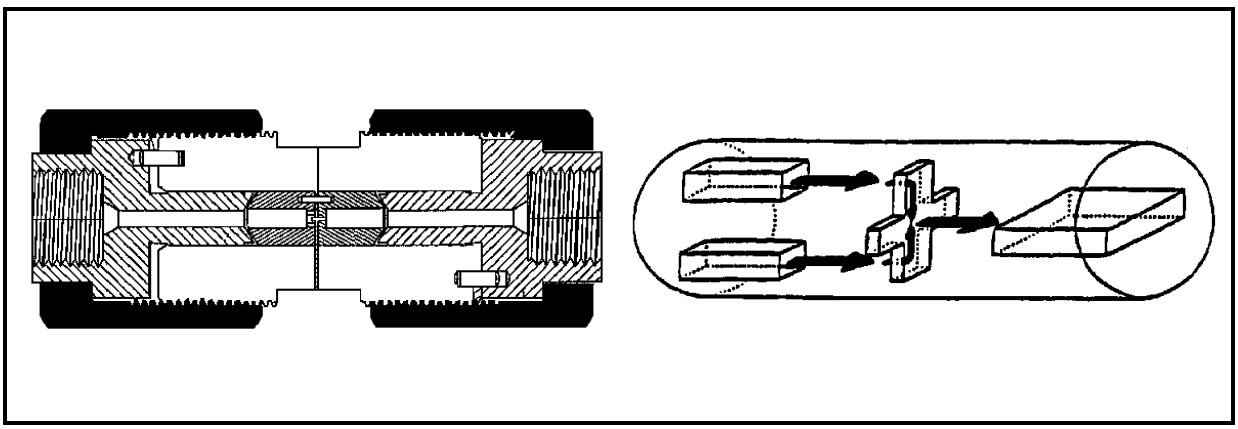

Fig. 16 Schematic cross-section through the dispersion zone of the Microfluidizer®, the so-called interaction chamber **(left)** and enlarged view of the liquid jet flow through the dissipation zone in the centre area of the interaction chamber **(right)**

This apparatus has been especially designed for lab-scale homogenisation with a total volume

of only 12 ml and a dead volume of only about 1 ml required for operation. Thus, small batches could easily be produced, as well as larger volumes by simply refilling crude emulsion in the reservoir and gathering the homogenised product at the outlet without recycling. For the experiments carried out here, it proved to be particularly useful not to use the continuous 'recycling' mode, as in that case only a proportion of about 6 ml per 'cycle' were processed through the 'interaction chamber' at once, and some unemulsified droplets and foam were still found floating on top of the liquid level, which never could be cycled through the dissipation zone, when the homogenised product was recycled to the product reservoir. By processing the whole batch once through the machine, a 'true' homogenisation cycle was carried out and no crude, unemulsified remainders were found after homogenisation.

Production of liposomes was achieved accordingly from the aqueous lecithin pre-dispersions. As Mayhew et al. [1984] reported, thus almost exclusively SUVs could be produced, which could be verified by Cryo-TEM investigations (see Chapter 3).

For production of SLNs from waxy materials (e.g. cetylpalmitate), the cooling coil was immersed in a heated, thermostatted water bath to allow operation above the melting point of the wax (approx. 54°C). After the final cycle, the product was collected in a beaker located directly in an ice bath and kept stirred for another 30 min to let the wax droplets solidify. The use of an additional in-line auxiliary processing module to achieve better dispersion results does not yield improved performance for low-viscosity O/W-emulsions [Broesel et al., 1998].

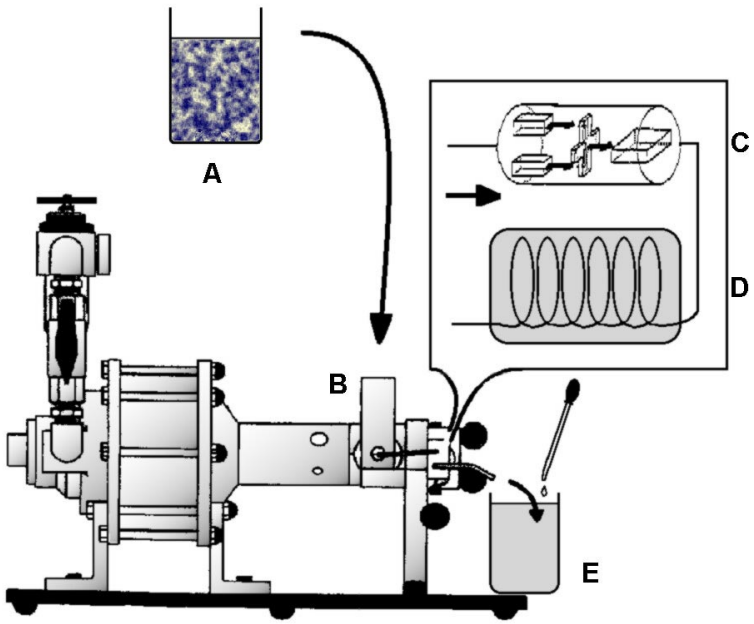

Fig. 17 Schematic drawing of the homogenisation process using the Microfluidizer 110S®

As illustrated in Fig. 17, the crude dispersions (A) were filled into the reservoir (B) and cycled through the dissipation zone (C), cooled or heated, respectively, by passing the heat exchange coil (D) and then collected at the outlet (E) to be refilled in the reservoir and recycled. After the final cycle, the pH of the aqueous phase was adjusted with 0.01 N sodium hydroxide solution to the desired value.

2.2.2.3 Sterilisation by Autoclaving

Samples were autoclaved in a Getinge GE 666 EC-1 (Getinge AB, Getinge, Sweden) autoclave with a LAB100 control unit using a fixed ramp heating and cooling program. Sterilisation conditions were recorded by a plotter and it was thus possible to verify that pharmacopeial requirements (121°C, 2 bar) were maintained for the selected treatment time. Cooling of the samples to 80°C was achieved after some 15 minutes and subsequently accelerated in iced water while being shaken.

2.2.3 Measurement of Particle Size

No single particle-sizing method can be capable of describing the complete particle size distribution of such complex submicron systems like the emulsions under examination here. Several methods were, therefore, used here, which however measure different properties of the dispersed particles to deduce their 'size', making the results obtained difficult to compare [Groves, 1984]. For more detailed descriptions of the methods applied, the reader is referred to Allen [1990].

2.2.3.1 Photon-Correlation Spectroscopy (PCS)

PCS covers the size range of about 5 nm - 3 µm and has, therefore, extensively been used for particle size analysis of submicron emulsions [Komatsu et al., 1995]. It has also been proposed for inclusion in a new monograph 'Globule Size Distribution in Intravenous Emulsions' for the next issue of the USP in the Pharmacopeial Forum [Ph.Forum, 1994].

Fluctuations of laser beam scattering intensity $I(t)$ from suspended particles in motion are detected and the auto-correlation function $G(\tau)$ calculated for the sampling interval (τ) [Allen, 1990].

$$G(\tau) = I(t) \cdot I(t+\tau)$$

Eq. 5 Measured auto-correlation function $G(\tau)$

Comparison of $G(\tau)$ with its theoretical behaviour, $g(\tau)$, enables calculation of the particles' diffusion coefficient *(D)*:

$$g(\tau) = e^{-2DK^2\tau}$$

Eq. 6 Fitted auto-correlation function $g(\tau)$
(K = scattering vector)

According to Eq. 6 and Eq. 7, a faster decay of the auto-correlation function is therefore observed for smaller particles. The diameter of the dispersed particles *(d)* can then be computed (assuming spherical particles) using the Stokes-Einstein equation [Weiner, 1984]:

$$d = \frac{k \cdot T}{3 \cdot \pi \cdot \eta \cdot D}$$

Eq. 7 The Stokes-Einstein equation

with k, the Boltzmann constant, absolute temperature T and the dynamic viscosity of the medium, η. The interference of the auto-correlation functions caused by polydispersity can be deconvoluted by cumulants analysis:

$$\frac{1}{2}\ln g(\tau) = a_0 + a_1\tau + a_2\tau^2 + a_3\tau^3 + \ldots$$

Eq. 8 The Cumulant-Fit method

a_0 yields an intensity-weighted mean diameter, the so-called '*z-average diameter*', and $a_1\tau$ gives the '*Polydispersity index*' *(PI)* which is an expression of the width of the particle size distribution, ranging between 0 (uniform) and 1 [Allen, 1990 / Mueller, 1991].

The analyses were carried out on a Malvern Autosizer-LoC with a 5 mW Diode-Laser emitting a wavelength of 670 nm and detection under a fixed angle of 90° coupled to a 7032 Multi-8 Correlator (Malvern, Herrenberg, Germany). The correlograms were evaluated using PCS for Windows V1.27 original software by Malvern. Each sample was recorded 5 times using 10 sub-run measurements at 20°C. Auto mode and cumulant analysis were used by default. To avoid multiple scattering effects, a maximum of 50-100 Kcounts/s was adjusted by dilution of the samples with sterilised and 0.22 µm-filtered glycerol/water (2.25 wt%). Liposomal dispersions could be measured in the undiluted state.

2.2.3.2 Laser Diffractometry (LD)

The 'Mie parameter' *(α)* relates the particle size *(r)* and the wavelength *(λ)* of the scattered light from dispersed particles:

$$\alpha = \frac{2 \cdot \pi \cdot r}{\lambda}$$

Eq. 9 The Mie parameter *(α)*

For $\alpha < 0.1$ (as for small particles), the *Rayleigh* approximation holds, where scattered light intensity *(I)* is found to be proportional to the sixth power of the particle diameter *(d)*. For $\alpha > 0.5$, the *Mie scattering theory* applies, and $I \sim d^2$ [Allen, 1990]. Furthermore, the angle of scattered incident light is inversely proportional to particle size. The scattered light intensity measured at defined angles can therefore be related to the particle size. *Fraunhofer theory* is frequently employed in conventional Laser Diffractometry and simplifies Mie scattering behaviour by assuming spherical particles larger than the wavelength of the incident beam ($d \geq 4\lambda$). It disregards the particles' optical properties, most importantly refractive index. If the refractive index is known, more complex calculations according to the Mie theory encompass scattering and absorption effects of particles smaller than the wavelength used (d about $\lambda/6$) [Plantz, 1984]. Modern Laser Diffractometers can size particles from approx. 100 nm – 2000 µm in size using either Mie or Fraunhofer calculation. The former allows sizing of smaller particle classes, but requires knowledge of refractive index of the dispersed phase, which in the case of phospholipid-stabilised emulsions can only be approximated. The latter is more sensitive to larger particles [Lucks, 1993 / Kohlrausch and Steffens, 1997].

A Coulter LS 230 (Coulter Electronics, Krefeld, Germany) equipped with PIDS technique and running in Mie mode was used, as well as a Malvern Mastersizer Micro (Malvern, Herrenberg, Germany) running in Fraunhofer mode. 100 µl of the emulsion samples were diluted into approximately 120 ml glycerol/water (2.25% v/v). As with PCS, higher concentrations of liposomal dispersions had to be used to achieve similar scattering intensities (about 4 ml into 120 ml). The Coulter LS 230 uses a laser of 750 nm and a double Fourier lens setup for focussing the scattered light on the ring-shaped detector setup (Fig 18). The detection range (angles) for diffraction is claimed to be 40 nm - 2000 µm, thus theoretically covering the size range expected here. The detector segments are arranged in three main areas: a low-angle detector (L) with 62 detector elements, mid- (M) and high-angle (H) detector comprised of 32 elements each, allowing high-resolution of a wide particle size range.

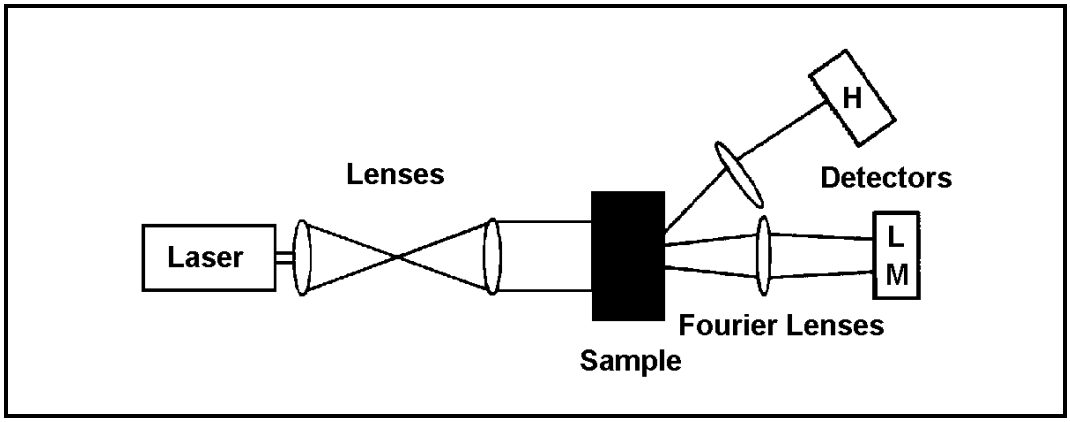

Fig. 18 Assembly of the Coulter LS230 Laser Diffractometer
(adapted from Schoofs [1990])

The PIDS-technique (*Polarisation Intensity Differential Scattering*) is used in-line with the conventional LD sample cell. Horizontally or vertically polarised light of three different wavelengths (generated by a filter wheel) is scattered by the sample and recorded at six different angles (Fig. 19). PIDS is claimed to be especially sensitive for scattering caused by the smallest particles and intended for additional submicron size analysis [Bott and Hart, 1991]. Using the Mie theory for evaluating both LD and PIDS scattering data, particle sizes for liposomes and oil droplets should be resolvable from a single sample measurement.

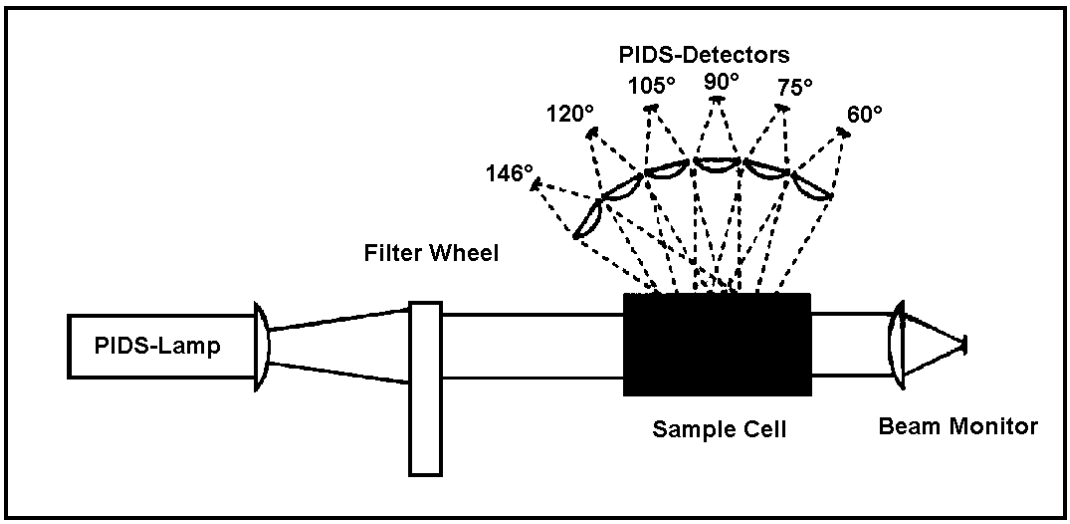

Fig. 19 Schematic drawing of the PIDS-cell of the Coulter LS230
(adapted from Bott and Hart [1990])

2.2.3.3 Asymmetrical Flow Field-Flow Fractionation (AFFF)

FFF is a separation method similar to liquid chromatography, but with no stationary phase in the separation channel (Fig. 20). A force field perpendicular to the channel flow concentrates the sample components in the direction of the lower accumulation wall according to their size. Asymmetrical Flow FFF uses hydrodynamic flow as the separating force, with diffusion back into the channel acting as a counter force. When both are balanced, particles are retained at a defined height in the channel according to their size: larger particles accumulate in thin, compressed layers at the walls (*Y* in Fig. 20) and smaller particles are gathered in thick, diffuse layers towards the centre of the channel (*X* in Fig. 20). In the parabolic flow profile between the channel walls, the sample components closer to the accumulation wall are transported slower than those higher up in the channel, causing smaller components to elute first. The lower channel wall is made of a frit covered with an ultrafiltration membrane, which is impermeable for the sample. The channel flow divides into one part eluting at the outlet to the detector and one part exiting as cross flow. The ratio between both flows is controllable by adjusting the back pressure on the outlets. Thus, AFFF allows high resolution separation of the sample components according to hydrodynamic radius and, accordingly, particle sizing is possible [Giddings, 1993].

A light scattering detector was used to determine on-line radii of the eluted fractions. Light scattering intensity was measured at 18 angles simultaneously as a function of time. From the angular dependence of scattering intensity the mean square radius can be calculated from first principles, if the Rayleigh-Debye-Gans approximation holds [Wyatt, 1993]. This has been assumed in all calculations and is justified by the scattering properties of both, liposomes and emulsions [van Zanten et al., 1991]. A UV detector was also used, but gives a complicated mix of absorption and scattering effects, which makes it highly non-linear to concentration. Sizes can be calculated without any concentration information from light scattering alone, and knowing the size and the refractive index increment, also concentration can be calculated from the response of the light scattering detector [Wyatt Technology, 1998].

The experiments were carried out on an AFFF channel as described by Tank and Antonietti [1996], equipped with an ultrafiltration membrane (10k cutoff, Hoechst AG, Frankfurt, Germany) and coupled to a DAWN® laser light scattering detector (Wyatt Technology Corp., Santa Barbara, USA) and a Hewlett Packard 1100 UV detector (Hewlett Packard, USA). Samples were eluted in water containing 50 mM $NaNO_3$.

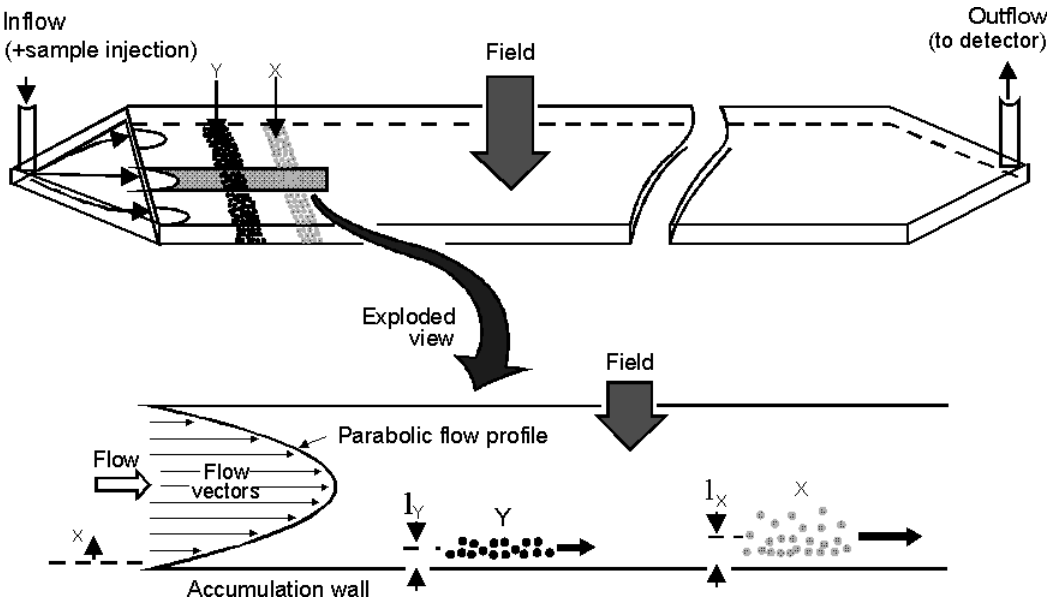

Fig. 20 Principle of separation in a Flow FFF channel

2.2.4 Structural Analysis

2.2.4.1 Centrifugation

High-speed centrifugation was performed on a Centrikon T-42K thermostatted centrifuge (Kontron Instruments, Neufahrn, Germany). Samples were pipetted into Beckman polyallomer tubes (No. 331374) and centrifuged using either an A-20 C type fixed-angle rotor at 19000 rpm (= approx. 33000 g) or a O-61 BC type swing-out-bucket rotor with a customised adapter to fit the tubes in the sample holders at 9000 rpm (= approx. 13000 g). Sample temperature was preset to 10°C and usually increased by about 4 - 5°C during centrifugation.

Ultracentrifugation was carried out on a Beckman model L centrifuge using either a 50 Ti fixed-angle rotor at 40000 rpm (= approx. 160000 g) or a SW 40 Ti swing-out rotor at 39000 rpm (= approx. 275000 g) and Beckman polyallomer tubes. Centrifugation temperature was also preset to 10°C, but in this case rose to about 20°C during centrifugation.

The polyallomer tubes were pricked with a syringe needle at the bottom of the tube to collect the subnatant (aqueous phase). Creamed oil phase and pelleted material could then be collected without further washing steps [Groves et al., 1985 / Férézou et al., 1994].

2.2.4.2 Freeze-Fracture Transmission Electron Microscopy (FF-TEM)

TEM can be used for the direct examination of particles in the size range 1 nm – 5 µm [Allen, 1990]. Thermal degradation or induced thermotropic phase transitions caused by the electron beam prevents, however, examination of samples containing lipids directly. The 'slush technique' was therefore used here. Samples were sandwiched between two gold platelets and cast into melting N_2 (-210°C) prepared by evacuating liquid N_2 with a vacuum-pump. Specimen vitrification with a cooling rate of 10^4-10^5 K/s was thereby achieved. Subsequently, the frozen samples were transferred into the Freeze-Fracture/Etching recipient (BAF 400 D, Balzers AG, Wiesbaden, Germany) under liquid N_2 of -150°C using a special sampler holder. The samples were fractured at exactly -100°C under a vacuum of $<10^{-6}$ mbar and subsequently shadowed with a 2 nm Pt layer (99.99% purity) at an angle of 45°. A final layer of pure carbon (20 nm) was added at 90°. Layer thickness was controlled by a swinging quartz assembly (QSG, Balzers AG, Wiesbaden, Germany). The replica were rinsed with chloroform:methanol (1:1 v/v), then with double-distilled water and transferred onto copper grids (400 mesh, Plano GmbH, Wetzlar, Germany). Finally, replica specimen were examined on a JEOL 100CX Transmission Electron Microscope using 80 kV acceleration voltage.

2.2.4.3 Cryo-Transmission Electron Microscopy (Cryo-TEM)

This technique was developed and first introduced to allow visualisation and examination of liposomal dispersions and proved to be particularly useful for determination of size and lamellarity of these [Nattermann Phospholipid GmbH, 1995]. Clear advantages of this technique over other TEM techniques is, that native, untreated systems can be examined, thus lowering the risk of producing any artifacts, and furthermore, clear discernment between SUVs and small emulsified oil droplets was possible, which could not be achieved e.g. by FF-TEM [Westesen and Wehler, 1992].

Copper grids (200 mesh, Science Services, Munich, Germany) were coated with a porous film (Triafol BN, Merck KGaA, Darmstadt, Germany) and subsequently vapour-deposited with carbon. The Triafol film was removed by washing the grids with ethylacetate to obtain a pure porous film of carbon. The size of the holes, varying between 2 and 12 µm, depended on the preparation conditions. For specimen preparation, a drop of the sample (which was pre-diluted with glycerol-water or double-distilled water, alternatively by 1:11 v/v) was put on the untreated coated grid. Most of the liquid was subsequently removed by means of blotting paper, leaving a thin film stretched over the holes. The best hole coverage could be achieved using a hydrophobic film surface. The specimens were then vitrified by plunging them into liquid ethane cooled to 90 K in a temperature-controlled freezing unit using liquid N_2 (Zeiss,

Oberkochen, Germany). Excess ethane was removed from the specimen using blotting paper. Subsequently, the specimen were transferred into a cryo-transfer holder and inserted into a Zeiss CEM 902 transmission-electron-microscope equipped with a cryo-stage. Examinations were carried out at a constant temperature of 90 K using an acceleration voltage of 80 kV and 12 µA beam current. A condensor diaphragm of 100 µm and an objective entrance aperture of 17 mrad was employed. Zero-loss filtered images (DE = 0 eV) were taken under low-dose conditions using the minimal dose focusing device to avoid excess heating of the focussed areas.

2.2.4.4 Polarised-Light Microscopy (PLM)

An Olympus IMT-2 microscope (Olympus Optical Co. Ltd., Tokyo, Japan) equipped with a photographic camera and crossed polarisers ($\lambda/4$ plates where indicated) was used. Lamellar phases exhibited typical anisotropic patterns and could thus be discerned from hexagonal or cubic phases which appear to be optically isotropic. Visual control of droplet sizes > 5 µm was also performed on this microscope.

2.2.4.5 X-Ray Diffraction Analysis

Wide-angle X-ray Diffraction (WAXD) examination of samples was performed on an X'Pert X-ray diffractometer (Philips, Kassel, Germany). The samples were equilibrated for 30 min at the respective temperatures before data collection and were analysed under N_2 purging. Thermostatting was achieved from 0°C - 90°C. 40 kV acceleration voltage and 40 mA current for generation of Cu-k_α radiation with $\lambda = 0.15419$ nm (Ni-filtered) were used for recording diffraction patterns.

2.2.4.6 ^{31}P-Nuclear Magnetic Resonance Spectroscopy (^{31}P-NMR)

With ^{31}P-NMR it is possible to follow changes in motional properties of phospholipid molecules in membranes and lipid vesicles and gain information on the state of order in those systems, e.g. which phases (lamellar, micellar, hexagonal etc.) are exhibited [Cullis and DeKruijff, 1978 / Seelig, 1978]. This is possible since the differences in the spectra obtained originate from the gel or liquid-crystalline like behaviour of the lipids, which means more or less restricted '*anisotropic*' motion due to the partially ordered structures taken within their aqueous dispersions. Commonly, '*isotropic*' motion is understood to take a molecule over all directions in space with equal probability and is defined by a *single* characteristic rotational time, whereas with '*anisotropic*' motion rotation about some molecular axes occurs at

different rates, so that at least *two* characteristic rotational times must be used to characterise a molecule's motion completely [Chan et al., 1981]. For non-bilayer arrangements (hexagonal phases, micelles etc.) additional motional averaging mechanisms lead to increased 'isotropic' movement, whereas typically, extended lamellar phases have been found to cause 'anisotropic' signals due to restricted motion in the bilayer plane [Cullis and De Kruijff, 1978]. One has to consider, however, that 'motion' as detectable by NMR encompasses motion within a molecule (e.g. trans-gauche rotations), motion of the molecule itself or even motion of larger molecular arrangements (e.g. tumbling of bilayer fragments or sheets). Due to overlayering of these effects, as a result, motional 'averaging' of the shift anisotropy might occur, leading to less information from the resulting spectra. However, ^{31}P-NMR has been widely used in examination of biomembranes and model membranes (liposomes) and can be reviewed in more detail e.g. in Chapman [1975], Seelig [1978] and Chan et al. [1981].

A Varian Unity 300 spectrometer was used in the Fourier transform mode. Unless otherwise stated, the sample temperature was controlled to 25±0.5°C with a standard variable temperature control unit. In all cases of multi-temperature measurements the alterations in the NMR spectra were reversible upon recooling of the specimen. All chemical shift values are reported in parts per million (ppm) from pure LPC micelles (0 ppm), positive values referring to low-field shifts. All spectra were obtained in the presence of a gated broad-band decoupling (10 W input power during acquisition) and accumulated free induction decays were obtained from 1200 transients. In some cases, and in order to improve signal to noise ratio, higher transient numbers were used, which are given in the respective spectra. A spectral width of 25 kHz, a memory of 16000 data points, 1.3 s interpulse time and a 90° radio frequency pulse were used. Prior to Fourier transformation, an exponential multiplication was applied resulting in a 100 Hz line broadening. The residual chemical shift anisotropy, $\Delta\sigma$, was measured as 3 times the chemical shift difference between the high-field peak and the position of isotropically moving lipid molecules at 0 ppm.

2.2.4.7 Fourier-Transform Infrared-Spectroscopy (FT-IR)

Fourier-Transform Infrared-Spectroscopy allows evaluation of infrared spectra with far better resolution and signal-to-noise ratio than with conventional spectrometers. It is thus possible to study multi-component samples and also follow temperature-induced peak-shifts owing to phase changes (e.g. melting or liquid crystalline phase transition of phospholipids). Especially carbonyl- and hydrocarbon-bands are susceptible for this approach [Fookson and Wallach, 1978 / Wallach et al., 1979 / Fringeli and Guenthard, 1981 / Casal and Mantsch, 1984]. This is achieved by recording and averaging high numbers of spectra, which is, when done conventionally, very time-consuming. Moreover, wavenumber accuracy is found to be in the

order of better than 0.01 for FT-IR, allowing detection of even slight peak-shifts. Owing to its high resolution, even faint signals are detectable, and by computing the spectral data of multi-component systems, subtraction (of e.g. water from aqueous dispersions) or deconvolution of the respective underlying signals of the single compounds can be achieved [Davies, 1987].

A Nicolet Magna-IR 550 was used with Nicolet Omnic V2.0 software for data recording and manipulation. The measuring compartment was constantly purged with air free from CO_2 and water by processing pressurised air through a KEN 6 TE type adsorption drier (Zander Aufbereitungstechnik GmbH, Essen, Germany). Different sample holders were employed which were mounted in temperature-controlled jackets and put on a motor-driven sample-shuttle to allow change of samples or background-samples. Temperature control between -10°C and 80°C was achieved by a Haake Fisons K 8752 type temperature bath connected to a second Pt-100 temperature sensor mounted directly into a small hole in the sample holder. To allow maintenance of equal sample thickness, conventional cuvettes from CaF_2 with different spacers (Graseby Specac, obtained from L.O.T. Oriel GmbH, Langenberg, Germany) were initially used. Spacers thinner than 10 µm are, however, not readily available and difficult to handle. A customised 'thin-film' cuvette (Fig. 21), also from CaF_2, was therefore made. The latter was cut on one side to yield films of 5.6 µm thickness [Hienerwadel, 1993]. Samples were prepared by application of 0.6 µl of the liquid onto the sample compartment of the lower cuvette window (see Fig. 21) and subsequent tightening of the cuvette in a special sample holder. Any excess liquid was squeezed into the outer ring (overflow channel), allowing exactly reproducible sample thickness on each preparation.

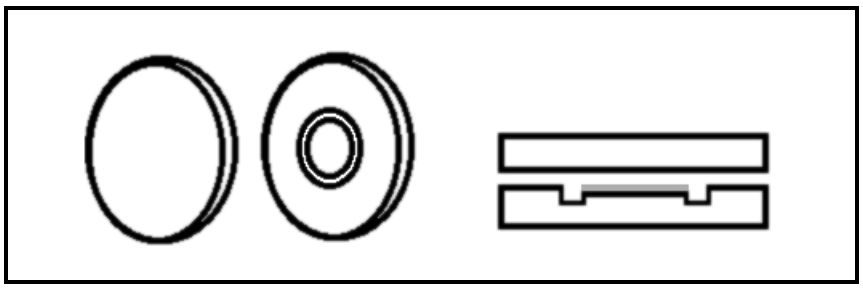

Fig. 21 Customised FT-IR thin-film cuvette (outer ∅: 20 mm, sample comp. ∅: 8.1 mm, sample thickness: 5.6 µm)

Alternatively, attenuated total reflection (ATR/FT-IR) technique was employed at room-temperature, which could not, however, be exploited for quantitative data. Total reflection occurs when a beam hits an interface from the optically denser medium (n2 in Fig. 22) towards the optically 'thinner' medium (n1), provided the incident angle ($\alpha 2$) exceeds a certain threshold angle. However, a part of the beam is able to penetrate into the 'thinner' medium for about a few wavelengths and then returns into the denser medium. By multiple reflection on

the contact interface, the 'thinner' medium (i.e. the sample) thus is allowed to absorb respective bands from the incident beam. Since penetration into the sample is, therefore, *inter alia* dependent on material properties like refractive indices and wavelength, an amplification for peaks in the lower wavenumber region results in ATR spectra [Nicolet Instrument Corporation, 1993]. To be able to compare ATR/FT-IR data with conventional spectra, this effect was corrected by performance of an 'ATR-correction' on the ATR/FTIR spectra. Samples were analysed on a horizontal ATR contact sampling plate from ZnSe (Spectra-Tech Europe Ltd., Warrington, U.K.), which is also water-resistant, but allows measurements of absorbance down to about 650 cm^{-1} and possesses a refractive index of n = 2.4.

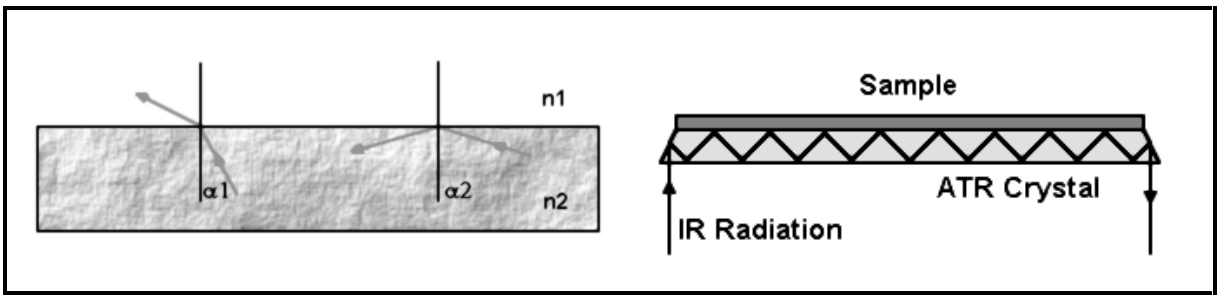

Fig. 22 Principle of Attenuated Total Reflection (ATR)/FT-IR **(left)** and of the horizontal ATR contact sampling technique **(right)** (adapted from Guenzler and Boeck [1993])

The analytical parameters and presets used for the FT-IR experiments were:

Parameters	Settings
Beam Source	He-Ne Laser (1mW, 632.8 nm)
Detector	DTGS KBr
Beamsplitter	KBr
Aperture	95
Spinning velocity	0.6329
Scans	128
Resolution	4 cm^{-1}
Apodisation	Happ-Genzel
Correction	None (or ATR-correction for ATR/FTIR-spectra)

2.2.4.8 Differential Scanning Calorimetry (DSC)

DSC allows determination of thermotropic phase transitions in a quantitative manner and is especially useful for the investigation of the complex behaviour of polymorphic lipids [Small, 1986 / Gennis, 1989]. Samples were analysed on a Differential Scanning Calorimeter PL (Rheometric Scientific, Bensheim, Germany). Typically, 8 - 15 mg of the sample were weighed into an aluminium pan and cold-sealed. The reference pan remained empty and was sealed in the same fashion. Heating and cooling rates of 3°C/min (or as indicated) were applied, recording at least two complete heating/cooling cycles.

2.2.4.9 Zeta Potential Measurement by Laser Doppler Anemometry (LDA)

For submicron parenteral emulsions, Zeta potential measurements via Laser Doppler Anemometry (LDA) are suitable. LDA allows fast determination of the electrophoretic mobility *(μ)* using laser light scattering. The electrophoretic mobility is defined by the following equation, where *E* is the field strength [Volt/cm] and *v* the velocity of a particle along the field [µm/s]:

$$\mu = \frac{v}{E} \quad \left[\frac{\mu m \cdot cm}{Volt \cdot s} \right]$$

Eq. 10 The Electrophoretic mobility *(μ)*

In the LDA setup (Fig. 23), a laser beam is first split and then interferes in the measurement zone located in the stationary layer of a capillary containing the sample. When particles following the electrical field move across this interference pattern, they cause a scattering of the laser light. This is frequency-shifted against the non-scattered parts of the beams ('Doppler effect'). From the frequency-shift (or Doppler frequency, f_d) measured, particle velocity through the capillary can be calculated according to Eq. 11, where λ is the laser wavelength and $\theta/2$ is the angle of detection by the photomultiplier.

$$f_d = v \cdot \frac{2 \cdot \sin\left(\frac{\theta}{2}\right)}{\lambda}$$

Eq. 11 Calculation of particle velocity *(v)* from the Doppler frequency *(f_d)*

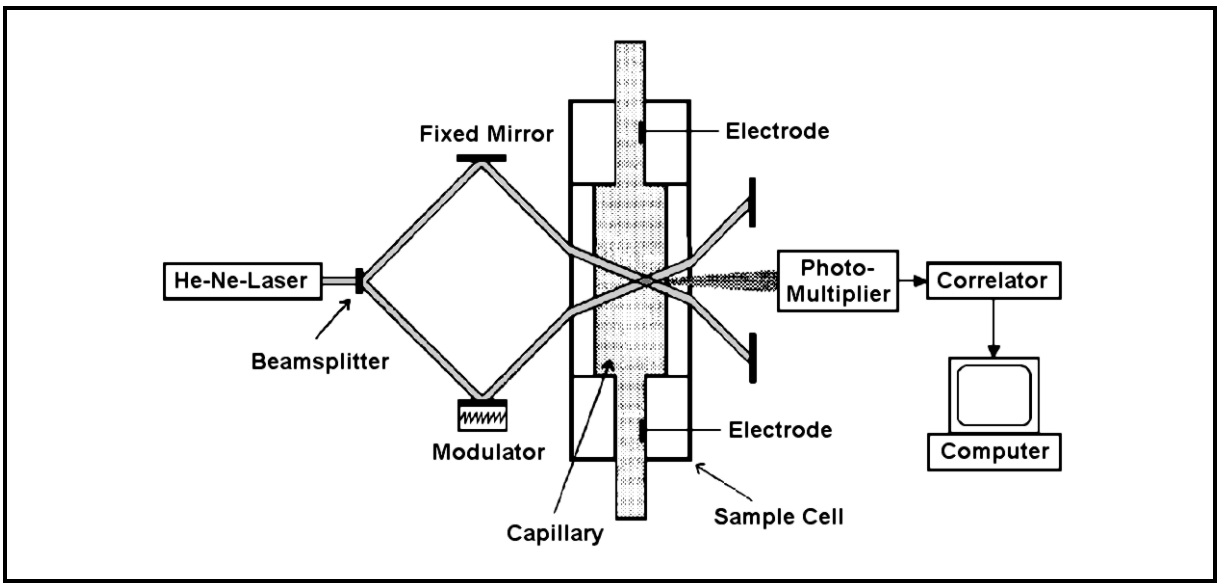

Fig. 23 Principle of Zeta Potential measurement by Laser Doppler Anemometry as employed in the Malvern Zetasizer series (after Mueller [1996])

The electrophoretic mobility is calculated from Eq. 10 and then the Zeta potential from the Henry equation. Alternatively, the Helmholtz-Smoluchowski approximation is used by the Zetasizer 3000, as the particles are assumed to be large compared with the thin electrical double-layer [Hunter, 1981].

$$\zeta = \frac{4 \cdot \pi \cdot \eta \cdot \mu}{E \cdot \varepsilon} \quad [mV]$$

Eq. 12 Calculation of Zeta Potential *(ζ)* from electrophoretic mobility *(μ)* according to the Helmholtz-Smoluchowski equation

In this approximation, the Zeta potential *(ζ)* is derived from μ and the electric field strength *(E)* applied, as well as the viscosity *(η)* and the dielectric constant *(ε)* of the dispersion medium at a given temperature.

Zeta potentials were determined using a Malvern Zetasizer 3000 (Malvern Instruments GmbH, Herrenberg, Germany) and are given as the mean of three measurements. Samples were diluted as described for PCS measurements (see Section 2.2.3.1), except that double-distilled and filtered (0.22 µm) water adjusted to the desired pH with 0.01 N HCl or NaOH solution was used for dilution. Measurements were carried out at 25°C ± 0.2°C unless stated otherwise. Calibration with a standard buffered sample (55 ± 5 mV) supplied by the manufacturer was performed before each set of measurements.

2.2.4.10 Measurement of Conductivity

The conductivity of samples was determined using a customised assembly. A small vessel (approx. volume = 1 ml) contained two electrodes in fixed position connected to a Metex M-3650 Multimeter. When W/O type systems or oil as the sole phase were examined, no conductivity or infinite resistivity occurred.

2.2.5 Compositional Analysis

2.2.5.1 Lyophilisation

Samples (5 ml of emulsions or lecithin dispersions containing approx. 1 - 4% lecithin which was equivalent to about $7.8 \cdot 10^{-5}$ mol) were pipetted to steel freeze-drying cups (∅ 6.5 cm) and transferred into a Delta 1-24 KD Model freeze-drier (Christ Medizinischer Apparatebau, Osterode a. Harz, Germany). The following parameters were used:

Parameter	Value
Shelf temperature during freezing	-45°C
Freezing time	2 h
Primary drying temperature	-20°C
Primary drying time	30 h
Primary drying pressure (Pirani)	0.16 mbar
Secondary drying temperature	-10°C to 15°C at 3°C / h
Secondary drying time	10 h
Secondary drying pressure (Pirani)	0.14 to 0.16 mbar

2.2.5.2 High-Performance Liquid Chromatography (HPLC)

Regarding the analysis of phospholipids by HPLC, numerous methods using various solvent mixtures have been reported, but owing to the complex nature of lecithins it is not straightforward, though. McCluer et al. [1986] give an overview of various methods and

detection techniques applied. Most of those report utilisation of silica columns with isocratic elution, e.g. IUPAC [Beare-Rogers et al., 1992] proposed a method utilising a silica column, isocratic elution with n-hexane:2-propanol:acetate buffer (8:8:1 v/v/v) and detection at 206 nm. Taking into account that the substances intended to be determined in this case consisted of unknown quantities of rather complex mixtures of phospholipids and their more hydrophilic degradation products, it seemed appropriate to use a method that allowed determination of all components in a single run without having to sacrifice peak resolution. Furthermore, it was desired to limit sample preparation and manipulation to a minimum extent and to allow analysis of lecithin-triglyceride-glycerol mixtures as they occur in the emulsions. Therefore, utilisation of an eluent gradient seemed necessary, which in turn limited detection possibilities, since e.g. refractive index (RI) detection is bound to isocratic eluents [McCluer et al., 1986]. Sotirhos et al. [1986b] describe the separation of a variety of soybean lecithin components using an eluent gradient and UV detection at 210 nm. This method seemed suitable to resolve the complexity of the samples in question and was found to give similar retention times as they had been reported.

The analyses were performed on a Perkin Elmer system running Turbochrom V4.1 software (Bodenseewerk Perkin-Elmer GmbH, Ueberlingen, Germany). This comprised an ISS 200 autosampler and a Series 200 LC binary pump, with sample detection using a Perkin Elmer model 785 UV/VIS detector. Solvent mixtures were purged with He and kept in gas-tight Schott flasks with tightly mounted purging and solvent pipelines through the cap. This was to prevent evaporation of solvents and decomposition of gradient ternary mixtures during analysis, which had been found to be critical for reproducibility. Preliminary experiments had shown that direct admixing of solvents with a ternary pump did not work due to volume contraction of the solvent mixture leading to unstable baselines caused by bubbling. Calibration was carried out by injecting and evaluating weight/area plots of different solutions of PC (Lipoid EPC®), PE (Sigma), LPC (Sigma) and LPC (Lipoid ELPC®) in (2-Propanol : n-Hexane / 1:1 v/v). Relative standard deviations between three successive injections were found to lie in the range of about 1.5% for higher concentrated, well-responding compounds like PC or PE and about 3% for low-response signals from LPC. These values were comparable to the reports of Sotirhos et al. [1986b], except LPC which was reported to be detected with a relative error of about 10%.

In preliminary experiments n-hexane : 2-propanol (1:1 v/v) was found to best dissolve all of the different substances of interest. Samples were therefore dissolved in 2-propanol : n-hexane (1:1 v/v) to give fixed volumes of injectable solution, whereby aqueous samples had been lyophilised in advance. In the case of more polar LPC, short and gentle heating helped to dissolve even larger amounts. Due to this fact, all samples were dissolved in

the same fashion and thus could be injected using the same solvent mixture. To avoid sample losses, no filtering of sample solutions prior to injection was applied, since the use of a precolumn gave satisfactory results. Each analysis comprised three injections from separate flasks. During each experiment an additional sample of each respective standard solution was also analysed. Even after 500 injections no backpressure increase was observed during HPLC analysis.

Parameter	Value
Column	30cm Waters µ-Porasil® 3,9mm ID (silica, 10µm size) Precolumn: Waters Guard Pak® with Resolve® Silica Inserts
Eluent gradient	א n-Hexane : 2-Propanol : Double dist. Water (6 : 8 : 0.5) (v / v / v) ℑ n-Hexane : 2-Propanol : Double dist. Water (6 : 8 : 1.5) (v / v / v)
	Over 20 min.: 90% א + 10% ℑ changing to 0% א + 100% ℑ (linear) For another 40 min.: 0% א + 100% ℑ
Eluent flow	0.8 ml/minute
Injected Volume	75 µl
Detection	UV, 210 nm, 0.0010 AUFS

Fig. 24 shows a typical chromatogram for a commercial parenteral emulsion (Intralipid 30®). It can clearly be discerned between various lipid and phospholipid components which were not all determined or evaluated quantitatively in this studies.

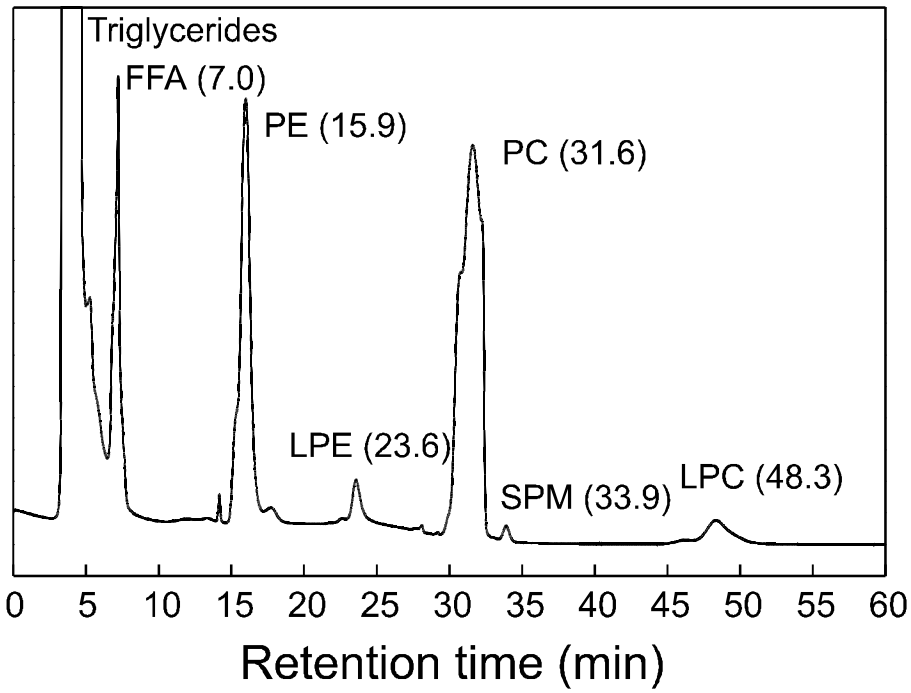

Fig. 24 HPLC-Chromatogram of Intralipid 30®, showing main components and respective retention times

2.2.5.3 High-Performance Thin-Layer Chromatography (HPTLC)

HPTLC compared to conventional TLC offers improved sample separation and requires only little equipment and time. Because other methods often have exhibited certain limitations and HPLTC offers a wide range of choices in stationary and mobile phases as well as in detection means, this technique is widely used in quantitative phospholipid analysis, e.g. by the forthcoming monograph of soya lecithin in the Ph.Eur. 1998. Two-dimensional HPTLC was employed to verify the lyso-phospholipid contents obtained from HPLC analysis. Sample solutions (2-Propanol : n-Hexane / 1:1 v/v) were pipetted on HPTLC plates using 10 µl DESAGA 'minicaps' microcapillaries (DESAGA, Heidelberg, Germany). On each plate three standard-solution dilutions (2-Propanol : n-Hexane / 1:1 v/v) were also applied and used for calibration. The trough was lined with filtration paper and allowed to saturate for 30 min. Elution was completed and the plate removed from the trough when the solvent front had travelled to about 1 cm away from the upper edge. The plate was dried with a fan and subsequently placed in the staining solution for 10 s. After drying away excess staining solution, the plate was developed in a conventional drying oven. After cooling to ambient temperature, the plate was scanned lane by lane using a Shimadzu CS-9301 PC Flying Spot Scanning Densitometer (Shimadzu Europe, Duisburg, Gemany). This kind of densitometer is especially suited for scanning of irregularly shaped spots and is also capable of evaluating data of non-homogeneously distributed spots [Marmer, 1985]. Spot absorption was compared with

a fitted function of standard absorptions using the Shimadzu original software for quantitation. Content values are reported as the mean of three runs.

Parameter	Value
HPTLC plate	Merck silica 60 F_{254} HPTLC plates (10x10cm)
Eluent	Chloroform : Methanol : NH_3 conc. : Double Dist. Water 75 : 25 : 2 : 2 (v / v / v / v)
Sample Volume	3 x 10 µl
Staining agent	$CuSO_4$-solution (10% w/v) in H_3PO_4 (6.8% v/v)
Developing conditions	45 minutes at 170°C
Detection	510 nm, reflectance mode, zig-zag scanning, 0.1 mm stepwidth

Fig. 25 shows a typical HPTLC-chromatogram after staining and scanned densitometric spectra which were integrated and quantitated subsequently.

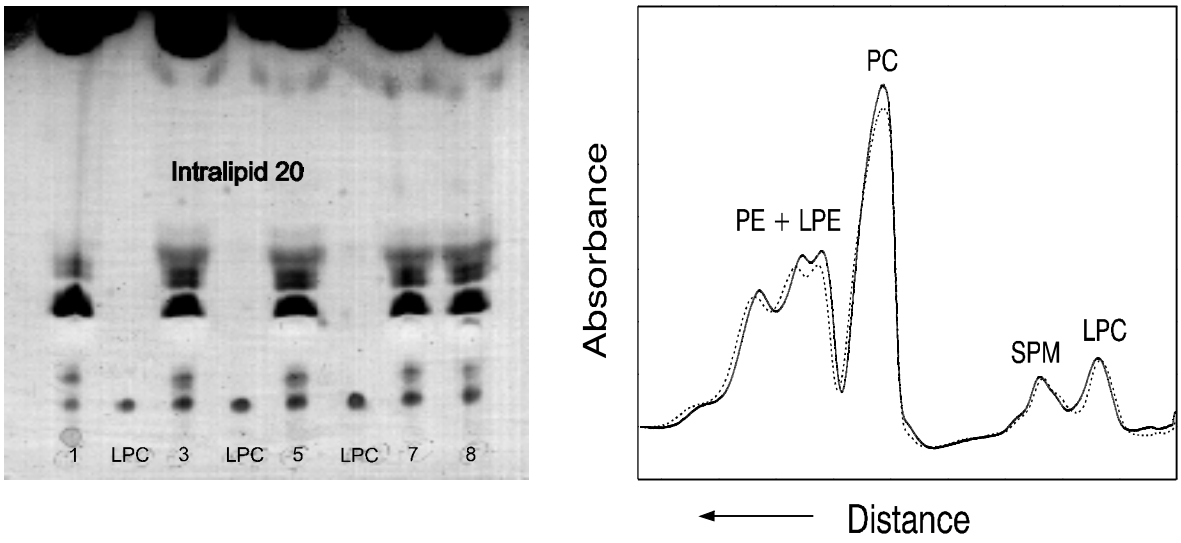

Fig. 25 HPTLC-Chromatogram of Intralipid 20® **(left, lanes 3 and 5)** and densitometric spectra thereof **(right)** showing lanes 3 (·····) and 5 (—) from the chromatogram

Under the conditions mentioned above the following approximate R_f-values were observed:

R_f-values observed	
Triglycerides (TG)	0.95
Free Fatty Acids (FFA)	0.83
Phosphatidylethanolamine (PE)	0.40
Phosphatidylcholine (PC)	0.29
Sphingomyelin (SPM)	0.22
Lysophosphatidylcholine (LPC)	0.10

2.2.5.4 pH-Measurement

A digital pH-meter type 640 (Knick, Berlin, Germany) with a glass electrode was used. Daily calibration with standard buffer solutions (pH 2.00 and pH 7.00 from Mettler Toledo, Steinbach, Germany) was employed. Measurements were carried out at room temperature on undiluted samples. See Chapter 3 for discussion of the measurement procedure.

Chapter 3 – Results and Discussion (I)
Production of Lecithin-Stabilised Emulsions

In this chapter, the physico-chemical characterisation of the egg lecithins and an examination of their emulsifying properties are given, followed by a step-by-step investigation of production parameters and their influence on emulsion size distribution, chemical composition and autoclaving stability.

3.1 Characterisation of Emulsifiers

For subsequent calculations, the molecular mass of the emulsifiers was estimated from the manufacturer's declaration on phospholipid content and fatty acid composition.

Emulsifier	Molecular Mass (g/mol)
DPPC	734.1
Lipoid EPC®	770.5
Lipoid E75®	~762
Lipoid E80®	~762
Egg-PE	728.4
Egg-LPC	513.9
Sodium Oleate	304.4

Tab. 7 Molecular mass estimated for the emulsifiers used (values calculated according to data from Marsh [1990])

3.1.1 Characterisation of Emulsifying Properties

3.1.1.1 Measurement of Droplet Coalescence Times

The influence of emulsifier film properties on parenteral emulsion stability using a coalescence cell has already been described by Hansrani [1980]. She reported differences in coalescence times depending on emulsifier concentration and composition, but used the lecithin dispersed in the water phase and did not investigate the influence of elevated temperatures on coalescence behaviour. In this work the phospholipids were incorporated in the oil phase, allowing equilibration at the interface to be examined.

Various empirical evaluations of experimental data on film-thinning and coalescence of droplets at a planar surface have been proposed [e.g. Cockbain and McRoberts, 1953 / Gillespie and Rideal, 1954]. Typically, the resulting droplet rest times before their coalescence into the oil phase show a wide distribution, which can be evaluated according to the Cockbain-McRoberts equation (Eq. 13). This assumes a two-stage process, the first being the thinning of the liquid film to its critical thickness, and the second, faster one, the actual coalescence following first-order kinetics:

$$\log N_t = -\frac{k_c \cdot t}{2.303} + const.$$

Eq. 13 Cockbain-McRoberts equation for droplet coalescence

The first-order half life of droplet coalescence *($T_{½}$)* is calculated from the slope ('coalescence rate constant', k_c) of a semi-logarithmic plot of the number of droplets not coalesced *(N_t)/(N_0)* against time *t*. Accordingly, the film drainage time *(t_d)*, where no coalescence has yet taken place, can also be obtained:

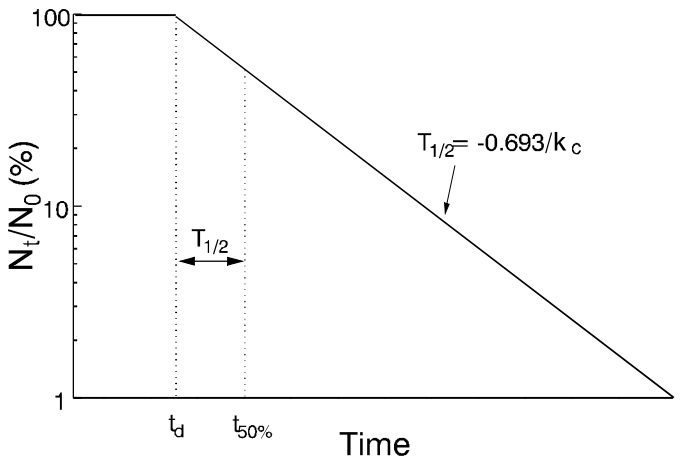

Fig. 26 Schematic of Cockbain-McRoberts plot for droplet rest-times

Hansrani's [1980] coalescence data showed that the addition of minor components like LPC and SPM led to reduced coalescence times compared with pure PC. PE also showed a marked effect, although different PE concentrations in PC:PE mixtures did not produce large differences in coalescence time. Most pronounced effects were observed with addition of LPC to the PC:PE premix, followed by SPM. However, none of the compounds attributed to exhibit stabilising effects by charge repulsion (e.g. PS or PA [Rydhag, 1979 / Szoka and Papahadjopoulos, 1980]) increased droplet coalescence time. Hansrani used a 10^{-4} molar

dispersion of PC:PE mixtures in water. Since, however, pure soybean oil gives similar values for $T_{1/2}$ (see later), it is likely that insufficient emulsifier was available at the interface at the time of coalescence in Hansrani's work. Furthermore, the dispersed lecithin vesicles she used would take a certain time to reorientate at the free oil interface (if at all). In the experiments reported here, the lecithin was, therefore, dissolved in the oil phase before layering onto the aqueous layer. It was expected that the lecithin would be more readily available at the oil/water interface compared with the aqueous vesicular dispersion, thus avoiding excess lecithin dispersed in the water phase without contributing to the film properties at the oil/water interface. Repeated measurements after various times were carried out in order to allow observation of interfacial 'ageing' phenomena.

With pure soybean oil, a clear effect of temperature on droplet coalescence rates is detectable (Fig. 27): increasing temperature decreases droplet stability, since film thinning is accelerated. Addition of lecithin to the soya oil produced a slow increase in droplet rest times. However, it took several hours to reach equilibrium rest times.

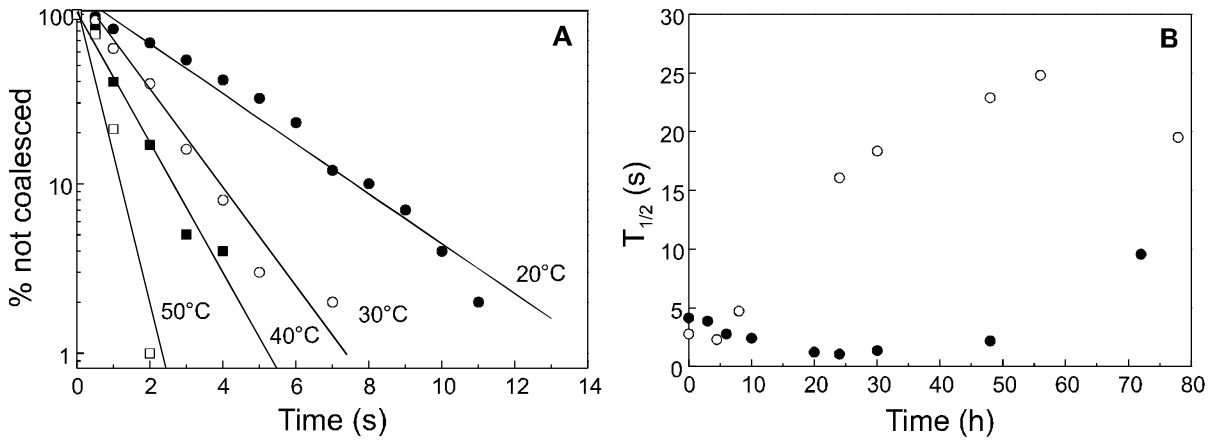

Fig. 27 **(A)** Droplet rest times of pure soya oil droplets in a Cockbain-McRoberts plot and **(B)** effect of prolonged equilibration times on $T_{1/2}$ of $7.6 \cdot 10^{-6}$ (○) and $3.3 \cdot 10^{-6}$ molar (●) Lipoid E80® in soya oil at 50°C

Soya Oil	$T_{1/2}$ (s)
20°C	4.4
30°C	2.6
40°C	1.8
50°C	0.5

Tab. 8 First-order droplet coalescence half-lives ($T_{1/2}$) for pure soya oil (Sigma)

Time to reach equilibrium was also dependent on lecithin concentration and took at least 48 h. Over a period of 72 h, a cloudy, viscous 'layer' gradually appeared at the interface, also dependent on the lecithin concentration. This 'layer' was assumed to consist of hydrated phospholipid (multilayer) structures. This observation supports the assumption that time-dependent life times are not just a result of slow diffusion of lecithin molecules through the oil phase. Remarkably, the $T_{1/2}$ values determined for pure soya oil (Tab. 8) are of the same magnitude as of those obtained for an aqueous 10^{-4} molar PC dispersion reported by Hansrani [1980]. As can be seen in Fig. 28, increasing concentrations of Lipoid E80® led to increased coalescence stability when measured after the same equilibration time. With $2.6 \cdot 10^{-5}$ mol Lipoid E80®, coalescence times at 70°C could be determined, whereas with $1.4 \cdot 10^{-5}$ mol coalescence was too fast to be measured (Tab. 9).

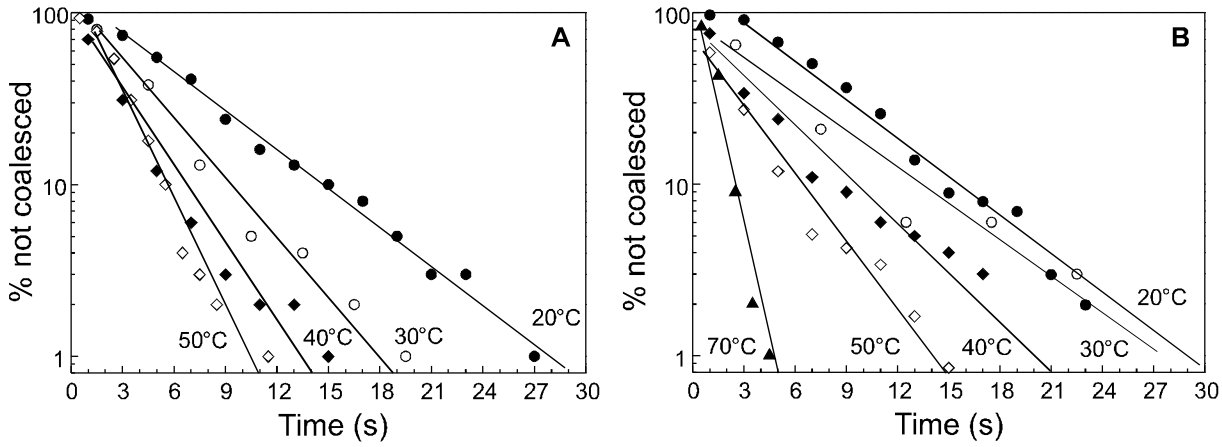

Fig. 28 Cockbain-McRoberts plots for **(A)** $1.4 \cdot 10^{-5}$ mol and **(B)** $2.6 \cdot 10^{-5}$ mol of Lipoid E80® at different temperatures after 12 h equilibration

Lipoid E80® ($1.4 \cdot 10^{-5}$ mol)	**$T_{1/2}$ (s)**	**Lipoid E80® ($2.6 \cdot 10^{-5}$ mol)**	**$T_{1/2}$ (s)**
20°C	9.3	**20°C**	8.4
30°C	7.0	**30°C**	9.5
40°C	5.4	**40°C**	8.3
50°C	3.3	**50°C**	5.7
70°C	-	**70°C**	1.3

Tab. 9 First-order droplet coalescence half-lives ($T_{1/2}$) for different Lipoid E80® concentrations at various temperatures after 12 h equilibration time

In order to obtain comparable droplet rest times of reasonable magnitude, phospholipids were employed in the range of some 10^{-6} mol/10 g of oil in subsequent experiments, and coalescence experiments were carried out at 50°C after 48 h equilibration (compare Fig. 27). It became evident, however, that the lecithin formed additional layers at the oil-water interface, which contributed to enhanced droplet rest times. According to reports on the emulsification properties of pure PC [Yeadon et al., 1958 / Rydhag and Wilton, 1981], and similar to the findings of Hansrani [1980], pure PC from egg yolk (Lipoid EPC®) gives more rapid coalescence than commercial egg lecithins containing increased content of minor compounds (Lipoid E75® and E80®) (Fig. 29). The latter contains approx. 80% PC and has a PC:PE ratio of 10:1, whereas Lipoid E75® possesses a PC:PE ratio of approx. 5:1 since about twice the amount of PE is contained. Yet, no difference in coalescence behaviour between both types is observed in Fig. 29 and Tab. 10.

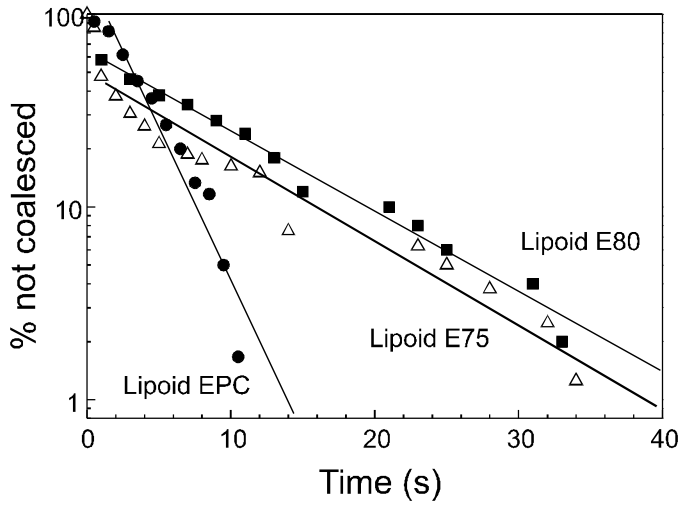

Fig. 29 Cockbain-McRoberts plots for different commercial egg lecithins ($7.7 \cdot 10^{-6}$ mol each) at 50°C after 48 h equilibration time

$7.7 \cdot 10^{-6}$ mol	**$T_{1/2}$ (s)**
Lipoid EPC®	5.2
Lipoid E75®	15.9
Lipoid E80®	16.7

Tab. 10 First-order droplet coalescence half-lives ($T_{1/2}$) for egg lecithins at 50°C

Fig. 30 shows the influence of increasing LPC content measured for droplet coalescence times on pure PC films.

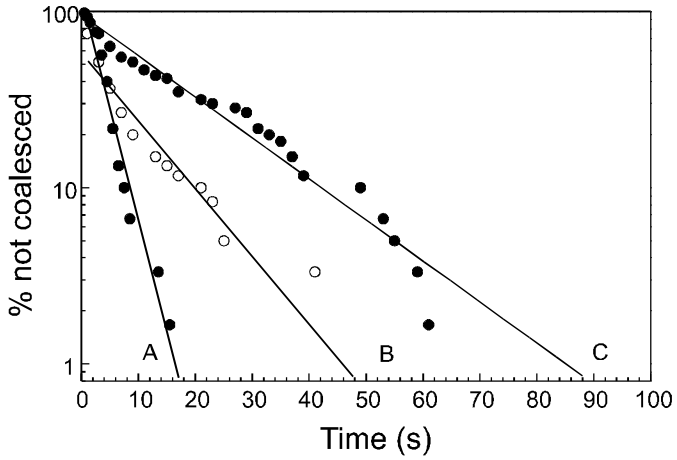

Fig. 30 Cockbain-McRoberts plots for different PC : lyso-PC (LPC)-mixtures (Lipoid EPC® : Sigma-LPC): **(A)** $7.7 \cdot 10^{-6}$ mol PC, **(B)** $7.1 \cdot 10^{-6}$ mol PC + $1.2 \cdot 10^{-6}$ mol LPC, **(C)** $5.2 \cdot 10^{-6}$ mol PC + $3.9 \cdot 10^{-6}$ mol LPC at 50°C after 48 h equilibration time

A clear effect of LPC admixture is evident (Tab. 11), which is not simply a result of increased total lipid concentration. A marked increase in $T_{1/2}$ is observed for 14.5 mol% LPC content and 42.9 mol% LPC in the mixtures, which is in agreement with Hansrani [1980], who did not find a levelling of LPC effect as in the case of PE content. Improved film properties were suggested, and possibly increasing stability of emulsions after partial hydrolysis of the emulsifier to LPC had taken place. Kumar et al. [1989] had also reported ^{31}P-NMR data indicating a stabilising effect of LPC on SUVs from PC. Despite the problems with Hansrani's method, it is clear that LPC improves droplet lifetime very effectively.

Lipoid EPC®	**$T_{1/2}$ (s)**
+ 0 mol% LPC	5.6
+ 14.5 mol% LPC	20.6
+ 42.9 mol% LPC	29.8

Tab. 11 First-order droplet coalescence half-lives ($T_{1/2}$) for PC+LPC at 50°C

With both Lipoid E75® and E80® a much smaller effect of added LPC on coalescence time

could be observed (Fig. 31). The 'minor components' already contained in Lipoid E75®/E80® evidently contribute to increased film stability. Increasing values for $T_{1/2}$ were, however, observed on addition of LPC (Tab. 12), there being no difference between the Lipoid® types, as seen before. Again it is clear that LPC increases droplet lifetime, even for impure Lipoid® E75 and E80, although, for a more pronounced effect, relatively high content of LPC was required.

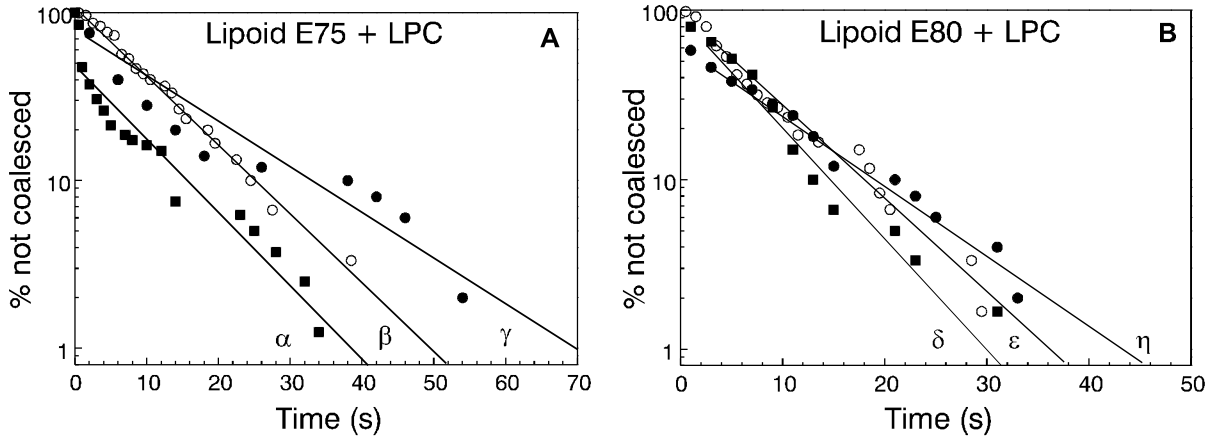

Fig. 31 Cockbain-McRoberts plots for **(α)** $7.7 \cdot 10^{-6}$ mol Lipoid E75®, **(β)** $7.3 \cdot 10^{-6}$ mol Lipoid E75® + $1.2 \cdot 10^{-6}$ mol LPC and **(γ)** $4.6 \cdot 10^{-6}$ mol Lipoid E75® + $3.9 \cdot 10^{-6}$ mol LPC **(A)** and for **(δ)** $7.8 \cdot 10^{-6}$ mol Lipoid E80®, **(ε)** $7.1 \cdot 10^{-6}$ mol Lipoid E80® + $1.2 \cdot 10^{-6}$ mol LPC and **(η)** $5.2 \cdot 10^{-6}$ mol Lipoid E80® + $3.9 \cdot 10^{-6}$ mol LPC **(B)** at 50°C after 48 h of equilibration time

Lipoid E75®	**$T_{1/2}$ (s)**	**Lipoid E80®**	**$T_{1/2}$ (s)**
+ 0 mol% LPC	15.9	**+ 0 mol% LPC**	16.5
+ 14.1 mol% LPC	16.8	**+ 14.5 mol% LPC**	17.7
+ 45.9 mol% LPC	27.4	**+ 42.9 mol% LPC**	23.7

Tab. 12 First-order droplet coalescence half-lives ($T_{1/2}$) for LPC admixtures on Lipoid E75®/E80® at 50°C

Muehlebach et al. [1987] determined 4.5 - 8.2% (presumably wt%) lyso-phospholipids by thin-layer chromatography in commercial Lipovenoes® and Intralipid® samples. Herman [1992] reported values corresponding to approx. 12 mol% LPC and about 4 mol% LPE for Intralipid 10%® as determined by HPLC with flame ionisation detection. For such LPC concentrations,

however, the results in Tab. 12 predict only an insignificant effect on coalescence behaviour. It is concluded that LPC in commercial lecithins is unlikely to be responsible for reducing droplet coalescence, thus confirming Herman [1992], who did not observe significant changes in emulsion stability after addition of lyso-PC, rather than Hansrani's prediction.

Sodium oleate is added as a co-emulsifying and pH-adjusting agent in certain commercial parenteral emulsions (see Section 1.2) and might also be formed during hydrolysis of lipids during production and storage. The influence of increasing amounts of sodium oleate (added to the aqueous phase) on the coalescence properties of PC-films is shown in Fig. 32.

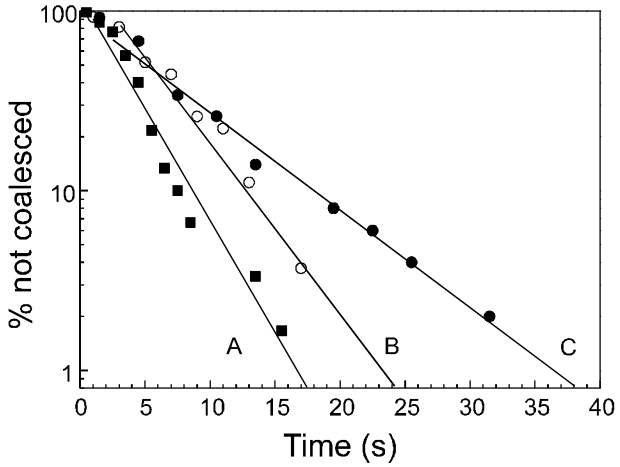

Fig. 32 Cockbain-McRoberts plots for different PC (Lipoid EPC®) : sodium oleate mixtures: **(A)** $7.7 \cdot 10^{-6}$ mol PC, **(B)** $7.8 \cdot 10^{-6}$ mol PC + $0.7 \cdot 10^{-6}$ mol sodium oleate, **(C)** $5.5 \cdot 10^{-6}$ mol PC + $3.3 \cdot 10^{-6}$ mol sodium oleate at 50°C after 48 hours

Lipoid EPC®	**$T_{1/2}$ (sec)**
+ 0 mol% Na-Oleate	5.6
+ 8.2 mol% Na-Oleate	8.0
+ 37.5 mol% Na-Oleate	12.5

Tab. 13 First-order droplet coalescence half-lives ($T_{1/2}$) for PC+Na-oleate at 50°C

Again, coalescence is retarded by addition of sodium oleate (Tab. 13), but with less efficacy than observed for the addition of LPC. In general, it can be deduced that droplet coalescence is strongly influenced by the presence of 'minor components'. Pure PC gives the least stable films, whereas sodium oleate and especially LPC both give enhanced coalescence stability.

Rydhag [1979] reported increased lamellar phase swelling when sodium stearate was added to lecithins, which is also a possible explanation for the stabilising effect of oleate addition observed in Tab. 13. Hydrolysis of phospholipids during production and storage of the emulsion would intuitively cause increased coalescence stability owing to emulsifier film stabilisation. Pronounced effects could, however, only be observed when large amounts of additives were present. Since coalescence occurs faster at higher temperatures (Tab. 9), it seems that stabilisation owing to mere film rigidity does not occur under high temperature stress (during autoclaving), but might become more important under milder conditions (e.g. during pre-emulsification or storage). In all cases, droplet lifetimes increased with equilibration time until a plateau was reached, showing that stabilisation by lecithin emerges slowly. Thus lecithin should exhibit weakest stabilisation efficacy where fast surface coverage is needed, e.g. during homogenisation using high pressure. This is of vital interest when considering the results of subsequent structural studies.

3.1.1.2 Measurement of Film Compressibility

The apparent surface area (A_0) covered by a single molecule [Å^2/molecule] can be obtained from isothermal film compressibility measurements when plotting area (A) against film pressure (π) [mN/m].

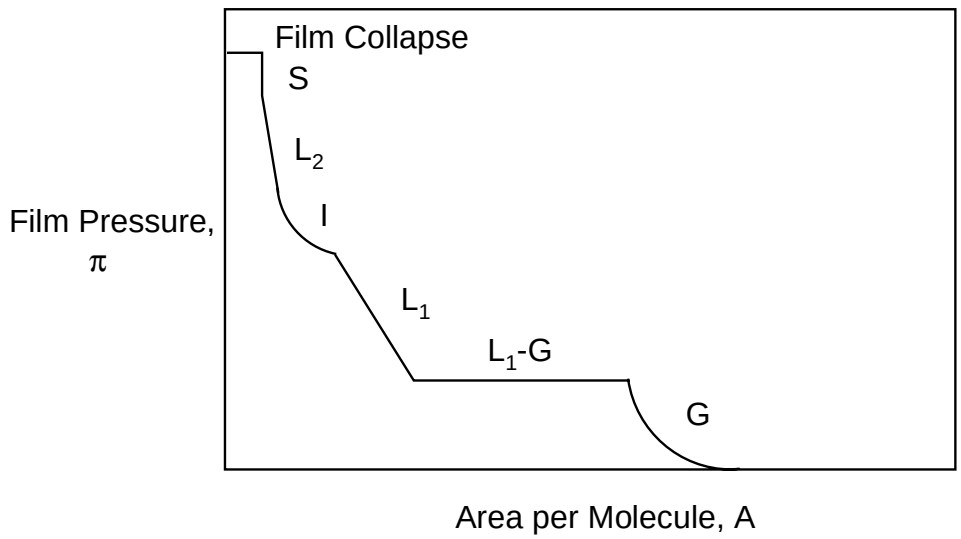

Fig. 33 π-A isotherm for an insoluble monolayer (after Hiemenz [1986])

For such data, Harkins [1952] discerned between gas-like molecules within a monolayer *(G)* which become more oriented towards each other upon increasing compression and are converted into the liquid expanded state $(L_1\text{-}G)$. This is a two-phase state where liquid domains coexist with 'gaseous' molecules. Upon further increase in pressure, the molecules are forced

further together to form a liquid expanded film *(L_1)*. The intermediate state *(I)* is assumed to consist of crystalline and 'liquid-like' domains coexisting. Further increase in pressure causes the chains to become strongly oriented (crystalline), the molecules still being tilted from the surface normal (L_2 or 'liquid-condensed phase'). Finally, the solid state *(S)* is reached, where the tightest possible packing for the headgroups and chains is achieved. Excess pressure on such films leads to eventual breakdown of the film (*Film Collapse Point*, π_c) [Gaines, 1966 / Hiemenz, 1986]. Molecular space requirements and film compressibility *(C^s)* (degree of deformation upon pressure applied) of film-forming, water-insoluble amphiphiles like e.g. lecithin can be obtained by extrapolating the linear parts of the π-A isotherm graph to A_0 (area requirement at zero film pressure) to obtain molecular area requirement. C^s can then be calculated from the slope of the linear regions of the π-A isotherm [Gaines, 1966]

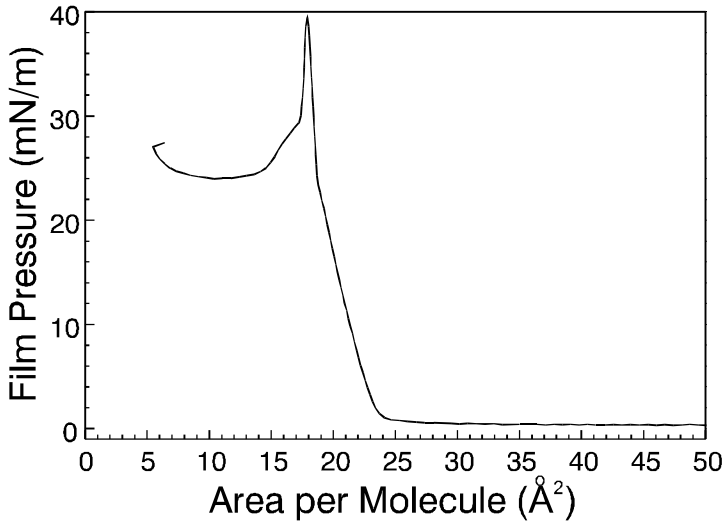

Fig. 34 π-A isotherm for palmitic acid at 20°C

Fig. 34 shows the π-A isotherm for palmitic acid, which was examined in order to evaluate film balance performance. A film of the S-type is seen, where compressibility for the films is very low, before the collapse pressure is reached. The area requirement per molecule (A_0=19.9 Å^2) is in good agreement with data from the literature [Schueckler, 1992 / Lauda, 1987]. The π-A isotherm for DPPC (Fig. 35) shows a two-phase region, where L_1 and G phases coexist (*L_1-G*), and either a second phase change or, more probably, incipient displacement occurring shortly before the collapse pressure was reached. Cevc and Marsh [1987] stressed that unsaturated phospholipids like DOPC remain in the L_1 state at 20°C even at high surface pressures, and show higher A_0 compared with saturated homologues. They also remarked that the formation of L_2 phases by saturated phospholipids also depends on temperature. The molecular space requirement A_0 determined for DPPC in Fig. 35 is similar, albeit slightly lower than e.g. reported by Lance et al. [1996].

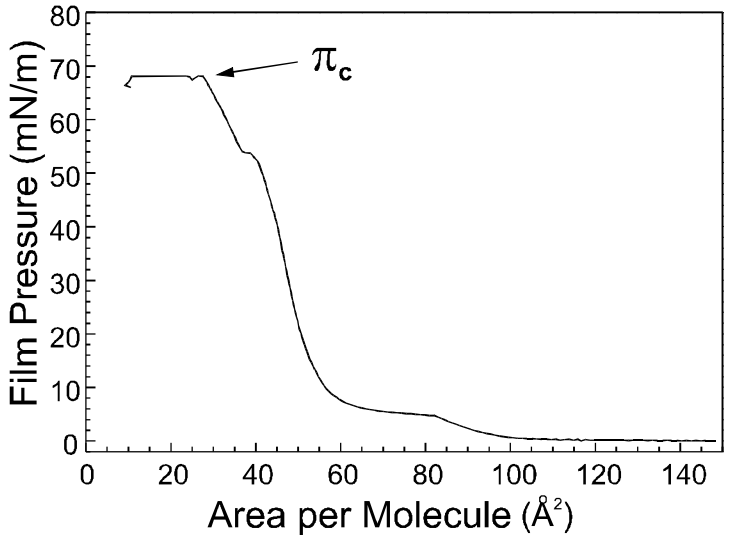

Fig. 35 π-A isotherm for Di-Palmitoyl-PC (DPPC) at 20°C

In contrast to DPPC, all Lipoid® lecithins appear to consist of only a single L_1-phase throughout the measurement range, since no discrete phase change is observed upon film pressure increase (Fig. 36). This behaviour is often found for unsaturated phospholipids (see above). This again supports the assumption that the distinct two-phase region observed for DPPC in Fig. 35 is a result of the fatty acid substituent profile, since pure PC having a large proportion of unsaturated fatty acids (Lipoid EPC®) shows L_1 behaviour and also increased A_0 (Fig. 36). No marked differences in overall phase behaviour of the films between Lipoid EPC® and the two less pure lecithins are seen in Fig. 36, except that molecular area requirement, parallel with the content of impurities, increases in the order Lipoid EPC® < Lipoid E80® < Lipoid E75®. Similar molecular area values were e.g. cited by Groves et al. [1985], who assumed a molecular area for lecithin of 62 $Å^2$ for interface coverage calculations. Broader, less sharp slopes than with DPPC are found for all lecithins, which is in agreement with the findings of Lance et al. [1996] for Lipoid E80®. These findings can be explained by the nature of the insoluble lecithin films, which contain mixtures of different lipids of both saturated and especially unsaturated fatty acid residues. They are therefore less easily compressed to an ordered arrangement, thus possessing higher compressibility values observed for the unsaturated residue lecithins.

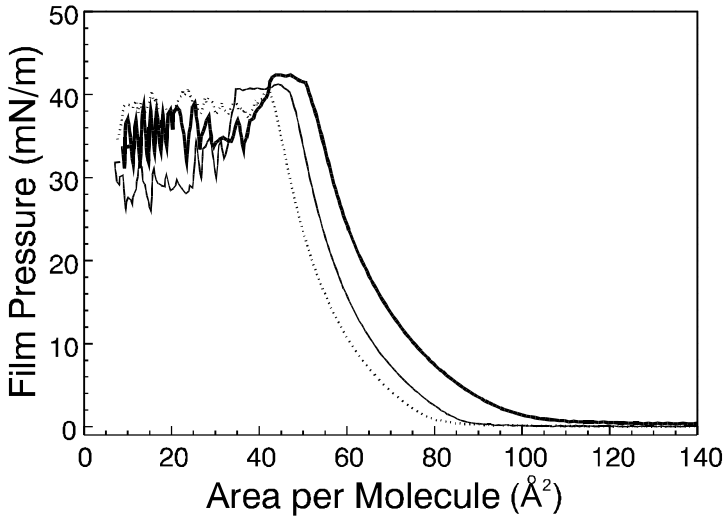

Fig. 36 π-A isotherms for Lipoid EPC® (·····), Lipoid E80® (—) and Lipoid E75® (44) at 20°C

Collapse pressure values of all three egg lecithins are markedly lower than that for DPPC (approx. 70 mN/m). Differences to the values quoted by Lance et al. [1996] can be explained by the higher film compression rate used in their experiments, since collapse pressure is known to be very sensitive to the compression rate applied [Hiemenz, 1986]. However, in general the lower collapse pressure arose from less densely-packed films with less molecular interactions compared with DPPC. This is a result of differences in fatty acid residues (homogeneity and degree of saturation) rather than of different phospholipid components, since all egg lecithins behaved similarly despite their different composition. As film collapse is subject to various influences, information from it has to be regarded with due care [Gaines, 1966] and is only limited. The slight differences in collapse pressure values observed (in the order Lipoid EPC® < Lipoid E80® < Lipoid E75®) indicate, however, ideal miscibility of components, which excludes separation or 'clustering' into separate PE or PC domains [Gaines, 1966]. For the case of the oil-water interface, increasing content of impurities should result in slightly less rigid emulsifier films. The more rigid films from pure PC were, however, less stable to droplet coalescence (see Tab. 10).

Insoluble monolayers of PE are known to be more easily tightly packed than for PC [Chapman, 1975], which is related to its higher chain melting transition temperature. Also its head group area is smaller than that of PC. Increasing content of PE in the commercial lecithins along with other minor impurities appears to cause the observed increase in apparent molecular area requirement and compressibility (Tab. 14). Molecular interaction between different phospholipid species are apparently decreased in the monolayer films. C^s values of commercial egg lecithin films are expectedly higher than for the more rigid DPPC layers and for the pure egg PC (Lipoid EPC®). The value for Lipoid E80® is a little lower than reported by Lance et

al. [1996]. But as their value for DPPC also ranged higher than the one given here, substantial agreement is assumed. Since, however, the C^s values of all Lipoid® lecithins were more similar to each other than e.g. compared with DPPC, the film properties alone do not explain, why Lipoid EPC® possessed remarkably worse emulsification properties than Lipoid E80® and E75®.

Electrostatic charge increases molecular area requirement owing to electrostatic repulsion [Hiemenz, 1986] and gives a possible explanation for the behaviour of Lipoid E75®/E80®, where more charged species are present and molecular area requirement is larger than with PC (Tab. 14). A similar explanation might apply for the case of higher subphase pH values (pH is adjusted to alkaline range before autoclaving emulsions), resulting in increased molecular area. However, this could not be investigated with the method used here, since Langmuir trough measurements require that the monolayer be completely insoluble in the subphase. Owing to hydrolysis and ionisation, fatty acids derived from the lecithin would dissolve at higher subphase pH values [Schueckler, 1992] and disappear from the monolayer film.

The molecular weight values used here for the molecular area calculations are taken from the declaration of composition and fatty acid profile by the manufacturer. Lance et al. [1996] estimated considerably lower values of molecular weight for Lipoid E80®, which accounts for the higher molecular area reported by these authors of 69 $Å^2$ for Lipoid E80®. This deviation also possibly resulted from the different method used (Wilhelmy plate) by these authors. Molecular area requirement for lecithin is, therefore, not straightforward to determine. As discussed before, however, the complicated mixtures of Lipoid E75®/E80® behave like a single species, which allows assumption of an average single molecular area.

Sample	Area per molecule ($Å^2$)	Compressibility (m/mN)
Palmitic acid	19.9	0.00244
DPPC	56.0	0.00469
Lipoid EPC®	60.0	0.00687
Lipoid E80®	64.6	0.00710
Lipoid E75®	71.9	0.00703

Tab. 14 Molecular area and compressibility values determined by the Langmuir film balance

3.1.2 Characterisation of Emulsifier Composition

3.1.2.1 Emulsifier Composition according to HPLC

Gradient HPLC analysis of the emulsifiers using UV-detection was successfully employed, showing that Lipoid EPC® contains slight, but detectable amounts of an impurity, which is assumed to be sphingomyelin (SPM). Lipoid E75® shows considerably more phosphatidylethanolamine (PE) and slightly less phosphatidylcholine (PC) than Lipoid E80®, and both contained similar trace amounts of SPM and faint traces of lyso-phospholipids. Fig. 37 shows the chromatograms of Lipoid EPC®, Lipoid ELPC®, Lipoid E75® and Lipoid E80®. Retention times are similar to those of Sotirhos et al. [1986b], who also described peaks of PI, PA and PS appearing in the region between PE and PC. The minor peaks observable at retention times between 16 and 25 min were not examined more closely here, as these components are not listed in the analysis reports of the manufacturer. The peak-splitting or shouldering observed at high concentrations is attributed to the different fatty acid substitution profile of the phospholipids, as previously reported by Herman [1992]. In this case co-integration of peak and shoulder was performed. Since UV-detection of phospholipids is a response of carbonyl and unsaturated sites [McCluer et al., 1986 / Herman, 1992], lyso-phospholipids are expected to yield a weaker absorbance. This was confirmed by a markedly reduced slope of the LPC-calibration curve compared with PE (largest slope) and PC. No differences could be found between Sigma and Lipoid LPC material, which is as an indication of similar fatty acid substitution (unsaturated/saturated fatty acid ratio) for both LPCs. As stated by McCluer and co-workers [1986] and Herman [1992], values for lyso-phospholipids are especially susceptible to the species of fatty acid cleaved from the phospholipid, since loss of an unsaturated fatty acid leads to a larger decrease in absorbance compared with loss of a saturated fatty acid. The LPC peaks are also split in 3-4 peaks (Fig. 37b), even though there is only a single fatty acid residue. It was hoped that by using egg-yolk compounds as standards, the influence of content variability in fatty acids on detection could be minimised.

As could be seen in Tab. 15, the HPLC assay for PC and PE are similar to the HPTLC results given by the supplier of the lecithins. In the case of LPC, however, unrealistically high values are found, although Sigma LPC and Lipoid® ELPC both gave reproducible results on repeated injection. The LPC contents are much higher than the correspondent decrease in PC concentration on hydrolysis (see later). Herman [1992] stated that hydrolysis of fatty acids would lower the UV molar absorbance coefficient of LPC in an unpredictable manner, making it impossible to be quantified by UV detection.

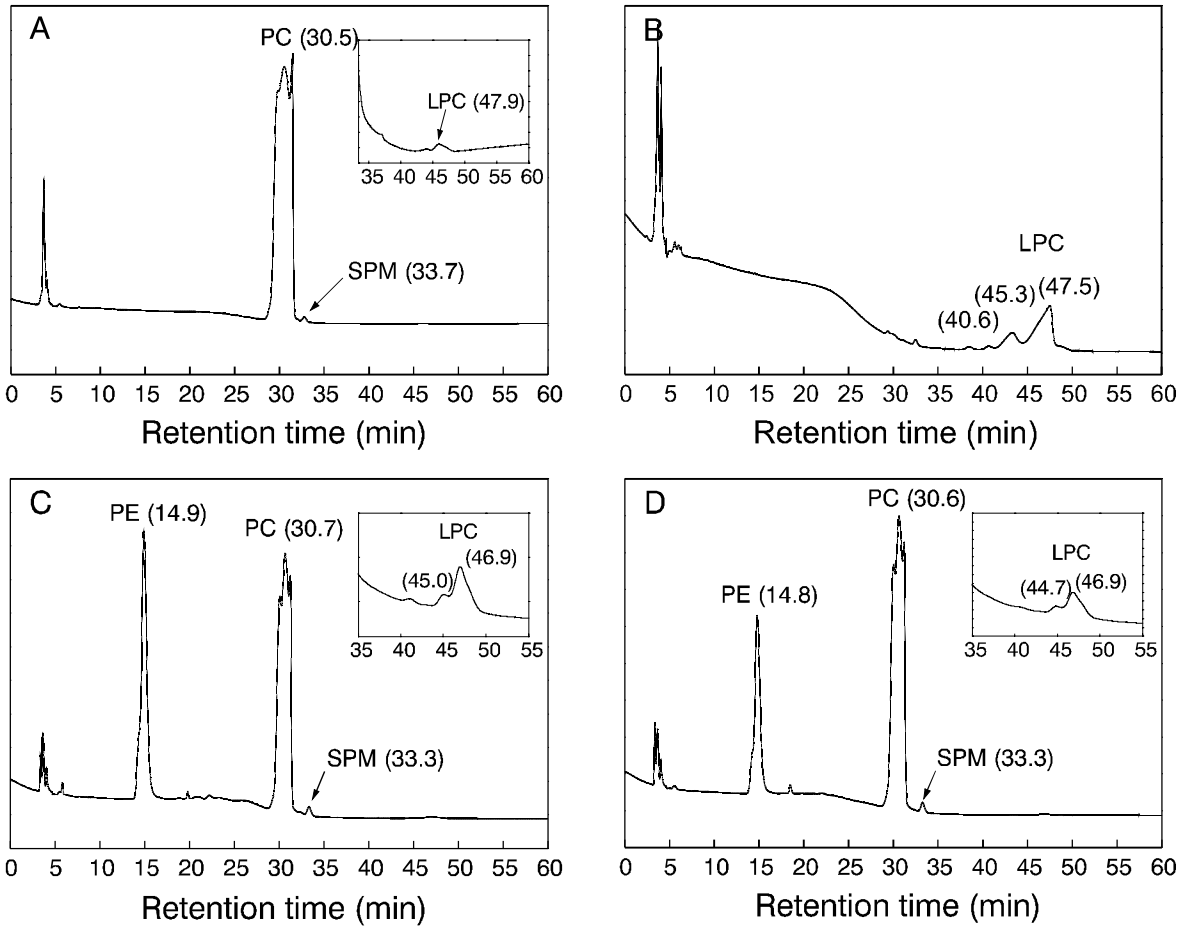

Fig. 37 HPLC chromatograms of **(A)** Lipoid EPC® (with enlarged section), **(B)** Lipoid ELPC® (enlarged), **(C)** Lipoid E75® (with enlarged section) and **(D)** Lipoid E80® (with enlarged section)

Sample	PC (mol%)	PE (mol%)	LPC (mol%)	Others
Lipoid E75®	76.0	19.5	19.5	SPM detectable
Lipoid E80®	82.3	10.9	14.5	SPM detectable

Tab. 15 Results for HPLC determination of emulsifier composition

Since the UV absorbance of LPC is low, measurement error was high owing to variations in the remaining fatty acid residue. It could, however, not be clarified why almost tenfold LPC contents are found compared with the supplier's declaration. LPC concentrations were, therefore, controlled by quantitative HPTLC measurements, as reported in the following section.

3.1.2.2 Emulsifier Composition according to HPTLC

Although only intended for lyso-PC, absorption values for other phospholipids could also be compared between different samples, allowing an estimation of compositional differences. As can be seen from Figs. 38 and 39, the HPTLC analysis demonstrated that Lipoid EPC® contains PC and minute amounts of SPM, but no detectable quantities of lyso-PC. However, for Lipoid E75® and E80® some LPC was clearly detectable. Lipoid E75® also contains more impurities in the form of PE and SPM than does Lipoid E80® (Fig. 39). Quantitation of each chromatogram was carried out by integration of the sample peak areas and using Sigma-LPC standard dilution stains.

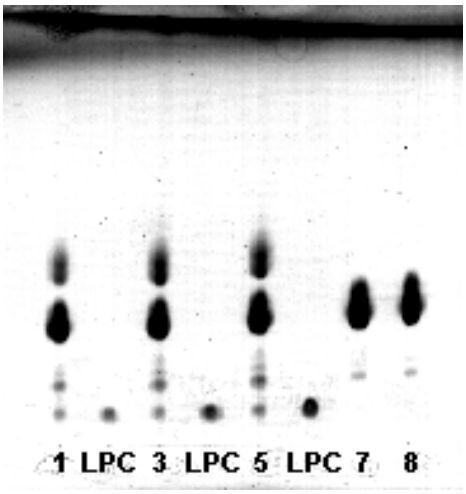

Fig. 38 HPTLC chromatogram of Lipoid E80® **(lane 1)**, Lipoid E75® **(lanes 3 and 5)** and Lipoid EPC® **(lanes 7 and 8)**

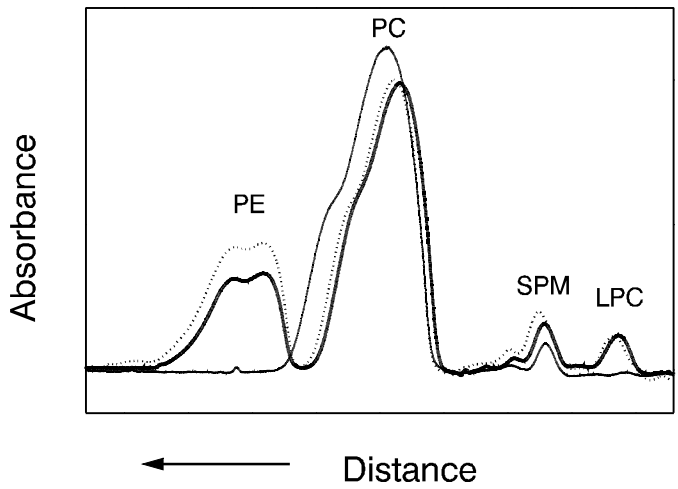

Fig. 39 HPTLC densitometric spectra of Lipoid EPC® (—), Lipoid E75® (·····) and Lipoid E80® (44)

Tab. 16 summarises the results for LPC content of the lecithins, clearly indicating lower values for all samples than determined by HPLC analysis.

Sample	LPC (mol%)	Others
Lipoid EPC®	not detectable	SPM detectable
Lipoid E75®	3.1	SPM detectable
Lipoid E80®	2.2	SPM detectable

Tab. 16 Results for HPTLC determination of LPC content

HPTLC analysis thus shows that the LPC content is in the range of the supplier's declaration, indicating that HPLC analysis yielded too high values for LPC and should not be used for LPC quantitation.

3.1.3 Physical Characterisation of Emulsifier

3.1.3.1 Thermoanalytical Characterisation

Comparison of lipid chain melting behaviour may be of importance for emulsification, where phospholipids are assumed to orientate more easily at the interface when in the molten α state [Diederichs, 1993]. As chain length and degree of saturation of fatty acid residues have a strong influence on packing behaviour (see Chapter 1), calorimetric properties of phospholipids also vary with their composition. Marsh [1990] gives main transition temperatures for fully hydrated, saturated PCs, which increase with chain length from -1.1°C (di-lauroyl-PC) to 64.5°C (di-arachidoyl-PC). Similarly, the transition enthalpies also increase with chain length. For PE, higher transition temperatures (di-lauroyl-PE: 30.2°C / di-arachidoyl-PE: 82.0°C) and enthalpies are cited. For di-substituted PCs, L_c-$L_{\beta'}$ phase transitions occur at about 21.2°C for palmitic residues, 28.0°C for stearic residues and 20.5°C for arachidic residues. $L_{\beta'}$-$P_{\beta'}$ pre-transitions lie at 34.2°C (di-palmitoyl-PC), 50.7°C (di-stearoyl-PC) and 63.7°C (di-arachidoyl-PC). L_α phases are formed by $P_{\beta'}$-L_α phase transitions ('chain melting') at 41.4°C (di-palmitoyl-PC), 55.3°C (di-stearoyl-PC) and 66.4°C (di-arachidoyl-PC). However, for unsaturated or mixed saturated/unsaturated phospholipids less exact data is available. Typically, lower transition temperatures are observed for PC with unsaturated chains, e.g. -21°C (di-oleoyl-PC), -16.2°C (1-stearoyl-2-linoleoyl-PC) or -13°C (1-stearoyl-2-α-linoleoyl-PC). Diederichs [1993] reported transitions for dry soya-PC with

mainly palmitic and stearic fatty acids at approx. 100°C, which is in agreement with e.g. Cevc and Marsh [1987] who quote 100°C and Small [1986], who quotes 110°C for the main transition of anhydrous DPPC. Diederichs also found a transition temperature for non-hydrated egg lecithin at around 25°C. Complex egg lecithin mixtures like Lipoid E80® should, therefore, show similar behaviour and exhibit broader transition peaks than more refined Lipoid EPC®.

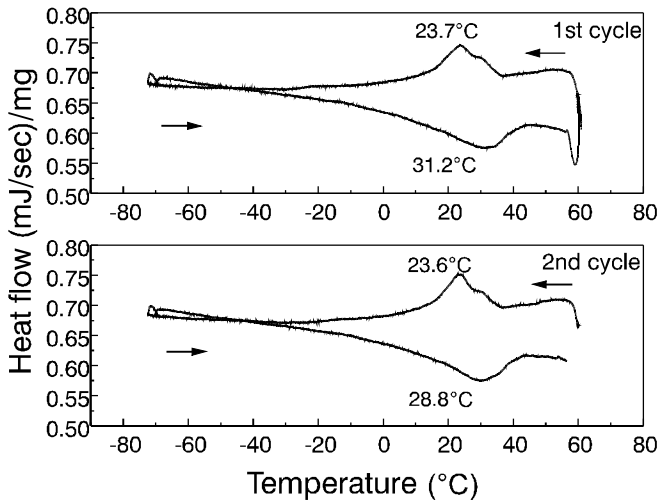

Fig. 40 DSC thermogram of desiccated Lipoid EPC® (at 3K/min)

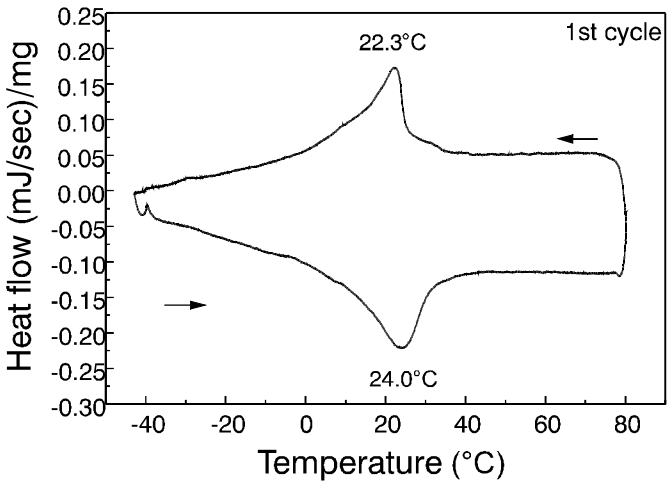

Fig. 41 DSC thermogram of desiccated Lipoid E80® (at 3K/min)

After drying under vacuum 12 h prior to examination, the unsaturated egg lecithins show melting slightly above room temperature (Figs. 40 and 41) as already reported by Diederichs [1993]. Nevertheless, Lipoid EPC® yields a narrower peak than Lipoid E80®, which shows a very broad transition stretching below 0°C. As the fatty acid profiles of both are comparable, this difference must be a result of the higher content of minor components present in the Lipoid E80®. In contrast to the reports of Diederichs [1993], who observed transition peaks at about

29.4°C and transition enthalpies of 24.5 mJ/mg, the latter were found to be 32.34 mJ/mg for Lipoid E80® and only 20.84 mJ/mg for Lipoid EPC®. However, according to the literature [Marsh, 1990], enthalpies of about 40 - 58.4 mJ/mg would be expected for PC containing unsaturated fatty acid chains (on the basis of the estimation of 770 mol/g). The deviations for the results reported here were probably owing to residual or re-adsorbed water content of the lecithins owing to their marked hygroscopicity [Small, 1986], as absorbed water may well account for the measurable lowering of the transition enthalpy. 7.2% w/w microfluidized liposomal dispersions in 2.25 wt% glycerol/water from Lipoid E80® show thermograms dominated completely by the sharp water freezing and melting peaks at -12.6°C and 2.6°C, respectively (not shown). No peaks arising from different lecithin concentrations could be observed. To shift the water peaks to lower temperatures and expose hereby the lecithin transitions, increasing amounts of glycerol were used in the dispersion medium. Thus, 30 wt% Lipoid E80® dispersed into 50 wt% glycerol/water (Fig. 42) shows a clear shift of the water freezing and melting peaks down to about -67°C and -31°C, respectively. This reveals broad solidification and melting peaks at about -11°C, similar in their width and shape to those observed for the desiccated lecithins. Similar behaviour has been reported for egg-yolk lecithin of unknown composition by Chapman [1975], who reported melting peaks at -15°C for the heating and -7°C for the cooling curve.

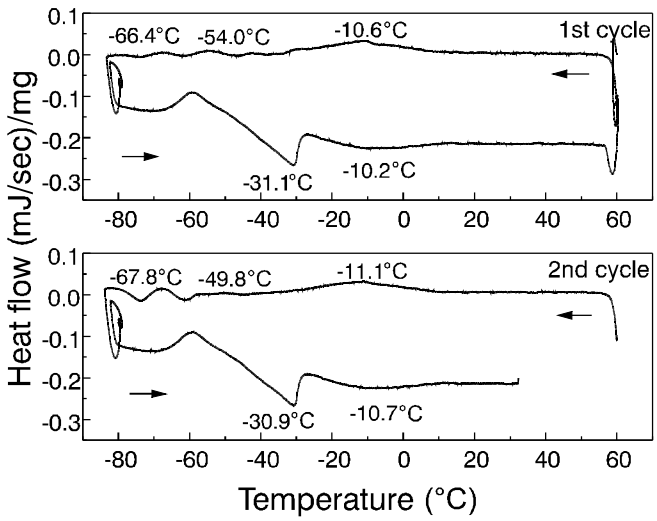

Fig. 42 DSC thermogram of 30 wt% Lipoid E80® in glycerol/water (50 wt%) at 3K/min

Diederichs [1993] reported broad transitions ranging from -35°C to +18°C with a peak maximum at about -10°C with 15% water content, and stressed that no peaks could be found at higher water contents. It is evident from Fig. 42 that the homogenisation temperature for emulsions stabilised with Lipoid E80® need not be above room temperature to yield an L_α

phase of the fully hydrated lecithin. To control the influence of factors like emulsifier hydration, diffusion and hydrolysis, which are strongly dependent on the temperature, model emulsions should, however, be predispersed at elevated temperatures to allow fast hydration of the emulsifier.

3.1.3.2 Characterisation by FT-IR

Using FT-IR, subtle shifts of the hydrocarbon- or carbonyl absorption bands of phospholipids can be detected, especially the CH_2-stretching and -scissoring modes reflecting the state of order in the acyl chains in the fatty acid residues [Fookson and Wallach, 1978 / Fringeli and Guenthard, 1981 / Casal and Mantsch, 1984]. Shifts towards higher frequencies, e.g. at 2850 cm^{-1} or 2920 cm^{-1}, indicate an increasing proportion of gauche to trans conformers, as occurs for the chain melting at the main transition of the lipid chains [Casal and Mantsch, 1984]. It is therefore possible to assess phase transitions using FT-IR by recording temperature-dependent spectra. A well-characterised example is DPPC [Fookson and Wallach, 1978], where hydrogen-bonding shifts the phosphoryl band at 1254 cm^{-1} to 1248 cm^{-1}. For DPPE, the same band appears at 1222 cm^{-1} owing to strong intermolecular hydrogen-bonding, which is also reflected in the spectra of mixed films of DPPC/DPPE, where the phosphoryl band lies in between those of the pure species and somewhat closer to the value of DPPC. The authors concluded that intermolecular hydrogen-bonding of the PE molecules is reduced and intermixing of both phospholipid classes becomes possible, especially at more alkaline pH where NH-O hydrogen-bonding becomes increasingly disrupted. Casal and Mantsch [1984] reported the main transition (chain melting) at 41.5°C for hydrated DPPC as determined from the CH_2-stretching modes. The pre-transition at 35°C was determined using the CH_2-scissoring modes. The carbonyl-stretching modes were also reported by these authors to be sensitive to the main transition, when head groups change conformation owing to chain movement. In the case of unsaturated egg-yolk PE, a L_α-H_{II} (lamellar-inverted hexagonal) transition was detectable, which occurred at lower temperatures when more unsaturated fatty acids residues were present. Fig. 43a shows that non-desiccated Lipoid EPC® contains water (arrows indicate OH-modes caused by water) which could not be detected by DSC measurements. To dry films prepared from chloroform solutions, residual solvent and water were therefore removed by evacuating the sample for 12 h, which now showed the absence of water OH-stretching modes in Fig. 43b.

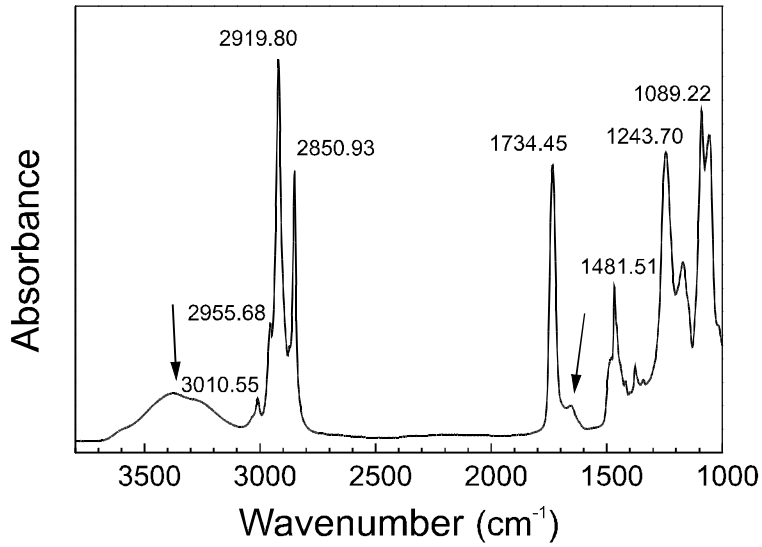

Fig. 43a ATR/FT-IR spectrum of non-dried Lipoid EPC® at ambient temperature

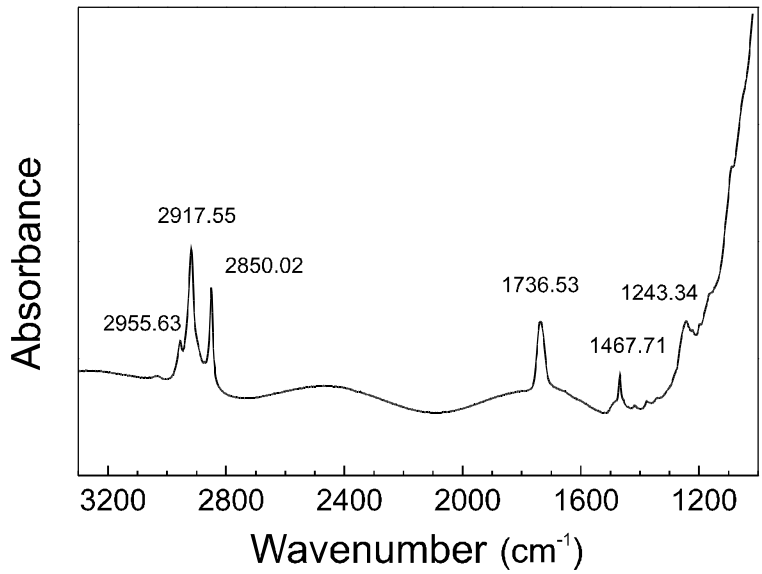

Fig. 43b FT-IR spectrum of desiccated DPPC from chloroform solution at 21°C

Tab. 17 gives an overview of the typical values of the bands most important for analysis of lipids and phospholipids examined here:

IR-Band	Wavenumber (cm^{-1})
C=O (sn-1 / sn-2) – stretching (in esters)	1742 / 1725
C-O – stretching	1170 + 1070
C=O – stretching (in acids)	1700-1725
CH_2 – stretching, antisymmetric	2920
CH_2 – stretching, symmetric	2850
CH_2 – deformation (scissoring)	1465
CH_2 – deformation (wagging)	1305
CH_2 – deformation (twisting)	1180-1345
CH_2 – deformation (rocking)	720
Terminal CH_3 – stretching, antisymmetric	2956
Terminal CH_3 – stretching, symmetric	2870
=C-H – stretching, antisymmetric	3010
CH_3 – stretching in $N(CH_3)_3$, antisymmetric	3040
$N-(CH_3)_3$ – stretching, antisymmetric	970
C-N – stretching, antisymmetric	945
PO_2 – stretching, symmetric	1085-1100
PO_2 – stretching, antisymmetric	1220-1250
P-O – stretching, antisymmetric	815-825
-OH – stretching	3200-3600

Tab. 17 IR-bands of importance for phospholipid analysis (after Fringeli and Guenthard [1981], Weers and Scheuing [1991] and Guenzler and Boeck [1993])

Fig. 44 shows the temperature dependence of the symmetric CH_2-stretching mode of DPPC, which was dispersed in water and heated to 60°C, vortexed and frozen to -20°C. This

freeze-thaw cycling followed by vortexing was repeated four times to achieve fully hydrated material. A clear shift of about 2 cm^{-1} is observed, indicating L_β-L_α chain melting at 39°C, which is the shift reported by Wallach et al. [1979] and Cortijo et al. [1982]. The deviation from the literature value of 41.5°C [Casal and Mantsch, 1984] is assumed to be a result of the slower heating rate of 0.2 K/min used here. The desiccated DPPC shows no shift in the range up to 80°C, as no transition is expected to occur below 110°C [Small, 1986]. This effect demonstrates the influence of water on the thermal behaviour of the phospholipids. Hydration of the head groups and subsequent head group packing rearrangement lead to a decrease in the transition temperature shift and its enthalpy [Cevc and Marsh, 1987]. The symmetric stretching mode has the advantage over the asymmetric band at about 2930 cm^{-1}, that it is less easily overlapped with other modes [Casal and Mantsch, 1984]. For DPPC, the main transition could be observed from the concomitant shift of the asymmetrical CH_2-stretching mode and the CH_2-scissoring mode.

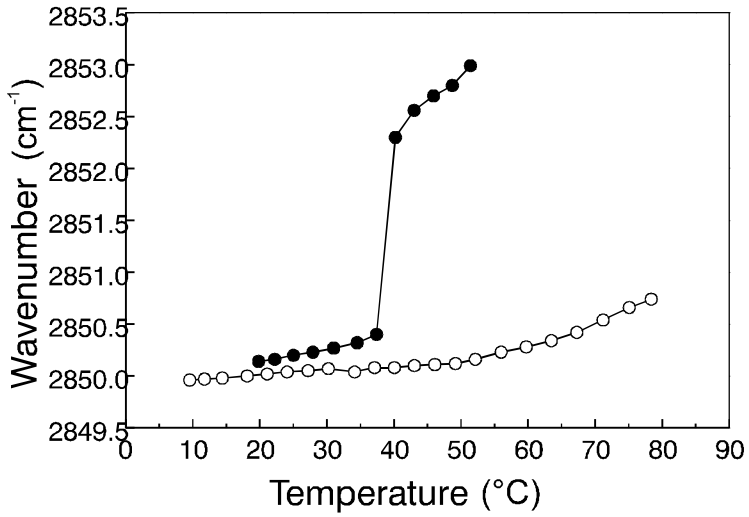

Fig. 44 Peak location for CH_2-symmetrical stretching modes of desiccated (○) and fully hydrated DPPC (●)

The commercial lecithins were dissolved in chloroform and dried as a thin film on a CaF_2-window under vacuum for about 12 h. Figs. 45 and 46 show clear shifts of the CH_2-stretching and -scissoring modes. The transition is, however, less sharp than that of hydrated DPPC in Fig. 44.

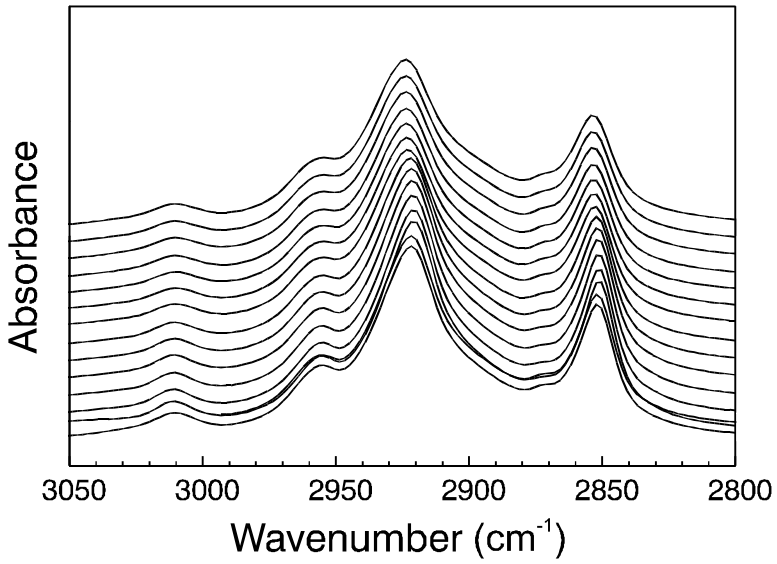

Fig. 45 FT-IR spectra of dry Lipoid E75® at 9-51°C with 3°C increment from bottom to top: region of the CH_2-stretching modes

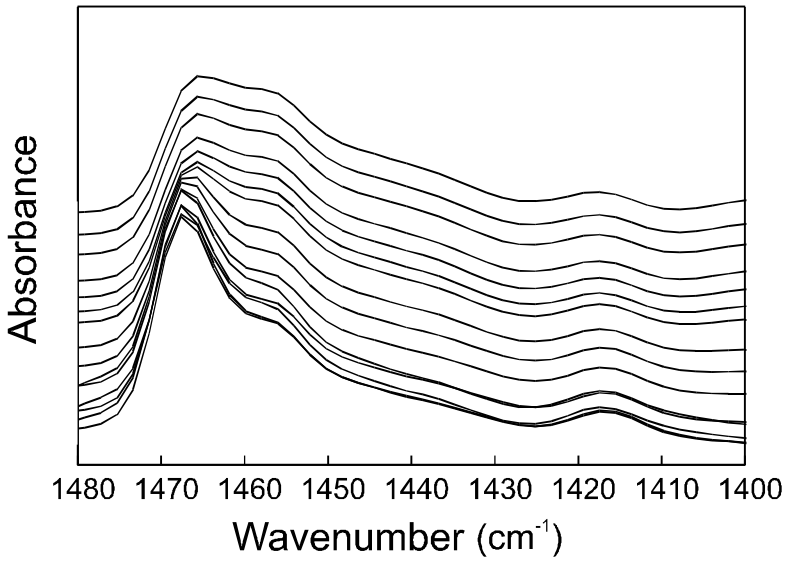

Fig. 46 FT-IR spectra of dry Lipoid E75® at 9-51°C with 3°C increment from bottom to top: region of the CH_2-scissoring bands

Figs. 47 and 48 summarise the temperature-frequency dependence of the CH_2-stretching and -scissoring modes for the different desiccated Lipoid® lecithin types. The wide transitions occur at approx. 43°C for Lipoid EPC®, 32°C for Lipoid E75® and 29°C for Lipoid E80® in desiccated samples. The desiccated lecithins possess, therefore, lower transition temperatures than dry DPPC (Fig. 44) owing to their higher content of unsaturated PC species. This is further lowered slightly by the higher content of impurities in Lipoid E75® and Lipoid E80®.

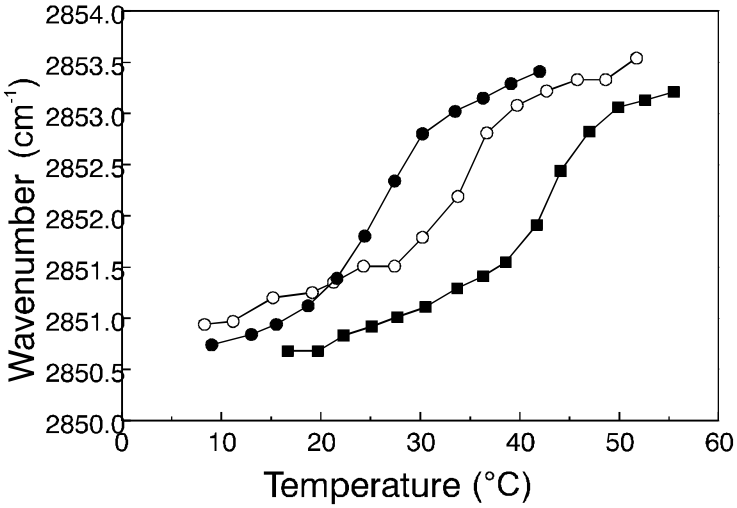

Fig. 47 Peak location for CH_2-symmetrical stretching modes of desiccated Lipoid E75® (○), Lipoid E80® (●) and Lipoid EPC® (■)

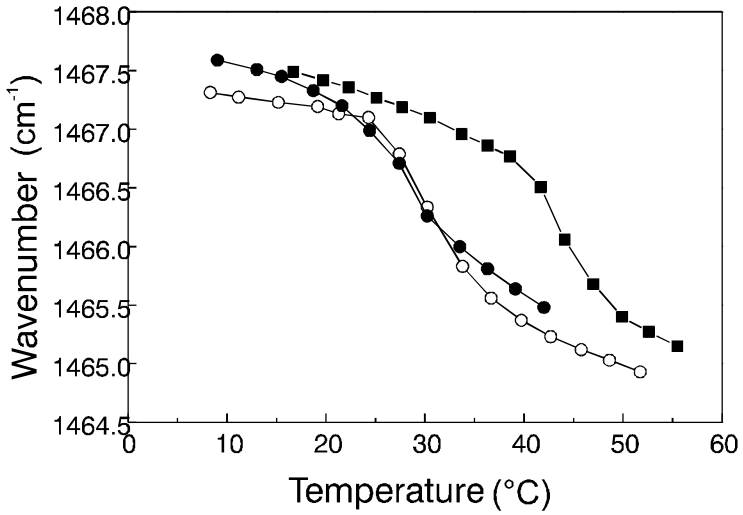

Fig. 48 Peak location for CH_2-scissoring modes of desiccated Lipoid E75® (○), Lipoid E80® (●) and Lipoid EPC® (■)

For Lipoid E75® and E80®, these chain melting transitions lie at similar values, although theoretically the 'purer' Lipoid E80® is expected to have a higher transition temperature than Lipoid E75®. Indeed, with Lipoid E80® the DSC peak maximum was 5°C lower. The residual water content in the DSC samples could not, however, be controlled as closely as with the FT-IR method. The main transition for Lipoid EPC® occurs 15°C higher than that determined from its DSC peak maximum (Fig. 40). This may again be a question of higher residual water content in the DSC samples, or simply reflect the difference between the two techniques.

Detection of the main transition for hydrated Lipoid E80® is shown in Figs. 49 and 50.

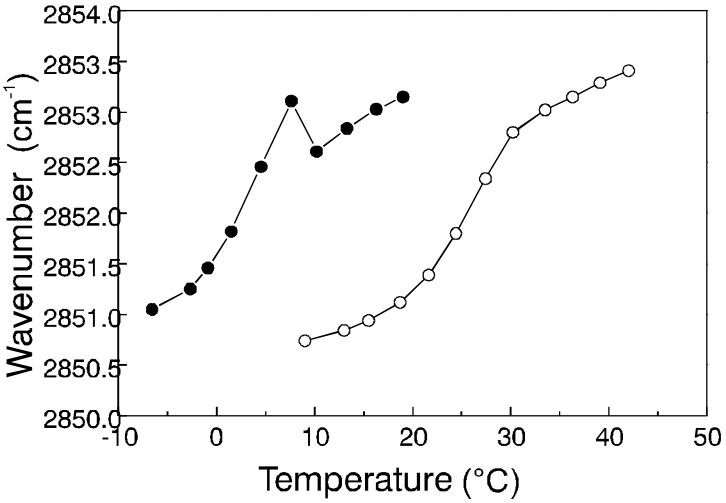

Fig. 49 Peak locations for CH_2-symmetrical stretching modes of desiccated (○) and fully hydrated Lipoid E80® (●)

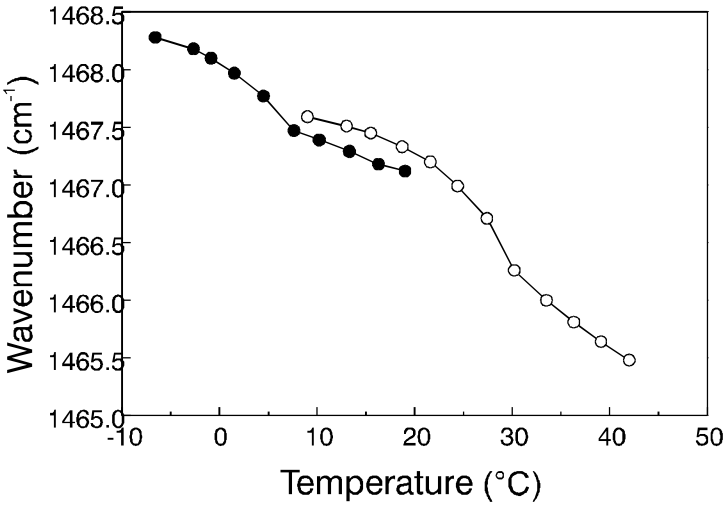

Fig. 50 Peak locations for CH_2-scissoring modes of desiccated (○) and fully hydrated Lipoid E80® (●)

In contrast to the DSC results (Section 3.1.3.1), it is thus possible to detect the gel-liquid crystalline phase transition for the fully hydrated Lipoid E80®. For the symmetrical CH_2-stretching mode an offset in the sigmoidal curve is apparent (Fig. 49), which can be assigned to the so-called 'ice-melting-induced shift', which usually is more easily detectable for modes which are strongly affected by hydrogen-bonding such as head group modes [Casal and Mantsch, 1984]. The detection of the gel-liquid crystalline transition is, however, not affected by this phenomenon and occurs at around 4.5°C, also about 15°C higher than the peak maximum determined from DSC data of the glycerol/water dispersion (Fig. 42). The DSC experiments gave, however, only a very broad transition ranging from -30°C to 10°C and thus do not enable assignation of distinct molecular mechanisms. From the FT-IR data, however, an

unequivocal correlation between acyl chain mobility and temperature is achieved, showing that upon hydration of Lipoid E80® a strong shift of the main transition occurs. All of the lecithin is present in the L_α-phase above approx. 10°C. The differences found for transitions determined by DSC and FT-IR could partly be a result of the slightly slower heating rate used for FT-IR (about 0.2 K/min.), which might have caused the DSC peaks to appear at a few °C lower than determined from FT-IR spectra. One of the most striking advantages of FT-IR is that even hydrated egg lecithin samples can be examined, whereas DSC thermograms quickly become overridden by the strong influence of peaks arising from water [Diederichs, 1993]. By computational subtraction of the typical water bands, the chain and headgroup bands of even minor compounds are detectable with FT-IR.

3.1.3.3 Characterisation by X-Ray Diffraction

From x-ray diffraction spectra it is possible inter alia to discern between anisotropic and isotropic phases. Following the Bragg equation, one can calculate molecular spacings from the typical scattering angles observed [Cevc and Marsh, 1987]. In Fig. 51, the temperature-dependent x-ray diffraction patterns for desiccated Lipoid EPC® are depicted, showing reflections (especially a sharp peak at 20.3° = 4.85 Å repeat distance) indicating crystalline chain-packing at room temperature [Small, 1986 / Larsson, 1986], which still is the case at 22°C. At 52°C, it exists in the molten state with no three-dimensional repeat-distances occurring.

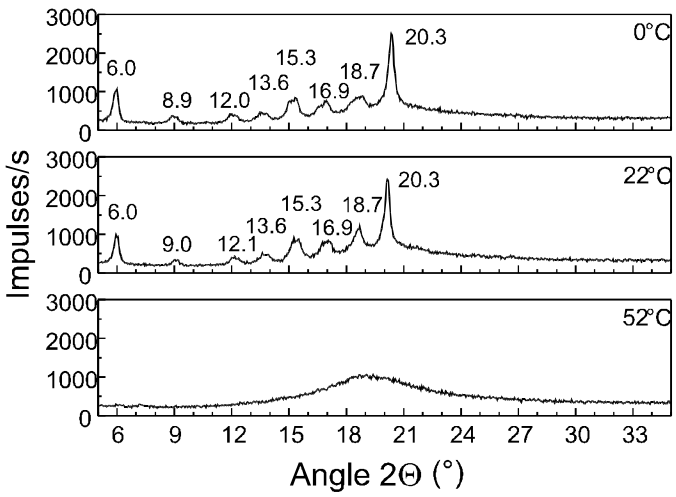

Fig. 51 X-Ray diffraction patterns for desiccated Lipoid EPC® at different temperatures

With Lipoid E80® (Fig. 52) and Lipoid E75® similar behaviour is found, confirming that complete melting of the lecithin crystals was achieved above 50°C. At 20°C, the diminished intensity of the reflection at 20.4° indicates incipient decrease in cristallinity.

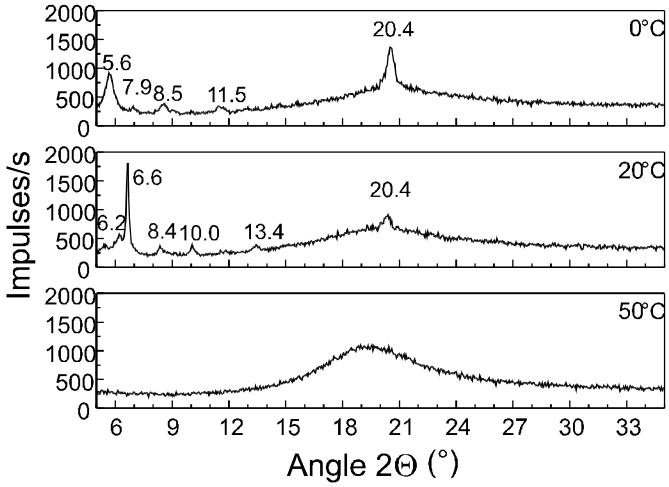

Fig. 52 X-Ray diffraction patterns for desiccated Lipoid E80® at different temperatures

These results confirm the data from DSC and FT-IR investigations.

3.2 Preparation of Emulsions, Solid Lipid Nanoparticles and Liposomes

The influence of emulsifier composition, its total content and manufacturing conditions on product properties were examined from measurement of particle size distribution, Zeta potential and emulsifier composition during production. Commercial formulations are reported for comparison.

3.2.1 Limitations on Determination of Particle Size

The most frequently employed methods for submicron emulsion particle analysis nowadays are PCS and LD [Groves, 1984 / Komatsu et al., 1995 / Schuhmann, 1995]. Other authors reported higher sensitivity for the largest droplet fractions using Coulter Counter sizing [Washington and Sizer, 1992 / Schuhmann et al., 1993], which, however possesses only a limited measurement range (> 700 nm), and prerequisite sample dilution in saline solutions promotes emulsion instability and coalescence [Schuhmann and Mueller, 1998]. Westesen and Wehler [1993] stated that the ‘intensity distributions’ obtained from PCS measurements were not useful for calculation of number or volume distributions. Preliminary experiments in this work showed, indeed, that monomodal cumulant analysis always yielded log-normal distributions even for broad, polydisperse distributions as expected for the emulsions investigated. Fig. 53 shows that samples were fitted to a perfect log-normal distribution by cumulant analysis, which does not necessarily represent their true distribution shape.

Liposomes present may, for example, form a second distribution which is not resolved. Only z-average values and polydispersity index (PI) are, therefore, reported here. Dilution of the emulsion samples did not alter the size distributions obtained as could be verified beforehand. PCS is limited to detection of particles undergoing Brownian motion [Mueller and Schuhmann, 1996], and particles larger than approx. 3 µm are therefore not detectable. As shown in Fig. 54, a visibly broken emulsion could not be correctly analysed with PCS. It was, nevertheless, possible to detect a pronounced increase in z-average and PI, which allowed coalescence to be qualitatively followed.

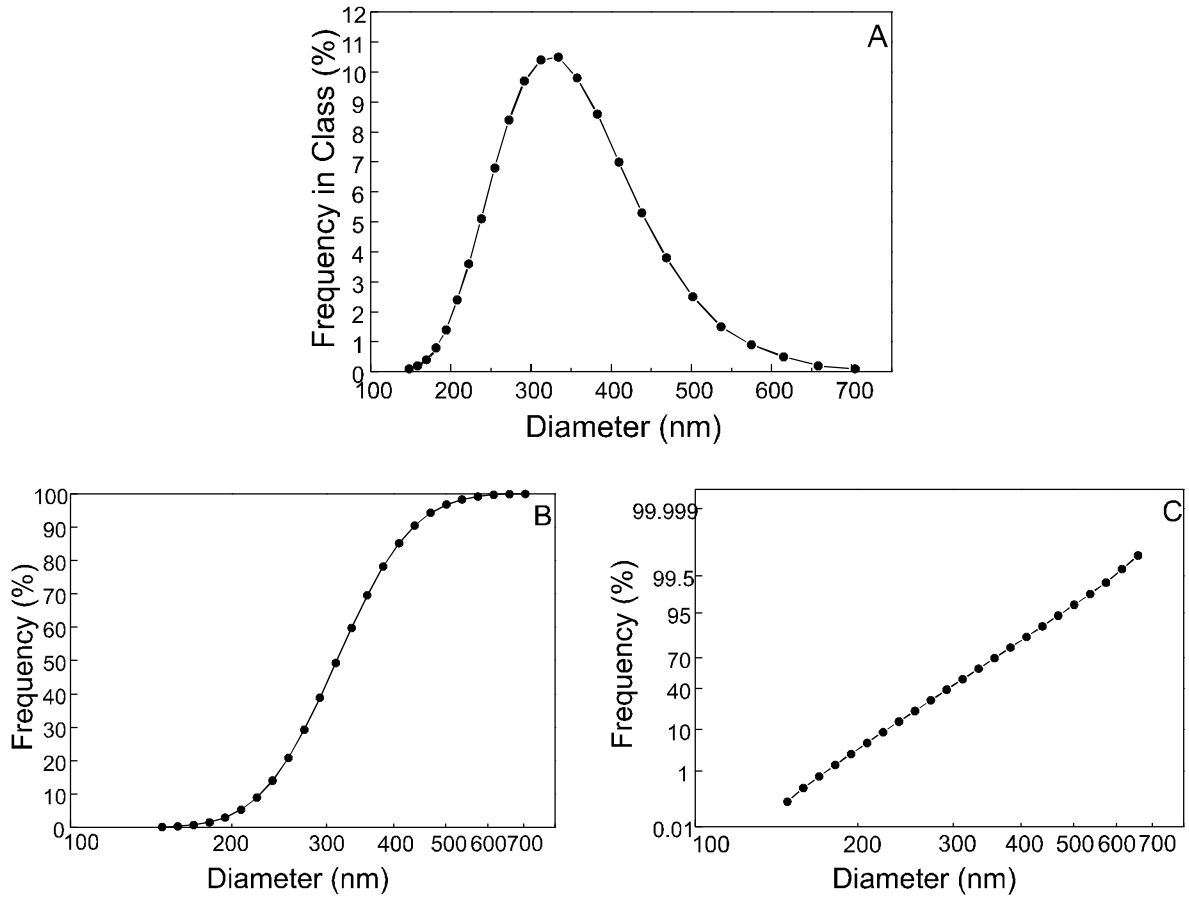

Fig. 53 PCS intensity distributions of a 20% soya oil emulsion **(A)**, cumulative percentage frequency curve in log-scale **(B)** and cumulative percentage frequency curve in log-probability scale **(C)**

Laser Diffractometry (LD) determines particle distribution from the actual intensities on the detector elements. Thus multimodal, polydisperse samples can also be resolved with high-resolution. To examine the upper region of emulsion size distributions which are of special interest regarding their parenteral use, better sensitivity towards larger particles could be

achieved by evaluating the diffraction data using the Fraunhofer approximation and presenting data in the form of volume distributions [Kohlrausch and Steffens, 1997]. However, more precise detection of the whole emulsion size range, especially at the lower size range, is achieved using the Mie approximation. As it is, however, difficult to determine the necessary values for the refractive index of the dispersed phase, Mie calculations were carried out assuming different refractive indices ranging from 1.33 (for water) to 1.59 (for polystyrene standard latex dispersions).

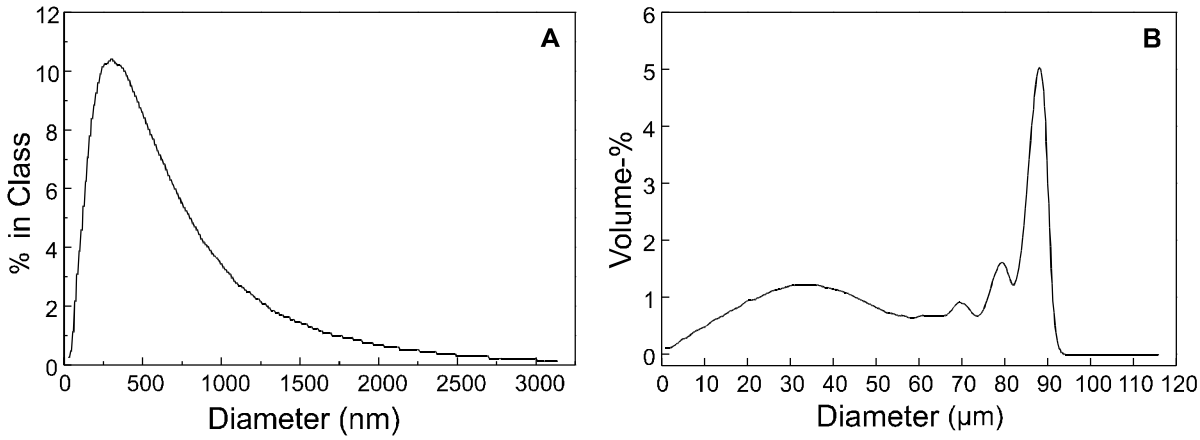

Fig. 54 PCS intensity distribution **(A)** and an LD (Fraunhofer) distribution **(B)** of a broken 20% soya oil emulsion

3.2.2 Influence of Emulsifier Concentration

The Microfluidizer® 110S is especially designed for lab-scale homogenisation with a volume of 12 ml and a dead volume of only 1 ml. Thus, small batches can easily be produced, as well as larger volumes by refilling crude product in the reservoir and gathering the homogenised product at the outlet. It proved useful not to use the continuous 'recycling' mode, as in that case only about 6 ml per cycle were processed through the interaction chamber, and some unemulsified droplets (in the case of emulsions) and foam were found floating on top of the liquid. Accordingly, this material could never be cycled through the dissipation zone. By processing the whole batch through the machine at once, no crude, unhomogenised material was evident. The collected sample was then refilled into the reservoir and recycled through the homogeniser.

Liposomes were prepared by microfluidization of the aqueous lecithin pre-dispersions. Mayhew et al. [1984] claimed that almost pure SUVs could thus be produced. PCS measurements of 1.2 wt% up to 7.2 wt% liposome dispersions were performed in their

undiluted state (Fig. 55) and showed that particle size constantly decreases during homogenisation, yielding almost exclusively small liposomes. Particle size falls drastically after the first homogenisation cycle and drops more slowly upon recycling, until final z-average diameters are in the range of approx. 50-120 nm after 11 cycles. Similarly, the width of size distribution detected by PCS (PI) dropped over 3 cycles, then remained constant at about 0.64, which indicates broadly distributed dispersions.

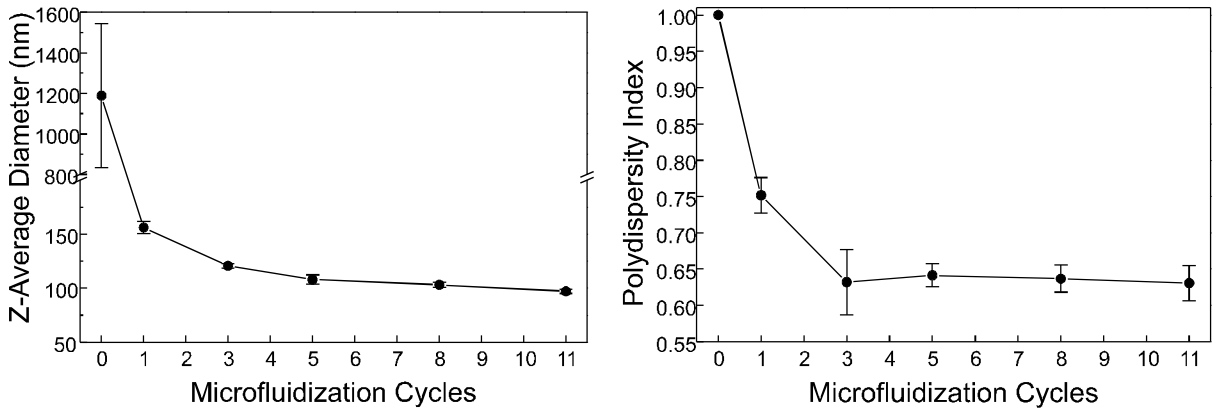

Fig. 55 Dependence of z-average diameter and polydispersity index of 7.2 % w/w Lipoid E80® (liposome) dispersions [homogenised at 1000 bar; n=5]

Fig. 56 shows the volume distributions for the example of a 3.6 wt% Lipoid E80® dispersion obtained from LD using PIDS and Mie calculation. Different assumptions of refractive index for the Mie calculation have an effect on the distribution, although not very pronounced. SUVs are, therefore, detectable with LD using the PIDS technique and Mie calculation. The best agreement with PCS measurements was observed for refractive indices of 1.33 and 1.44.

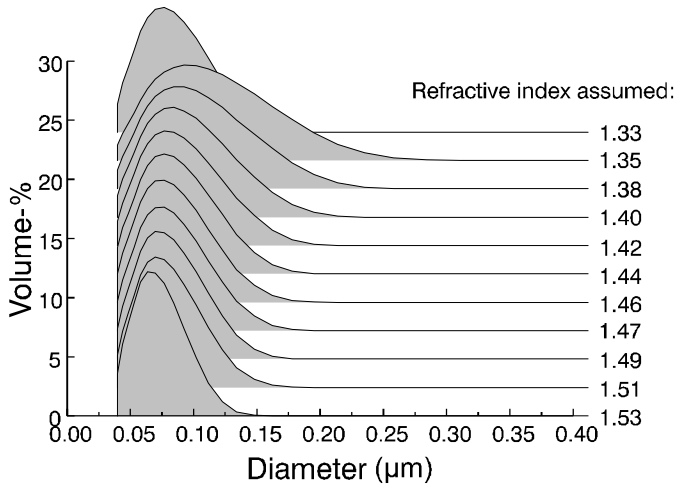

Fig. 56 Volume distribution of a 3.6 wt% Lipoid E80® (liposome) dispersion homogenised at 1000 bar and measured by LD with PIDS using different refractive indices for Mie calculation

However, liposomal dispersions showed weak diffraction intensities, which necessitated as much as 4 ml of the dispersions to be diluted to 150 ml. As liposomes represent hollow spheres, it is also unclear what value for their refractive index is valid. As is shown later, this causes problems when determining liposomes in the presence of oil droplets in emulsions (Section 4.3.2).

Ishii et al. [1990] and Chaturvedi et al. [1992] reported that submicron emulsions with 10% or 20% oil were less stable when lecithin was reduced below 1.2% w/v. Reduction of lecithin in commercially available 10% emulsions to 0.6% w/v has, however, already been realised. In commercial emulsions, lecithin:oil ratios of 0.12 (the older 10% emulsions), 0.06 (the newer 10% and 20% emulsions) and 0.04 (30% emulsions) are available. To examine the influence of this lecithin:oil ratio on emulsion properties, different oil contents of 5% up to 30% w/w emulsions were employed at fixed homogenisation pressure and amount of emulsifier. Fig. 57 shows the results for 10% and 20% w/w emulsions homogenised at 700 bar.

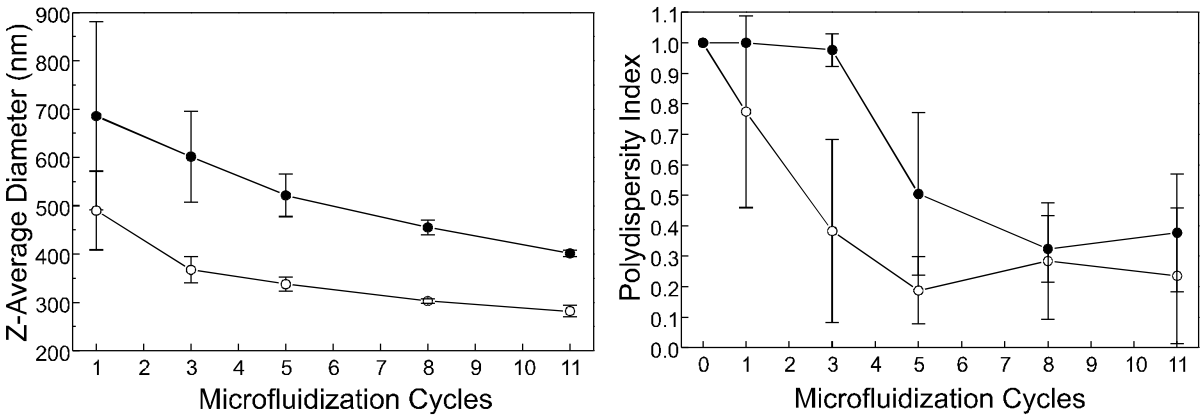

Fig. 57 Dependence of z-average diameter and polydispersity index on soya oil content of emulsions using 1.2 wt% Lipoid E80®:
20 wt% soya oil (●) and 10 wt% soya oil (○) [homogenised at 700 bar; n=5]

It is evident that particle size reduction and homogeneity are a function of number of cycles, as has been reported by Washington and Davis [1988] and Bock et al. [1994]. Contrary to their findings, however, particle size reduction and narrowing of distribution width continues until the last cycle, especially when a higher oil content is emulsified. Therefore, subsequent emulsions were homogenised for 11 cycles. Although the homogenised samples were kept at 30°C after each cycle, it can be assumed that on passing the interaction chamber they were heated by approx. 20°C before being cooled again by the heat exchange coil [Microfluidics International Corp., 1996]. For constant emulsifier concentration and homogenisation conditions, the dependence of z-average mean diameters on oil phase content yields a sigmoidal curve (Fig. 58), reported similarly by Ishii et al. [1990].

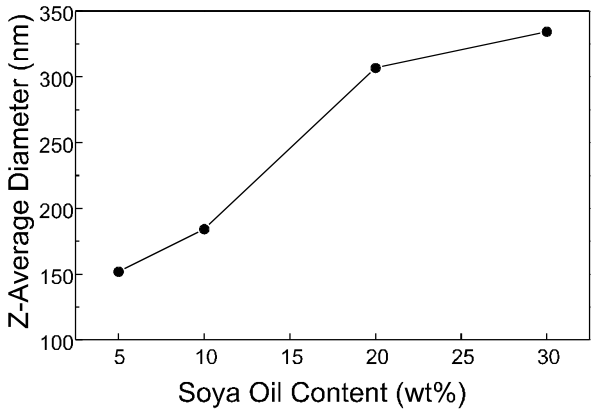

Fig. 58 Dependence of z-average diameter on soya oil content of emulsions using 1.2% w/w Lipoid E80® [homogenised for 11 cycles at 1000 bar; n=5]

Commercial and model 10% emulsions with reduced lecithin content show larger PCS z-average diameters (see Tab. 18) than with 1.2% lecithin. This could be caused either by larger emulsion droplets or by less emulsifier excess, which would, as liposomes, reduce the overall particle size measured. Fig. 59 illustrates the effect of reduced lecithin content on 10% model emulsion particle diameters. No difference in PI can, however, be seen.

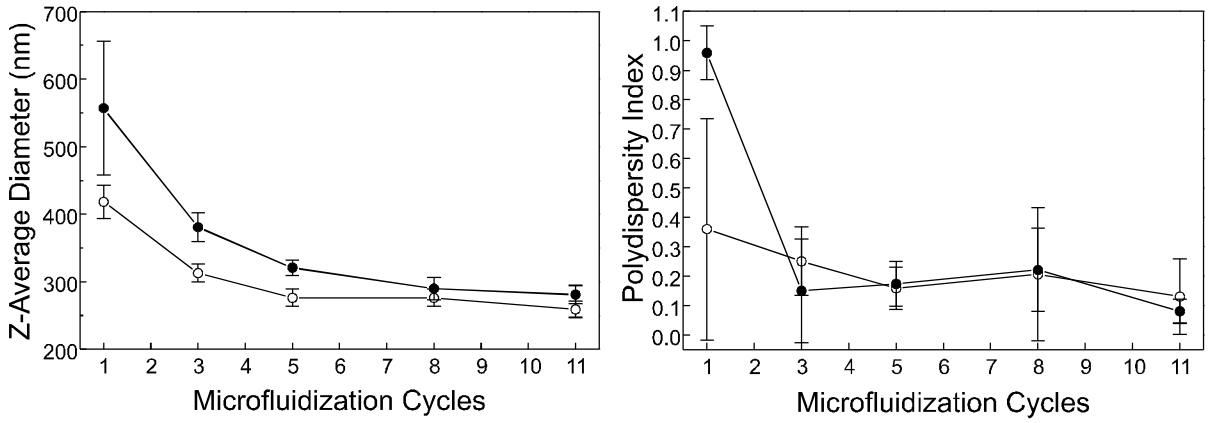

Fig. 59 Dependence of z-average diameter and polydispersity index of 10 wt% soya oil emulsions on Lipoid E80® concentration: 0.6 wt% lecithin (●) and 1.2 wt% lecithin (○) [homogenised at 1000 bar; n=5]

Bock [1994] suggested that increasing emulsifier content in the oil phase counteracted droplet disruption by increasing dispersed phase viscosity. This could not be confirmed to have any influence on the 10% emulsion formulations investigated here.

3.2.3 Influence of Emulsifier Composition

Emulsions could not be stabilised using pure PC; Hansrani [1980] and Yamaguchi et al. [1995b] reported that certain 'impurities' were necessary to form stable emulsions. Emulsions from 1.2 wt% Lipoid® EPC (pure PC) indeed cracked immediately when 20% oil phase was incorporated, and showed measurable coarsening for 10% oil on 12 weeks' storage. Surprisingly, the addition of only 0.02 wt% of sodium oleate yielded stable emulsions even with 20% oil (Tabs. 18 and 21), which showed similar particle size to emulsions containing Lipoid E80® (Fig. 61). The droplet interface coalescence experiments implicated, however, that addition of such small amounts of sodium oleate does not lead to such a pronounced effect on coalescence stability (Fig. 32). A clear effect of oleate could, however, be observed on the Zeta potential-pH-plots for Lipoid® EPC emulsions (Fig. 60), which may explain the remarkable increase in emulsion stability [Yamaguchi et al., 1995a].

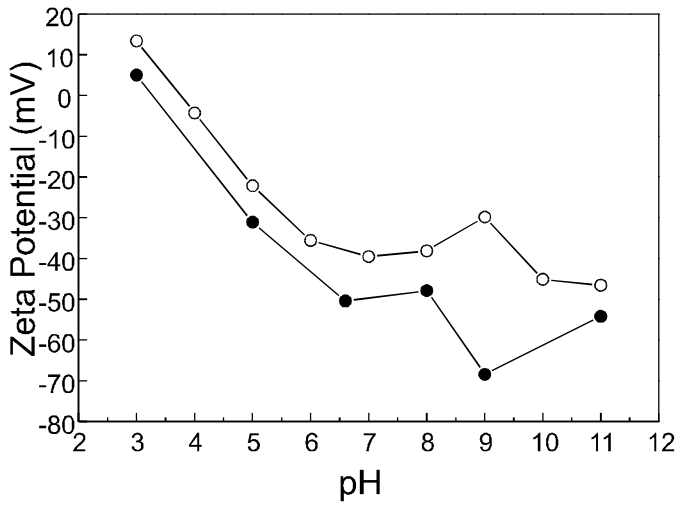

Fig. 60 Influence of pH on Zeta potential for non-autoclaved 10% w/w soya oil emulsion stabilised with 1.2% w/w Lipoid EPC® (○) and 20% w/w emulsion with 1.2% w/w Lipoid EPC® + 0.02% w/w sodium oleate (●)
[homogenised at 1000 bar]

Muchtar et al. [1991] reported that emulsions made with pure PC showed Zeta potential values of -30 mV, whereas stable emulsions from purified lecithin admixed with negatively-charged minor components exhibited values of -45 to -57 mV. The influence of pH and Zeta potential will be discussed in more detail in Section 3.2.5.

PC alone is obviously insufficient to stabilise the freshly-formed interface during high-pressure homogenisation. A water-soluble co-emulsifier like sodium oleate would locate at the interface faster and thus be more effective than PC. Fatty acids are either incorporated at the oil-water interface, possibly increasing repulsive surface charge by forming an integral part of

the emulsifier film, or allow at least short-time stabilisation of the new interface until PC gradually becomes available and replaces the fatty acids. Sodium oleate added to emulsions prepared from Lipoid E80® also showed a slight reduction in z-average diameter (Fig. 61). However, a more pronounced effect was detectable for the early stages of homogenisation (cycles 1-3) where most of the uncovered, unstable oil-water interface was being created. Since the z-average diameter dropped faster for the admixed emulsions, a more rapid and effective stabilisation occurred for the systems containing the co-emulsifier. During cycles 4-11, where mainly disruption of remaining larger droplets occurs, the difference effectively disappears, as recoalescence becomes less important at this stage.

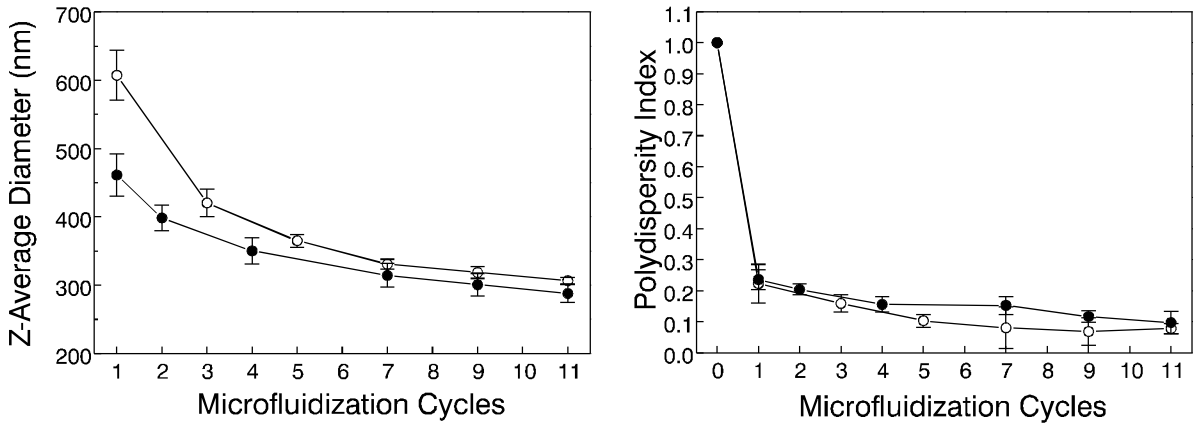

Fig. 61 Z-average diameter and polydispersity index of 20% w/w soya oil emulsions with 1.2% w/w Lipoid E80® (○) and additional 0.03% w/w sodium oleate (●) [homogenised at 1000 bar; n=5]

An even stronger effect is observed when Pluronic® F68 (dissolved in water) is used as the sole water-soluble emulsifier. It stabilised the newly-created interface immediately (Fig. 62). Within only one homogenisation cycle maximum dispersity is already reached and cannot be further reduced by repeated homogenisation. As Pluronic® F68 is a non-ionic emulsifier and produces sterically-stabilised emulsions [Eccleston, 1992], effects on Zeta potential were not assumed to be responsible for these findings. To allow application of high homogenisation pressure to improve dispersity of the emulsions and concomitantly avoid recoalescence during homogenisation, addition of a water-soluble compound such as fatty acid salts is very effective in improving the emulsification properties of lecithin. Depending on the duration of the pre-emulsification step, incipient hydrolysis of the lecithin could provide in situ production of fatty acids and, perhaps, also lyso-phospholipids (see Section 3.2.5.3). Since lyso-PC also reduces coalescence rates in the droplet/interface coalescence experiments (Fig. 30/ Tab. 11) and is more water-soluble than PC, the presence of both hydrolysis products may enhance stability against recoalescence during homogenisation. A marked effect of fatty acids on electrostatic

repulsion during homogenisation is, however, only expected at alkaline pH, thus increasing their degree of ionisation (see also Section 3.2.5).

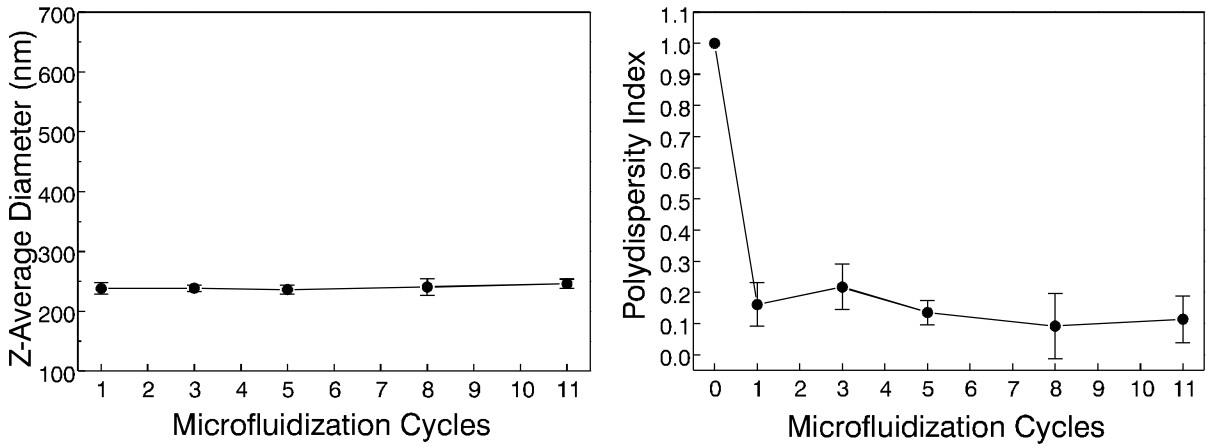

Fig. 62 Z-average diameter and polydispersity index of 20% w/w soya oil emulsions with 1.2% w/w Pluronic F68® [homogenised at 1000 bar; n=5]

Emulsions prepared from Lipoid E75® gave similar particle sizes as with Lipoid E80®. PCS results for homogenised lecithin dispersions also yielded comparable size values for the different lecithin types employed (Tab. 19).

3.2.4 Influence of Homogenisation Conditions

According to Washington and Davis [1988], Ishii et al. [1990] and Bock et al. [1994], the most important homogenisation parameters for controlling droplet size are *homogenisation pressure, temperature* and *duration* (number of cycles). From Washington and Davis [1988] and Bock [1994] it is known that higher temperature results in more effective disruption of droplets, but according to Bock et al. [1994] slightly broader particle size distributions and larger diameters for the largest droplets result when high temperature is used together with high homogenisation pressure for more than three cycles. This can be regarded as a typical case of overprocessed emulsions, where dispersion efficacy exceeds the stabilisation capability of the emulsifier. Stang and Schubert [1997] reported that stability against recoalescence could be considerably improved when critical droplet collisions are minimised by using a turbulent pipe flow adjacent to the dispersion zone. A conventional valve homogeniser was used, however, where cavitation was responsible for droplet disruption, and which yields larger particles for the same energy density compared with jet homogenisers like the Microfluidizer® [Schubert, 1997]. This might also account for their observation of generally broader size distributions.

Temperature was not varied in the following experiments to avoid irreproducible influence on chemical degradation (hydrolysis) of the lipids during homogenisation.

Fig. 63 gives the results for variation of microfluidization pressure for the example of model 20% emulsions. Higher emulsification pressure produces more rapid reduction of particle size and more homogeneous samples (as indicated by the more rapid reduction of PI values). This trend is consistent with the findings of Washington and Davis [1988], although these authors reported that homogenisation for only 6 cycles at approx. 700 bar yielded better dispersity than observed for 700 bar in Fig. 63. However, final particle sizes were also found to be the lowest for all samples where the highest pressure (1000 bar in our case) had been used.

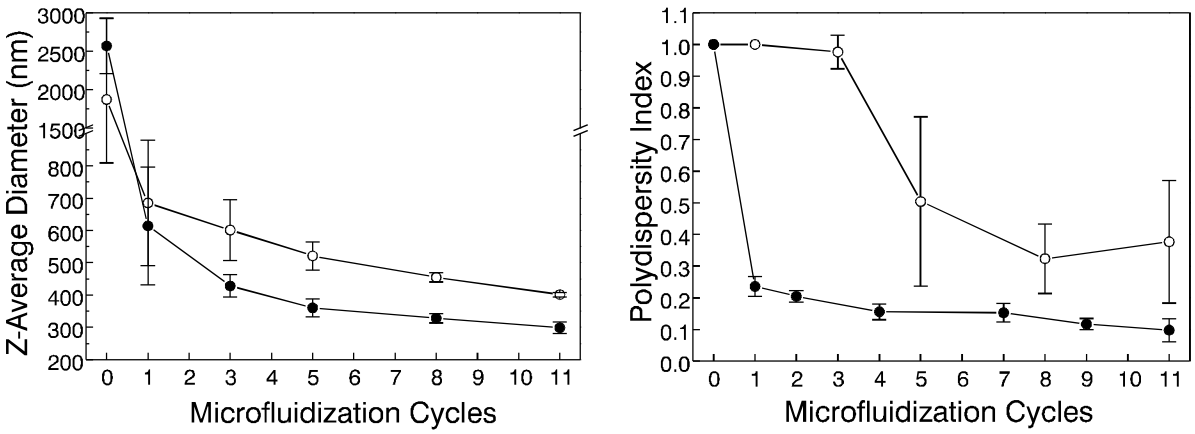

Fig. 63 Influence of different homogenisation pressure on z-average diameter and polydispersity index of 20% w/w soya oil emulsions using 1.2% w/w Lipoid E80®: 1000 bar (●) and 700 bar (○); [n=5]

Evidently no overprocessing occurred for the samples at these conditions (1000 bar, 30°C). Judging from this result, emulsions should be homogenised at the highest pressure and for as many cycles as possible to achieve the smallest particle sizes and to disperse the emulsifier efficiently and thus reduce free lecithin content. However, to produce sufficiently small mean diameters with fewest proportion of droplets > 1 µm, just 3 - 5 cycles seem to suffice. To exploit more effectively the energy density applicable during homogenisation and yet avoid recoalescence, addition of a co-emulsifying agent like e.g. sodium oleate could improve the homogenisation results.

Tab. 18 and Tab. 19 summarise typical particle sizes (according to PCS and LD measurements) obtained for model emulsions and commercial formulations, as well as model liposome dispersions. These values will be referred to continually in the following sections.

Emulsion	Z-Average (nm)	Polydispersity index	LD $d50_{Vol}$ (nm)	LD $d90_{Vol}$ (nm)
5%, 1000 bar, 1.2% LipoidE80®	151.8	0.124	270	840
Intralipid 10® (68460-51)	320.3	0.107	500	920
Lipovenoes 10 PLR®	348.1	0.098	450	790
Lipofundin 10% N®	347.1	0.161	450	800
Lipofundin MCT 10®	274.4	0.071	310	570
10%, 400 bar, 1.2% LipoidE80®	291.8	0.146	n.d.	n.d.
10%, 700 bar, 1.2% LipoidE80®	233.6	0.073	n.d.	n.d.
10%, 1000 bar, 0.6% LipoidE80®	239.6	0.057	330	750
10%, 1000 bar, 1.2% LipoidE80®	184.2	0.081	270	580
10%, 1000 bar, 1.2%LipoidEPC®	232.4	0.106	350	810
Intralipid 20® (85375-51)	365.4	0.165	480	880
Lipovenoes 20®	374.3	0.088	390	730
Lipofundin 20% N®	370.0	0.137	490	870
Lipofundin MCT 20®	282.5	0.073	350	590
20%, 700 bar, 1.2% LipoidE80®	401.6	0.377	n.d.	n.d.
20%, 1000 bar, 1.2% LipoidE80®	306.6	0.078	480	910
20%, 1000 bar, 1.2%LipoidE80® 0.03% sod.oleate	287.8	0.098	400	760
20%, 1000 bar, 1.2%LipoidEPC® 0.02% sod.oleate	309.6	0.119	410	710
20%, 1000 bar, 1.2%PluronicF68®	268.0	0.111	460	900
Intralipid 30® (87537-51)	513.5	0.127	570	960
30%, 1000 bar, 1.2%LipoidE80®	334.3	0.050	450	950

Tab. 18 Typical particle size distributions of commercial and model parenteral emulsions by PCS (intensity distribution) **(left)** and Laser Diffractometry [Mastersizer Micro, Fraunhofer Mode, 50% and 90% of volume distribution] **(right)**

For LD measurements volume distributions are typically reported as few larger particles can be detected more easily [Groves, 1984]. Similarly, presentation of diffraction data by Fraunhofer theory achieves better sensitivity towards larger droplets (> 5 µm) than using Mie theory [Kohlrausch and Steffens, 1997]. It can be seen that model emulsions produced at 1000 bar possess very small mean diameters, but are slightly broader in distribution than the commercial samples (d_{90} values). The smallest droplets are contained in the Lipofundin MCT® formulations, although the same amount of lecithin is contained in the LCT emulsions of the same manufacturer. As discussed above, the influence of oil phase content and emulsifier/oil ratio can also be deduced.

Lecithin dispersion	Z-Average (nm)	Polydispersity index
1.2% Lipoid E80®, 1000 bar	49.5	0.474
1.2% Lipoid EPC®, 1000 bar	88.4	0.695
3.6% Lipoid E80®, 1000 bar	74.1	0.557
3.6% Lipoid EPC®, 1000 bar	75.0	0.567
7.2% Lipoid E80®, 1000 bar	97.1	0.589

Tab. 19 PCS diameters of different microfluidized liposomal dispersions

For preparation of solid lipid nanoparticles as ‘solidified’ model emulsion systems, several waxes and solid fatty acids were tested. The best homogenisation (melting) and stability behaviour was found for cetylpalmitate. However, higher amounts of emulsifier for stabilisation had to be used, yielding particle size distributions similar to those for parenteral emulsions although somewhat broader. Dilute SLN dispersions *without emulsifier* were also prepared by solidification of the fluid droplets by pouring the microfluidized stream directly into a beaker placed in an ice bath with stirring until solidification. Considerable amounts of large aggregates resulted, however, which had to be removed by centrifugation, and the remaining SLNs aggregated within a few days. The sizes reported in Tab. 20 are in agreement with data from the literature (e.g. Mueller et al. [1995]). Lecithin was found to be more effective as an emulsifying agent compared with Pluronic F68®, as aggregation occurred with dispersions prepared with the latter after prolonged storage in the refrigerator.

SLN dispersion [w/w]	Z-Average (nm)	Polydispersity index
10% Cetylpalmitate, 4.8% Lipoid E80®, 1000 bar	178.5	0.176
10% Cetylpalmitate, 2.5% Pluronic F68®, 1000 bar	221.6	0.174

Tab. 20 PCS diameters of microfluidized solid lipid nanoparticle dispersions

3.2.5 Influence of pH Adjustment and Autoclaving

Various emulsions and liposome dispersions were steam-sterilised for different times under pharmacopeial conditions (121°C, 2 bar). Particle size was monitored with PCS and Laser Diffractometry, together with microscopical evaluation, to follow droplet stability. Chemical degradation of the emulsions' ingredients was determined by chromatographic analyses, which was also used to trace possible redistribution of lecithin components between aqueous and oil phase during autoclaving as had been reported by Groves and Herman [1993].

As had been proposed by Herman [1992], pH values in emulsions were measured after addition of increasing amounts of a saturated KCl-solution. By doing so, adsorption of ions onto the charged emulsion droplets ('dispersion effect'/ see Lee et al. [1989]) should be reduced. A similar procedure is also used for pH determination of dextrose solutions according to USP23/NF18 [1995], where ions other than H^+ and OH^- are absent. pH-values obtained for addition of increasing proportions of saturated KCl-solution to 8 ml of commercial emulsion samples are shown in Fig. 64. The pH values drop markedly by approx. one unit upon addition of KCl-solution, although KCl-solution was presumed to possess neutral or slightly acidic pH of 6-7. pH reached a plateau after addition of 500 µl solution to the original samples. However, Herman and Groves [1993] who added 50 µl to 2 ml of emulsion samples, reported that only half of this amount was necessary. Bock [1994], however, observed that electrode equilibrium is reached more slowly when electrolyte solution is added. Thus it was decided to measure pH in the subnatant aqueous phase obtained after centrifugation for 24 h at approx. 13000 g. pH measured in this way did not, however, differ from pH determined by direct measurement in the emulsions, showing that the dispersion effect does not occur. Values given here were therefore obtained from the untreated emulsions.

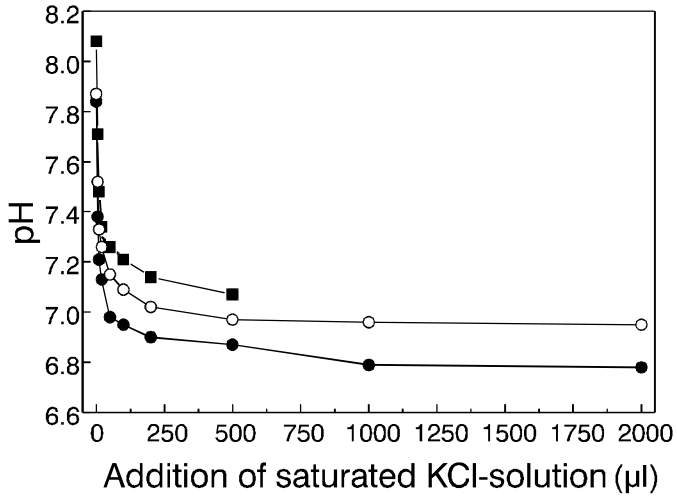

Fig. 64 Influence of addition of saturated KCl-solution on pH of commercial parenteral emulsions: Lipofundin 20% N® (○), Intralipid 10® (●), Lipovenoes LCT 20® (■)

3.2.5.1 Zeta Potential

Spooner et al. [1990] reported an apparent pK_a for oleic acid of 7.4 - 7.5 determined by NMR spectroscopy for an equal distribution of the fatty acid between phospholipid bilayers and lecithin on the surface of emulsion droplets. Similarly, Spector [1975] stated that the pK_a of long-chain fatty acids ranged in a more 'hydrophobic' environment from about 4.7 - 5.0, although 6 - 8 had also been reported by other authors. Villalaín and Gómez-Fernández [1992] determined the apparent pK_a of palmitic acid in multilamellar vesicles to be about 8.7 using FT-IR spectroscopy. Accordingly, Herman [1992] argued that the influence of charged fatty acids located at the oil-water interface on emulsion stabilisation should be negligible. To estimate the influence of pH on free fatty acid ionisation, Fig. 65 shows dissociation curves for the example of oleic acid according to its higher and its possible lower pK_as. Even with pK_a = 7.5, considerable ionisation occurs for pH values between 9 and 11. Although electrostatic repulsion owing to free fatty acids might not be enhanced at neutral pH (as in the final product), a stabilising effect might be postulated, nevertheless, for the emulsification and autoclaving steps where alkaline pH values exist. It can also be seen from Fig. 65 that emulsions prepared from either pure PC or non-ionic emulsifier Pluronic F68® exhibit low negative or even slightly positive Zeta potential values under acidic conditions and become shifted to more negative values with increasing pH. Nevertheless, the change of Zeta potential with pH shift from neutral to alkaline (where ionisation of fatty acids would be expected to become more important) is not very pronounced. Little contribution of Zeta potential to droplet stabilisation would, therefore, be expected in the case of pure PC.

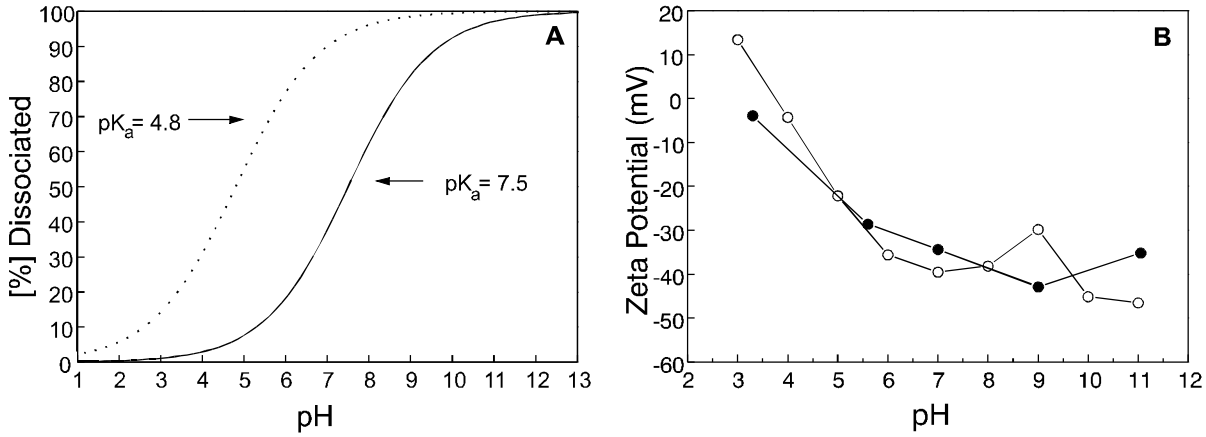

Fig. 65 Influence of pH on **(A)** dissociation of oleic acid and on **(B)** Zeta potential for non-autoclaved 10% w/w soya oil emulsions stabilised with 1.2% w/w Lipoid EPC® (○) and 1.2% w/w Pluronic F68® (●) [homogenised at 1000 bar]

Only small amounts of free fatty acid can be present before autoclaving, since otherwise they would increase Zeta potential considerably.

Zeta potentials of Lipoid E80®-stabilised emulsions were found to increase by some 10 - 20 mV during autoclaving, accompanied by a parallel drop in emulsion pH. Emulsions autoclaved without addition of NaOH to adjust pH to alkaline showed cracking and shifting of pH towards 3 - 4, although these emulsions finally exhibited the highest Zeta potential values. The example of a 20% emulsion (pH 6.5 before autoclaving and pH 3.5 after autoclaving for 30 min) is depicted in Fig. 66. The autoclaved, cracked emulsion possesses nominally higher Zeta potential at pH > 5, but < pH 5 both emulsions have similar Zeta potentials. Taking pK_a-values of 11.25 (DLPE, NH_3), <1 (DPPC, PO_4), about 6 (DPPS, COOH) and 3.87 (egg-PA, PO_4), (Marsh [1990]), about 10% of PS carboxylic groups are still dissociated at pH 5, whereas long-chain fatty acids would be expected to be almost entirely undissociated (Fig. 65, pK_a = 7.5). Free fatty acids possibly produced by hydrolysis during autoclaving are therefore not able to increase Zeta potential under acidic conditions and fail to enhance emulsion stability. pH adjustment to alkaline values has not only to be regarded as a means to 'pre-adjust' final emulsions to blood pH, but is rather a prerequisite to allow autoclaving of parenteral emulsions [Bock, 1994].

Addition of sodium oleate to emulsions stabilised with pure PC (Lipoid EPC®) influenced Zeta potential in a similar fashion (Fig. 60). Also, only the oleate-admixed emulsions could be sterilised without cracking, and not those with pure PC alone, although in all cases pH had been adjusted to > 9.0 before autoclaving. Stabilisation owing to increased electrostatic repulsion thus appears only to be effective at Zeta potentials > approx. -50 mV for emulsions containing PC.

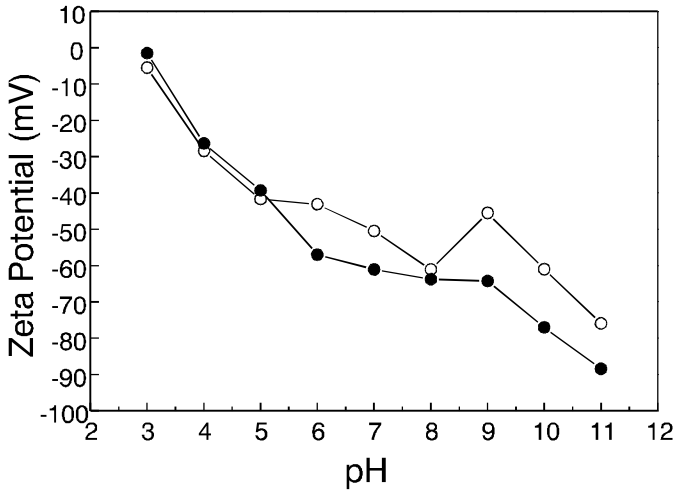

Fig. 66 Influence of pH on Zeta potential for 20% w/w soya oil emulsion stabilised with 1.2% w/w Lipoid E80® non-autoclaved (○) and after autoclaving for 30 min at 121°C without prior pH adjustment (●) [homogenised at 1000 bar]

However, even for pH values < 5, oleate-admixed emulsions showed Zeta potentials approx. 10 mV higher than those with pure PC (Fig. 60). It is also evident from the high Zeta potentials of broken emulsions that high Zeta potential alone cannot be regarded as an indicator for stability. However, as a pronounced effect could be observed for droplet stability during heat stress, it is important to control pH and resulting Zeta potential values *before* autoclaving. Bock [1994] recommended adjusting of emulsions to alkaline pH prior to homogenisation instead of prior to autoclaving, thus resulting in larger Zeta potentials with less variability in final pH.

In the case of commercial emulsions similar Zeta potentials and dependency on pH were observed. Both Lipofundin MCT® 10% (5 months prior to expiration) containing oleate admixture, as well as Intralipid 20® (6 months prior to expiration) containing no additional oleate, showed Zeta potentials of approx. -50 mV at pH 7. Higher values occurred at stronger alkaline pH, which is not seen with the Lipoid EPC®-emulsions where Zeta potentials reach a plateau within the alkaline pH range (Fig. 65). Since the Lipoid E80®-emulsions show a similar pH-dependency before and after autoclaving (Fig. 67), higher Zeta potentials of the commercial emulsions can be attributed to additional minor lecithin components which were absent in the emulsions containing pure PC. The Point of Zero Charge (PZC) of the emulsions lay around or below pH 3, which is in agreement with reports by Dawes and Groves [1978] and Lucks [1993] for Intralipid® formulations.

To verify that Zeta potentials measured at 25°C reflect accurately those values existing at elevated temperature during production, Zeta potential measurements were also carried out on Intralipid 20® at various temperatures using sample dilutions of pH 8 and pH 9. Similar to the

reports of Yamaguchi et al. [1995b], only slight changes of the Zeta potentials were observed (Fig. 68). This is an additional indication of the validity of the importance of electrostatic repulsion for autoclaving stability of these emulsions at high temperature.

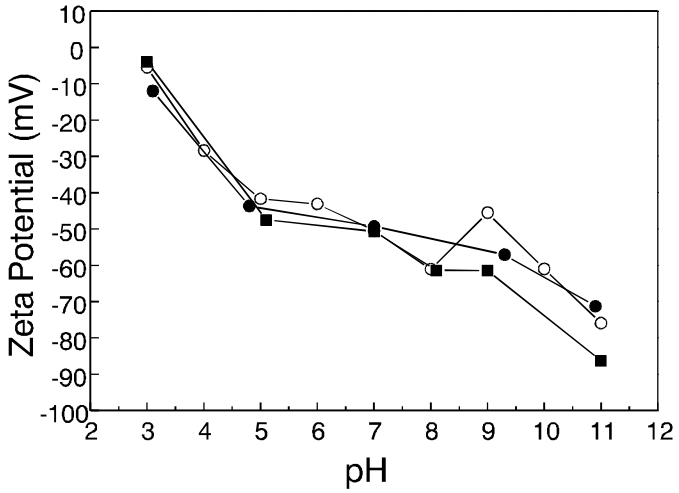

Fig. 67 Influence of pH on Zeta potential for Intralipid 20® [batch 85375-51] (■), Lipofundin MCT® 10% [batch 6023A81] (●) and non-autoclaved 20% w/w model emulsion stabilised with 1.2% w/w Lipoid E80® (○) [homogenised at 1000 bar]

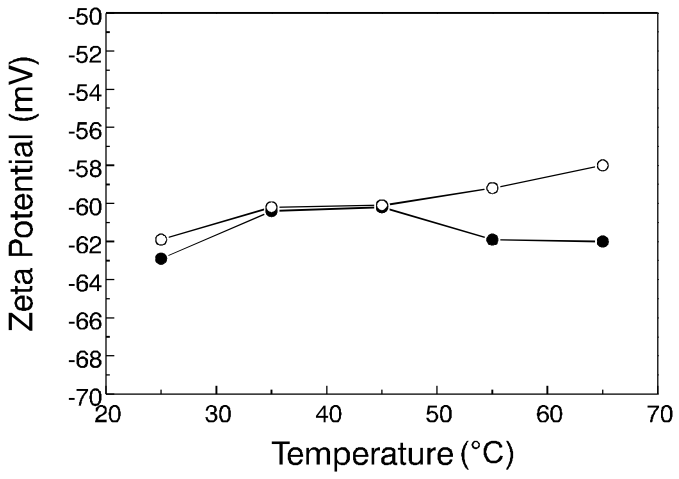

Fig. 68 Influence of temperature on Zeta potential for Intralipid® 20 [batch 85375-51] at pH 8 (○) and pH 9 (●)

Model emulsions consisting of liquid paraffin as the dispersed phase instead of soya oil, showed a similar drop in pH and increase in Zeta potential on autoclaving. This effect owes therefore more to the emulsifier than to hydrolysis of the dispersed phase.

Essentially, these Zeta potential values confirm data reported for similar emulsions by Washington and Davis [1987], Washington et al. [1989], Chaturvedi et al. [1992] and Yamaguchi et al. [1995a]. They contradict reports by Muchtar et al. [1991], who claimed that emulsions prepared with purified lecithin, enriched in negatively-charged phospholipids, experienced neither changes in Zeta potentials nor pH values when different autoclaving times were used. The production of hydrolysis products of lecithin during autoclaving would be expected to enhance surface charge of oil droplets, but also to lower pH leading to diminished proportion of ionised species (and thus lower Zeta potential), as reported by Washington and Davis [1987] by adding oleic acid to parenteral emulsions. As no difference between Zeta potentials of emulsions containing 0.6% or 1.2% lecithin could be observed, reports by Ishii et al. [1990] could not be confirmed. These authors found Zeta potential values to be maximally negative at 1.2% lecithin content, but did not state the pH of their emulsions. It appears therefore that Zeta potential and with it also droplet stability during autoclaving are not affected by reduction of excess emulsifier, although the latter could theoretically serve as a 'reservoir' of hydrolyseable phospholipids and thus as a source of free fatty acids. Older reports on emulsion Zeta potential refer to the outdated Intralipid 10® formulation containing excess lecithin. This might, however, also have affected their admixing stability, since charged lipids might be able to buffer ion admixing. However, Rubino [1990] stressed that emulsions to which sodium oleate had been added or 'aged' commercial emulsions (which contain more hydrolysed lecithin) exhibited increased flocculation upon the addition of Ca^{2+}-ions, whereas addition of sodium-PA gave best stabilisation against flocculation. Also Washington et al. [1990] used determination of critical flocculation concentrations of added Ca^{2+} to determine 'stability' of emulsions. They reported that increase in pH markedly increased stability of Intralipid® against Ca^{2+} addition, which was even further improved when glucose solution was contained.

3.2.5.2 Physical Stability

Tab. 21 shows to which degree particle sizes of different emulsions were affected by autoclaving. According to reports in the literature [Lee and Groves, 1981 / Groves and Herman, 1993], autoclaving of model emulsions was expected to yield only a slight decrease in PCS z-average diameters, if at all. The former finding reflects the disappearance of few larger particles from the measurement range owing to aggregation or coalescence. However, in these experiments, particle size remained practically unchanged for the pH-adjusted emulsions, whereas the emulsions whose pH had not been adjusted before autoclaving showed marked coarsening (see 3.2.5.1). The addition of sodium oleate clearly increased the autoclaving-stability of emulsions stabilised with pure Lipoid EPC®.

Emulsion	Z-Average (nm)	Polydispersity index	LD $d50_{Vol}$ (nm)	LD $d90_{Vol}$ (nm)
10%, 1000 bar, 0.6%LipoidE80®	239.6	0.057	330	750
10%, 1000 bar, 0.6%LipoidE80®	245.1	0.035	330	800
10%, 1000 bar, 1.2%LipoidE80®	184.2	0.081	270	580
10%, 1000 bar, 1.2%LipoidE80®	186.7	0.075	n.d.	n.d.
10%, 700 bar, 1.2%LipoidE80®	233.6	0.073	n.d.	n.d.
10%, 700 bar, 1.2%LipoidE80®	236.4	0.079	n.d.	n.d.
10%, 1000 bar, 1.2%Lipo.EPC®	232.4	0.106	340	780
10%, 1000 bar, 1.2%Lipo.EPC®	1235.9	0.200	1360	2390
20%, 1000 bar, 1.2%LipoidEPC® 0.02% sod.oleate	309.6	0.119	410	710
20%, 1000 bar, 1.2%LipoidEPC® 0.02% sod.oleate	305.9	0.080	410	720
20%, 1000 bar, 1.2%LipoidE80®	256.3	0.056	400	745
20%, 1000 bar, 1.2%LipoidE80®	263.4	0.060	400	730
20%, 1000 bar, 1.2%LipoidE80®, no pH adjustmnt.	1387.0	0.250	n.d.	n.d.
Intralipid 20® [batch 85375-51]	342.0	0.134	480	880
Intralipid 20® [batch 85375-51]	351.1	0.095	480	890
30%, 1000 bar, 1.2%LipoidE80®	334.3	0.050	450	950
30%, 1000 bar, 1.2%LipoidE80®	344.9	0.057	420	810

Tab. 21 Typical particle size distributions of commercial and model parenteral emulsions by PCS (intensity distribution) **(left)** and Laser Diffractometry [Mastersizer Micro, Fraunhofer Mode, 50% and 90% of volume distribution] **(right)** before (plain) and after (shaded) autoclaving for 15 min at 121°C

Repeated autoclaving of commercial emulsions also was not found to lead to major changes in

their particle size distributions.

Although liposomal dispersions generally showed broad size distributions, PCS results suggest, that liposomal structures and sizes were maintained during autoclaving up to 5 h duration. This was not seen when pH had not been adjusted to alkaline values before autoclaving and accordingly dropped to acidic values. Liposome size was similarly stable for pure egg-PC (Lipoid EPC®) and the less purified blend (Lipoid E80®) and therefore independent of emulsifier composition.

Sample	Z-Average (nm)	Polydispersity index
1.2% Lipoid E80®, 400 bar	156.5	0.546
1.2% Lipoid E80®, 400 bar	142.2	0.499
1.2% Lipoid E80®, 700 bar	115.4	0.752
1.2% Lipoid E80®, 700 bar **(5 h, pH 9)**	100.4	0.682
1.2% Lipoid E80®, 700 bar **(5 h, pH 6)**	376.5	0.265
4.0% Lipoid EPC®, 1000 bar	75.0	0.567
4.0% Lipoid EPC®, 1000 bar	75.5	0.600
4.0% Lipoid E80®, 1000 bar	74.1	0.557
4.0% Lipoid E80®, 1000 bar	77.8	0.612

Tab. 22 Particle size distributions of microfluidized liposomal dispersions of egg lecithin by PCS (intensity distribution) before (plain) and after (shaded) autoclaving for 15 min at 121°C or as indicated

3.2.5.3 Chemical Composition

2-propanol : n-hexane (1:1 v/v) was found to be the best solvent for the lyophilised combined triglycerides, fatty acids, polar and apolar lipids. In some cases, dissolution could be accelerated by short-time gentle heating of the samples. No filtering or pre-purification was needed, and after 500 injections no backpressure increase was observed during HPLC analysis. The relative standard deviations between three successive injections were all approx. 1.5% for PC or PE and about 3% for the low-response signals from LPC. These values are comparable

to the reports of Sotirhos et al. [1986b], except LPC which was reported to be detected with a relative error of about 10%.

Despite the relatively slow pump rate, no serious tailing of the solvent front was observed, as reported by Herman [1992]. The elution of triglycerides (together with the solvent front) and free fatty acids, approximately 1-2 minutes later, could therefore be observed. This could be confirmed by spiking samples with oleic and myristic acid. The first phospholipid of interest, PE, eluted well-separated from the oil-related lipids after about 15 min. LPC eluted at about 47 min, after which the gradient was returned to the initial conditions. Although this procedure required relatively long analysis times, reliable separation was achieved. Higher flow rates or more hydrophilic gradient conditions could probably have reduced run times or improved peak shape [Herman, 1992]. Quantitation of egg lecithin samples is, however, very complex and tedious, and the results reported here are sufficient for the purpose of characterisation of the samples under investigation. For more detailed studies and reviews on different solvents and detection techniques the reader is referred to McCluer et al. [1986], Herman [1992], Beare-Rogers et al. [1992] and Balazs et al. [1996].

Consistent with the reports of Herman [1992], Herman and Groves [1992] and Grit et al. [1989], hydrolysis of PC in both model and commercial emulsions occurs according to first order kinetics (Fig. 69). PC in liposomal dispersions undergoes faster degradation than in the 20% model emulsions. Contrary to Herman and Groves' suggestion, any catalyst effects of a buffered aqueous medium can be ruled out.

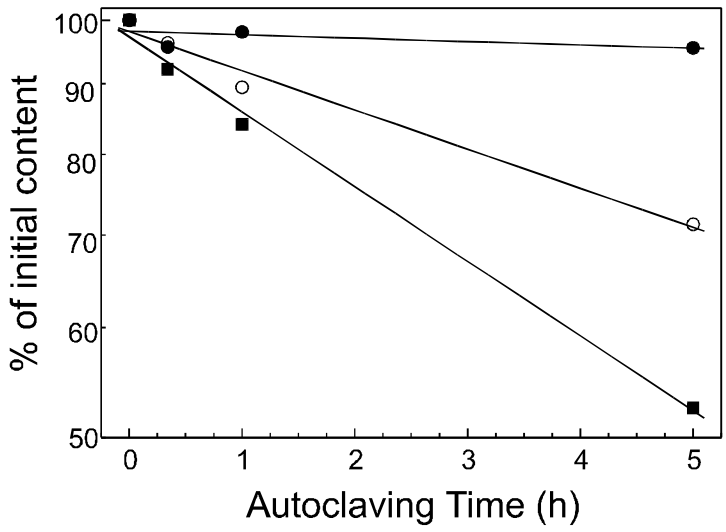

Fig. 69 Semilogarithmic plot for PC degradation during autoclaving of Intralipid 20® [batch 70178-51] (●), 20% w/w model emulsion stabilised with 1.2% w/w Lipoid E80® without pH adjustment [pH ≅6.6] (○) and 1.2% w/w Lipoid E80® dispersion [pH≅6.2] (■)

A possible explanation is that the PC located in the lamellar bilayers was more easily

hydrolysed by the surrounding water than in the more lipophilic environment at the emulsions' oil-water-interface. As a result, the higher the initial content of excess lecithin in an emulsion the greater should be the lyso-PC content in the final product. Herman [1992] and Herman and Groves [1992] give various values for Arrhenius activation energies (E_a) for PC and PE hydrolysis in their model emulsions. They, however, found that phospholipid hydrolysis was independent of the purity of the oil used as the dispersed phase. Intralipid 20® shows less degradation of PC when re-autoclaved compared with the model dispersions being autoclaved for the first time. Consequentially, its pH also decreased less (Fig. 70). Confirming the report of Herman [1992], the drop in pH during the first 15 min interval is greater than can be related to mere hydrolysis of the phospholipids. Yet, the extent of decrease (2-3 units) cannot clearly be related to the pH adjusted prior to autoclaving (Fig. 70). Bock [1994] observed that even non-autoclaved emulsions which had been pH-adjusted after homogenisation showed a drop in pH of about 1-2 units within 24 h, whereas those whose pH had been adjusted prior to homogenisation did not change pH remarkably. He attributed these findings to neutralisation reactions or incipient triglyceride hydrolysis which had been accelerated by the homogenisation process. This might also explain the initial pH drop in Fig. 70, as all systems were examined immediately after preparation.

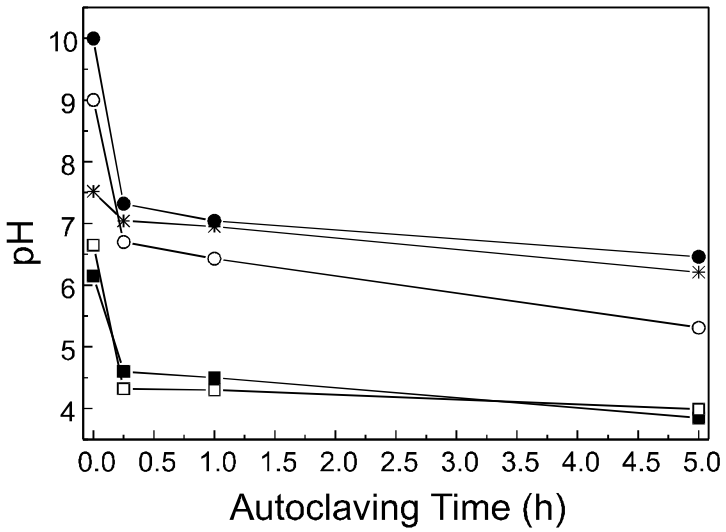

Fig. 70 Drop in pH during different autoclaving intervals: Intralipid 20® [batch 70178-51] (Σ), 20% w/w model emulsion stabilised with 1.2% w/w Lipoid E80® without prior pH adjustment (□), adjusted to pH 9 (○) and pH 10 (●), as well as 1.2% w/w Lipoid E80® dispersion without prior pH adjustment (■)

To maintain stability of the emulsions it appears, therefore, that pH adjustment before autoclaving must be controlled carefully to avoid a subsequent shift during autoclaving to lower pHs. This can be achieved by adjusting pH of the aqueous phase before homogenisation (as suggested by Bock [1994]) or by adjusting pH to about 10 after homogenisation, taking

into account the subsequent drop of almost 3 pH units to be expected (Fig. 70). Many authors reporting difficulties with autoclaving stability either did not report pH or probably oversaw these pH changes.

The chromatograms of 20% model emulsions depicted in Fig. 71 show that with decreasing intensity of PE (Fig. 71, **2**) and PC signals (Fig. 71, **4**), free fatty acids, lyso-PC and also a third signal at about 22 min are detected. From the retention times reported by Sotirhos et al. [1986b], this signal could be related to the formation of lyso-PE. The values observed for first-order rate constants were in agreement with the one which could be derived from the cited reports of Herman on PC hydrolysis after application of high-temperature stress towards model emulsions (Tab. 23).

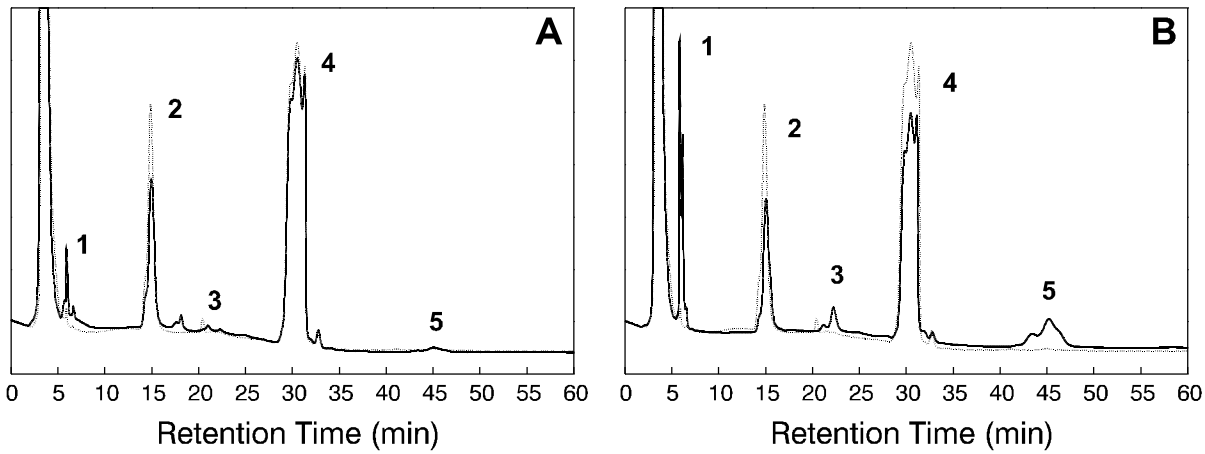

Fig. 71 HPLC chromatograms of native 20% w/w model emulsions stabilised with 1.2% w/w Lipoid E80® [pH ≅6.6] (·····) and after autoclaving for **[A]** 15 min (—) and **[B]** 5 h (—) without prior pH adjustment:

1-FFA **2**-PE **3**-LPE **4**-PC **5**-LPC

Fig. 71 and Tab. 23 also indicate that PE is in most cases hydrolysed faster than PC, whereas Herman and Groves [1992] reported almost equal hydrolysis rates for both compounds. However, hydrolysis rates are clearly found to be pH-dependent, and different pHs used in their emulsions might account for these different outcomes. PE yielded increased hydrolysis rates at alkaline pH, whereas PC appeared to be most stable at pH 9. This was surprising, since Håkansson [1966] had predicted hydrolysis to appear at the slowest rates at pH of 6.5. Since the detection of PC was in agreement with the data of Herman and Groves, this inexplicable deviation can only in part be caused by the method of detection applied (UV vs. FID used by Herman and Groves).

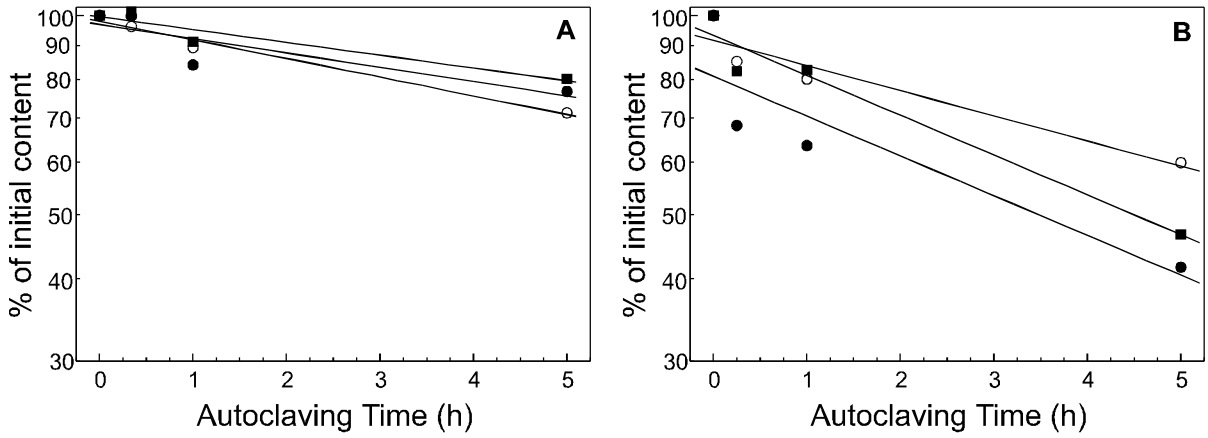

Fig. 72 Semilogarithmic plots for **(A)** PC and **(B)** PE degradation during autoclaving of 20% w/w model emulsions stabilised with 1.2% w/w Lipoid E80®, adjusted to pH 9.0 (■), pH 10.0 (●) and without prior pH adjustment [pH≅6.6] (○)

Tab. 23 summarises the first-order hydrolysis rates observed for PC and PE:

Sample (pH before autoclaving)	**k_{obs} [1/h]**	
	PC	**PE**
1.2% Lipoid E80® liposomal dispersion (6.2)	0.1241	0.1023
20% Model Emulsion (6.6)	0.0651	0.0875
20% Model Emulsion (9.0)	0.0446	0.1386
20% Model Emulsion (10.0)	0.0497	0.1383
Intralipid 20® [batch 70178-51] (7.52)	0.0056	0.0338
20% Emulsion (8.5) *	0.0501	0.0446

Tab. 23 First-order hydrolysis rate constants for PC and PE in 20% emulsions autoclaved at 121°C as determined by HPLC
(***** calculated from Herman [1992])

Emulsifier degradation during only 15-20 minutes' autoclaving proceeds slowly, making it difficult to obtain reliable degradation data from change in PC or PE content. Therefore, corresponding LPC values as determined by HPLC analysis are depicted in Fig. 73.

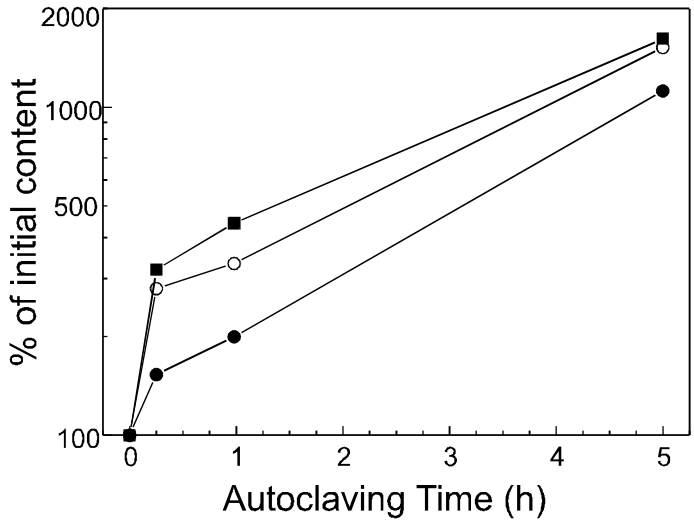

Fig. 73 Semilogarithmic plot for increase of LPC content during autoclaving: 20% w/w model emulsion stabilised with 1.2% w/w Lipoid E80® without prior pH adjustment [pH≅6.6] (○), adjusted to pH 9.0 prior to autoclaving (●), and non-adjusted 1.2% w/w Lipoid E80® dispersion [pH≅6.2] (■)

Despite the limitations regarding LPC quantitation by UV-absorbance (see Section 3.1.2.1), substantially the same dependency between hydrolysis and pre-autoclaving sample pH are seen. However, LPC content does not increase parallel to PC degradation and deviates from first-order kinetics. Herman [1992] and Herman and Groves [1992] suggested that ongoing hydrolysis of LPC to GPC is an explanation for this behaviour, and Chaturvedi et al. [1992] stated that direct hydrolysis of PC to GPC occurred especially at alkaline pH. Indeed, after prolonged autoclaving two new peak shoulders (indicated by the arrows in Fig. 74) emerge. Herman and Groves [1992] and Herman [1992] reported more detailed data on GPC/GPE content.

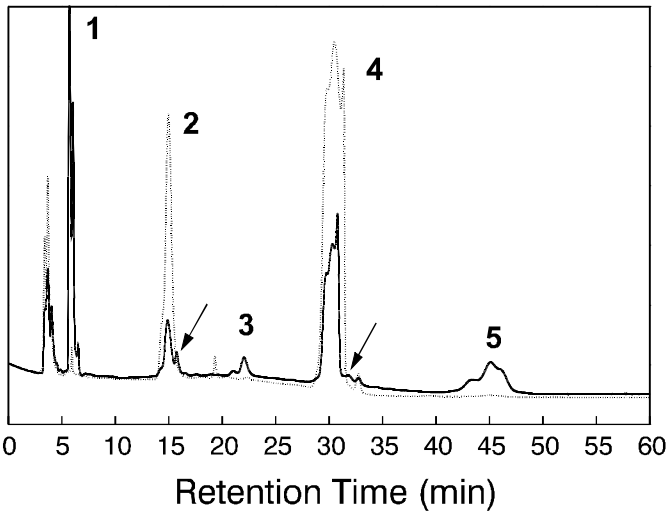

Fig. 74 HPLC chromatograms of native 1.2% w/w Lipoid E80® dispersion [pH ≅6.2] (·····) and after autoclaving for 5 h (—) without prior pH adjustment:

1-FFA **2**-PE **3**-LPE **4**-PC **5**-LPC

HPTLC measurements gave LPC contents ranging from about 3 to almost 19% (mol:mol total phospholipid) in various emulsion samples (Tab. 24). Phospholipid hydrolysis had, therefore, obviously begun before autoclaving, owing to the initial dispersion stages where elevated temperatures had been used. It may be assumed, therefore, that addition of NaOH at this stage may also have produced dissociation of free fatty acids before the homogenisation step. As in commercial products Na-oleate is added (approx. $6 \cdot 10^{-4}$ to $1 \cdot 10^{-3}$ mol/l) to adjust the pH of the aqueous phase before homogenisation, a co-stabilising effect of free fatty acids may be possible by phospholipid hydrolysis before homogenisation.

Sample (pH before autoclaving)	**LPC (mol%) before**	**LPC (mol%) after**
20% Model Emulsion (6.6)	3.2	5.8
Intralipid 20® * [batch 70178-51] (7.52)	18.6	19.7

Tab. 24 Results for HPTLC determination of LPC content of non-pH-adjusted emulsion before and after autoclaving for 15 min at 121°C (***** analysed 2 months after expiry)

Comparison with Intralipid 20® (Tab. 24) also confirms, that LPC content rises further during storage, producing concentrations well above 10% around the time of expiry, which is in agreement with earlier reports from Muehlebach et al. [1987] and Herman [1992] who had found up to about 10% LPC in emulsions still within their shelf-life by HPTLC and HPLC analysis. This supports the prediction of Hansrani [1980] and Washington and Davis [1987] that stability was better in aged emulsions than in freshly produced samples.

Using HPLC analysis it was also possible to reveal differences in emulsifier composition between different commercial products and compare their composition with the model emulsions. Model emulsions (adjusted to pH 9.0) showed only slightly detectable degradation when analysed before and immediately after autoclaving (Fig. 75a). Identical chromatograms can be seen, and only a slight increase in free fatty acid peaks together with minor signals for LPC and LPE are detectable. From Fig. 75b it is evident that Lipofundin 10%N® and Lipovenoes LCT 20® possess almost identical phospholipid composition, with a PC:PE ratio similar to that for the model emulsions. These emulsions were analysed shortly before their expiry, and clearly contain pronounced amounts of free fatty acids and lyso-phospholipids, whereas both PC and PE content are diminished compared with the model emulsions. This observation emphasises again that hydrolysis of the phospholipids continued during storage. In Fig. 75c, Lipofundin MCT 10%® is shown to contain substantially more hydrolysis products than Intralipid 10®. The total amount of phospholipids in Lipofundin MCT 10%® is, however,

nominally twice the amount used in Intralipid 10®. Nevertheless, PE is present in equal amounts in both emulsions, indicating that the Intralipid® formulation possessed a higher PE:PC ratio, as could also be seen from Tab. 25, and had similarly been reported by Muehlebach et al. [1987].

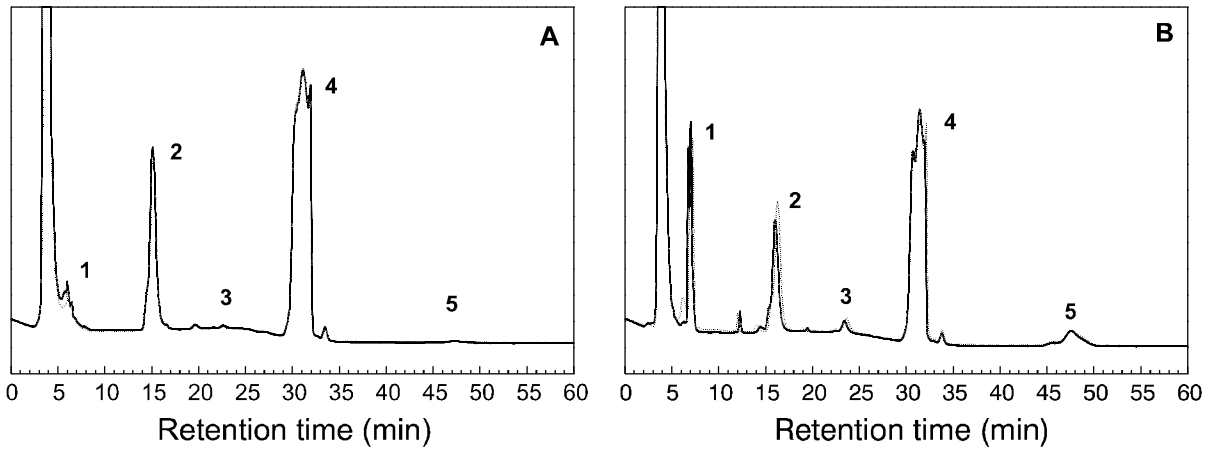

(A) 20% w/w model emulsions stabilised with 1.2% w/w Lipoid E80® and adjusted to pH 9.0, before (·····) and after autoclaving (—) for 15 min at 121°C
(B) Lipofundin 10% N® [1 month prior to expiry] (—) and Lipovenoes LCT 20® [1 month prior to expiry] (·····)

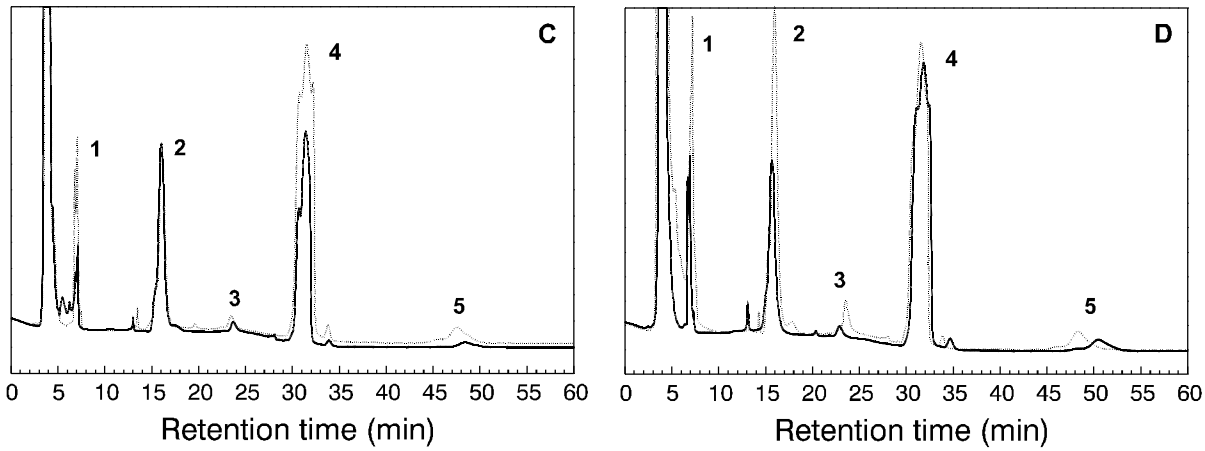

(C) Lipofundin MCT 10%® [1 month prior to expiry] (·····) and Intralipid 10® [batch 87535-51, 12 months prior to expiry] (—)
(D) Lipofundin MCT 20%® [1 month prior to expiry] (—) and Intralipid 30® [batch87537-51, 12 months prior to expiry] (·····)

Fig. 75 HPLC chromatograms of commercial and model parenteral emulsions:
1-FFA **2**-PE **3**-LPE **4**-PC **5**-LPC

A similar result is depicted in Fig. 75d, showing the phospholipid compositions of Lipofundin MCT 20%® and Intralipid 30%® which are both formulated with 1.2% lecithin. Intralipid® also in this case shows more intense PE and LPE peaks compared with the Lipofundin® emulsion. Intralipid 30® [batch 88555-71] contained less PC but more PE than found in Intralipid 10® and 20®, which was consistent with reports by Férézou et al. [1994]. These authors found increased contents of PE and PI at the expense of PC in Intralipid 30®. However, duplicate analysis of the three emulsion types from batches one year ahead of their expiry did not confirm such differences between the three formulations and suggests that the former finding was simply batch-to-batch variations of the emulsifier. From Fig. 75d it can, however, be seen that Intralipid 30® contains more free fatty acids than usually observed for 10% or 20% emulsions. As Intralipid 30® samples had been analysed well before expiry, either more hydrolysis of lecithin owing to heat stress had taken place, or, more likely, more free fatty acids had been introduced by the increased proportion of the oil phase. This may occur either by the inherent free fatty acid content of the soya oil, or by hydrolysis of the latter during production and storage. For emulsions stabilised with Pluronic F68®, homogenised and autoclaved under the same conditions, no substantial amounts of free fatty acids were released during autoclaving (Fig. 76). Thus the oil phase is not the source of fatty acids. Free fatty acid release under autoclaving conditions is therefore a result of degradation of phospholipids.

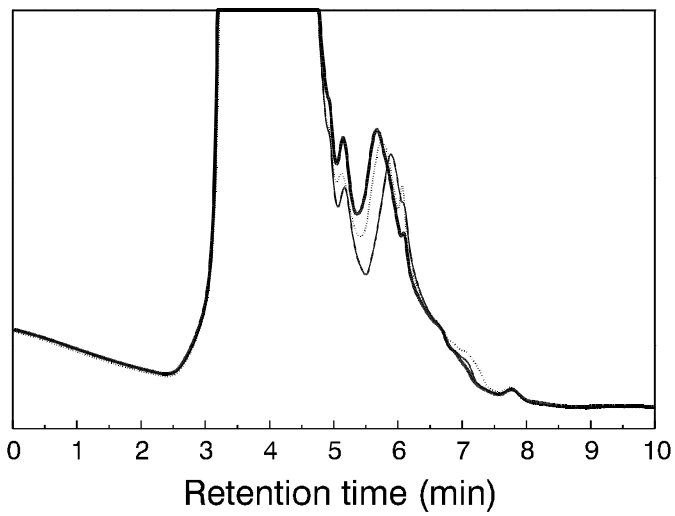

Fig. 76 HPLC chromatograms of native 20% w/w emulsion stabilised with 1.2% w/w Pluronic F68® [pH ≅5.5] (·····) and after autoclaving for 20 min at 121°C without prior pH adjustment (—) and after adjustment to pH 9.0 (44) [enlarged section showing typical free fatty acid retention times]

Fig. 77 shows the same section of the chromatograms of a 20% w/w emulsion stabilised with Lipoid EPC® and 0.02% w/w sodium oleate before and after autoclaving. Due to the

addition of sodium oleate, a pH of 9.26 was observed and therefore, no additional NaOH was used to control the pH. It is evident that hydrolysis led to formation of further free fatty acids, and that the initial oleate content is small compared with the usual content of hydrolysis-derived FFAs (compare with Fig. 75).

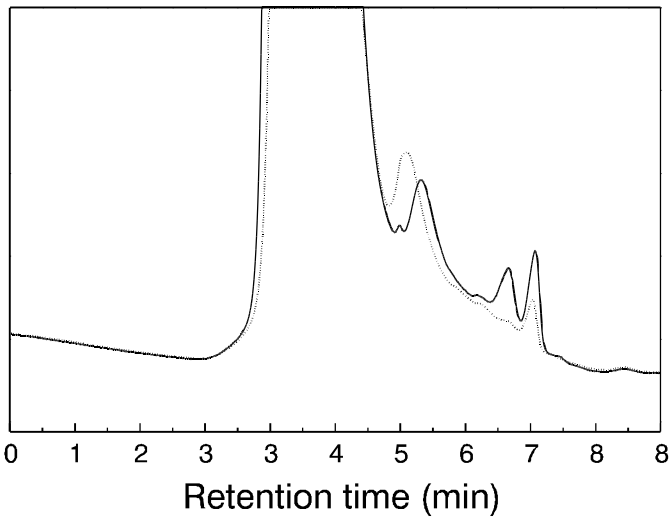

Fig. 77 HPLC chromatograms of native 20% w/w emulsion stabilised with 1.2% w/w Lipoid EPC® and 0.02% w/w sodium oleate before [pH = 9.26] (·····) and after autoclaving for 15 min at 121°C (—) [enlarged section showing typical free fatty acid retention times]

Since the composition of the lecithin in the emulsions, especially the ratio of PC:PE, are regarded as important for emulsion stability [Hansrani, 1980 / Groves and Herman, 1993], PC and PE contents of various commercial and autoclaved model emulsions determined by HPLC analysis are summarised in Tab. 25. The PC and PE composition of the model emulsions possess highest PC:PE ratios but were similar to the Lipofundin® and Lipovenoes® formulations. In contrast, Intralipid® formulations in general possess lower PC:PE ratios. However, molar contents of total phospholipids in Intralipid® batches sometimes ranged at the upper end or even exceeded the amount theoretically contained. This can again be explained by differences in the fatty acid substitution of the phospholipids, which influence also the molar mass. The variations in lecithin composition observed in Tab. 25 are, however, not relevant for emulsion autoclaving stability.

Emulsion	PC (mol/l)	PE (mol/l)	PC+PE (mol/l)	PC:PE ratio
Intralipid 10® [1] (batch 68460-51)	$5.534 \cdot 10^{-3}$	$1.405 \cdot 10^{-3}$	$6.939 \cdot 10^{-3}$	3.9 : 1
Intralipid 10® [12] (batch 87535-51)	$6.312 \cdot 10^{-3}$	$1.761 \cdot 10^{-3}$	$8.073 \cdot 10^{-3}$	3.6 : 1
Lipovenoes 10 PLR®	$5.980 \cdot 10^{-3}$	$8.030 \cdot 10^{-4}$	$6.783 \cdot 10^{-3}$	7.4 : 1
Lipofundin MCT10®	$1.163 \cdot 10^{-2}$	$1.514 \cdot 10^{-3}$	$1.314 \cdot 10^{-2}$	7.7 : 1
10%, 1000 bar, 1.2% LipoidE80®	$1.081 \cdot 10^{-2}$	$1.215 \cdot 10^{-3}$	$1.202 \cdot 10^{-2}$	8.9 : 1
Intralipid 20® [1] (batch 70178-51)	$1.026 \cdot 10^{-2}$	$2.861 \cdot 10^{-3}$	$1.312 \cdot 10^{-2}$	3.6 : 1
Intralipid 20® [12] (batch 85375-51)	$1.169 \cdot 10^{-2}$	$3.188 \cdot 10^{-3}$	$1.488 \cdot 10^{-2}$	3.7 : 1
Lipovenoes 20®	$1.127 \cdot 10^{-2}$	$1.677 \cdot 10^{-3}$	$1.295 \cdot 10^{-2}$	6.7 : 1
Lipofundin 20% N®	$9.363 \cdot 10^{-3}$	$1.661 \cdot 10^{-3}$	$1.102 \cdot 10^{-2}$	5.6 : 1
Lipofundin MCT20®	$9.903 \cdot 10^{-3}$	$1.877 \cdot 10^{-3}$	$1.178 \cdot 10^{-2}$	5.3 : 1
20%, 1000 bar, 1.2% LipoidE80®	$1.277 \cdot 10^{-2}$	$1.501 \cdot 10^{-3}$	$1.427 \cdot 10^{-2}$	8.5 : 1
20%, 1000 bar, 1.2%LipoidEPC®, 0.02% sod.oleate	$1.230 \cdot 10^{-2}$	-	$1.230 \cdot 10^{-2}$	-
Intralipid 30® (batch 88555-71)	$1.212 \cdot 10^{-2}$	$3.766 \cdot 10^{-3}$	$1.589 \cdot 10^{-2}$	3.2 : 1
Intralipid 30® (batch 87537-51)	$1.325 \cdot 10^{-2}$	$3.673 \cdot 10^{-3}$	$1.692 \cdot 10^{-2}$	3.6 : 1
30%, 1000 bar, 1.2%LipoidE80®	$1.376 \cdot 10^{-2}$	$1.671 \cdot 10^{-3}$	$1.543 \cdot 10^{-2}$	8.2 : 1

Tab. 25 PC and PE content of commercial and model emulsions as determined by HPLC analysis

(**1-**analysed 1 month prior to expiry, **12-**analysed 12 months prior to expiry)

3.2.5.4 Emulsifier Distribution

Heat stressing of lecithin-stabilised emulsions has been reported to lead to irreversible redistribution of emulsifier compounds within oil and aqueous compartments [Herman, 1992 / Groves and Herman, 1993]. PC and PE were reported to move from the aqueous continuum towards the dispersed oil phase. Emulsion oil and aqueous compartments were separated by centrifugation in a swing-out rotor at 13000g for approx. 18h (described in more detail in Chapter 4) which allowed phase separation without destruction of the oil droplets. As shown in Fig. 78, the aqueous phase of centrifuged Intralipid 30® contained measurable amounts of phospholipids and, indicated by the intense, broad peak around the solvent front, a large proportion of triglycerides. This is in agreement with the reports of Rotenberg et al. [1991], Westesen and Wehler [1992] and Férézou et al. [1994], who reported many oil droplets in the subnatant. Owing to enhanced Brownian motion, acceleration was too low to separate the smallest oil droplets during centrifugation.

Most of the hydrolysis products (LPC, LPE and free fatty acids) were still associated with the oil droplets and had not moved to the aqueous compartment to form micelles (see Tab. 26). Westesen and Wehler [1992] did not find large amounts of lyso-phospholipids in the aqueous phase either, which suggests that hydrolysis products remain within the emulsifier film, enhancing electrostatic repulsion as well as influencing film properties (see Section 3.1.1.1). Also Herman [1992] reported LPC content of the oil to the aqueous phase of about 7:1, and that approximately twice the amount of LPC was located in the oil phase than could be accounted for according to its initial proportion of the total phospholipid content. He also observed a relocation of PC from the aqueous to the oil phase owing to heat-stress which occurred faster than for PE. Thus, PC:PE ratio of the oil phase increased during autoclaving. This has *inter alia* been suggested to be the cause of reversible cubic phase formation of the lecithin upon thermal stress, possibly responsible for enhanced autoclaving stability [Groves and Herman, 1993].

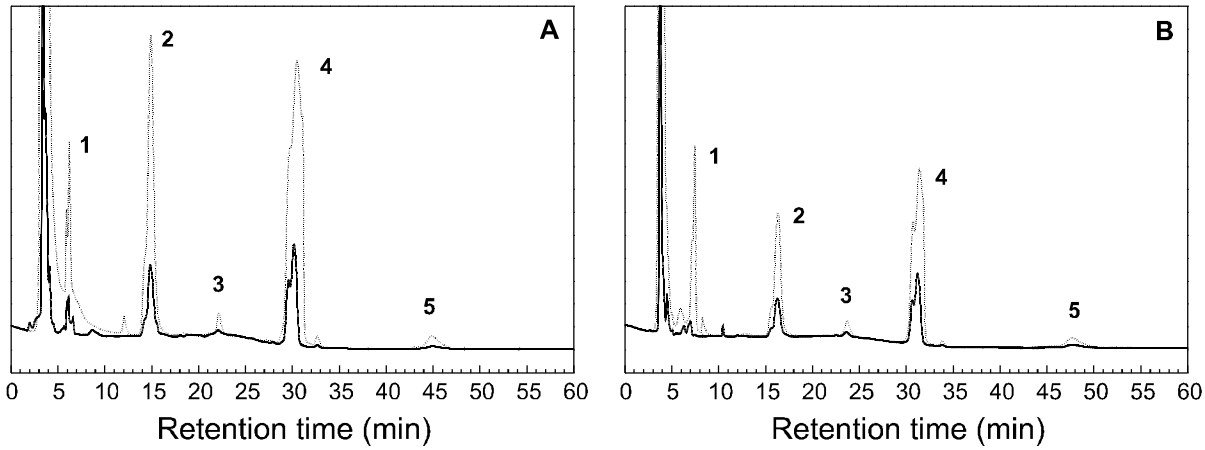

(A) Intralipid 30® [batch 88555-71, 15 months prior to expiry] cream layer (·····) and aqueous subnatant (—) after centrifugation
(B) Intralipid 10® [batch 68460-51, 1 month prior to expiry] cream layer (·····) and aqueous subnatant (—) after centrifugation

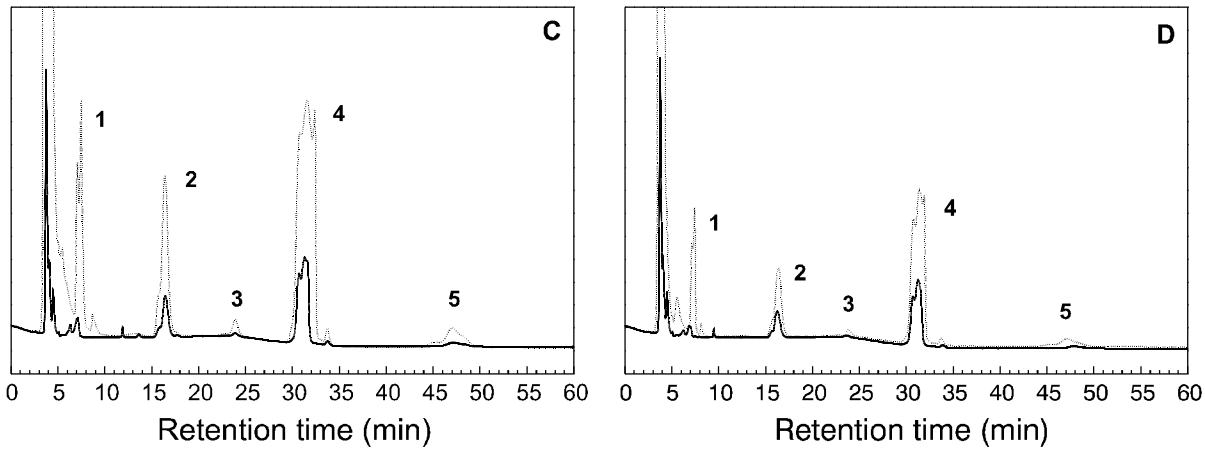

(C) Lipovenoes LCT 20® [1 month prior to expiry] cream layer (·····) and aqueous subnatant (—) after centrifugation
(D) Lipovenoes LCT 10 PLR® [6 months after expiry] cream layer (·····) and aqueous subnatant (—) after centrifugation

Fig. 78 HPLC chromatograms of creamed oil phase and aqueous subnatant of a selection of commercial parenteral emulsions:

1-FFA **2**-PE **3**-LPE **4**-PC **5**-LPC

Fig. 79 shows that also for model emulsions a fraction of the triglycerides and all types of phospholipids were present in the aqueous phase after centrifugation. Compared with commercial emulsions (Fig. 78 and Tab. 26), however, less phospholipid is contained in the aqueous phase; it is present mainly in association with the oil phase.

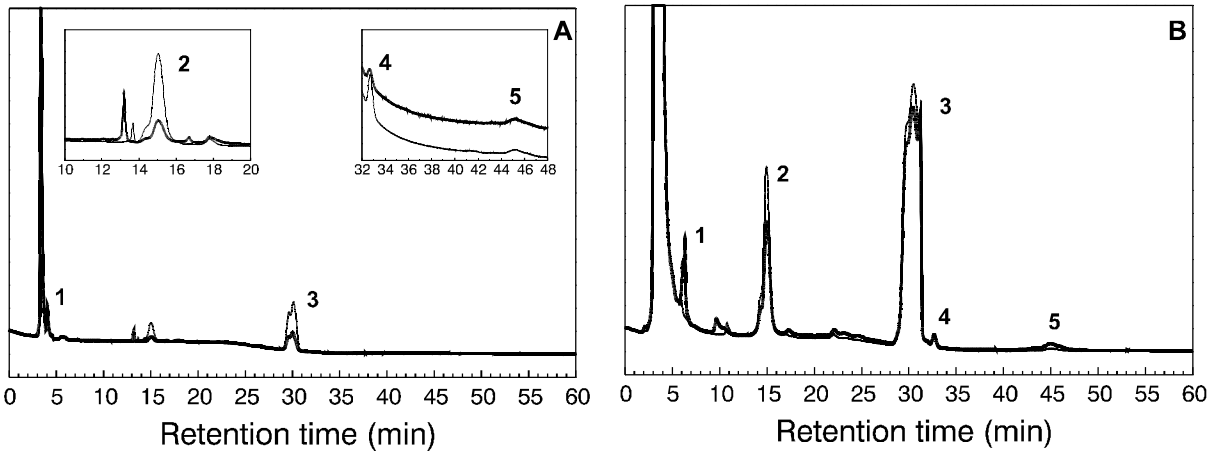

Fig. 79 HPLC chromatograms of a 30% model emulsion stabilised with 1.2 wt% Lipoid E80®, adjusted to pH 9.0:
(A) Aqueous subnatant prior to autoclaving (—) and after autoclaving for 20 min at 121°C (44) after centrifugation **(with enlarged inserts)** and **(B)** respective cream layer before (—) and after autoclaving (44)

1-FFA **2**-PE **3**-PC **4**-SPM **5**-LPC

However, a clear reduction in PE and PC is observed for the aqueous compartment as a consequence of autoclaving. LPC and FFA contents are, surprisingly, not changed by phospholipid hydrolysis during heat stress. PC and PE content in the cream layer also decreases upon autoclaving, however the ratio of the intact phospholipids in the cream layer to the water phase is greatly increased (Tab. 26). This is accompanied by a notable increase in free fatty acid and LPC peaks. It appears that hydrolysis products were distributed in favour of the oil compartment, and those formerly present in the water were largely relocated to the oil-water-interface. For those phospholipids associated to the O/W-interface, their hydrolysis products remain at the interface. This would counteract the formation of micelles from LPC or FFAs in the aqueous phase. Kumar et al. [1989] and Herman [1992] suspected similarly that incorporation of these compounds into vesicles and emulsion droplets would account for the reduced haemolytic toxicity found for these systems. SPM is also reduced in the aqueous subnatant after autoclaving, yet no corresponding changes are seen for the cream layer.

Fig. 80 shows how for 10% w/w model emulsions produced at 1000 bar a redistribution of phospholipids can be observed.

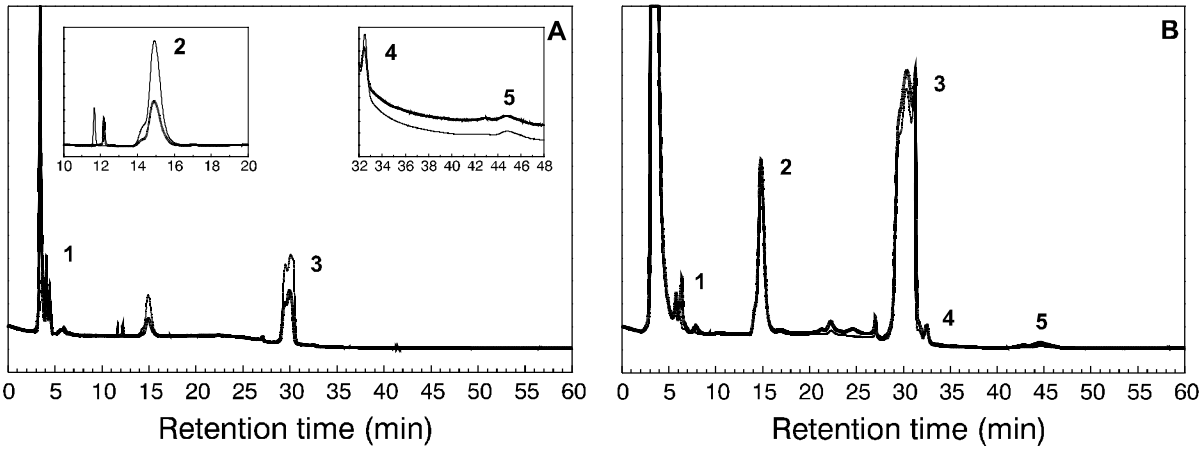

Fig. 80 HPLC chromatograms of a 10% model emulsion stabilised with 1.2 wt% Lipoid E80®, adjusted to pH 9.0:
(A) Aqueous subnatant prior to autoclaving (—) and after autoclaving for 20 min at 121°C (44) after centrifugation **(with enlarged inserts)** and **(B)** respective cream layer before (—) and after autoclaving (44)

1-FFA **2**-PE **3**-PC **4**-SPM **5**-LPC

The PC and PE peaks are clearly diminished in the aqueous compartment after autoclaving, whereas LPC and FFAs remain unchanged. Surprisingly, PC is enhanced in the cream layer and PE unchanged, although markedly increased hydrolysis peaks are seen. This also indicates a redistribution of phospholipids from the aqueous to the oil compartment, as was reported by Herman [1992]. Compared with Fig. 79, the total phospholipid concentration of the aqueous compartment of the 10% formulations was greater than for the 30% emulsion, supporting the assumption that excess lecithin in the 10% formulation is present in the aqueous phase.

It was, however, not possible to confirm the reports of Herman [1992] and Groves and Herman [1993] that PC redistributes preferentially from the aqueous to the oil compartment upon heating, thus producing a higher PC:PE ratio in the cream layer of their model emulsions. In contrast to their findings, no clear trend for redistribution of distinct phospholipids in the autoclaved model emulsions and the commercial formulations is observed (see Tab. 26). The PC:PE ratio of the aqueous phase is enhanced as faster hydrolysis of PE takes place here. As the native model emulsions prepared by Herman [1992] possessed similarly low PC:PE ratios as Intralipid® (and thus higher PE contents) PC redistribution is not observed so strongly for the model emulsion systems and commercial emulsions reported here, containing higher PC:PE ratios than the former. Despite the differences found for the model emulsions, the results for Intralipid® are in agreement with Herman [1992], who however could not verify substantially increased PC:PE ratios for the cream layer of commercial emulsions. The data presented by Groves and Herman [1993] were also only based upon PC and PE concentrations of the

separated phases, which underestimates the influence of phospholipid disappearance owing to lyso-phospholipid formation. Furthermore, an interaction or aggregation of vesicular aqueous phospholipids with the dispersed oil phase must also be taken into account (see Chapter 4).

Differences to HPLC data in the literature are probably owing to different sample dilution and detection procedures. Chloroform, which was used by Herman [1992], did not dissolve the amounts of lyso-compounds present in the samples reported here, necessitating use of 2-propanol:n-hexane (1:1 v/v). Herman and Groves [1993] also stated that flame ionisation detection (FID) was difficult to handle, excluding thereby the use of various buffers and solvents. As refractive index detection is not applicable for gradient analysis, evaporative light scattering detection seems most promising to solve analytical problems with phospholipid quantitation, but has also proved to show only narrow response linearity [Balazs et al., 1996]. The availability and the ease of operation of UV detection together with various gradient eluents makes this method still valuable for phospholipid analysis, and the accuracy achieved here is sufficient for the desired description of chemical changes in the emulsions.

HPTLC is frequently used for phospholipid quantitation (as e.g. in Ph.Eur. 1998), but even using flying-spot scanning shows a higher analytical error (~10%) than HPLC analysis, confirming reports by Marmer [1985]. This lets this method seem advantageous only where clear systematic detection errors by HPLC detection inhibited accurate quantitation (e.g. lyso-phospholipid detection). Analysis of various phospholipid compounds in one sample would require considerable effort for additional plates and different staining agents to allow concomitant analysis of standard dilutions and duplicate samples.

Tab. 26 shows the distribution behaviour of PC and PE between aqueous and oil compartments after centrifugation of some model emulsions before and after autoclaving for 20 min at 121°C, as well as for selected commercial emulsions. From the ratios between the phospholipid contents in the cream layer and the aqueous phase, it becomes evident that model emulsions contained more PC and PE associated with the cream layer, which appeared enhanced after autoclaving by a factor of 2-4, compared with commercial emulsions. This can either be explained by formation of larger oil droplets from the smallest ones, thus becoming separated into the cream layer more easily, or by association of additional phospholipids with the oil droplets present, as Groves and Herman [1993] suggested. However, this question could only be clarified by microscopical evidence (see Chapter 4).

Emulsion	PC (mol/g)	PE (mol/g)	Total PC:PE ratio	PC in CL:AS ratio	PE in CL:AS ratio
5%, 1000 bar, 1.2% Lipoid E80®, CL	$7.041 \cdot 10^{-5}$	$6.109 \cdot 10^{-6}$	11.5 : 1	9.5 : 1	7.2 : 1
5%, 1000 bar, 1.2% Lipoid E80®, AS	$7.440 \cdot 10^{-6}$	$8.433 \cdot 10^{-7}$	8.8 : 1		
5%, autoclaved, CL	$6.075 \cdot 10^{-5}$	$5.986 \cdot 10^{-6}$	10.1 : 1	16.4 : 1	17.6 : 1
5%, autoclaved, AS	$3.713 \cdot 10^{-6}$	$3.396 \cdot 10^{-7}$	10.9 : 1		
10%, 1000 bar, 1.2% Lipoid E80®, CL	$5.317 \cdot 10^{-5}$	$6.646 \cdot 10^{-6}$	8.0 : 1	15.9 : 1	14.6 : 1
10%, 1000 bar, 1.2% Lipoid E80®, AS	$3.352 \cdot 10^{-6}$	$4.551 \cdot 10^{-7}$	7.4 : 1		
10%, autoclaved, CL	$6.002 \cdot 10^{-5}$	$7.266 \cdot 10^{-6}$	8.3 : 1	42.5 : 1	54.7 : 1
10%, autoclaved, AS	$1.413 \cdot 10^{-6}$	$1.329 \cdot 10^{-7}$	10.6 : 1		
Intralipid 10® (batch 68460-51/CL)	$2.672 \cdot 10^{-5}$	$6.763 \cdot 10^{-6}$	3.9 : 1	13.9 : 1	14.7 : 1
Intralipid 10® (batch 68460-51/AS)	$1.929 \cdot 10^{-6}$	$4.600 \cdot 10^{-7}$	4.2 : 1		
Lipofundin 10%N®, CL	$3.214 \cdot 10^{-5}$	$3.202 \cdot 10^{-6}$	10.0 : 1	7.6 : 1	7.8 : 1
Lipofundin 10%N®, AS	$4.205 \cdot 10^{-6}$	$4.106 \cdot 10^{-7}$	10.2 : 1		
Intralipid 20® (batch 70178-51),CL	$3.000 \cdot 10^{-5}$	$8.019 \cdot 10^{-6}$	3.7 : 1	7.9 : 1	6.7 : 1
Intralipid 20® (batch 70178-51),AS	$3.790 \cdot 10^{-6}$	$1.190 \cdot 10^{-6}$	3.2 : 1		
Intralipid 30® (batch 88555-71),CL	$2.737 \cdot 10^{-5}$	$8.853 \cdot 10^{-6}$	3.1 : 1	6.7 : 1	6.3 : 1
Intralipid 30® (batch 88555-71),AS	$4.112 \cdot 10^{-6}$	$1.411 \cdot 10^{-6}$	2.9 : 1		
30%, 1000 bar, 1.2% Lipoid E80®, CL	$2.519 \cdot 10^{-5}$	$3.985 \cdot 10^{-6}$	6.3 : 1	12.5 : 1	15.7 : 1
30%, 1000 bar, 1.2% Lipoid E80®, AS	$2.012 \cdot 10^{-6}$	$2.542 \cdot 10^{-7}$	7.9 : 1		
30%, autoclaved, CL	$2.693 \cdot 10^{-5}$	$3.181 \cdot 10^{-6}$	8.5 : 1	55.2 : 1	38.5 : 1
30%, autoclaved, AS	$4.883 \cdot 10^{-7}$	$8.264 \cdot 10^{-8}$	5.9 : 1		

Tab. 26 PC and PE content of centrifuged oil and aqueous compartment of selected commercial and model emulsions as determined by HPLC analysis (**CL**-cream layer / **AS**-aqueous subnatant / values given as mol of lipid per weight of separated phase)

3.3 Conclusions

The film rigidity of egg lecithin films clearly increases with degree of saturation of fatty acids. Although thermoanalytical and monolayer film properties of Lipoid EPC® were similar to the less refined Lipoid E75® and E80®, it showed weaker emulsifying properties. As could be shown by droplet-to-planar-surface coalescence studies, the incorporation of minor components (as contained in Lipoid E75® and E80®) resulted in prolonged droplet stability. The amount of hydrolysis products required for marked reduction of film thinning rates were, however, too high to be solely responsible for the stabilising effect in the emulsions. Zeta potential and particle size measurements implied, however, that the presence of additional sodium oleate resulted in very effective stabilisation of Lipoid EPC® emulsions during homogenisation and autoclaving. A faster adsorption of these more water-soluble amphiphiles to the freshly-created interface could also have accounted for a more effective homogenisation process. High homogenisation pressure for 5-10 cycles yielded finely dispersed emulsions with smaller droplet diameters than commercial samples.

Phospholipids contained in liposomes were shown to hydrolyse faster during heat stress than in association with the oil droplets. Hydrolysis of PE occurred faster than of PC in all cases. It could also be shown that the hydrolysis products produced within emulsions remain largely in association with the oil phase. Hydrolysis products forming during autoclaving and storage should therefore be expected to even enhance droplet stability. pH was found to have an important influence on autoclavability of the emulsions, possibly by maintaining droplet Zeta potential above -50 mV.

Emulsions from Lipoid E80® showed lecithin composition and distribution similar to Lipovenoes® and Lipofundin® formulations. However, Intralipid® emulsions showed a lower PC:PE ratio and contained even more PE than was reported by Kuksis [1985] (Tab. 3). The variability of PC:PE ratios observed did, however, not influence the stability of the emulsions.

Phospholipid relocation from the aqueous to the dispersed oil phase occurred within the emulsions during autoclaving. This points to an interaction of the phospholipids with the oil droplets, with a possible influence on their autoclaving stability [Groves et al., 1985]. Contrary to the reports of Groves and Herman [1993], the relocation of PC and PE did not alter their respective ratios during autoclaving. This contradicts the authors' suggestion of a cubic phase formation during autoclaving, since these phases are usually observed at higher PE and low water content [Eriksson et al., 1985 / Small, 1986]. The presence of additional phospholipid material at the O/W-interface will be demonstrated in Chapter 4.

Chapter 4 – Results and Discussion (II)
Structures formed within Lecithin-Stabilised Emulsions

The results are divided into three groups, one for the investigations carried out on the undiluted samples, a second, where dilution with 2.25% aqueous glycerol had to be carried out before measurement, and finally, measurement on fractions obtained after centrifugal separation of the emulsions into an upper cream layer and an aqueous subnatant. After prolonged centrifugation a third layer in the form of a sediment appeared at the bottom of the tube, which however could not be obtained from samples containing Pluronic F68® as the only emulsifier.

4.1 Separation of Emulsions by Centrifugation

High-speed centrifugation as described by Groves et al. [1985] and Férézou et al. [1994], was sufficient for separation of oil droplets and most of the aqueous phase. During prolonged centrifugation (approx. 48 h) considerable breakdown of the emulsions was achieved, revealing that model emulsions were more easily cracked than commercial emulsions, especially when pH had not been adjusted to alkaline. Smith and Mitchell [1976] questioned, however, the validity of comparison between droplet coalescence under ambient conditions and accelerated coalescence during centrifugation. As will be seen, the results need therefore to be interpreted with great care. After an initial interval of cream layer formation, where most of the oil droplets were forced to the top of the tube and compressed, incipient formation of free oil was observed only after 12 h when a fixed-angle rotor at 33000 g was used. At the same time the aqueous layer became less turbid, and after 24 h the formation of a yellowish sediment at the bottom of the tube occurred. After approx. 48 h separation did not proceed any further. To completely break down the emulsions, ultracentrifugation for 24 h was employed to yield most of the free oil even from commercial emulsions. Some authors report that the addition of electrolyte solutions accelerates phase separation [Vold and Groot, 1962 / Rotenberg et al., 1991]. As this should alter Zeta potential and destabilise droplet hydration behaviour [Groves and Yalabik, 1975], the phase behaviour and structures present may be changed considerably [Vold and Groot, 1964]. For this reason no additives were used here. As depicted in Fig. 81, strong coalescence usually proceeded the formation of the pellet. Pelleting was, however, also observed before marked separation of oil had occurred. Autoclaving led to enhanced formation of a pellet, which now appeared to be of darker colour. The rate and degree of pellet formation also depended upon centrifugation technique, with the swing-out rotor in the case of both high-speed and ultracentrifugation yielding less pelleted material than did the fixed-angle rotor.

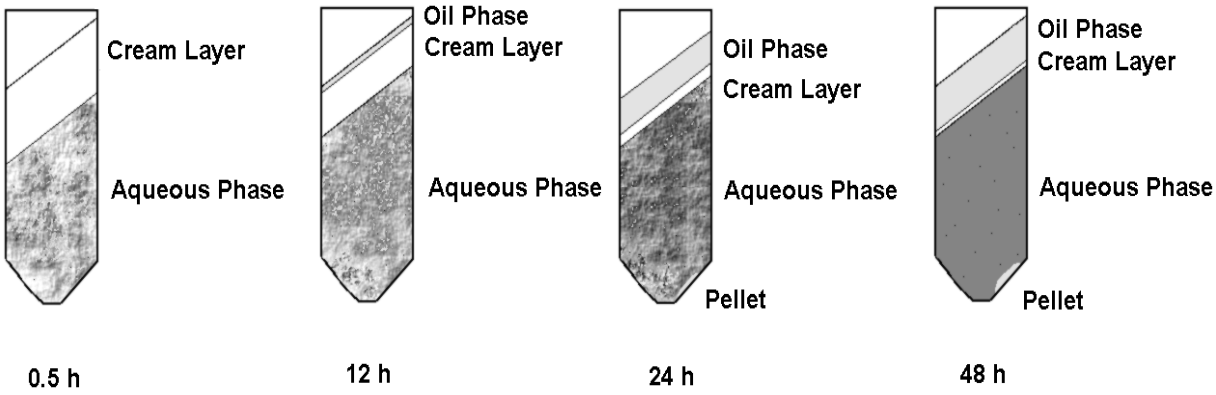

Fig. 81 Schematic of separation of emulsions in a fixed-angle rotor during 48 h at 33000g

4.1.1 Analysis of Separated Oil Phase

The separated oil phase of model emulsions and of Intralipid 20® contained no measurable amounts of phospholipids as determined by DSC and FTIR. However, the Intralipid® oil phase was practically colourless in appearance, whereas the Sigma soya oil used for the model emulsions was considerably more yellow. The DSC thermograms in Fig. 82 of pure soybean oil and the oil phase of Intralipid 20® show similar but not identified melting and freezing peaks. The most evident freezing peaks occur at -13.6°C (-11°C for Intralipid®), -40°C (-37°C) and -66°C (-62°C). The corresponding melting peaks appear at -8.5°C (-8.8°C for Intralipid®), -28.0°C (-27.5°C) and -37.7°C (-46.0°C). There is only one difference in peak positions between the 1st and the 2nd cycle for soya oil. Despite tempering at 50°C before each measurement to ensure complete melting of the triglycerides, the Sigma soya oil shows two peaks between -30°C and -80°C in the first scan, which upon recycling only appear as a single peak. It is, however, known that mixtures of triglycerides where unsaturated fatty acids like linoleic acid (54% in the case of Sigma soya oil) and oleic acid (21.7%) dominate do not give uniform DSC behaviour owing to polymorphism [Small, 1986]. As no data is available in the literature on the thermal behaviour of mixtures of asymmetrically substituted triacylglycerols, no characterisation of the DSC thermograms will be given here. However, melting points ranging below 0°C are an indication of the predominance of unsaturated triacylglycerols in both oils [Larsson, 1986 / Small, 1986]. The transitions certainly represent formation of metastable α (and possibly β') modifications at the low cooling rate of 3K/min used. This would not have allowed formation of the stable β modifications during the time scale of the experiment.

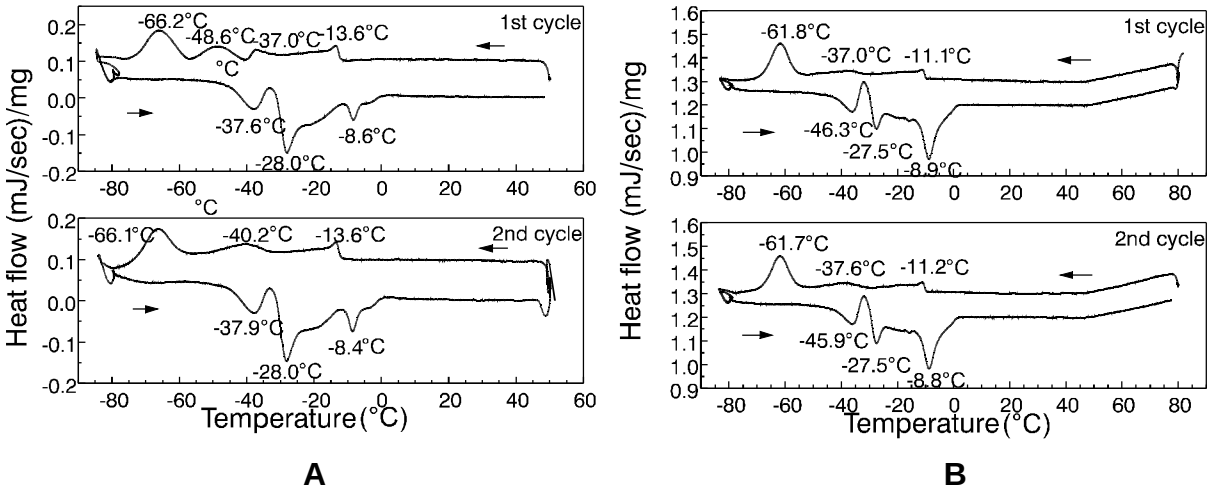

Fig. 82 DSC thermograms of **(A)** Sigma soya oil and of **(B)** separated oil phase from Intralipid 20® [batch 70178-51] at 3K/min

The identical spectra from FT-IR (Fig. 83) for Sigma soya oil and separated oil phase confirm the same composition of both samples, within the sensitivity expected for FT-IR. It is clear, however, that that no phospholipids are present in the separated oil phase, there being no PO_2-peaks in the range 1300-1000 cm^{-1}. HPLC investigation of the oil samples confirmed these results, since no peaks other than those arising from triglycerides and FFAs could be detected.

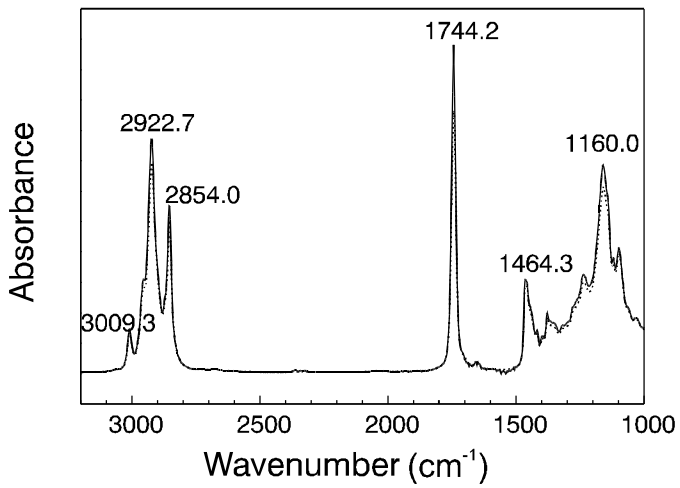

Fig. 83 ATR/FT-IR spectra of Sigma soya oil **(—)** and of separated oil phase from Intralipid 20® [batch 70178-51] **(·····)**

4.1.2 Emulsified Oil Droplets

In agreement with Smith and Mitchell [1976] and Vold and Groot [1964], who examined emulsions in the micrometer range, the parenteral emulsions show distorted, polyhedral-shaped oil droplets after high-speed-centrifugation (Figs. 84 and 85).

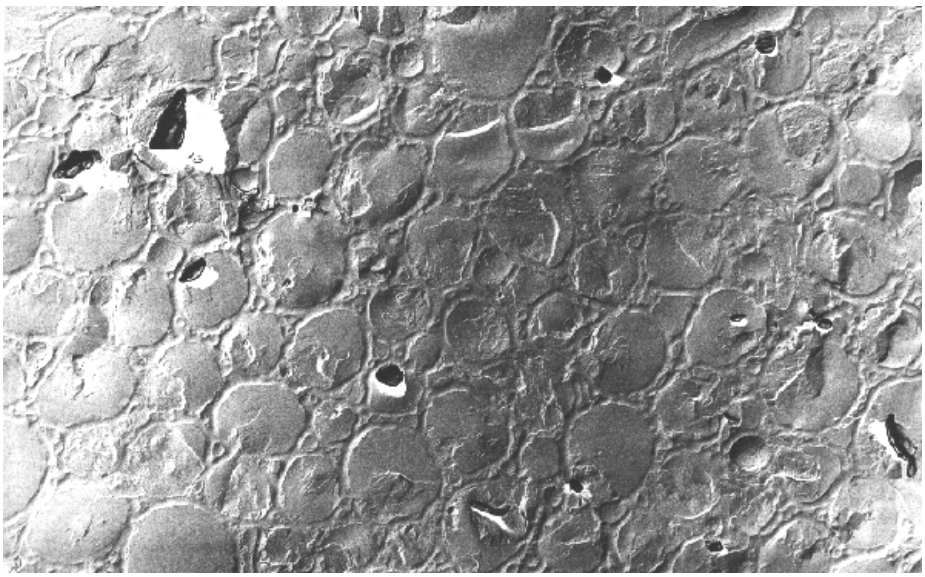

Fig. 84 FF-TEM micrograph of the centrifuged cream layer (1h, 33000 g) of non-autoclaved 20% w/w model emulsion with 1.2% w/w Lipoid E80® (4444 = 640 nm)

The oil droplets are still intact and spaced by a thin film of aqueous continuum. Measurement of conductivity of the centrifuged emulsion phases confirmed that all phases, including the cream layer, were still of the oil-in-water type. During prolonged centrifugation (up to 48 h), the cream layer was further compressed to such a degree that a semi-solid, highly viscous layer resulted. The cream layer volume decreased continually.

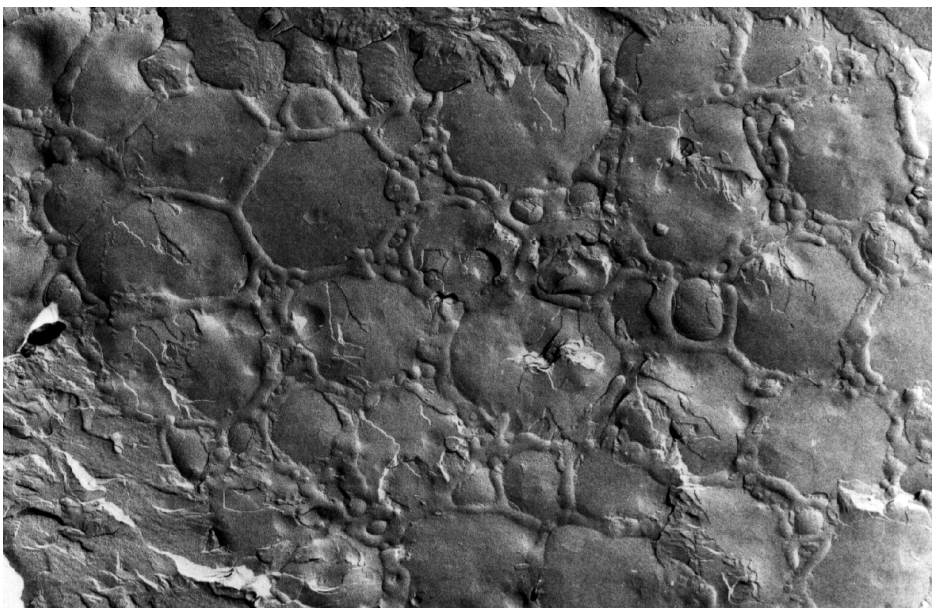

Fig. 85 FF-TEM micrograph of the centrifuged cream layer (1 h, 33000 g) of non-autoclaved 20% w/w model emulsion with 1.2% w/w Lipoid E80® showing hexagonally distorted droplets (4444 = 410 nm)

For Pluronic F68®-stabilised emulsions, no complete cracking could be achieved on

centrifugation. At an early stage a gel-like cream layer was formed which reduced droplet floatation and also subsequent coalescence. SLN dispersions, which consisted of rigid cetylpalmitate spheres, showed much less compression of the cream layer. In contrast the oil emulsions show very tight packing, since in Fig. 86 (upper left corner) it can be seen that smaller globules (either oil droplets or small vesicles) are intercalated between the spaces between larger droplets.

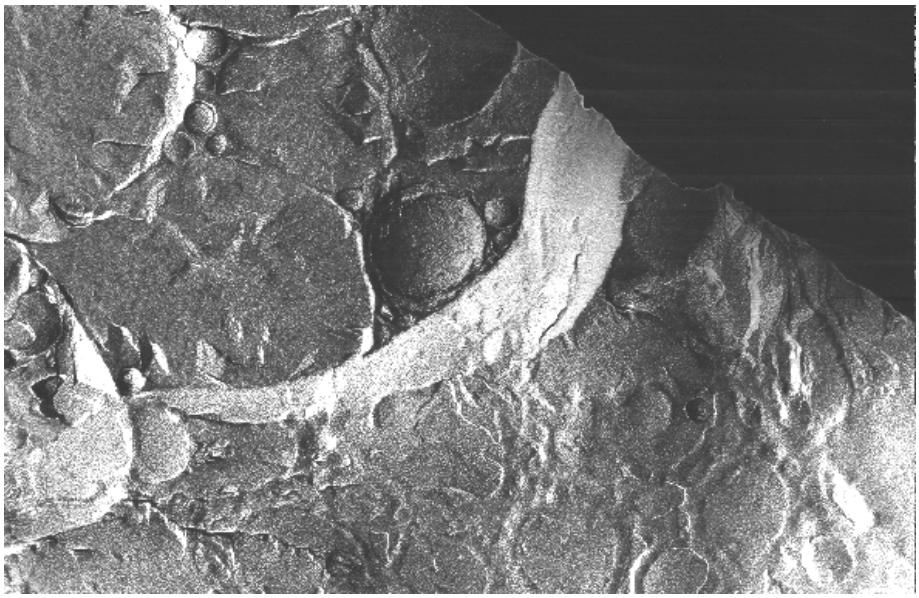

Fig. 86 FF-TEM micrograph of the centrifuged cream layer (1 h, 33000 g) of non-autoclaved 20% w/w model emulsion with 1.2% w/w Lipoid E80® showing densely packed droplets (4444 = 260 nm)

Other structures found in the model emulsions include vesicles (Fig. 87). Here, either a multivesicular, or more likely, a large vesicle with multiple fractures at its interface is seen.

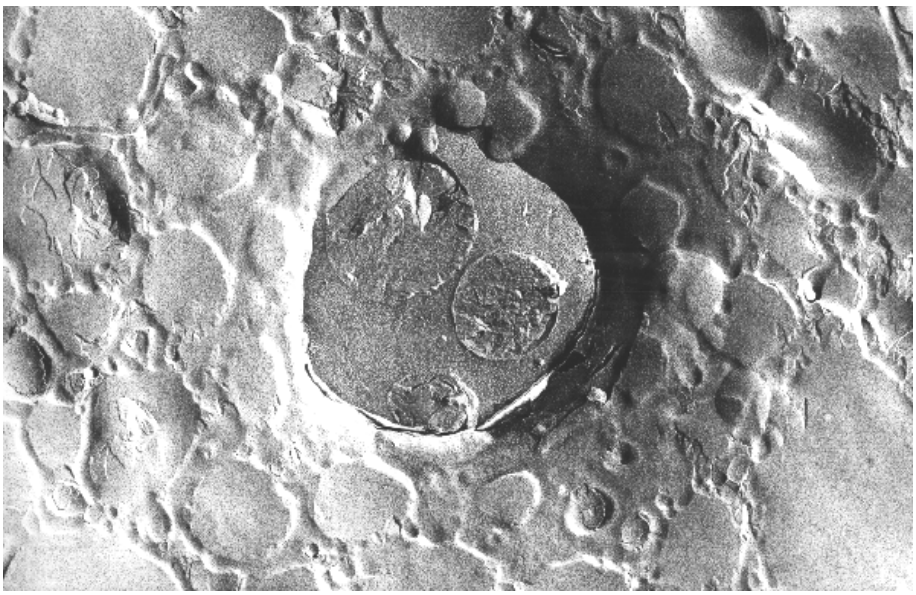

Fig. 87 FF-TEM micrograph of the centrifuged cream layer (1h, 33000 g) of non-autoclaved 20% w/w model emulsion with 1.2% w/w Lipoid E80® showing cross-fractured globule (4444 = 420 nm)

After 25 hours' centrifugation (Fig. 88), the cream layer still contains intact, tightly-packed oil droplets neighboured by smaller droplets or vesicles. As claimed by Westesen and Wehler [1993], (larger) oil droplets are evidently readily fractured, whereas smaller droplets or vesicles remain intact. It is therefore not possible to determine their type and structure unequivocally by FF-TEM.

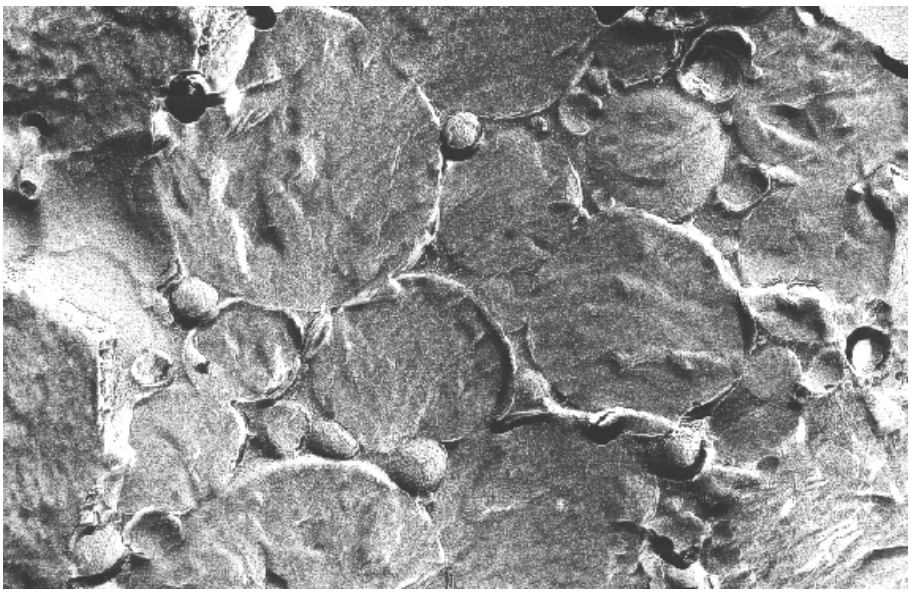

Fig. 88 FF-TEM micrograph of the centrifuged cream layer (25 h, 33000 g) of non-autoclaved 20% w/w model emulsion with 1.2% w/w Lipoid E80®
(4444 = 196 nm)

After 48 hours' centrifugation (Fig. 89) considerable cracking could be observed

macroscopically, and the cream layer exhibits large oil droplets and also multilamellar vesicular structures. Neither of these could be detected in the non-centrifuged samples.

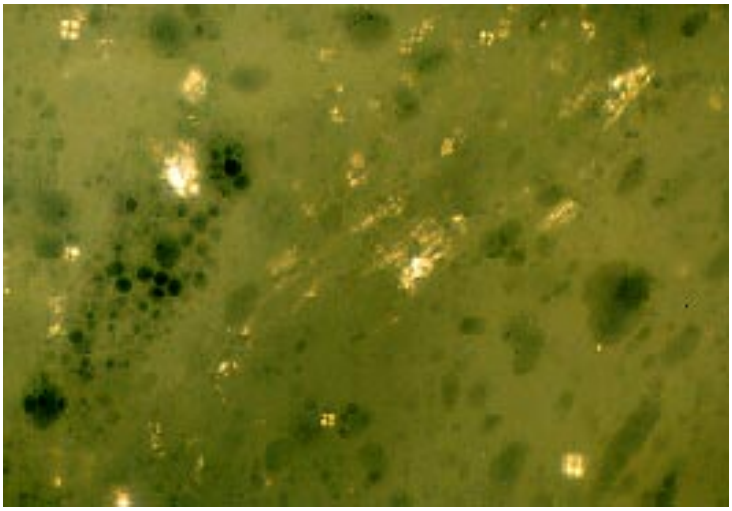

Fig. 89 PLM picture (without λ/4-platelet) of the centrifuged cream layer of a 20% w/w model emulsion after 48h centrifugation (4444 = 84 µm)

The darker globules of oil are visible in Fig. 89, as well as the brighter Maltese crosses arising from anisotropic, multiple phospholipid bilayers (see later). It was concluded therefore, that multilamellar structures are formed during centrifugation, as caused by coalescence of emulsified droplets. The presence of such structures in centrifuged emulsions is therefore an artifact, i.e. they were not present in the original emulsions. This finding is supported by analysis of a coalesced cream phase which had been left to dry over $CaCl_2$ for 24 h and then admixed with water. Large coalesced oil droplets were observed, as well as spontaneously emerging lamellar myelin sheets, typical for (free) lecithin (Fig. 90). The lamellar sheets were, however, transformed rapidly into closed lipid multilayers (MLVs).

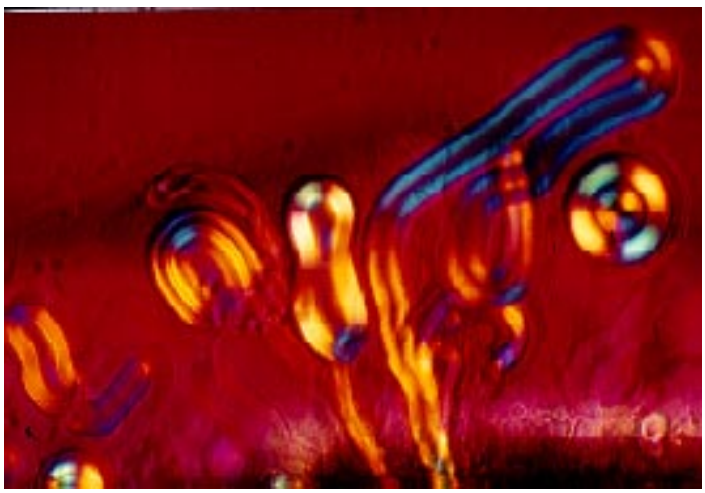

Fig. 90 PLM picture of dried cream layer (1 h, 33000 g) of autoclaved 20% w/w model emulsion after addition of double-distilled water (4444 = 45 µm)

HPLC and FT-IR analysis of the dried, aqueous phase obtained from centrifugation showed measurable amounts of triglycerides, in agreement with reports by Dickinson and Stainsby [1988], Westesen and Wehler [1993] and Férézou et al. [1994]. This can be explained by calculations from Stokes' law; soya oil droplets ($\rho = 0.92$ g/cm^3) of 70 nm cream at $6.2 \cdot 10^{-4}$ cm/d and small liposomes of the same size ($\rho = 1.010$ g/cm^3 [Férézou et al., 1994]) sediment at only $7.7 \cdot 10^{-5}$ cm/d using 33000 g, which clearly exceeds any practical time scale for centrifugation. Therefore, very small particles ought to be present in the centrifuged samples. Fig. 91 shows the FT-IR spectrum of the vacuum-dried aqueous phase of a 10% w/w model emulsion stabilised with 0.8% w/w Pluronic F68® obtained by high-speed centrifugation. As with the lecithin-stabilised emulsions, the separated aqueous phase was slightly opaque in appearance and possessed a PCS z-average diameter of 60 nm.

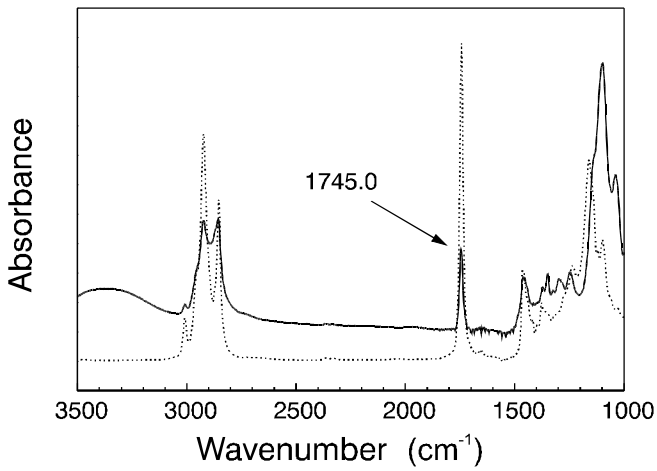

Fig. 91 ATR/FT-IR spectra of commercial soya oil **(·····)** and of dried separated aqueous subnatant of a 10% w/w model emulsion stabilised with 0.8% w/w Pluronic F68® **(—)**

Bands typical for triglycerides can clearly be seen in Fig. 91, especially the carbonyl mode at 1745 cm^{-1}. This comes from an ester and could only stem from the soya oil triglycerides. Furthermore, the peak seen at about 3010 cm^{-1} arises from alkene double-bonds, which shows the presence of unsaturated fatty acids of the soya oil. Apart from emulsifier and glycerol, the aqueous subnatant does therefore clearly contain a small proportion of triglyceride.

4.1.3 Liposomal Phospholipid Material in Emulsions

To separate the triglyceride-rich dispersed phase from possible excess lecithin material prolonged centrifugation can be used, similar to the prolonged ultracentrifugation method reported by Groves et al. [1985]. These authors observed separation of a 'yellow layer' out of the cream layer with time, and also a sediment at the bottom of the tube which they did not examine any further. It is known that liposomes (especially larger vesicles like MLVs) are

easily concentrated from the aqueous supranatant by high-speed centrifugation to form a 'pellet' [New, 1990]. As was shown above, SUVs have a very low sedimentation velocity since their densities are only marginally different from the aqueous medium. PCS measurements of the centrifugation subnatant of various parenteral emulsions gave mean particle diameters of about 70 - 80 nm, similar to those yielded by SUV dispersions (see Section 3.2.2, Tab. 19 and Fig. 92). Similar particle sizes for the subnatant have also been reported by other authors [Groves et al., 1985 / Rotenberg et al., 1991 / Westesen and Wehler, 1993 / Férézou et al., 1994 / Bach et al., 1996]. Furthermore, this phase was estimated to contain about 1/3 - 1/6 of the total phospholipids present in the emulsion [Lutz et al., 1990 / Westesen and Wehler, 1993 / Férézou et al., 1994], depending on the triglyceride-lecithin-ratio of the emulsions. The phospholipid analyses reported in Chapter 3 showed, however, the presence of only about 1/7 - 1/14 of the total PC and PE in the aqueous subnatant of commercial emulsions. However, even lower proportions were found for the model emulsions. It was therefore speculated e.g. by Herman [1992] that aggregates of phospholipids and triglycerides were present in the centrifuged subnatant. However, FF-TEM analysis of this layer showed only small, globular shapes (data not shown), which visually could be either oil droplets or liposomes. In this size range the spheres do not cross-break, which would have allowed identification of particle morphology by the appearance of the enclosed phase [Westesen and Wehler, 1993]. This is illustrated in Fig. 92 showing the FF-TEM morphology of centrifuged small liposome dispersions.

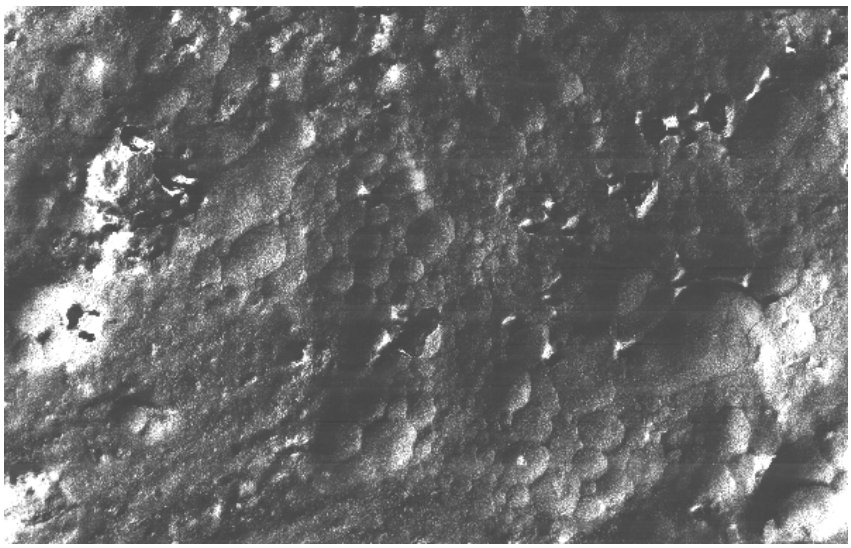

Fig. 92 FF-TEM micrograph of the middle aqueous phase layer of microfluidized and centrifuged (15 h, 33000 g) 1.2% w/w Lipoid E80® dispersion
(4444 = 260 nm)

The PLM pictures of the pellet obtained by centrifuging a 20% model emulsion (Fig. 93a and 94) show remarkable similarity to a non-centrifuged MLV dispersion (Fig. 93b).

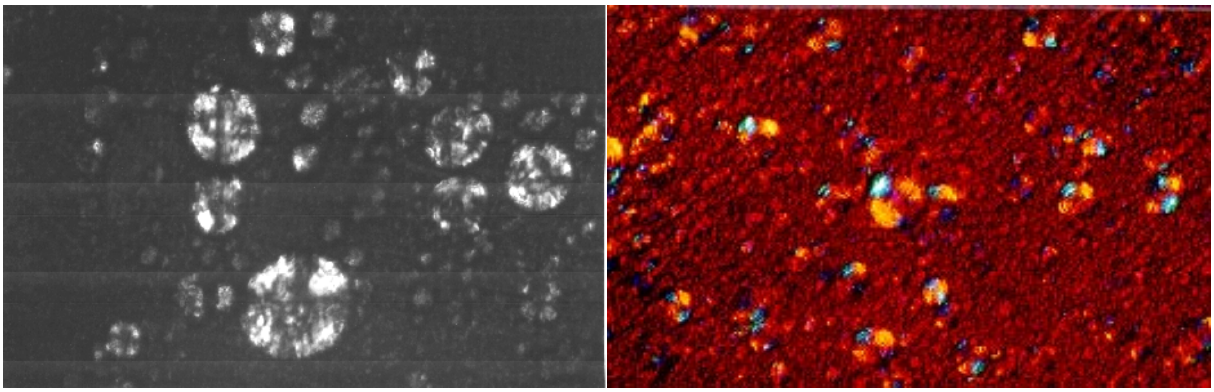

Fig. 93 **A** (4444 = 65 µm) **B** (4444 = 65 µm)

PLM pictures of **(A)** the centrifugation pellet (47 h, 33000 g) of a 20% model emulsion showing typical multilamellar structures and **(B)** non-centrifuged MLV dispersion from Lipoid E80®:Double-distilled water (1:2 w/w)

Note especially from Fig. 94, that the typical birefringence of Maltese crosses from the multilamellar phase can still be observed within the pellet.

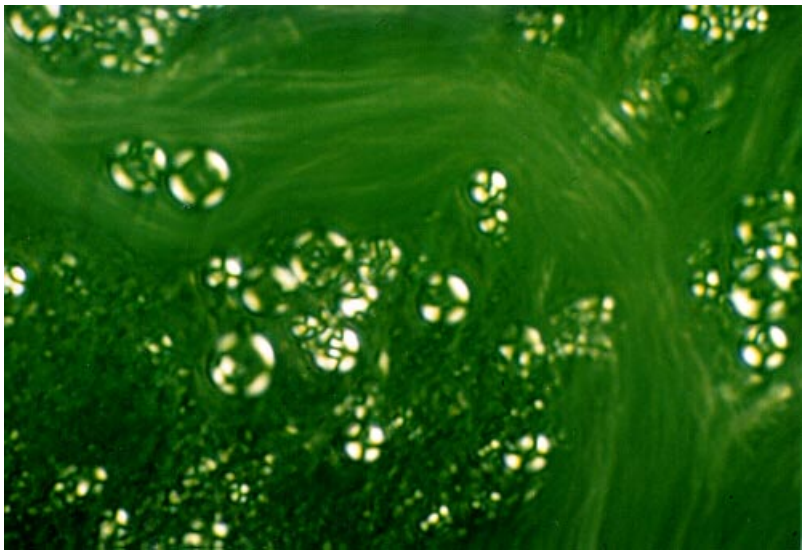

Fig. 94 PLM picture (without λ/4-platelet) of the centrifugation pellet of a 20% model emulsion showing typical Maltese crosses (4444 = 21 µm)

However, when Na-lauryl-SO_4 was admixed to the emulsions to about 50 mol% of the lecithin before centrifugation, these typical Maltese crosses disappeared (Fig. 95). This was attributed to the interaction of the surfactant with the lecithin, inhibiting the formation of the lamellar vesicles.

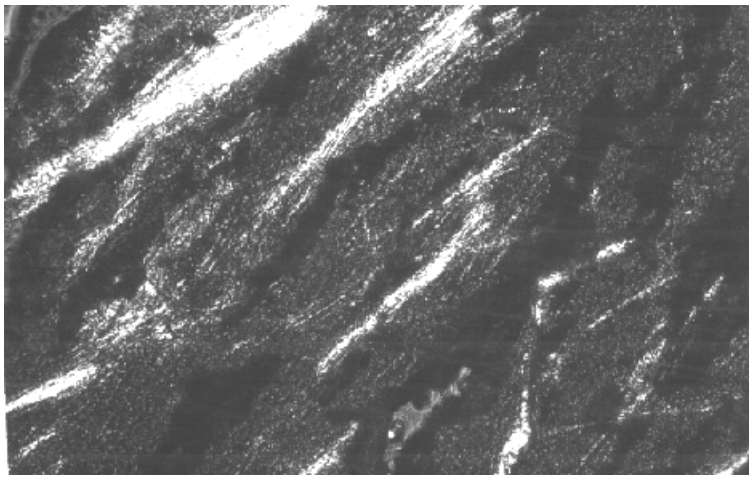

Fig. 95 PLM picture (without λ/4-platelet) of the centrifugation pellet of a 20% model emulsion admixed with Na-lauryl-SO_4 (4444 = 70 µm)

To prove a multilamellar structure for the pelleted material, FF-TEM was employed. Indeed, the pellet appears to consist of extensive, multilamellar sheets (Figs. 96 and 97). The amount of pellet obtained was larger for emulsions already cracked before centrifugation, as e.g. in the case of 20% w/w soya oil emulsion stabilised with Lipoid EPC®. More pellet was also obtained with lecithin-stabilised SLNs, where higher amounts of lecithin than typically used for emulsions had to be used to stabilise the dispersions. It can be concluded, therefore, that the amount of pellet produced is directly related to the excess of lecithin present.

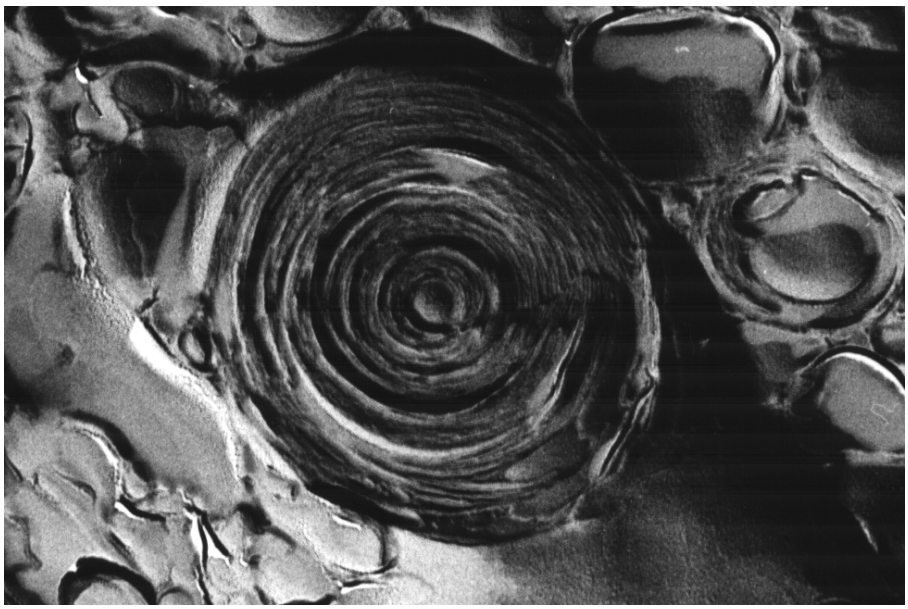

Fig. 96 FF-TEM micrograph of the centrifugation pellet (25 h, 33000 g) of non-autoclaved 20% w/w model emulsion showing typical multilamellar structures (4444 = 167 nm)

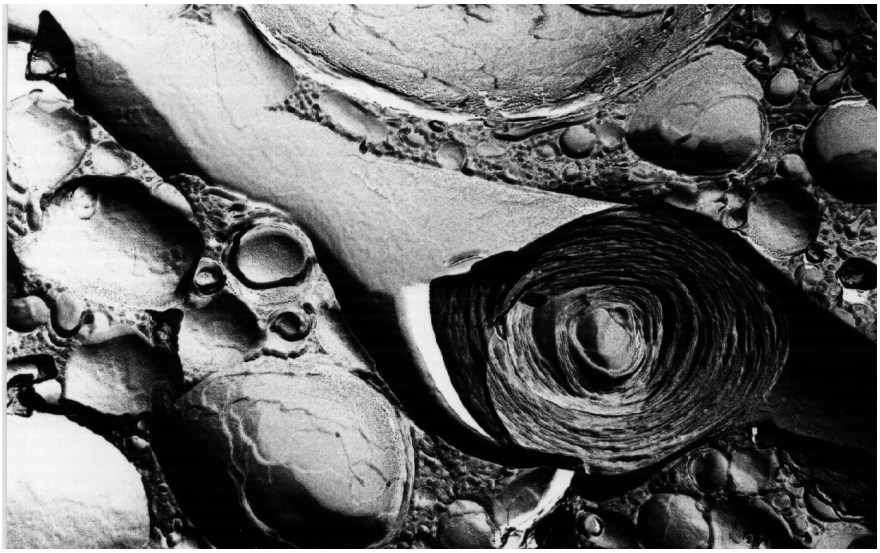

Fig. 97 FF-TEM micrograph of the centrifugation pellet (25 h, 33000 g) of a non-autoclaved 20% w/w model emulsion showing multilamellar tubular structures (4444 = 367 nm)

It is assumed that the large aggregated structures in the pellet are derived from globular precursors in the range of LUVs and small SUVs. It is clearly seen that multilamellar phases are formed in the pellet, which could only come from the phospholipids. Since these aggregates are much larger than could be expected within the original emulsion, the pellet structures must have been produced by aggregation of small phospholipid vesicles during high acceleration on centrifugation. The structure and amount of pellet indicates that excess lecithin was present in the emulsion, yet does not represent its original state of dispersion.

Since the colour of the pelleted sediment varied according to the dispersed phase used, it is evident that some of the oil phase was still associated with the sedimented lecithin. The pellets obtained from paraffin model emulsions and from Lipofundin® or Intralipid® were practically colourless, whereas the pellets from soya oil model emulsions and cetylpalmitate SLNs appeared increasingly yellowish in this order. FT-IR analysis of the vacuum-dried pellets proved the essential conformity between pellet and native egg-yolk phospholipids (Fig. 98). Moreover, the presence of glycerol out of the aqueous phase could also be detected (underlying bands at 1415 cm^{-1} and 1030 cm^{-1} and strong mode around 3100-3500 cm^{-1} indicating extensive H-bonding although water had largely been removed by drying).

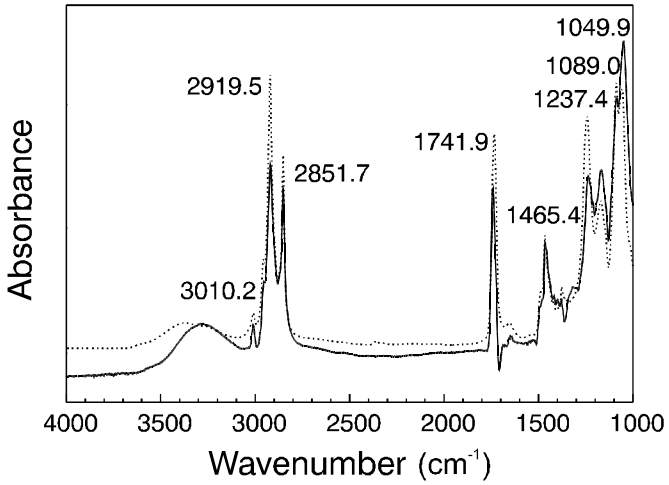

Fig. 98 ATR/FT-IR spectra of commercial egg lecithin (Lipoid E80®) **(·····)** and of dried separated pellet from Intralipid 20® [batch 70178-51] **(—)**

Centrifugation pellets also give similar melting and freezing transitions with DSC analysis to liposomal dispersions also containing glycerol. For example, the pellet obtained from Intralipid 20® (Fig. 99) shows similarly broad freezing and melting peaks to those obtained from Lipoid E80® liposomal dispersions (Figs. 42 and 122) containing glycerol. Owing to the glycerol-content of the emulsion pellet, the predominant freezing and melting peak of water is shifted away from 0°C, to reveal the lecithin signals. Thus, the freezing peak maximum at about -11°C is exposed. The shift in the water peaks is, however, less pronounced than observed for 50 wt% aqueous glycerol (Fig. 42). Therefore, in Fig. 99, the melting peak of water still overlaps the melting peak of the lecithin. Another melting peak visible at about -28°C may come from the triglycerides present in the pellet, since a similarity is found with pure soya oil thermograms (Fig. 82).

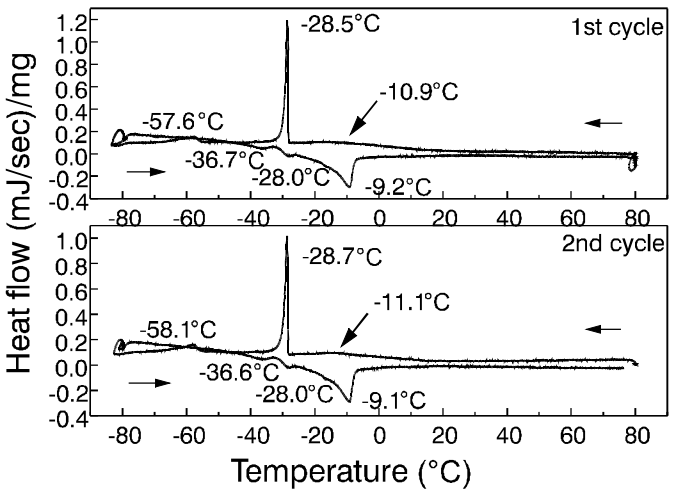

Fig. 99 DSC thermogram of the centrifugation pellet from Intralipid 20® [batch 70178-51] at 3K/min

According to HPLC analysis, the pellets were comprised mainly of PE, PC and lyso-phospholipids. Owing to the small amounts of pellet which could be isolated from emulsions, however, only weak peaks were obtained (Fig. 100). Small amounts of triglycerides and FFAs could also be discerned from the chromatograms.

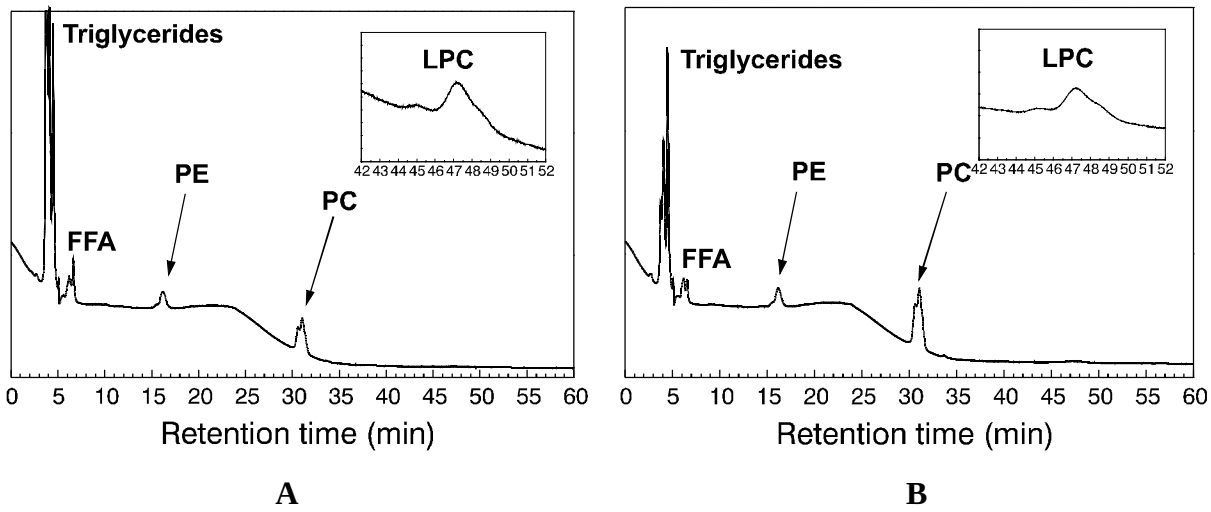

Fig. 100 Enlarged HPLC chromatograms of centrifugation pellets from **(A)** Intralipid 20® [batch 70178-51] and **(B)** Lipovenoes LCT 20® with magnified inserts

As was shown in Fig. 89, multi-lamellar structures were formed during coalescence of the dispersed phase. This explains why a pellet was also obtained when the cream phase had been harvested, redispersed in aqueous glycerol and again be centrifuged for another 12 h. This pellet therefore resulted only from droplet coalescence and thus was not related to excess lecithin initially present in the emulsion.

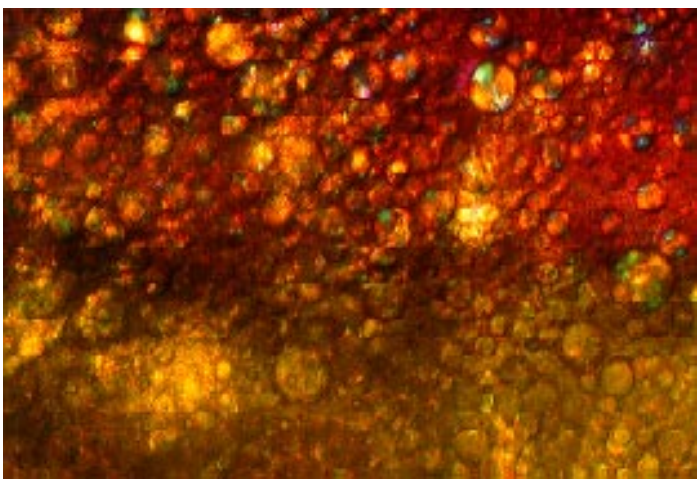

Fig. 101 PLM picture of the centrifugation pellet obtained after redispersing the cream layer of a 20% w/w model emulsion in aqueous glycerol and centrifuging it for additional 12 h at 33000 g ($_{4444}$ = 53 µm)

This finding shows that examination of the emulsions by centrifugation has to be carried out with great care, and is liable to produce liposomal structures which were not present in the native emulsions.

4.1.4 Other Possible Structures

Micelle-forming compounds like FFAs and lyso-phospholipids were mostly found at the oil/water-interface (Figs. 78-80). The ^{31}P-NMR results (see below) also do not suggest the enhanced formation of micelles of LPC. The presence of micelles from FFAs or lyso-compounds in the aqueous phase is therefore only minimal.

4.2 Separation of Emulsions by Asymmetrical Flow Field-Flow Fractionation

Asymmetrical Flow Field-Flow Fractionation (AFFF) is a new separation method among the Field-Flow Fractionation techniques. It was intended to attempt separation of emulsion droplets and liposomes in the emulsions according to their sizes. Earlier reports had tried Sedimentational Field-Flow techniques in order to separate parenteral emulsions [Caldwell, 1984 / Li et al., 1993 / Levin and Klausner, 1995]. Theoretically, emulsion droplets and liposomes would be expected to be separable by their different densities (0.92 g/cm^3 for soya oil and 1.010-1.030 g/cm^3 for the particles contained in the aqueous subnatant [Férézou et al., 1994]). Levin and Klausner [1995] could not, however, obtain separation of a distinct liposomal fraction, as had been suggested for centrifugational separation by Groves et al. [1985]. In the current study, however, it has been shown that the emulsions underwent unpredictable changes under centrifugational forces, yielding artifacts (Section 4.1). Using AFFF it was hoped to yield a high resolution separation of the emulsions without producing artifacts by centrifugation.

The first objective was to characterise separately the size distributions for a microfluidized 4 wt% liposomal dispersion and for a 10 wt% emulsion produced with 1.2 wt% Lipoid E80®. Fig. 102 shows the scattering intensities of the diluted liposomal dispersion for 9 scattering angles plotted against elution time. A strong dependence of the scattering angle can clearly be seen for the larger particle sizes. The root mean square (rms-) radii were calculated from the slope of scattering intensity vs. angle [Wyatt, 1993].

The third peak in Fig. 102 has a large slope, indicating visually that large liposomes must be contained in the sample. These were, however, not resolvable by PCS measurements.

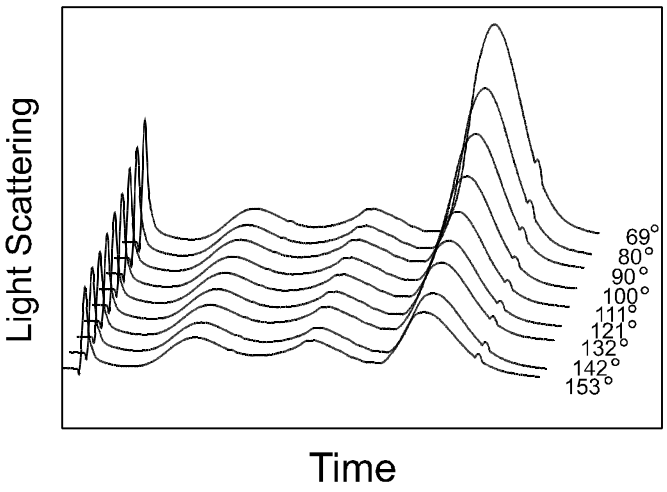

Fig. 102 Plot of scattering intensity of a 0.4% w/w liposome sample vs. elution time for 9 scattering angles as determined by AFFF

The first liposome fraction in Fig. 103 shows a retention time of 3-6 min, using elution at 1.0 ml/min channel flow rate and 1.0 ml/min cross flow rate. After 10 min elution time the flow rates were changed to 1.55 and 0.45 ml/min, allowing larger sizes to elute. Two additional peaks appeared after 14 and 16 min, indicating that the largest particles ranged up to 700 nm rms-radius, probably being larger liposomal aggregates.

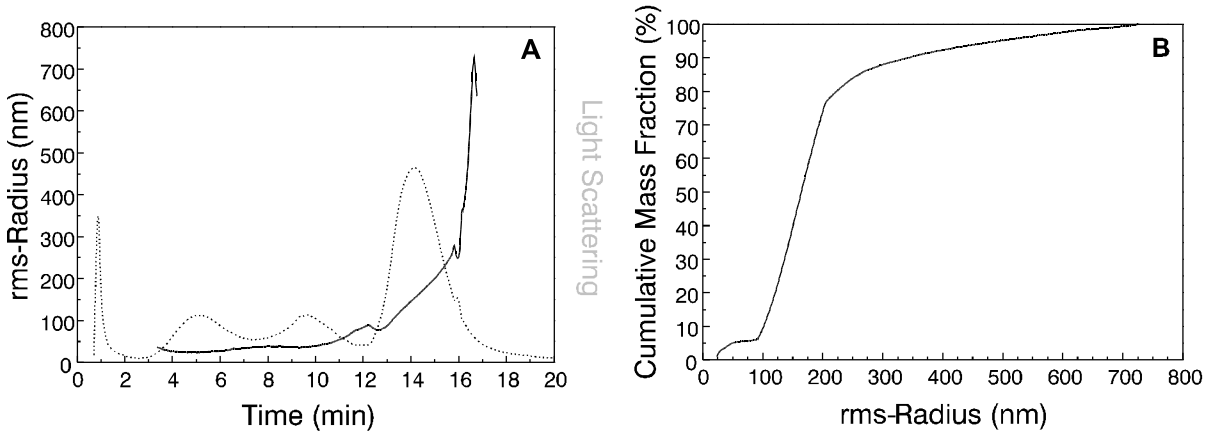

Fig. 103 Plots of **(A)** scattering intensity of a 0.4% w/w liposome sample vs. elution time at 90° light scattering trace (·····) and calculated rms-radius of the liposomes (—) as a function of elution time and **(B)** resulting cumulative mass distribution

Particle sizes determined by AFFF are somewhat larger than those determined by PCS or LD measurements (Fig. 56, Tab. 19), indicating more sensitive response towards small fractions of larger particles. FFF theory predicts a linear increase in radius with elution time at a constant cross flow rate. This is seen with the calculated rms-radii in Fig. 103b and Fig. 104b. At higher elution times the cross flow rate was reduced, leading to deviation from a linear increase. There is no indication of Mie scattering effects even at the largest calculated radii. Extrapolations are linear with excellent correlation using the Berry function.

Under the same separation conditions, a 10% w/w model emulsion (homogenised with 1000 bar) shows only the tailing flank of a high system peak resulting from oversized particles well above 1µm in geometrical diameter (Fig. 104). After 13 min elution time, the flow ratio was changed to 1.95 and 0.05 ml/min to allow fast elution of the larger droplet sizes.

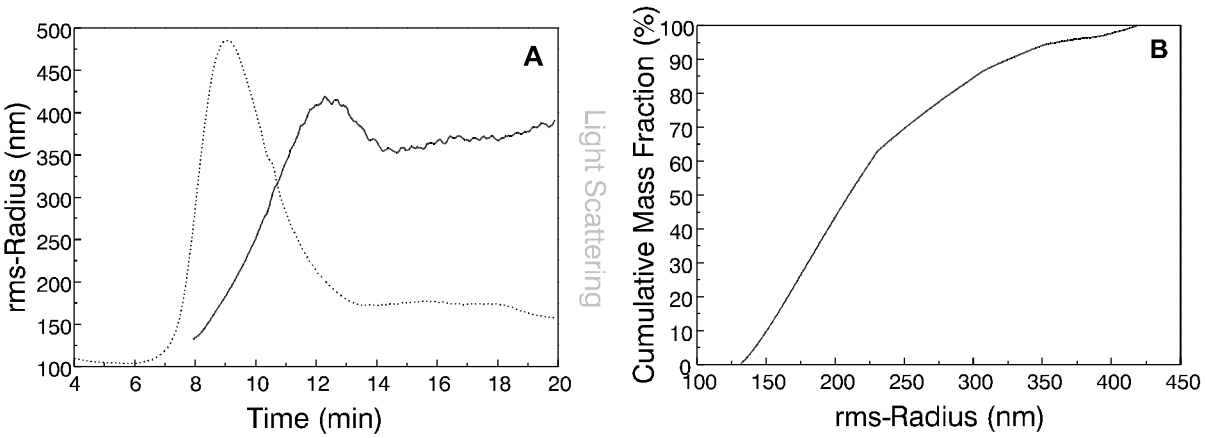

Fig. 104 Plots of **(A)** scattering intensity of a 10% w/w emulsion sample vs. elution time for 90° light scattering trace (·····) and calculated rms-radius of the liposomes (—) as a function of elution time and **(B)** resulting cumulative mass distribution

Accordingly, the emulsion does not show any particles < 100 nm rms-radius, but ranged up to 450 nm rms-radius. If free liposomes were present, they should be easily detectable within the emulsion sample after approx. 5 min, which surprisingly is not the case. To ascertain if liposomes could in principle be detected in the presence of emulsion droplets, emulsion and liposome preparations were mixed immediately before injection into the AFFF. Fig. 105 shows the 90° light scattering signals for the liposomal dispersion, the emulsion and their mixture.

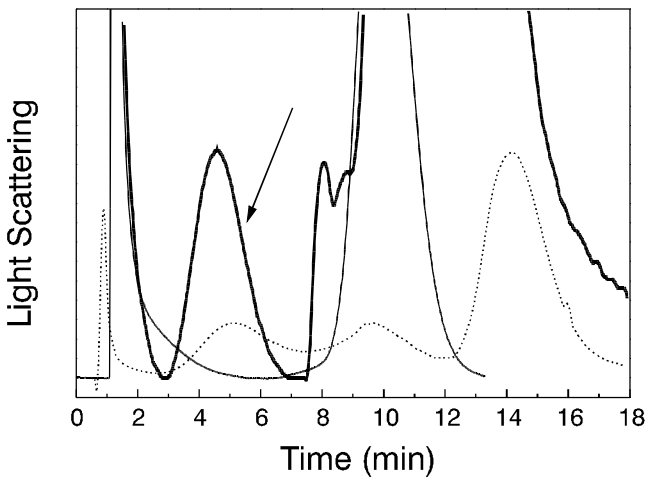

Fig. 105 Plot of scattering intensity of liposome dispersion and emulsion sample vs. elution time for 90° scattering angle as determined by AFFF: 10% w/w emulsion (—), 0.4% w/w liposome dispersion (·····) and enlarged section of mixture of liposomes and 10% w/w emulsion (44)

The liposomes elute, as found in Fig. 103, after 3-6 min. The 10% w/w emulsion, however, shows no peak in this elution time window. But in the mixture, a liposome peak can be clearly detected. Since the liposomal dispersion was contained diluted to approx. 0.4 wt% lecithin, a calculation based on signal-to-noise characteristics gives an estimated free liposome concentration in the pure emulsion that cannot exceed 0.01 wt%. This is surprising, since 10% O/W-emulsions with 1.2 wt% lecithin are thought to contain a 50% lecithin-excess over that required to cover the oil droplets [Férézou et al., 1994]. It can be concluded therefore that if any lecithin excess occurred, it did not exist as free liposomes within the emulsion. However, these results do not rule out the formation of liposome aggregates, e.g. with emulsion droplets. Such aggregates would not have been separated, as their size would overlap with that of the emulsion droplets.

4.3 Examination of Unfractionated Samples

4.3.1 TEM Analysis

10% w/w model emulsions containing 1.2% w/w lecithin, which was therefore presumed to be contained in excess, were examined by Cryo-TEM by 1+10 dilution with 2.25% w/w aqueous glycerol. No differences could be observed for emulsions diluted with double-distilled water, indicating that vitrification of the samples was achieved without producing any artifacts arising from the presence of glycerol. Hamilton et al. [1980] claimed that MLV dispersions were transformed into SUV dispersions under high pressure conditions. Similarly Mayhew et al. [1984] reported the production of SUVs with a Microfluidizer®. For TEM analysis of lecithin-stabilised emulsions, negative staining (mainly with OsO_4) has frequently been used [Kleinberger and Pamperl, 1983 / Groves et al., 1985 / du Plessis et al., 1986 / Cornelus et al., 1993]. Negative staining of liposomal dispersions can, however, easily result in artifacts, since small liposomes can be disrupted to larger MLV structures owing to the manipulation of the sample [Miyamoto and Stoeckenius, 1971]. Small liposomal material may therefore erroneously appear to be in multilamellar state in the emulsions. Fig. 106 shows clearly emulsified oil droplets of a 10% model emulsion. These appear as dark spheres on a lighter background, with apparently no lamellar structures in view.

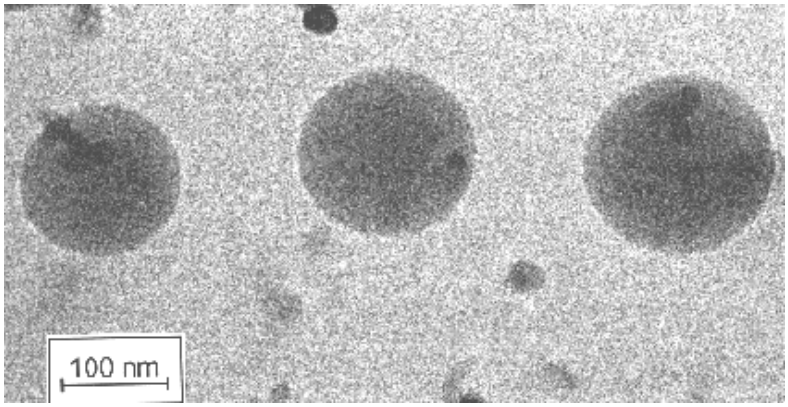

Fig. 106 Cryo-TEM picture of a non-autoclaved 10% w/w model emulsion produced with 1.2% w/w Lipoid E80® at 700 bar

Lipofundin MCT 10%® has essentially the same appearance (Fig. 107); dark oil droplets but no visible multilamellar sheets.

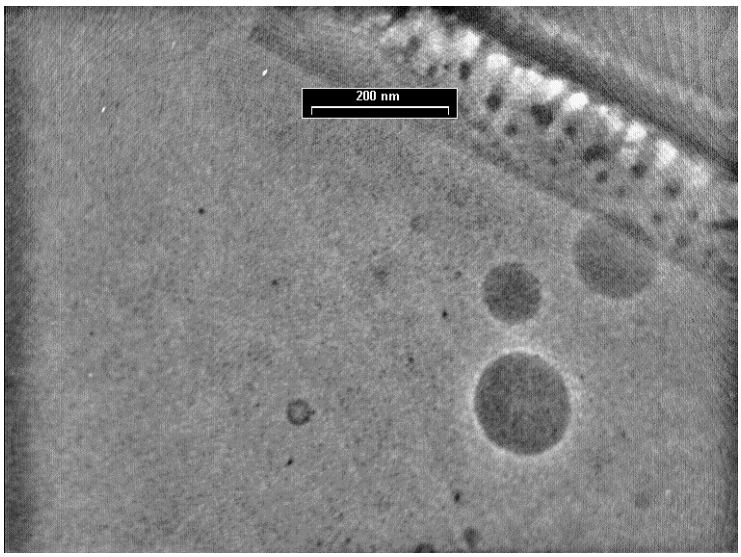

Fig. 107 Cryo-TEM picture of Lipofundin MCT 10%® produced with 1.2% w/v egg lecithin **(bar represents 200 nm)**

As a comparison Fig. 108 shows Cryo-TEM pictures of liposomal dispersions. The picture in Fig. 108a was published by Nattermann Phospholipid GmbH [1995], showing a liposomal dispersion obtained under low-shear conditions, resulting in large tube-shaped structures. Such structures were, however, found extremely rarely in microfluidized Lipoid E80® dispersions (Fig. 108b).

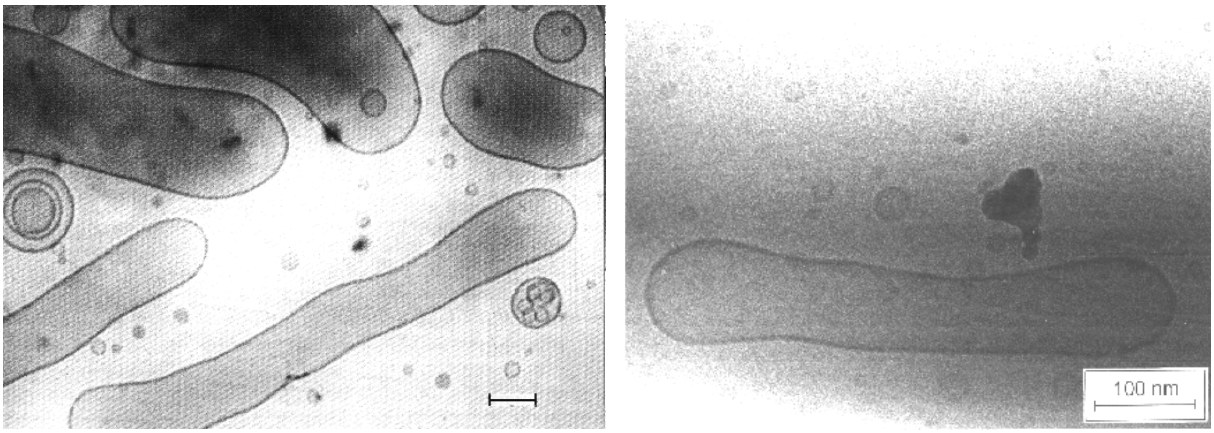

A **B**

Fig. 108 Cryo-TEM pictures of **(A)** liposome dispersions manufactured at lower energy input (from Nattermann Phospholipid GmbH [1995]) and **(B)** homogenised 1.2% w/w Lipoid E80® dispersion **(bars represent 100 nm)**

The high homogenisation pressure used (up to 1000 bar), evidently disrupted the multilamellar precursors to yield mainly SUVs of mean diameter ranging well below 100 nm (Fig. 109). LUVs (as in Fig. 108) could rarely be found.

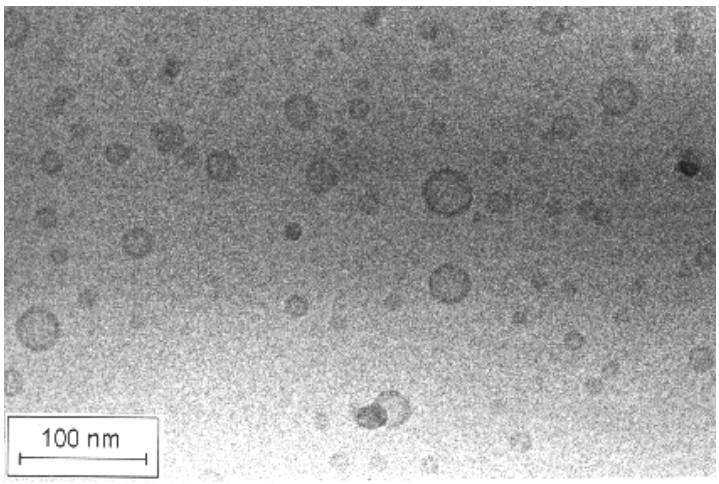

Fig. 109 Cryo-TEM picture of homogenised 1.2% w/w Lipoid E80® liposome dispersion, showing typically-seen SUVs

Liposomes with multiple bilayers could also only be observed rarely (Fig. 110) and, if present, had only small diameters. It is therefore concluded, that liposomal material in emulsions prior to autoclaving is present in the form of SUVs rather than multilamellar vesicles. This is also the case for the model emulsions as well as for commercial emulsions.

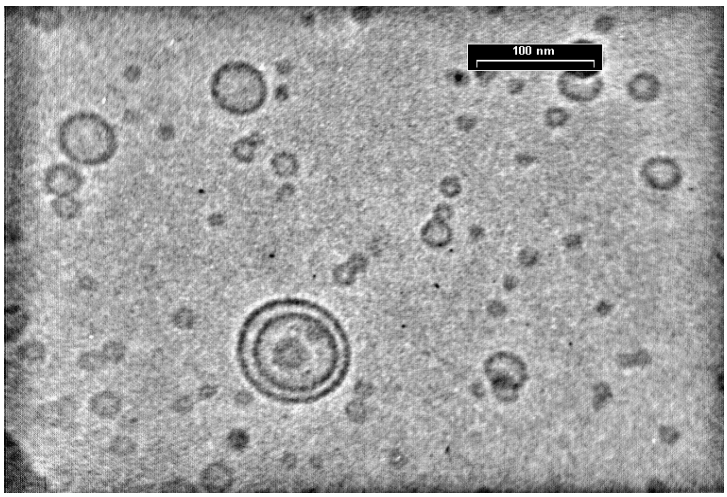

Fig. 110 Cryo-TEM picture of homogenised 1.2 wt% Lipoid E80® liposome dispersion, showing multiple bilayer structure **(bar represents 100 nm)**

Hollow liposomes of size predictable from pure liposome dispersions are seen in the emulsions, together with darker oil droplets (Figs. 111-113). Neither the model emulsions before autoclaving (Figs. 112+113), nor commercial Lipofundin MCT 10%® (Fig. 111) contain multilamellar structures which had been reported for lecithin-stabilised O/W-emulsions by Friberg et al. [1976] and Groves et al. [1985].

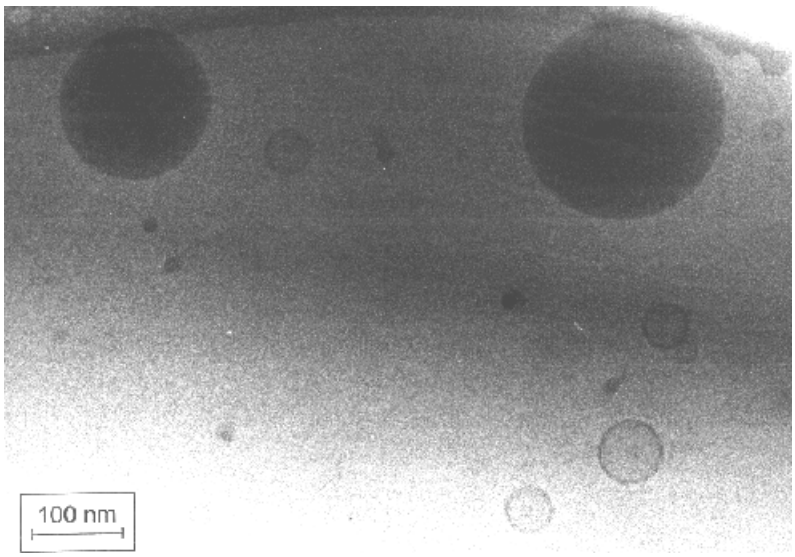

Fig. 111 Cryo-TEM picture of Lipofundin MCT 10%® stabilised with 1.2% w/v egg lecithin

Du Plessis et al. [1986] and Westesen and Wehler [1993] reported negative staining TEM and FF-TEM, respectively, to determine particle size distributions of parenteral fat emulsions. Both

techniques measure, however, cross-sections of the droplets for diameter analysis, which does not reflect the true particle diameters. Cryo-TEM yields the exact projection diameters of the spheres. The oil droplets found in the model emulsions are of the size range expected from PCS and LD data (Tabs. 18+21), although it was also observed that droplets larger than the sample film thickness (a few hundred nm) were forced out of the film into the grid areas and thus were less readily detected. Therefore, calculation of size distributions from the Cryo-TEM micrographs was not attempted.

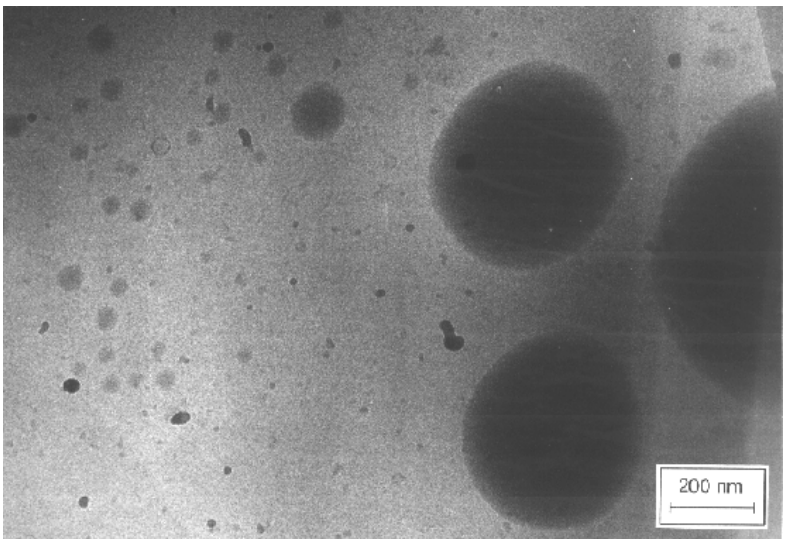

Fig. 112 Cryo-TEM picture of non-autoclaved 10% w/w emulsion with 1.2% w/w Lipoid E80® homogenised at 400 bar

It appears, however, that 10% emulsions with presumed emulsifier excess contain more liposomes when being homogenised at 400 bar (Fig. 113) than at higher pressures, which could well be explained by their larger mean droplet diameter.

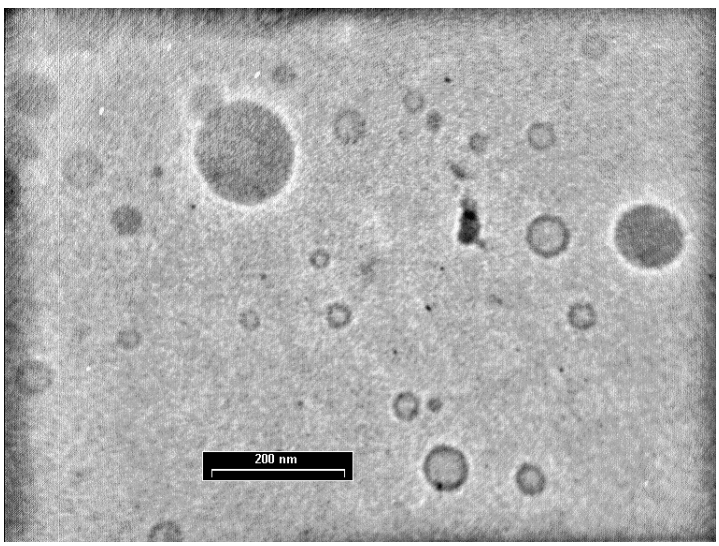

Fig. 113 Cryo-TEM picture of autoclaved 10% w/w emulsion with 1.2% w/w Lipoid E80® homogenised at 400 bar, showing many excess SUVs **(bar represents 200 nm)**

4.3.2 Particle Size Analysis using Laser Diffractometry equipped with PIDS

A direct determination of liposomal excess in the form of SUVs in unfractionated emulsions was attempted using a Laser Diffractometer equipped with the PIDS technique and operating in the Mie mode. With this apparatus high resolution sizing from 40 nm up to the upper µm range is possible, which should allow determination of the complete particle size distribution expected in parenteral fat emulsions. However, evaluating light scattering data using the Mie evaluation is known to underestimate the proportion of the largest emulsion droplets [Kohlrausch and Steffens, 1997]. It also requires knowledge of optical properties of the sample. Since the true refractive indices for soya oil droplets, SLNs and liposomes are unknown, the size distributions were calculated here according to the Mie model, but using various refractive indices as optical models for the dispersed phase. The values varied from 1.33 (water) up to 1.59 (refractive index of polystyrene latices, which were also admixed to dispersions for comparison purposes). The imaginary part of the optical model was set to 0 in all cases, even though absorption of the incident light by the dispersed particles could not be ruled out for emulsions and liposomes. However, by reflectometric measurement of solid cetylpalmitate, its refractive index was determined to 1.42 and no absorption was detected. Typically, emulsion and SLN samples were diluted by about 1:3000 with 2.25% v/v aqueous glycerol to achieve acceptable obscuration values. As reported in Section 3.2.2, liposome samples showed low scattering intensities, making it necessary to use a 40 - 80 fold lower dilution.

Initially the resolution capability of the method for polydisperse systems possessing different optical properties was examined. Liposomal dispersions were admixed with increasing amounts of a 210 nm polystyrene latex dispersion.

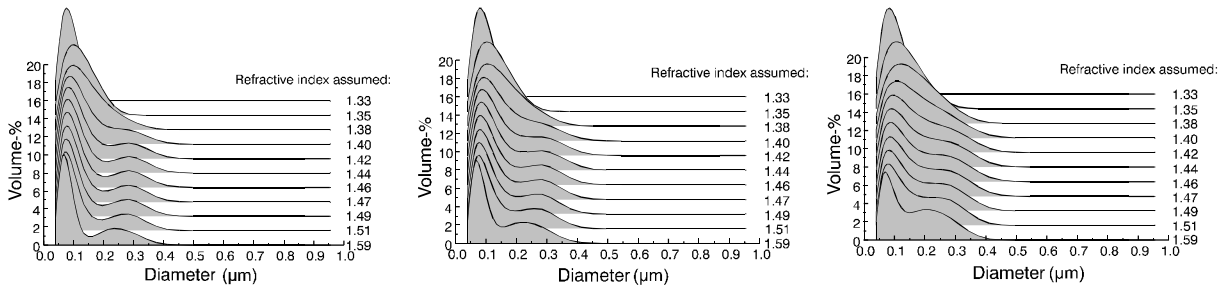

Fig. 114 Volume distributions of 3.6% w/w Lipoid E80® SUV dispersion admixed with increasing amounts of 210 nm latex standard as determined with LD with PIDS in the Mie mode using various refractive indices for optical model calculations

Liposomes:latex **(A)** 81:1 v/v **(B)** 41:1 v/v **(C)** 17:1 v/v

The results in Fig. 114 show clearly that polydisperse particles of different optical properties can be detected, even when the different particles possess similar mean diameters. The discrimination of the two peaks at approx. 70 nm (liposomes) and 210 nm (latex) improves with increasing refractive index used for the Mie calculation. This typifies the problems when examining a system containing two different disperse phase populations of different refractive indices. For the Mie calculation only a single refractive index is used, which clearly cannot display the correct distribution of two populations. Although the liposome peak in Fig. 114 remains at approx. 70 nm for all refractive indices, the discrimination between both populations is better at refractive indices in the range correct for the latex (1.59). The discrimination is good with little added latex (Fig. 114b), but shows incipient fusion of the peaks with increasing amount of added latex (Fig. 114b+c). It thus appears that the expected bimodal particle size distributions in the parenteral emulsions may be able to be resolved by this method. Fig. 115 shows the results for Intralipid® 10 and 20 by varying the optical model as before.

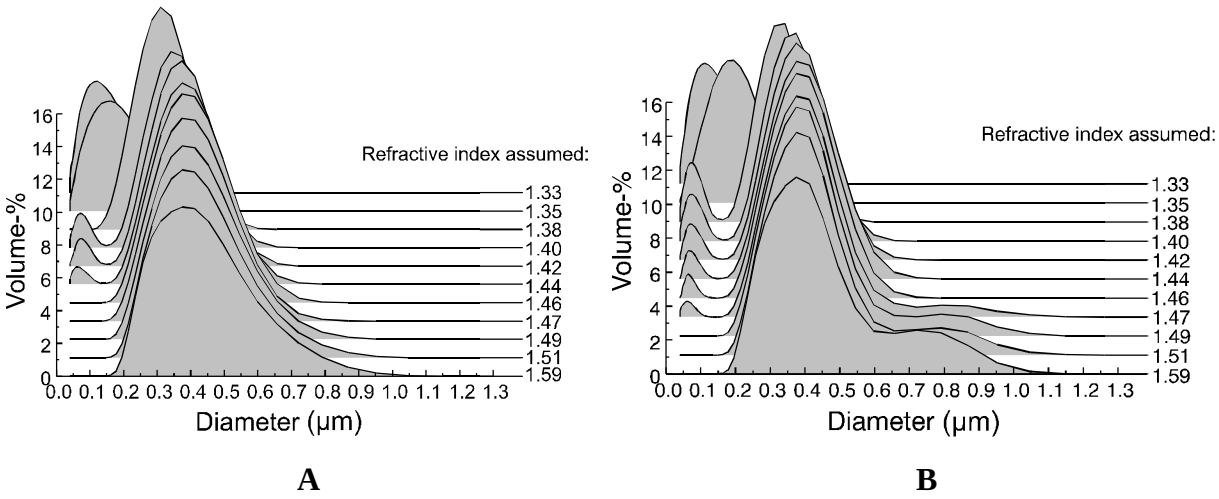

Fig. 115 Volume distributions of **(A)** Intralipid 10® [batch 68460-51] and **(B)** Intralipid 20® [batch 70178-51] as determined with LD with PIDS in the Mie mode using various refractive indices for optical model calculations

Contrary to the results for the liposomal and latex dispersions (Figs. 56+114), alteration in the refractive index greatly influences the result for the emulsions. By increasing refractive index a broadening of the distributions and a tendency to shift towards greater particle sizes is observed. The refractive index of pure soya oil in the dispersed phase is about 1.47, although the influence of the interfacial layer(s) is unknown. The mean particle sizes are, however, strongly dependent on the refractive index chosen. Compared with PCS data, the results obtained with refractive indices from 1.44-1.47 are closest (Tab. 27). It is, however, remarkable that both emulsions show a second particle population at those refractive indices and at that size where liposomal dispersions could be detected with the LS 230 (Fig. 56).

Refractive index	Intralipid 10®	Intralipid 20®
1.33	121 nm	114 nm
1.35	139 nm	162 nm
1.38	307 nm	209 nm
1.40	264 nm	247 nm
1.42	298 nm	285 nm
1.44	325 nm	316 nm
1.46	386 nm	330 nm
1.47	389 nm	345 nm
1.49	397 nm	395 nm
1.51	415 nm	398 nm
1.59	399 nm	400 nm
PCS Z-Average	320 nm	361 nm

Tab. 27 LD mean diameter of volume distribution for Intralipid 10® and Intralipid 20® samples depending on the refractive index assumed, compared with PCS z-average data

The Intralipid 10® formulation, which contains reduced emulsifier excess, shows less strong signals for this second population at around 100 nm. It is tempting to assume that this population represents liposomes (SUVs) present in the aqueous phase.

To evaluate the influence of preparation method and emulsifier excess on the size distributions, two 10% w/w model emulsions were prepared in different ways: one with 1.2% w/w lecithin at 1000 bar assumed to contain lecithin in excess; a second one prepared by diluting a homogenised (1000 bar) 20% w/w emulsion with aqueous glycerol solution down to 0.6% w/w emulsifier, was equivalent to that contained in Intralipid 10®. Fig. 116 shows that substantial differences occur between the two emulsions. The 10% model emulsion appears to consist of two populations, although the smaller fraction appears rather as a shoulder on the main distribution. Particle size is considerably lower than for the commercial 10% sample (Fig. 115), which confirmed previous PCS measurements (Tabs. 18+21). Either a larger interfacial area had reduced emulsifier excess, or more excess emulsifier was present, shifting the distribution towards smaller particle sizes.

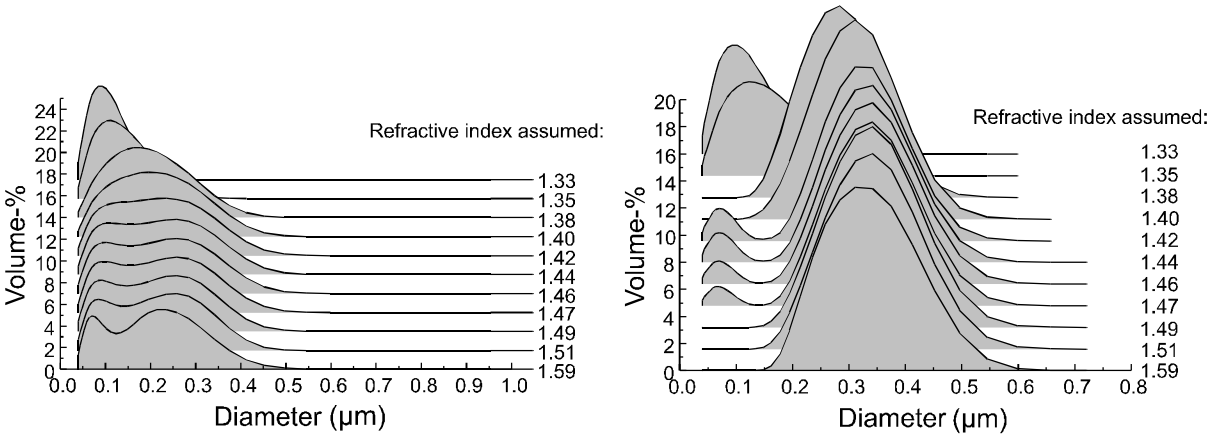

Fig. 116 Volume distributions of **(A)** 10% w/w model emulsion prepared with 1.2% w/w Lipoid E80® and of **(B)** 10% w/w emulsion prepared by dilution from 20% w/w emulsion as determined with LD with PIDS in the Mie mode using various refractive indices for optical model calculations

The second 10% emulsion prepared by diluting a 20% system appears to be similar to a 20% emulsion. Again, two separate distributions appear, suggesting again that small amounts of liposomes are detectable. Droplet sizes are, however, larger, confirming the size data reported in Tab. 18 and Figs. 57+58, where higher dispersed phase content resulted in greater mean particle size. The attempt to reduce emulsifier excess by dilution of a more concentrated system prepared with less emulsifier excess, thus led to larger particle size.

The size distributions obtained with model emulsions prepared with paraffin (liquid and viscous paraffin combined to yield the same viscosity as soya oil, η = 69.2 mPa·s) containing excess lecithin (Fig. 117b), and also with solidified cetylpalmitate melts (SLNs) stabilised with excess lecithin (Figs. 117a) also both show clear signals below 100 nm indicative of liposomes.

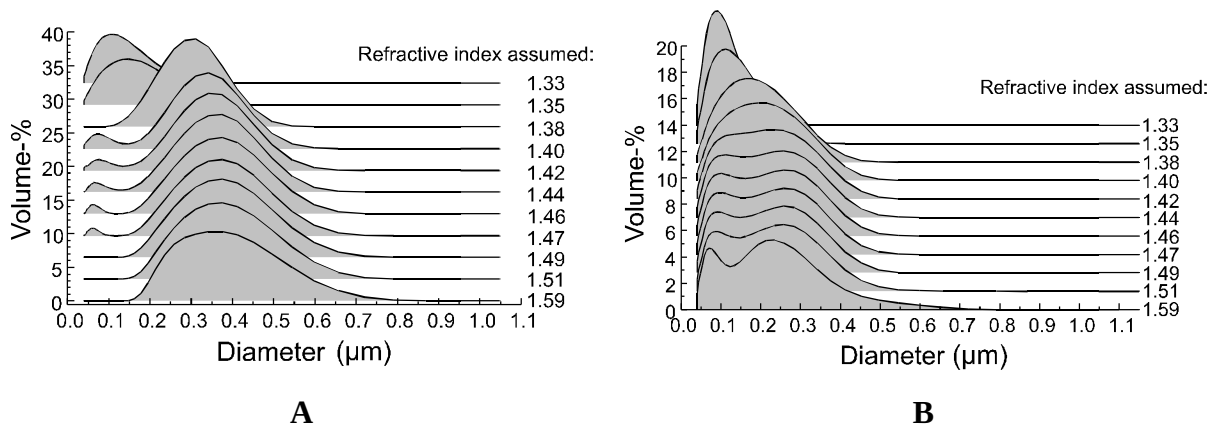

Fig. 117 Volume distributions of **(A)** 10% w/w cetylpalmitate SLN dispersion prepared with 4.8% w/w Lipoid E80® and of **(B)** 9.3% w/w paraffin emulsion prepared with 1.2% w/w Lipoid E80® as determined with LD with PIDS in the Mie mode using various refractive indices for optical model calculations

SLNs are not subject to coalescence on admixing with emulsions since they are rigid spheres. Liposomes or SLNs were therefore added to emulsions to determine whether the bimodal distributions observed could be related to distinct particle populations (Fig. 118). Changes in peaks on addition of increasing amounts of SLNs or liposomes are clearly detectable in Fig. 118. The lecithin-stabilised SLNs have an average diameter of approx. 400 nm (Fig. 117a) and when added to a 10% model emulsion, increased the signal at 400 nm (Fig. 118b) attributed to the oil droplets. Similarly, addition of liposomes of average diameter 70 nm (Fig. 56, Tab. 19) to an Intralipid 20® emulsion increased the signal < 100 nm (Fig. 118a) attributed to liposomes of excess lecithin. These admixture experiments show that polydisperse systems possessing different optical properties (i.e. liposomes with oil droplets) are resolvable into individual distributions by LD with PIDS. It remained, however, unequivocally to be proven if the peak at about 80 nm in the emulsions solely reflects a liposomal fraction.

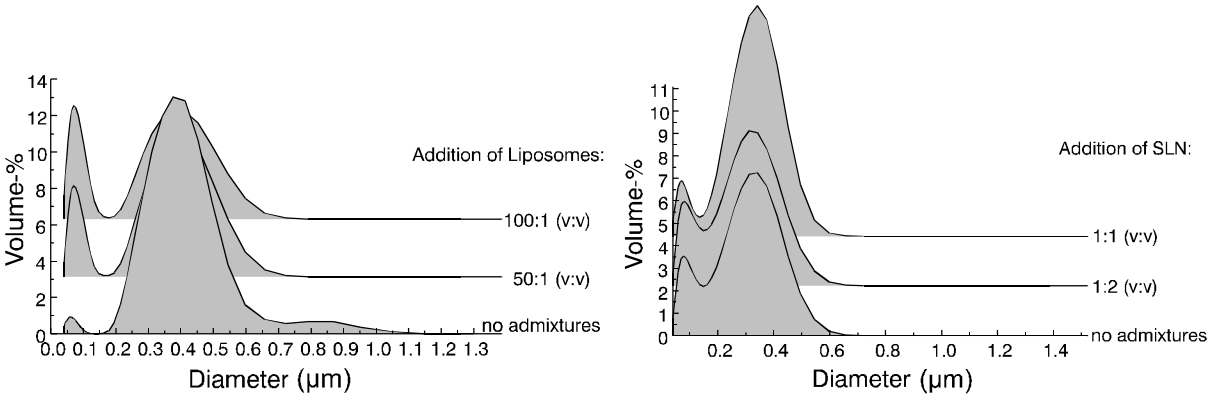

Fig. 118 Volume distributions of **(A)** Intralipid 20® [batch 70178-51] admixed with increasing amounts of 3.6% w/w Lipoid E80® SUV dispersion and of **(B)** 10% w/w model emulsion prepared with 0.6% w/w Lipoid E80® with increasing admixing of SLN dispersion as determined with LD with PIDS in the Mie mode using a refractive index of 1.47 for optical model calculations

To this end, model emulsions and SLN dispersions were produced with Pluronic F68® as emulsifier. These should show only monomodal distributions, since the emulsifier is more water-soluble than lecithin and is not expected to form any vesicular aggregates above 40 nm. Pure Pluronic F68® solutions did not give any measurable scattering nor size distributions with either PCS and LD. Surprisingly, bimodal distributions were also observed for the SLNs (Fig. 119a) and the emulsions (Fig. 119b). Since the presence of liposomes is not possible in these dispersions, the conclusion must be drawn that the scattering data generates artifacts (ghost peaks) for broadly distributed samples in the size range close to the lower limit.

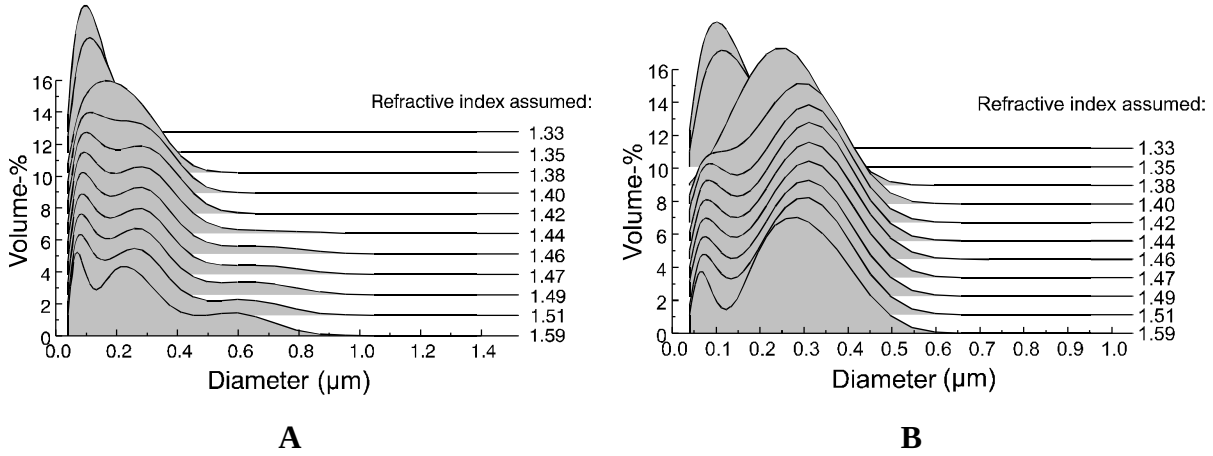

Fig. 119 Volume distributions of **(A)** 10% w/w cetylpalmitate SLN dispersion prepared with 1.6% w/w Pluronic F68® and of **(B)** 10% w/w model emulsion prepared with 0.8% w/w Pluronic F68® as determined with LD with PIDS in the Mie mode using various refractive indices for optical model calculations

The initial promising results for mixed liposome and emulsion samples do not therefore prove the existence of liposomes besides oil droplets within the emulsions. A further point is that liposomes show a very weak light scattering response, which would make reliable quantitation of a small liposomal excess impossible. To conclude the LD results, it is not possible to judge to which extent lecithin is present in the form of liposomes in native emulsions.

4.3.3 DSC Analysis

Diederichs [1993] claims that the direct thermal analysis of lecithin within emulsions is possible. According to her data, egg phospholipid melting was detected at about -10°C and the respective freezing at -25°C. It was, however, not reported, if these lecithin transitions come from bilayer (liposomes) or monolayer (emulsion interface) phospholipids.

The thermograms of native emulsions are completely dominated by the freezing and melting peaks of water (Fig. 120). This was observed in all cases, regardless of the oil phase content of the samples. When the same amount of soya oil was incorporated in 2.25% aqueous glycerol with an Ultra Turrax stirrer without addition of an emulsifier, the freezing point depression of the water is larger (-17.6°C) and also numerous small freezing and melting peaks of soya oil are evident (compare enlargement in Fig. 120 with Fig. 82 for soya oil). This different behaviour of emulsion and soya oil/water coarse dispersion is related to the degree of dispersity of the soya oil. In the coarse dispersion without surfactant it rapidly coalesced, allowing coincident melting and freezing of the separated oil phase.

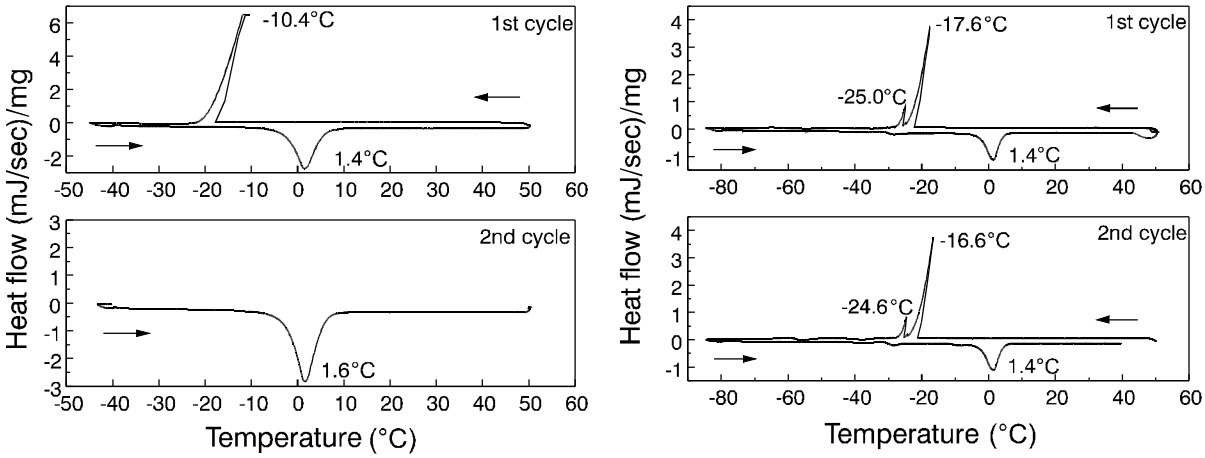

A **B**

(A) 20% w/w model emulsion at 4K/min and
(B) 20% w/w soya oil coarsely dispersed in aqueous glycerol without emulsifier

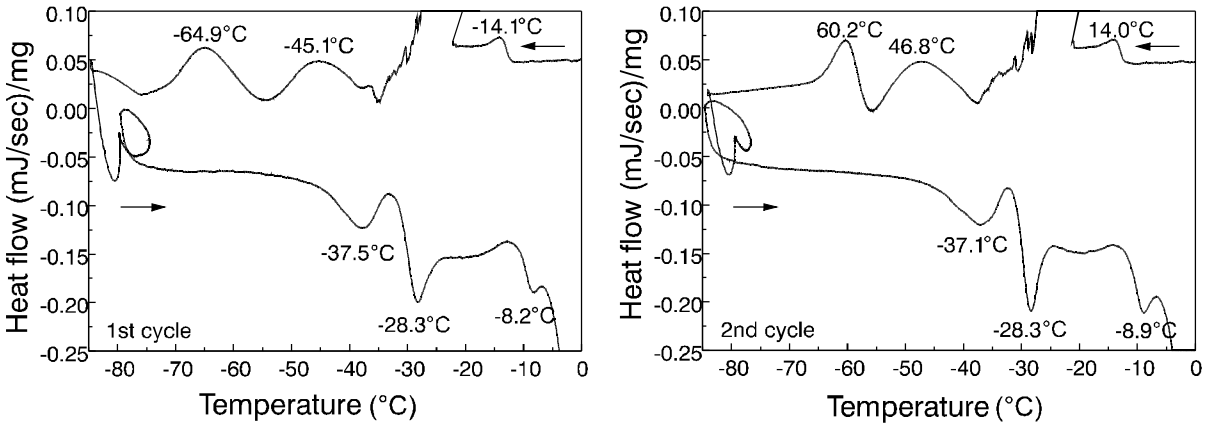

C **D**

20% w/w soya oil coarse dispersion in aqueous glycerol without emulsifier (enlarged)

Fig. 120 DSC thermograms of lecithin-stabilised soya oil emulsion and soya oil dispersion at 3K/min

In the stable emulsion the individual oil droplets clearly do not melt or freeze together by virtue of their size and the increased Laplace pressure at their surfaces, or thermal transitions are hidden by the thermal capacity of the aqueous medium. The appearance of a second freezing peak at -25°C cannot be readily explained, since soya oil freezes at -11°C, which would be overlapped by the water freezing peak.

The influence of the state of dispersity of the oil phase on DSC behaviour was examined further using a coarse pre-emulsion containing Lipoid E80® prepared with an Ultra-Turrax. Its mean particle diameter was approx. 18 µm as determined by LD and therefore considerably larger than the submicron range for the homogenised emulsion in Fig. 120. The DSC thermograms for this coarse emulsion are shown in Fig. 121.

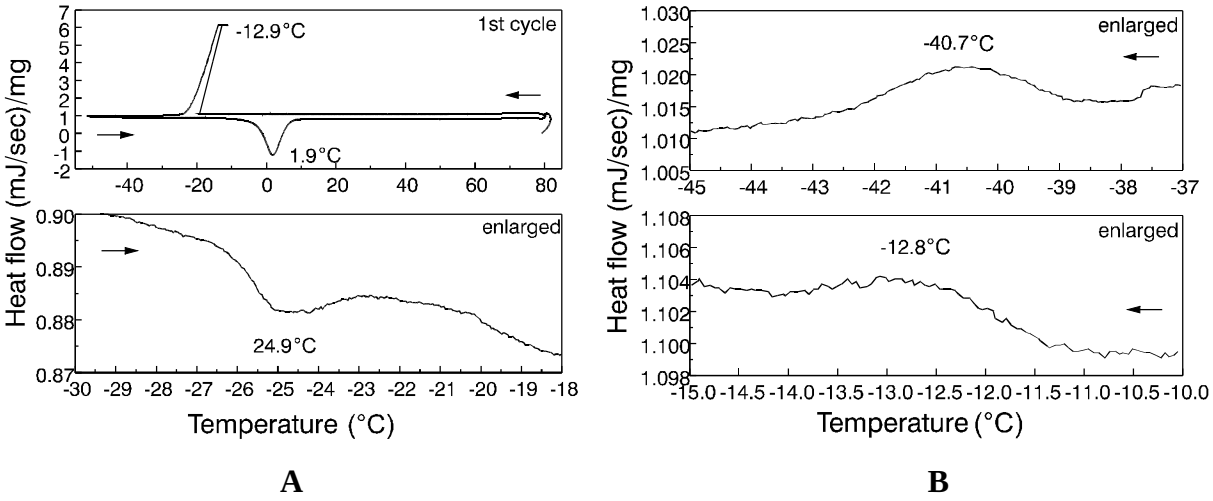

Fig. 121 DSC thermogram of coarse soya oil emulsion stabilised with 1.2% Lipoid E80® at 3K/min showing **(A, bottom)** melting and **(B)** freezing transitions

Peaks for soya oil freezing and melting are evident, but are smaller than seen with the coarse dispersion and can only be observed after considerable magnification. Only the most prominent soya oil peaks can be seen; the melting peak at -24.9°C and the freezing signals at about -40.7°C and -12.8°C. Other peaks seen with the coarse dispersion were too small to be detected. Since the oil content is the same in both systems, increasing the degree of dispersity attenuates the enthalpy flux stemming from the dispersed phase.

To determine if phospholipid transitions are hidden under the water freezing peak of the emulsion in Fig. 120, emulsion and SUV liposomal dispersions were vacuum-dried over $CaCl_2$ at room temperature for up to 94 h. As already shown in Section 3.1.3.1, reducing the water content of the emulsions should shift the water freezing and melting peaks as the relative glycerol concentration increases. This may reveal possible underlying signals arising from the lecithin.

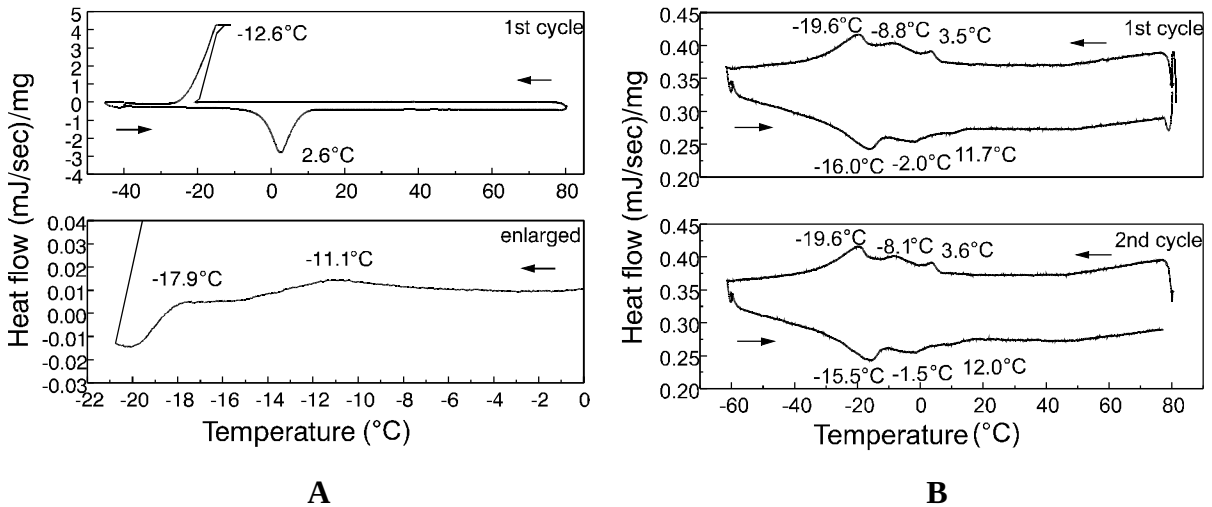

Fig. 122 DSC thermograms of **(A)** microfluidized 7.2% w/w Lipoid E80® SUV dispersion in glycerol/water (2.25 wt%) at 4K/min and **(B)** after 94 h of drying at 3K/min

For a dried liposomal dispersion peaks are indeed seen (Fig. 122b), whereas the native dispersion shows only the expected water transitions; only after large magnification two small peaks of very weak intensity are revealed (Fig. 122a). Therefore, the emulsion was dried to three reduced water contents (Fig. 123): the transitions visible on reduced water content (especially with 35.9%) can, however, only be attributed to the respective soya oil transitions (cf Fig. 120). The shifts achieved in the water peaks by drying are weak, and only the undercooling of the water freezing transitions exposes the freezing peaks of the oil. This makes it impossible to detect lecithin in mixtures with soya oil at such concentrations.

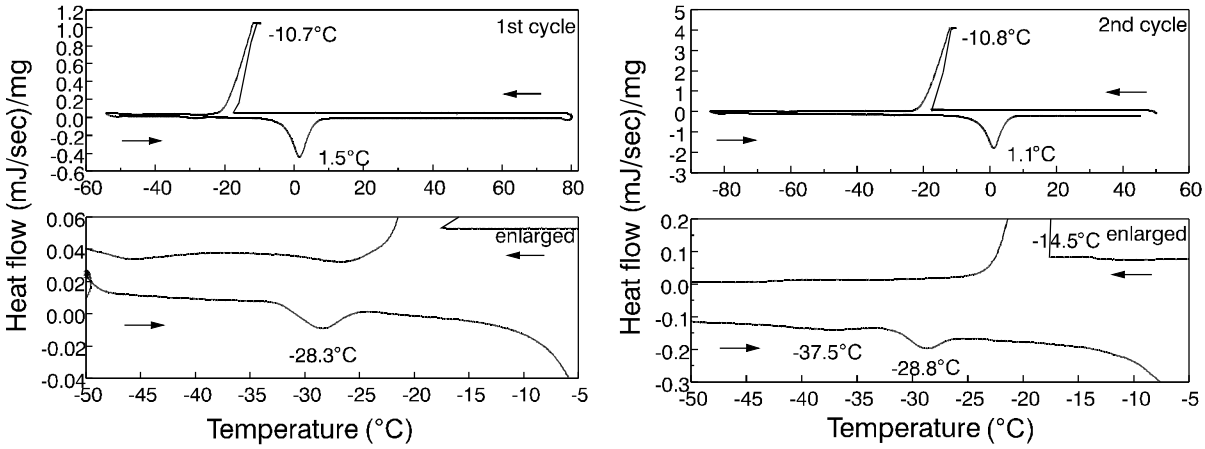

A **B**

20% w/w model emulsion **(A)** dried to 72.6% w/w water content
and **(B)** dried to 66.2% w/w water content

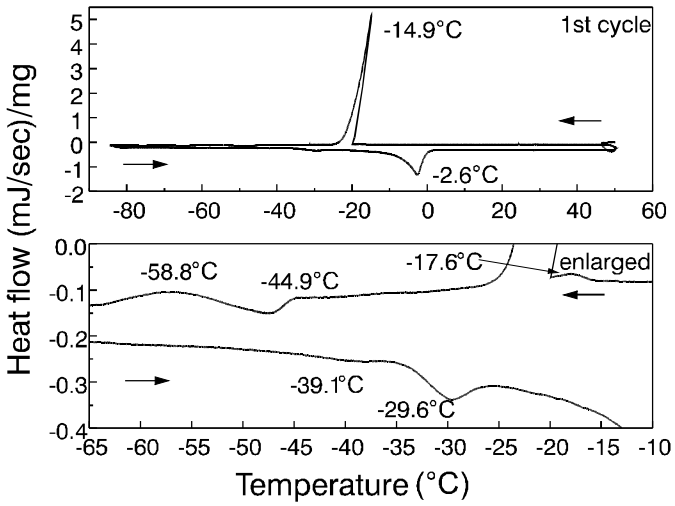

C

20% w/w model emulsion dried to 35.9% w/w water content

Fig. 123 DSC thermograms of a dried 20% (w/w) soya oil emulsion with 1.2% (w/w) Lipoid E80® with reduced water content at 3K/min

Only peaks arising from the oil can be detected besides the water peaks. Thermograms of lecithin-stabilised SLN dispersions similarly show only freezing and melting transitions of the dispersed cetylpalmitate. Although 4.8% w/w Lipoid E80® were used, no transitions belonging to the lecithin can be seen.

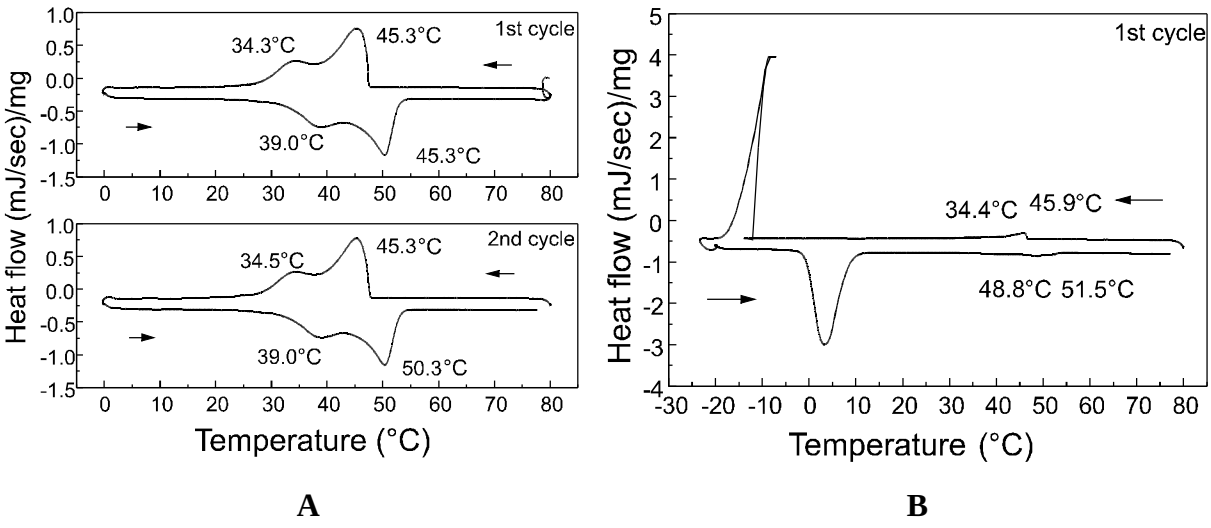

Fig. 124 DSC thermograms of **(A)** pure cetylpalmitate and **(B)** 10% w/w SLN dispersion with 4.8% w/w Lipoid E80® at 3K/min

In summary, with DSC the model and commercial emulsions and their components could be analysed and their similarity proved. However, characterisation of the emulsifier by the analysis of native or water-reduced emulsions proved difficult. The results contradict Diederichs' [1993] description of a lecithin freezing peak at -25°C detectable within the emulsions, although results obtained for liposomal dispersions are grossly similar. By using a heating rate of 3K/min it was possible to resolve various peaks of the soya oil phase within emulsion samples. Diederichs used 5K/min and could not resolve any of these peaks. It is clear that egg lecithin is not detectable in the presence of high amounts of triglycerides (approx. 1:17 w/w in this case). The peaks reported by Diederichs [1993] were therefore most likely from the oil phase rather than the lecithin. Moreover, it is therefore not possible to distinguish between interfacial and excess liposomal phospholipids in emulsions by DSC analysis.

4.3.4 FT-IR Analysis

The major difficulty in analysing aqueous samples is the strong absorption of the water, which lowers the signal strength of other compounds in the sample. By reducing the sample film thickness to 5.6 µm using the customised 'thin-film cuvette' (Fig. 21), an excellent signal to noise ratio was obtained, much superior to the results obtained using conventional cuvettes equipped with 25 µm Teflon spacers. By thermostatting sample and reference during the

measurement, it was assured that film thickness was kept equal. Fig. 125 shows how the lipid spectra were obtained by subtraction of water absorbance from an emulsion spectrum.

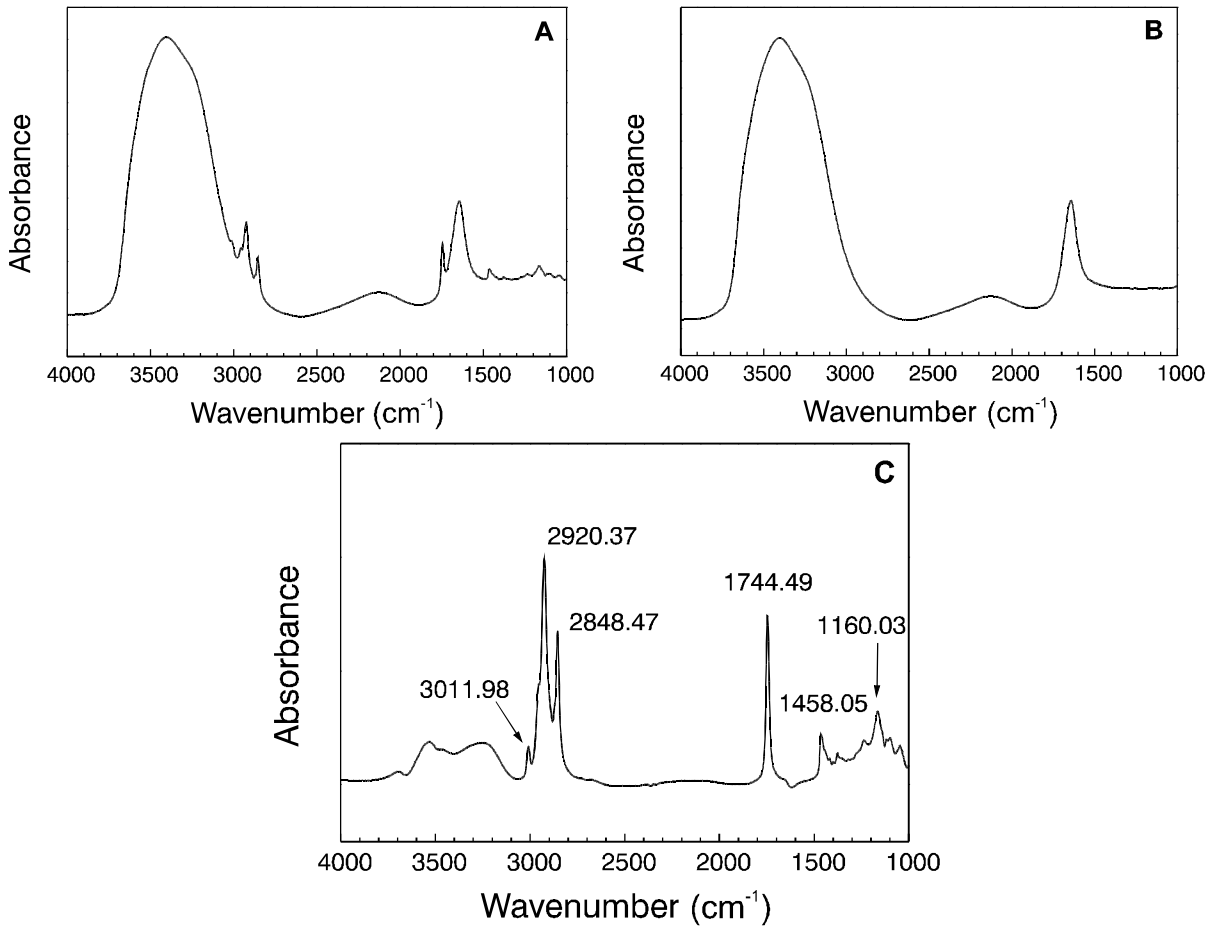

Fig. 125 FT-IR spectra of **(A)** Intralipid 20® at 20°C, **(B)** double-distilled water at 20°C and **(C)** resulting difference spectrum

The strong absorption bands of water which partially overlap the lipids' carbonyl mode at 1744 cm^{-1} in the emulsion spectrum are removed almost completely by this operation. The exposed CH_2-stretching modes at 2848-2920 cm^{-1} and the alkene peak at 3012 cm^{-1} come from the fatty acid residues. To observe temperature-dependent changes in lecithin, it is necessary to identify those IR-modes belonging to the phospholipids that are temperature sensitive. As, however, both carbonyl- and CH_2-stretching modes occur for lecithin and triglycerides, mixtures of lecithin in soya oil were investigated to clarify whether lecithin could be detected at all. Although the CH_2-stretching modes are practically identical for soya oil and egg lecithin in Fig. 126a, increasing concentrations of Lipoid E80® can be detected. The pronounced PO_2-stretching modes clearly indicate the presence of lecithin. A shift in the C=O-mode is also evident for the mixtures, from 1743.7 cm^{-1} for pure soya oil to 1735.0 cm^{-1} for 12% w/w Lipoid E80® admixture.

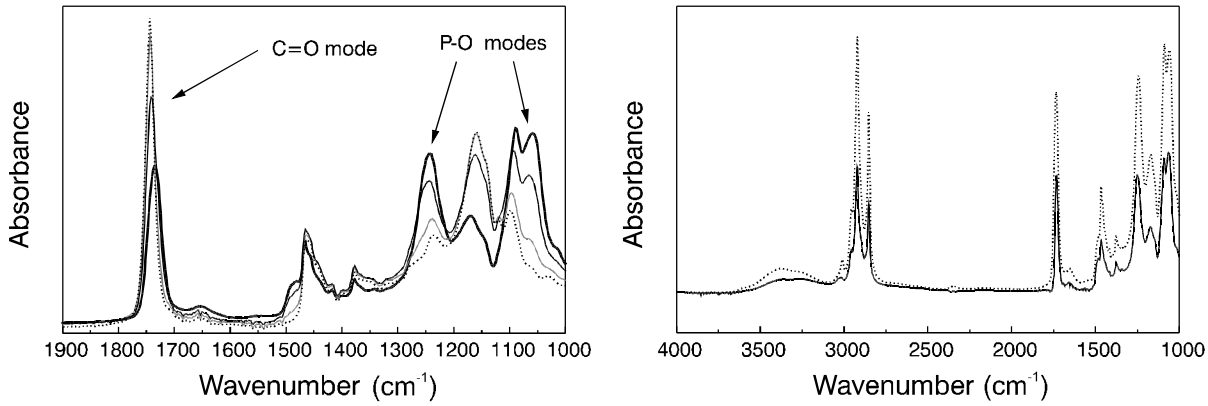

Fig. 126 ATR/FT-IR spectra of **(A)** pure soya oil **(·····)** and pure Lipoid E80® **(**44**)**, as well as 6% w/w **(**44**)** and 12% w/w **(—)** Lipoid E80® in soya oil at RT;
(B) spectrum of 12% w/w Lipoid E80®/soya oil after subtraction of soya oil spectrum **(—)** and of pure Lipoid E80® **(·····)** at RT

This is a result of the difference in their respective ester bonds. By subtraction of the soya oil spectrum from the mixtures (Fig. 126b), a practically identical spectrum to that for the pure lecithin was obtained. It is thus possible to detect the phospholipid signals within the oil phase at those molar ratios of lecithin:oil found in the emulsions. The lecithin headgroup modes ($P\text{-}O_2$) cannot, however, be used to detect thermal transitions. Additionally, the $P\text{-}O_2$ stretching modes are weakened owing to increasing absorption of the CaF_2 windows at these low wavenumbers (< 1300 cm^{-1}). In the case of an emulsion it was necessary to use a twofold subtraction (for water and oil), which introduced considerable error into the resulting double difference spectra. Consequently, thermally-induced peak shifts could not be detected reproducibly for the emulsions.

This situation was not improved when the ratio of lecithin+oil:water was increased. To circumvent the overlapping of the carbonyl peaks of oil and lecithin in the emulsions, the formulation had to be changed. Model emulsions were prepared with a dispersed phase free of ester bonds and giving no carbonyl signals. Among the compounds tested were silicon oils as well as octyldodecanol or dioctylether, which, however, failed to yield stable emulsions. Excellent results were obtained, however, with fluid paraffins. A mixture of viscous and liquid paraffin (3:7 w/w) had the same viscosity as soya oil, and similar dispersing behaviour was obtained. Its refractive index of 1.469 is also very close to that of soya oil (1.470), important for particle size measurement (see Fig. 117b). No differences to soya emulsions were found for 9.3% and 18.6% w/w paraffin emulsions in both their particle sizing and ^{31}P-NMR behaviour (see later). Fig. 127 shows the ATR-spectra of 5.7% w/w Lipoid E80®/paraffin mixture and an 18.6% w/w paraffin emulsion (volume-equivalent to 20% soya oil) after subtraction of the spectra of the aqueous phase.

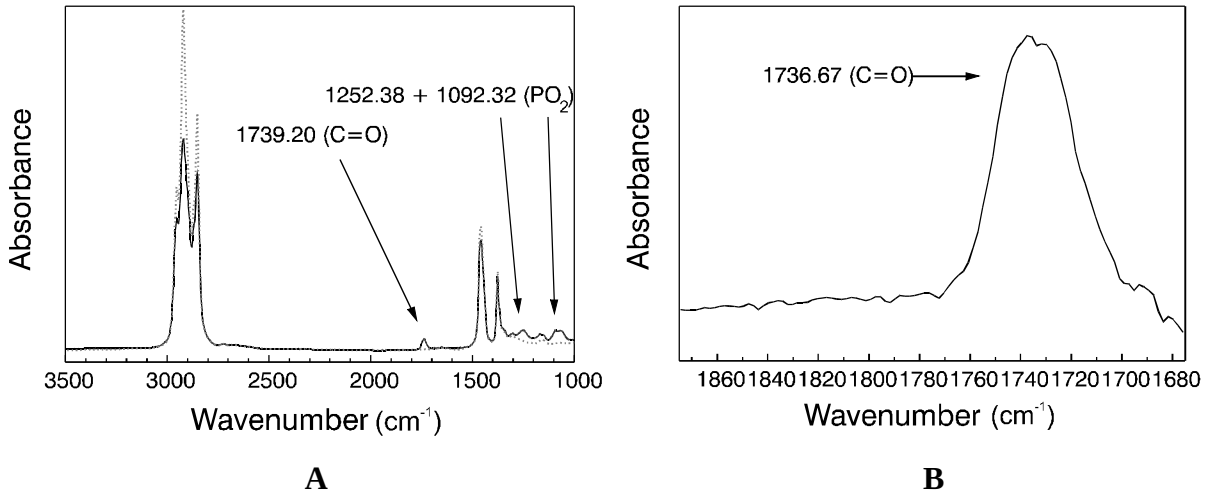

Fig. 127 ATR/FT-IR spectra of **(A)** 5.7% w/w Lipoid E80® in fluid paraffin mixture **(—)** and paraffin mixture (viscous:liquid paraffin 3:7 w/w) **(·····)** at RT;
(B) enlarged spectrum of 18.6% w/w paraffin emulsion with 1.2% Lipoid E80® after subtraction of aqueous glycerol spectrum **(—)** at RT

As hoped, the C=O peak of the phospholipids is clearly detectable within the mixture of lecithin in paraffin (Fig. 127a) as well as within the difference spectrum of the paraffin emulsion (Fig. 127b). This also demonstrates that lecithin was detectable at a concentration of only 1.2 wt% in the presence of about 76.6 wt% water. The subtraction procedure did not, however, yield satisfactory results in all cases, which can be seen in Fig. 128. In an aged 18.6% w/w paraffin emulsion it is not possible to detect the phospholipid C=O peak besides the residual water peak. The carbonyl mode appears broadened with an underlying shoulder (Fig. 128a, bottom). When the sample was vacuum-dried it became evident that the carbonyl signal had split into the usual ester bond signal and an additional signal at lower wavenumbers, typical for carboxylic acids (Fig. 128a, top). This acid peak emerged owing to the formation of hydrolysis products on ageing, which also would explain the concomitant decrease in the ester bond mode at 1734 cm^{-1}. It is therefore possible to detect hydrolysis of the lecithin within the emulsions using FT-IR. To verify this, paraffin emulsions were autoclaved for intervals up to 2 h and analysed. HPLC analysis confirmed that considerable hydrolysis of the emulsifier had occurred. Again, the split carbonyl peaks were found for the subtraction spectrum of the autoclaved samples, owing to the formation of free fatty acids. This was also confirmed by analysis of the native sample to which 0.6 wt% oleic acid had been admixed. The subtraction spectrum in Fig. 128b also clearly shows a carboxylic acid peak.

The utility of FT-IR for examining phase transitions in the emulsions is thus limited, and in general the results are more useful for qualitative analysis of emulsion composition in their native state.

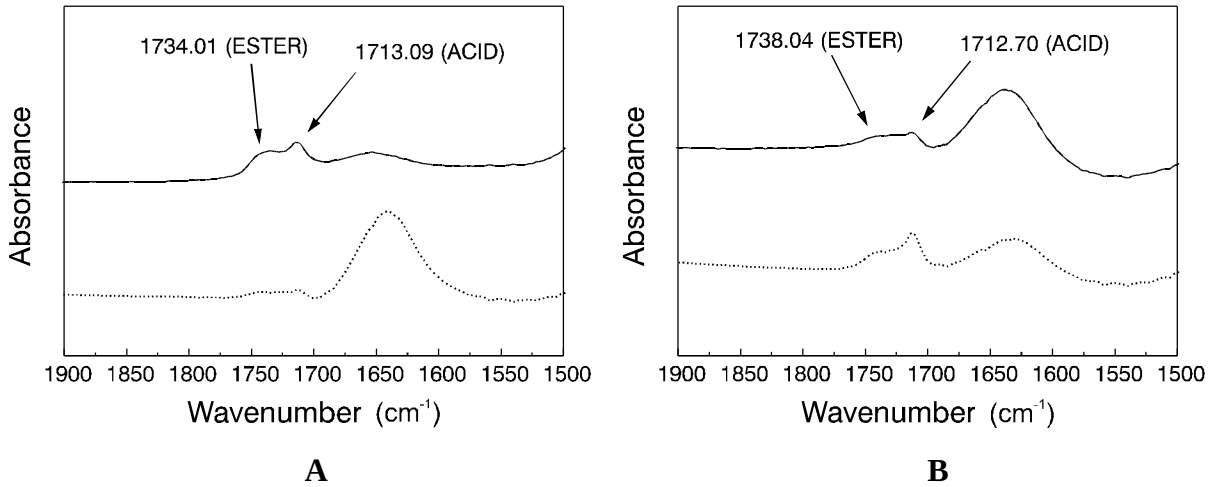

Fig. 128 Enlarged FT-IR spectra of **(A)** aged, non-autoclaved 18.6% w/w paraffin emulsion with 1.2% w/w Lipoid E80® after subtraction of aqueous glycerol **(**.....**)** and after drying of the sample **(—)**, recorded at 20°C;
(B) enlarged subtraction spectra of **(—)** 18.6% w/w paraffin emulsion with 1.2% w/w Lipoid E80® after autoclaving for 2 h at 121°C and **(**.....**)** after addition of 0.6% w/w oleic acid, recorded at 20°C

The main drawback is, as found with DSC, the small amounts of phospholipids present in the emulsions. Future thermal analysis of emulsions using FT-IR could therefore focus on analysis of the centrifuged cream layer, since phospholipid signals are enhanced in these samples and difference spectra can be obtained more precisely. By using C^{13}-labelling of the phospholipids, the respective C=O stretching modes are shifted [Blume et al., 1988], which would result in two separate carbonyl peaks, each well accessible for FT-IR analysis. This might allow examination of thermal effects within the emulsions. This approach, however, requires labelling of different phospholipid species in order to mimic the composition of egg lecithin.

4.3.5 ^{31}P-NMR Analysis

The mobility of phospholipid molecules can be characterised by ^{31}P-NMR [Seelig, 1978 / Chan et al., 1981]. This might offer a way to distinguish between the different states taken by the phospholipid molecules in the emulsions, viz monolayers and bilayers. Sotirhos et al. [1986a] also reported quantitative phospholipid analysis using ^{31}P-NMR. Moreover, samples can be analysed in their native state, which reduces the risk of dilution-induced artifacts. The different polymorphic molecular arrangements should produce different phospholipid spectra [Cullis and De Kruijff, 1978]. The high three-dimensional mobility of the phospholipid molecules in solutions yields a symmetric (isotropic) signal, since all molecules move in all directions at equal probability. This three-dimensional motional averaging is found also in lyso-PC micelles, which were therefore used as a reference for symmetric, isotropic peaks (Fig. 129a).

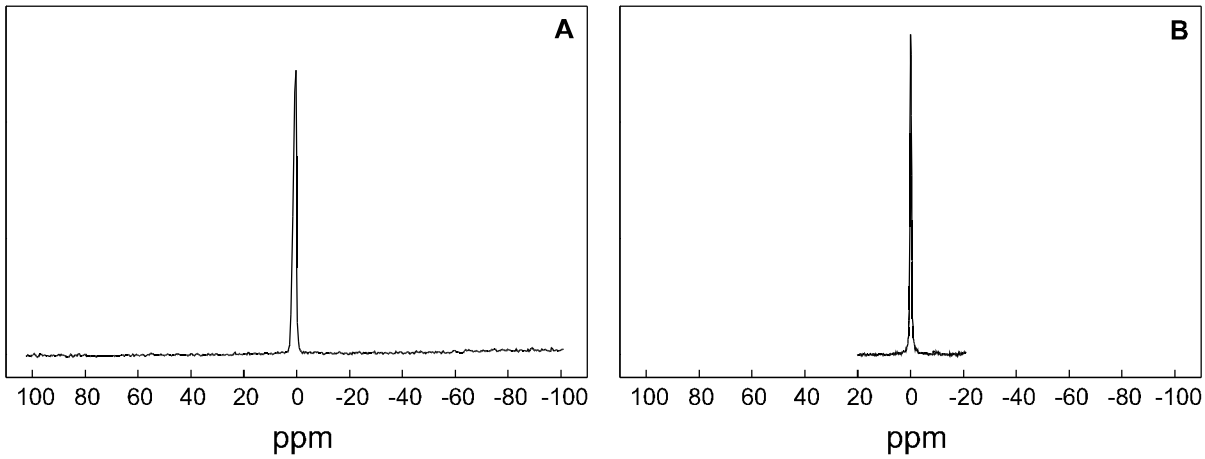

(A) Lyso-PC micelles and **(B)** microfluidized 4% w/w Lipoid E80® dispersion

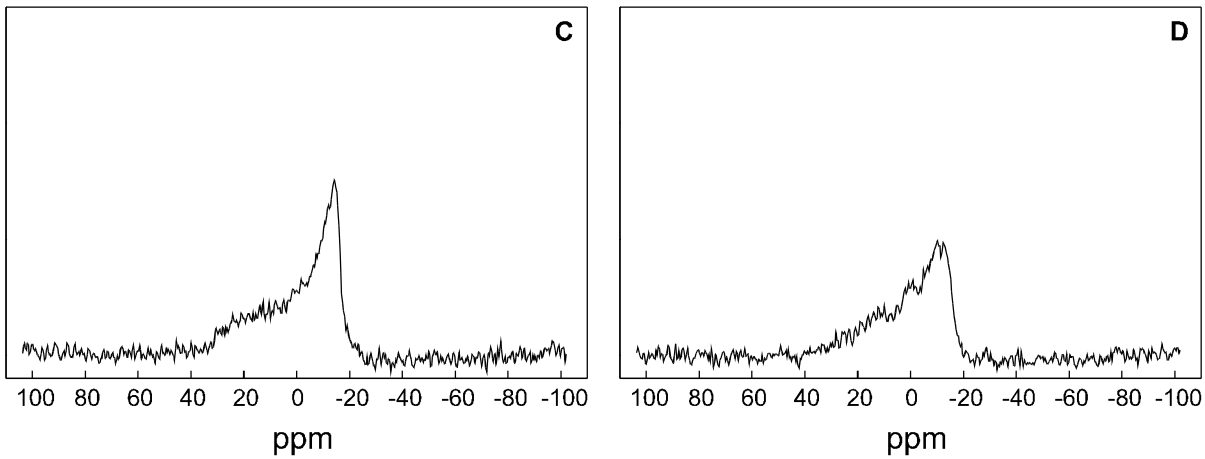

(C) MLVs from 4% w/w Lipoid EPC® and **(D)** MLVs from 4% w/w Lipoid E80®

Fig. 129 ^{31}P-NMR spectra of different egg-lecithin dispersions

Chemical shift anisotropy subsequently refers always to this peak of Palmitoyl-LPC (0 ppm). The signal for microfluidized Lipoid® dispersions is of similar appearance (Fig. 129b), although multilamellar liposomes give more broader, anisotropically shifted peaks (Fig. 129c+d). This change to broader peaks can be explained by the restricted mobility of phospholipid molecules in the bilayer plane of the MLVs. The paradoxical appearance of the microfluidized SUV dispersions (Fig. 129b), which also consisted of lamellar bilayers, is related to the increasing influence of Brownian motion of the SUVs, which effectively increases the molecules' mobility. Burnell et al. [1980] and Westesen and Wehler [1992] also reported such isotropic peaks for liposomes < than 100 - 200 nm.

The ^{31}P-NMR spectra of model emulsions show a clear dependence on the triglyceride:lecithin ratio, as has similarly been reported by Férézou et al [1994]. The isotropic signals appear to decrease with increasing dispersed phase content (Fig. 130), and the anisotropic peak becomes enhanced. This could be explained by a progressive decrease in the amount of small liposomes together with an increase in multilamellar structures.

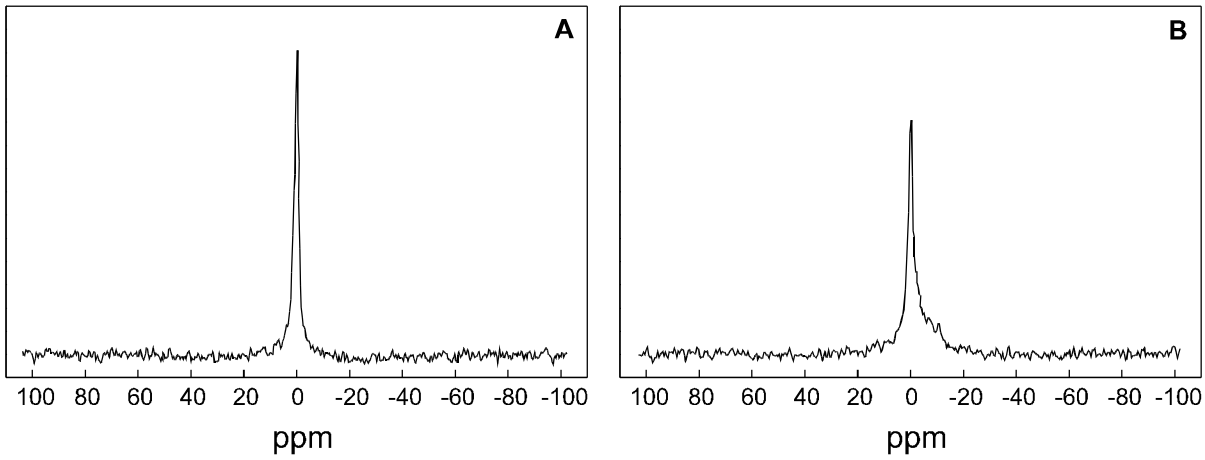

(A) 5% w/w emulsion and **(B)** 10% w/w emulsion

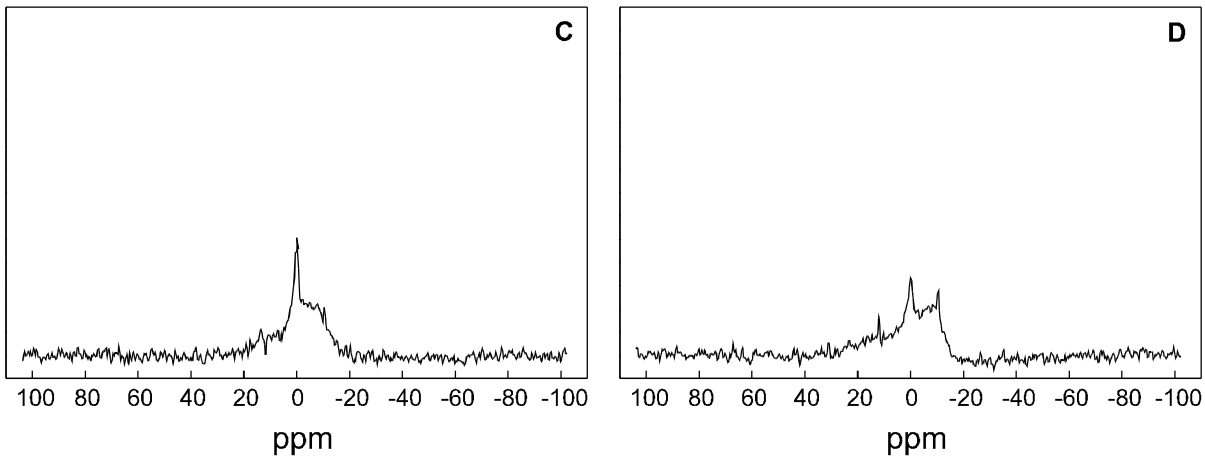

(C) 20% w/w emulsion and **(D)** 30% w/w emulsion

Fig. 130 Intensity-normalised ^{31}P-NMR spectra of non-autoclaved model parenteral emulsions stabilised with 1.2% Lipoid E80® and homogenised at 1000 bar

From the PLM and Cryo-TEM results presented above it is, however, evident that no multilamellar phases are formed with increasing oil phase content. Excess emulsifier will be reduced with increasing oil phase content, which could also account for the reduction in the isotropic signals. Additionally, an increase in mean particle size with the larger amounts of oil phase would result in less contribution of Brownian motion to the isotropic signal. The enhanced anisotropic signals may be related to the increased amount of emulsifier located at the oil-water interface, which would also be expected to show restricted mobility within the emulsifier film. This was indeed assumed by Férézou et al. [1994], who proposed that the more lipophilic environment of the phospholipids at the oil-water interface would account for this anisotropic behaviour. An increase in homogenisation pressure reduced the isotropic signal of the NMR spectrum of 10% emulsions (Fig. 131a+b), which clearly cannot be explained by increasing particle diameter, and particle size measurements confirmed the expected reduction in droplet sizes. This may reflect more the reduction of free SUV excess, since more lecithin was required to cover the increased interfacial area.

Similarly, when 10% emulsions were produced with only half of the lecithin amount, their isotropic peak was decreased greatly (Fig. 131c). This cannot be explained only by their somewhat larger droplet size, since 20% emulsions possessing similar droplet diameters (see Tab. 18) gave even smaller isotropic signals. The clear reduction in the isotropic peak for the 10% formulation with 0.6 wt% lecithin arose therefore from the reduction in liposomal excess compared with 1.2% emulsifier.

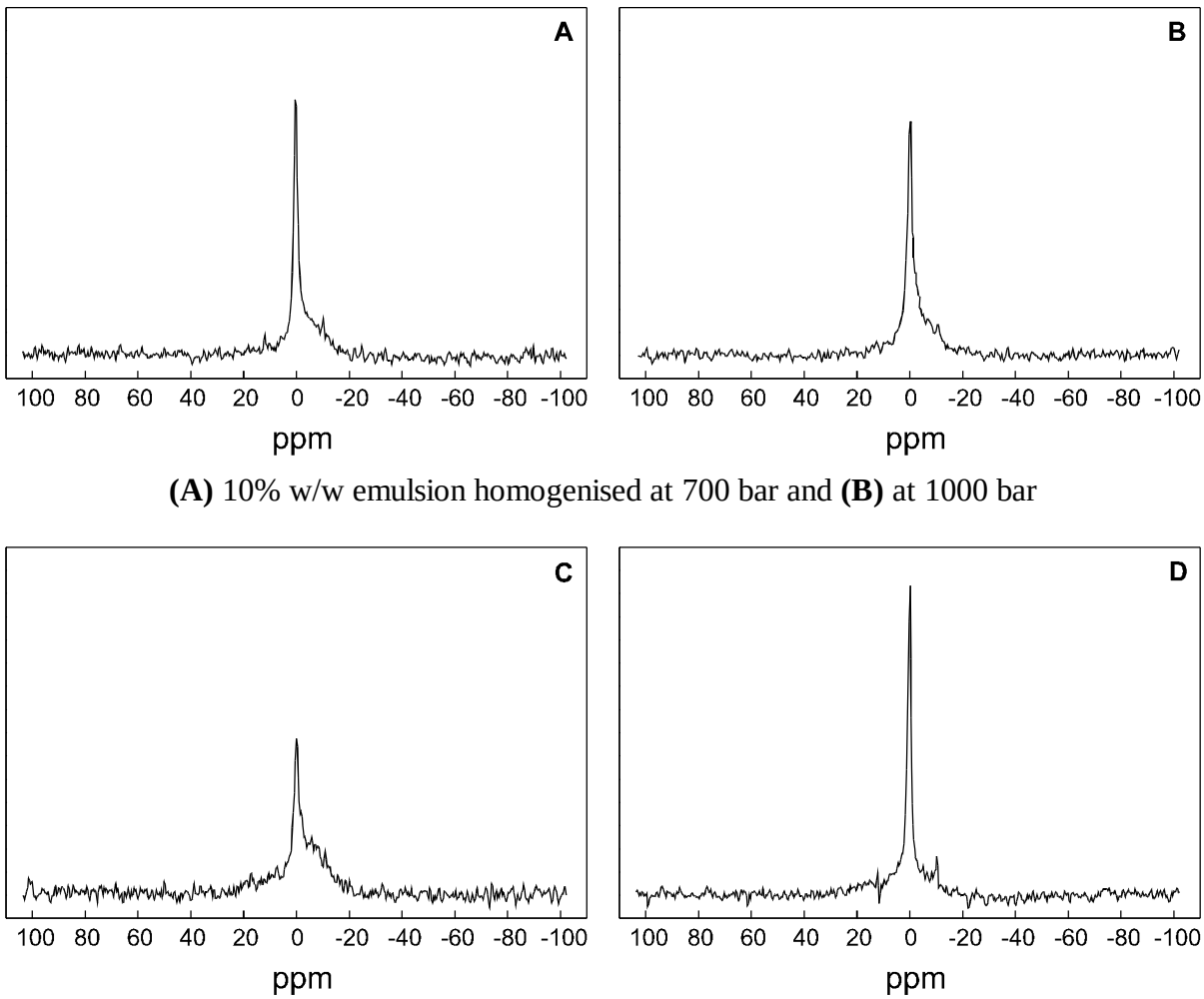

(A) 10% w/w emulsion homogenised at 700 bar and **(B)** at 1000 bar

(C) 10% w/w emulsion with 0.6% Lipoid E80® and **(D)** with 1.2% Lipoid EPC®

Fig. 131 Intensity-normalised ^{31}P-NMR spectra of non-autoclaved 10% w/w model emulsions stabilised with different emulsifier and/or content

With Lipoid EPC® (Fig. 131d), the oil phase has been dispersed less effectively, and more emulsifier is left as liposomes, causing smaller anisotropic and larger isotropic signals. This was confirmed by the larger mean diameters of the Lipoid EPC® formulation.

The spectra of commercial emulsions show interesting differences. The emulsions with reduced ratio of emulsifier:oil exhibit as expected smaller isotropic signals (Fig. 132a+d) than those with 1.2% lecithin (Fig. 132b+c). For Lipofundin 10% N®, which had the same mean diameter as Lipovenoes 10 PLR®, particle size effects can be excluded. It is concluded therefore that the excess emulsifier used in Lipofundin 10% N® was mainly present in the form of SUVs. Although Lipofundin MCT 10%® also contained marked emulsifier excess, it possessed the smallest mean diameter of all the commercial 10% emulsions. This is seen from the slightly larger anisotropic peak, indicating more interfacial coverage.

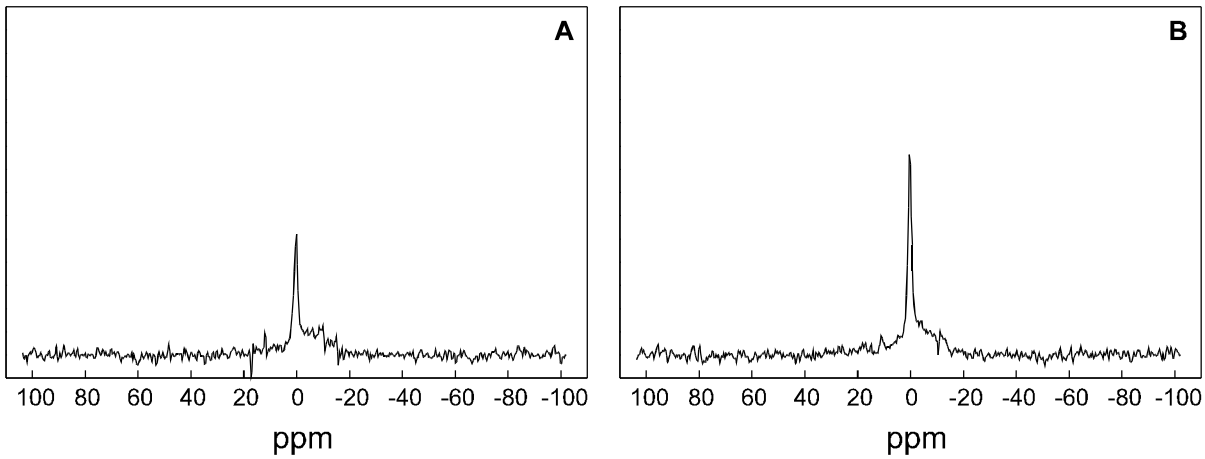

(A) Intralipid 10® [batch 87535-51] and **(B)** Lipofundin 10% N®

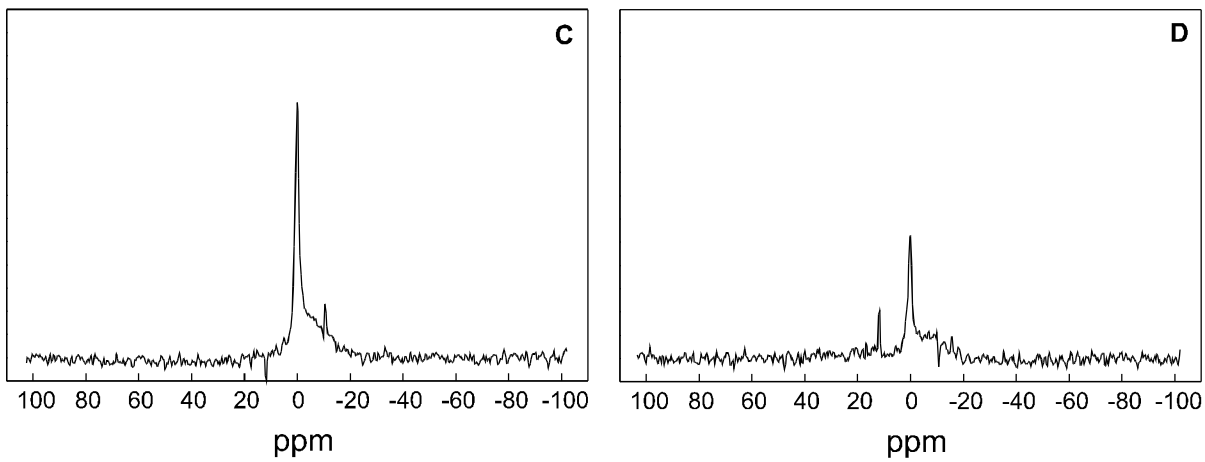

(C) Lipofundin MCT 10%® and **(D)** Lipovenoes LCT 10® PLR

Fig. 132 Intensity-normalised ^{31}P-NMR spectra of commercial 10% parenteral emulsions

The results in Fig. 133 for commercial 20% and 30% emulsions show similar differences in their spectra.

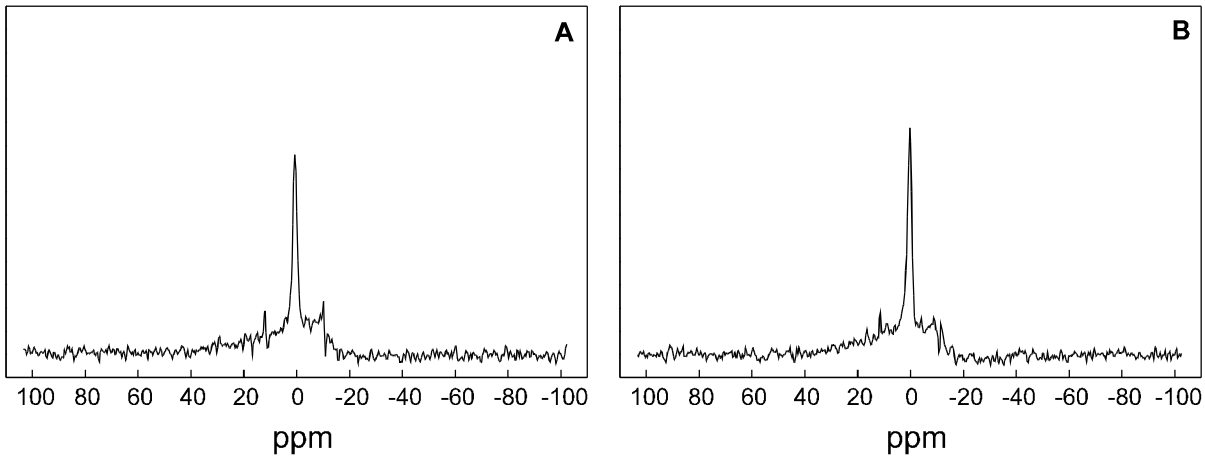

(A) Intralipid 20® [batch 70178-51] and **(B)** Lipofundin 20% N®

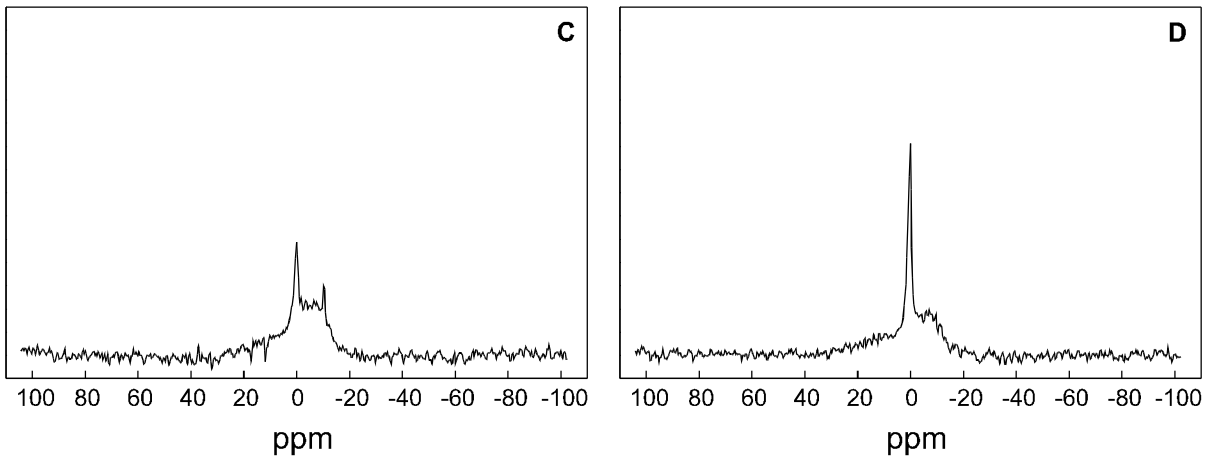

(C) Lipofundin MCT 20%® and **(D)** Lipovenoes LCT 20®

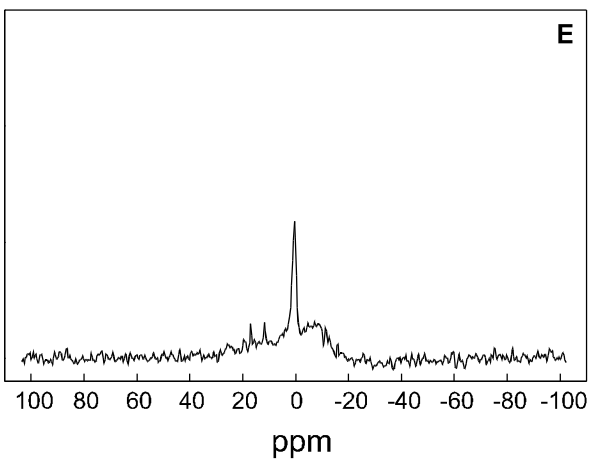

(E) Intralipid 30%® [batch 88555-71]

Fig. 133 Intensity-normalised ^{31}P-NMR spectra of commercial 20% and 30% parenteral emulsions

All of the emulsions shown in Fig. 133 contained nominally the same amount of emulsifier, yet Intralipid 30® and especially Lipofundin MCT 20%® show clearly reduced isotropic peaks. The

latter emulsion had a mean diameter some 90 nm less than those determined for the other 20% emulsions. As this does not cause an increase in the isotropic signal, the larger interfacial coverage had evidently also reduced the liposomal emulsifier excess. It is evident therefore that emulsion structure, droplet size and liposome content do not only depend on the lecithin:oil-ratio, but also on the homogenisation conditions applied. This point is underestimated in the literature.

The cream layer and aqueous subnatant fractions of centrifuged model emulsions show anisotropy for the cream layer (Fig. 134a) and isotropy for the aqueous phase (Fig. 134b), respectively. After resuspension of the centrifuged cream layer in aqueous glycerol (2.25 wt%), its ^{31}P-NMR spectrum showed no isotropic peak. This confirmed the above assumption, that the lecithin-covered oil droplets are mainly detected as the anisotropic signal. The aqueous phase contains mainly SUVs and small emulsion droplets which are detected as an isotropic signal. Férézou et al. [1994] and Westesen and Wehler [1992] tried to determine the amount of excess vesicular emulsifier by addition of shifting reagents to the emulsions, resulting in shifts for the anisotropic and isotropic signals accessible to the aqueous phase. The inside of liposomes would, however, still remain detectable as non-shifted isotropic peaks. Westesen and Wehler examined 25% w/v model emulsions with 1.8% w/v lecithin, and determined that 1/3 of the total emulsifier was located in liposomes. For Intralipid 30®, Férézou and co-workers reported eight times less liposomal material than for the old Intralipid 10® emulsions prepared with 1.2% w/v lecithin.

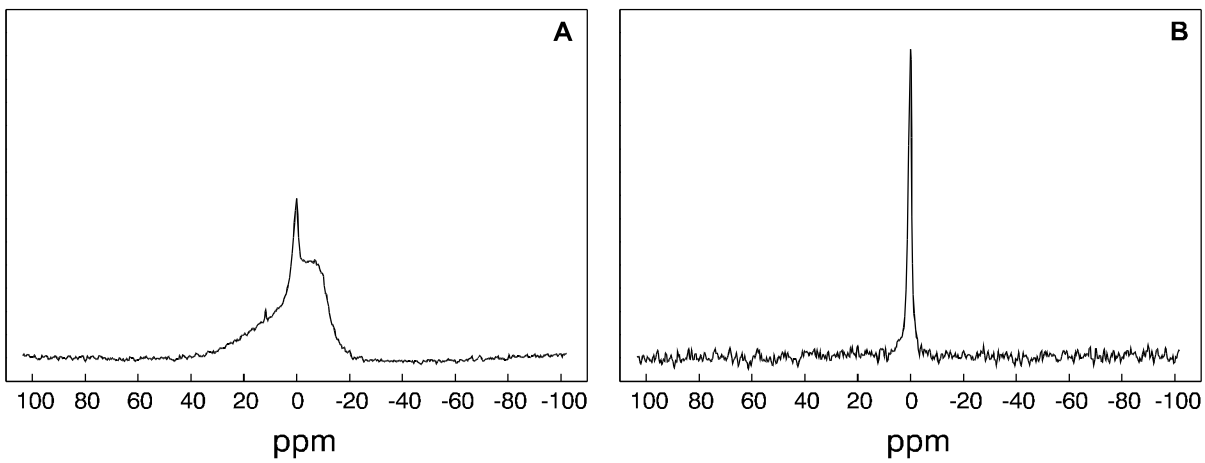

Fig. 134 ^{31}P-NMR spectra of **(A)** centrifuged cream layer of 10% w/w emulsion stabilised with 1.2% Lipoid E80®, homogenised at 700 bar (9000 transients recorded) and **(B)** respective aqueous subnatant (1200 transients recorded)

The results reported here confirm these findings, but it was also demonstrated that comparison can only be made on the basis of knowledge of the particle size distribution and emulsion structure as e.g. determined by Cryo-TEM.

The influence of temperature increase on the appearance of the ^{31}P-NMR spectra is shown in Fig. 135.

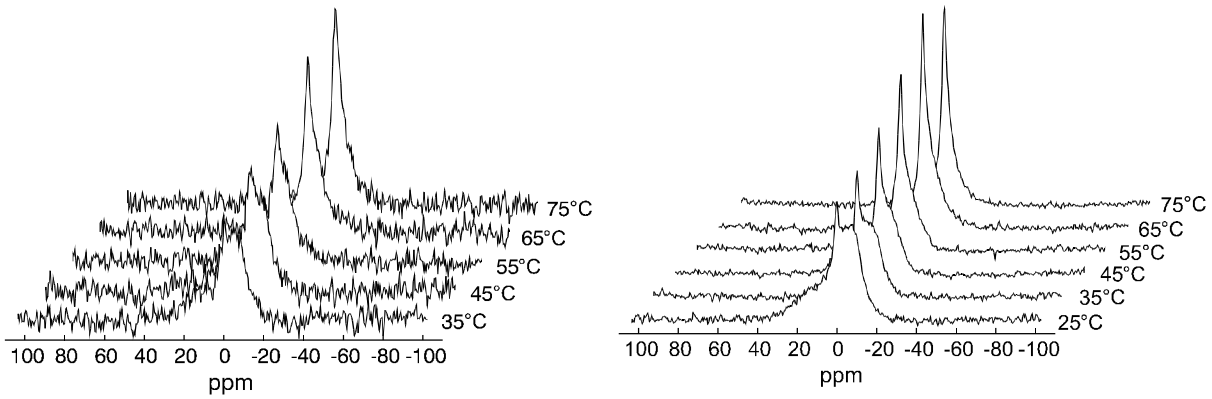

Fig. 135 ^{31}P-NMR spectra of **(A)** 20% w/w model emulsion after autoclaving at 121°C for 20 min (1000 transients recorded) and of **(B)** centrifuged cream layer of 10% w/w model emulsion stabilised with 1.2% Lipoid E80®, homogenised at 700 bar (2500 transients recorded)

With increasing temperature the signals are converted progressively into the isotropic type, which was reversible on cooling to 25°C. The more dense cream layer obtained by centrifugation shows similar behaviour, which, however, does not arise from reversible phase transitions. More likely is an increasing mobility of the phospholipid molecules at the interfacial layer and the overall increased motion of oil droplets with temperature, causing enhanced isotropic motional averaging. It could not, however, be clarified from these experiments whether cubic phases formed at elevated temperatures, as suggested by Groves and Herman [1993]. A cubic phase would also show ^{31}P-NMR spectra of isotropic motional averaging. Formation of an additional lamellar phase could not be detected in these experiments.

4.3.6 Intermediate Conclusions

The results show that all emulsions consisted of oil droplets in the submicron range together with small unilamellar liposomes (SUVs) expressing an excess of lecithin. Multilamellar liposomes could only be observed as artifacts after centrifugation by TEM. It must be concluded that the TEM data of Intralipid® reported by Groves et al. [1985] also are artifactial, with multilamellar structures possibly formed during negative staining [Miyamoto and Stoeckenius, 1971] or during centrifugation stress. Since in FF- and Cryo-TEM experiments no lamellar interphase on the oil droplets could be detected, the ability of excess lecithin in the form of liposomes to enhance the stability of the emulsions towards coalescence during autoclaving was investigated.

4.4 Influence of Autoclaving on Structure and Stability of Liposomal Dispersions and Emulsions

According to the particle size measurements (Section 3.2), the stability of the emulsions to heat stress is very sensitive to pH during autoclaving. The following section shows the concomitant structural changes which occur within the emulsions.

When comparing Fig. 136 with the non-autoclaved liposomal dispersions (Fig. 109+110) it can be seen that the liposomes could be autoclaved after pH adjustment to alkaline and remained practically unchanged in structure and size. The dispersions still consist of single, freely mobile SUVs of about 80-100 nm diameter. This corresponds well to the ^{31}P-NMR spectra (Fig. 138a+b) which show slight peak broadening, but still possess a prominent isotropic peak owing to the small vesicles and no indication of an underlying anisotropic signal coming from multilamellar or larger liposomes. During autoclaving only minimal changes in the liposomes thus occur and there is no formation of larger, multilamellar structures.

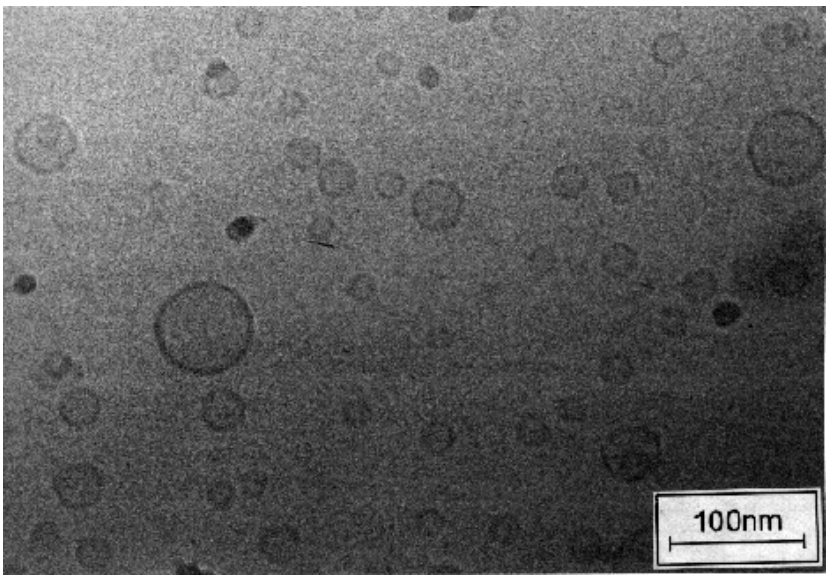

Fig. 136 Cryo-TEM picture of SUV dispersion from 1.2 wt% Lipoid E80® after autoclaving for 20 min

In contrast, the ^{31}P-NMR spectra obtained for autoclaved emulsion samples show a reduction in their isotropic peaks during autoclaving (Figs. 138c-f), without an associated change in particle size distribution. Since the anisotropic part of the NMR signal is not increased, structural changes must have arisen in the smallest particles, which contribute most to the isotropic peak. However, the Cryo-TEM pictures (Fig. 137) confirm that the autoclaved emulsions still contain considerable amounts of small liposomes, which had not been transformed into a lamellar phase associated with the oil droplets nor into MLVs.

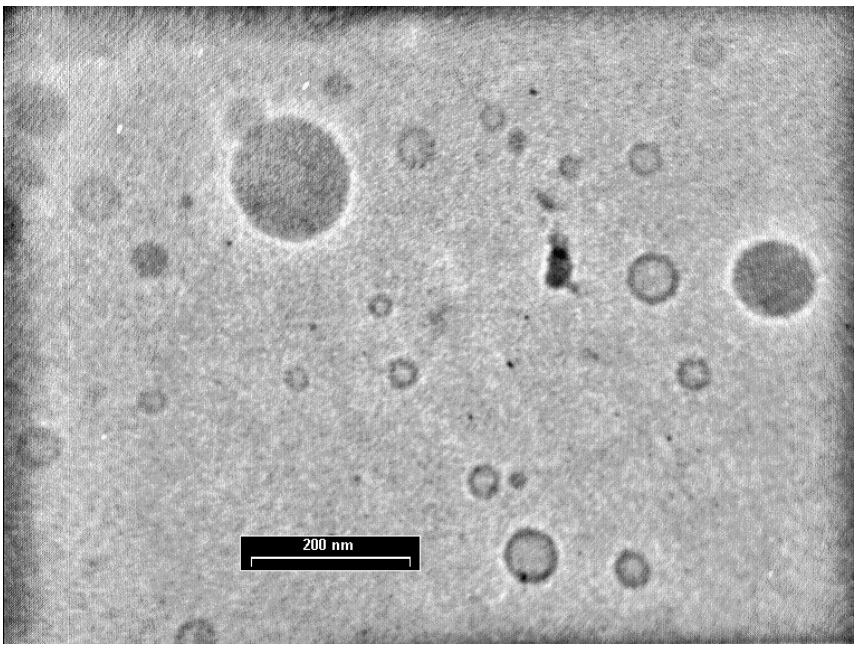

Fig. 137 Cryo-TEM picture of a 10 wt% model emulsion with 1.2 wt% Lipoid E80® homogenised at 400 bar and autoclaved for 20 min at 121°C
(bar corresponds to 200 nm)

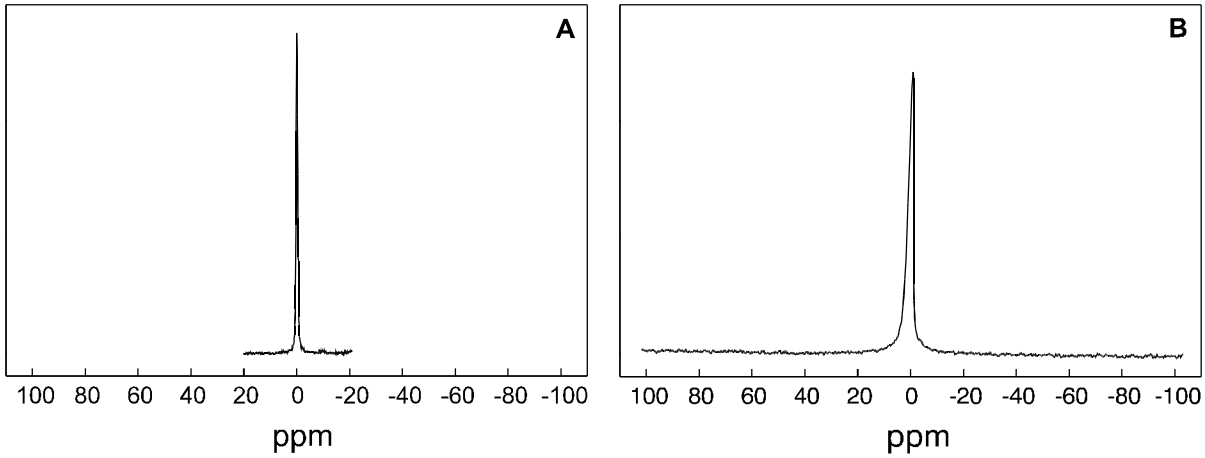

Microfluidized Lipoid E80® (4 wt%) dispersion **(A)** before and **(B)** after autoclaving

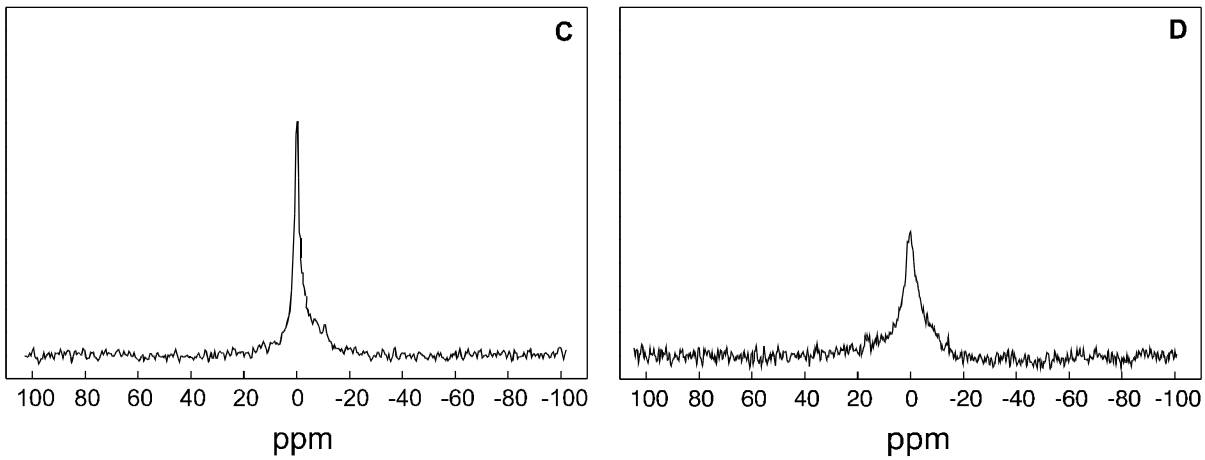

10% w/w emulsion with 1.2 w/w Lipoid E80® **(C)** before and **(D)** after autoclaving

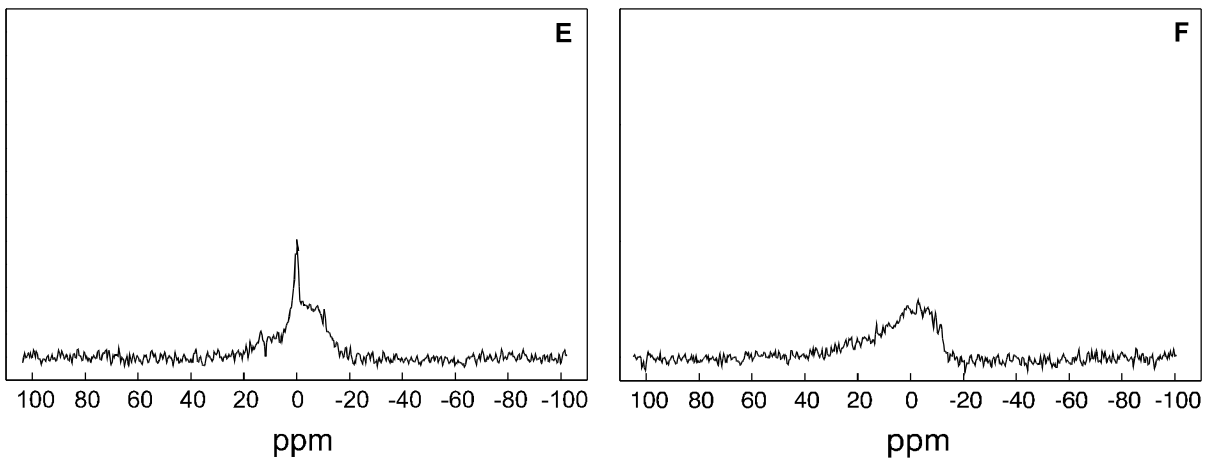

20% w/w emulsion with 1.2 w/w Lipoid E80® **(E)** before and **(F)** after autoclaving

Fig. 138 Intensity-normalised ^{31}P-NMR spectra of pH-adjusted model parenteral emulsions and liposome dispersion before and after autoclaving for 20 min at 121°C

The appearance of Lipofundin MCT 10%® (formulated with 1.2% w/v lecithin) shown in Fig. 139 is similar to the 10% model emulsions with 1.2% lecithin which were homogenised at 400 bar and thus exhibit more liposomal lecithin excess. Since this Lipofundin® formulation was formulated with excess lecithin, it is not surprising to find considerable amounts of liposomes (Fig. 140) and sometimes even bilamellar vesicles (Fig. 141).

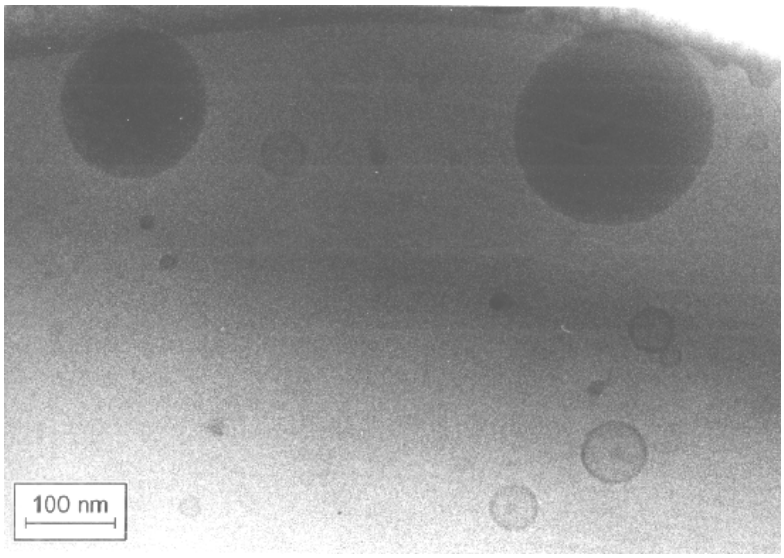

Fig. 139 Cryo-TEM micrograph of Lipofundin MCT 10%® stabilised with 1.2% w/v lecithin

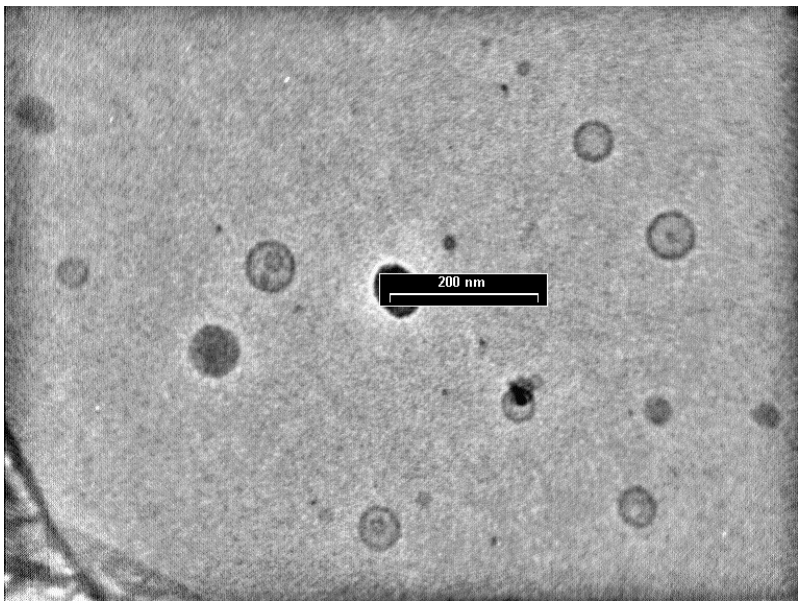

Fig. 140 Cryo-TEM picture of Lipofundin MCT 10%® stabilised with 1.2% w/v lecithin **(bar corresponds to 200 nm)**

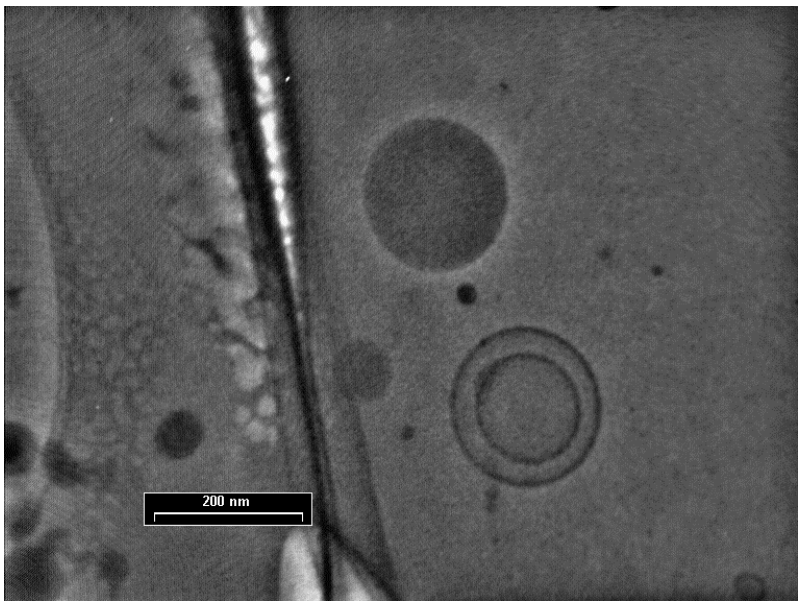

Fig. 141 Cryo-TEM picture of LipofundinMCT 10%® stabilised with 1.2% w/v lecithin **(bar corresponds to 200 nm)**

Autoclaved emulsions were also frequently found to contain liposomes adhering to the surface of the emulsion droplets (Figs. 142+143). This was not observed in the non-autoclaved emulsions and appeared more frequently as the number of liposomes was increased, e.g. when homogenised at lower pressure.

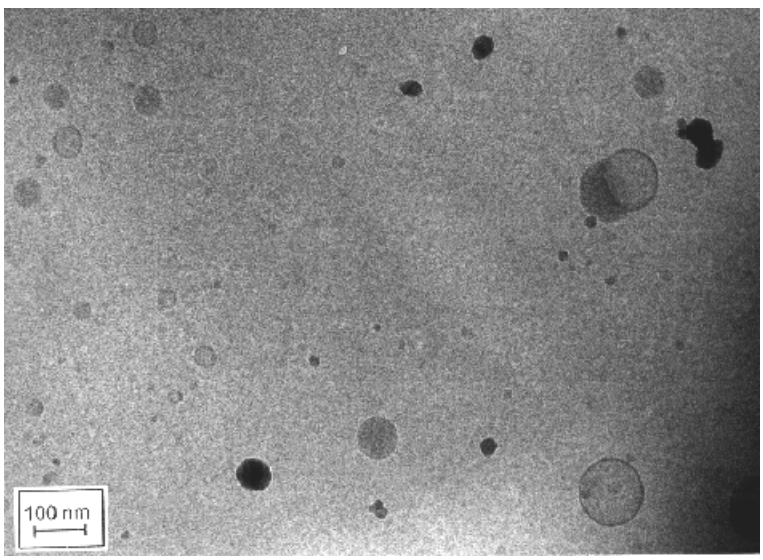

Fig. 142 Cryo-TEM picture of a 10 wt% model emulsion with 1.2 wt% Lipoid E80® homogenised at 400 bar and autoclaved for 20 min at 121°C

The aggregates of liposomes and oil droplets seen in Fig. 142+143 are expected to move less rapid owing to Brownian motion. This may explain why the NMR spectra of autoclaved emulsions show decreased isotropic signals (Fig. 138), suggesting the disappearance of the

SUVs. The smallest droplets and liposomes had, however, not coalesced, but were rather immobilised by aggregation. It is noteworthy that the bilayers apparently resisted complete fusion with the emulsion droplets, which may be a result of repulsive charges preventing film thinning and coalescence.

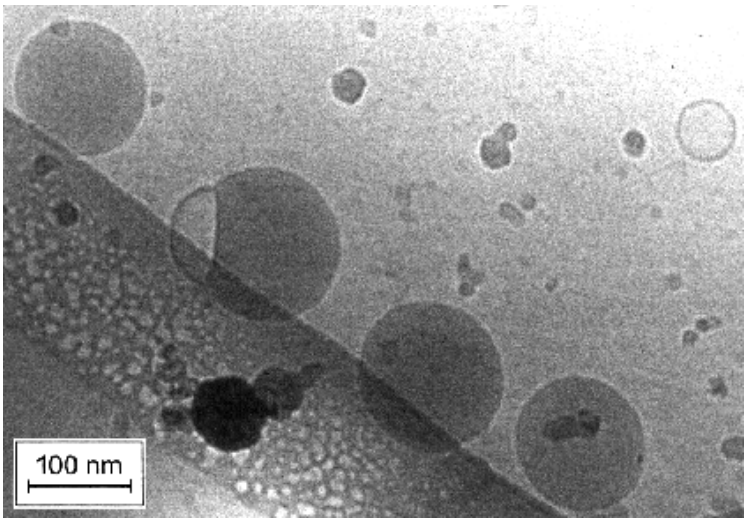

Fig. 143 Cryo-TEM picture of a 10 wt% model emulsion with 1.2 wt% Lipoid E80®, homogenised at 1000 bar after autoclaving for 20 min at 121°C

Similar aggregates could also be found in the commercial emulsions, as can be seen from Fig. 144 (left and centre). Both populations, liposomes and emulsion droplets, do interact and cannot be seen as mere bimodal distributions.

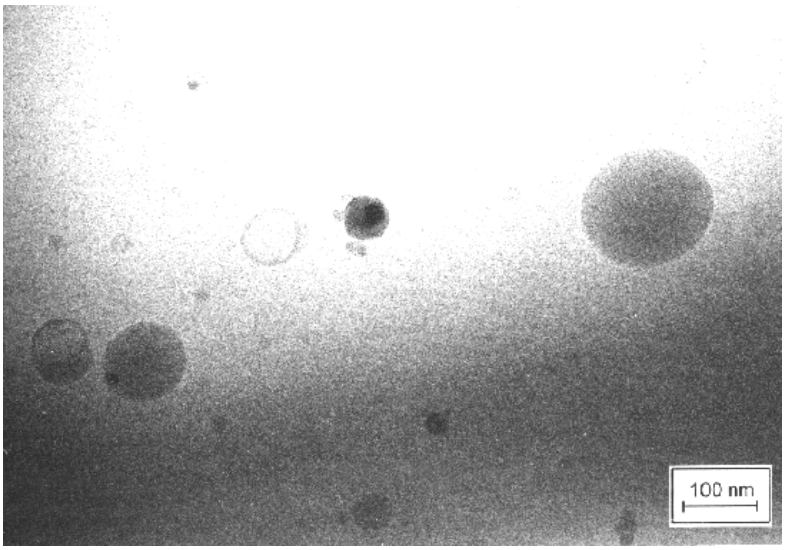

Fig. 144 Cryo-TEM picture of Lipofundin MCT 10%® stabilised with 1.2% w/v lecithin

It is, however, unclear to which degree these aggregates influence emulsion stability during or after autoclaving. Nattermann Phospholipid GmbH [1995] reported similar aggregation

behaviour for liposome dispersion/oil-mixtures (Fig. 145), when high energy input was used. It was claimed that these liposomes were able to solubilise the oil and thus stabilise the emulsions.

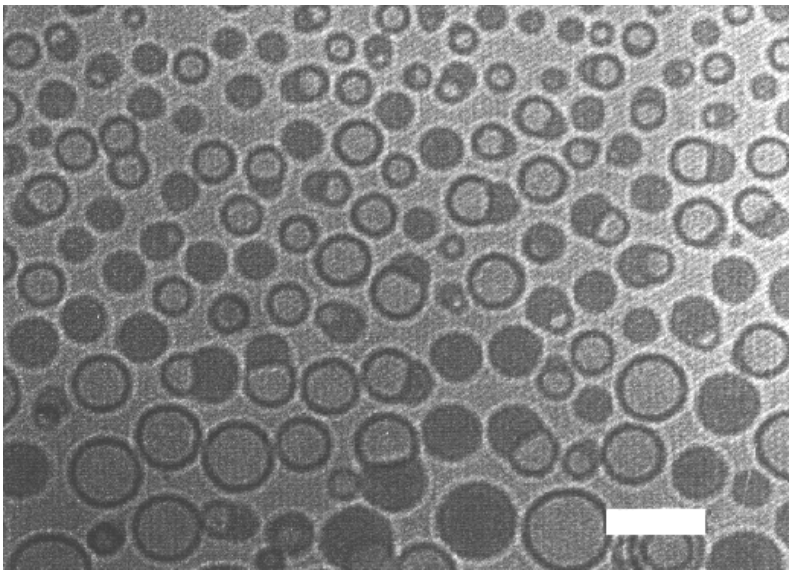

Fig. 145 Cryo-TEM micrograph of liposomes stabilising safflower oil droplets (6:4) after homogenisation at high energy (from Nattermann Phospholipid GmbH [1995]) **(bar corresponds to 200 nm)**

At high lecithin/oil ratios so-called 'propeller liposome' structures were seen (Fig. 146), which consisted of unilamellar liposomes clustered in flocks around small oil droplets, thus inhibiting coalescence of the emulsion.

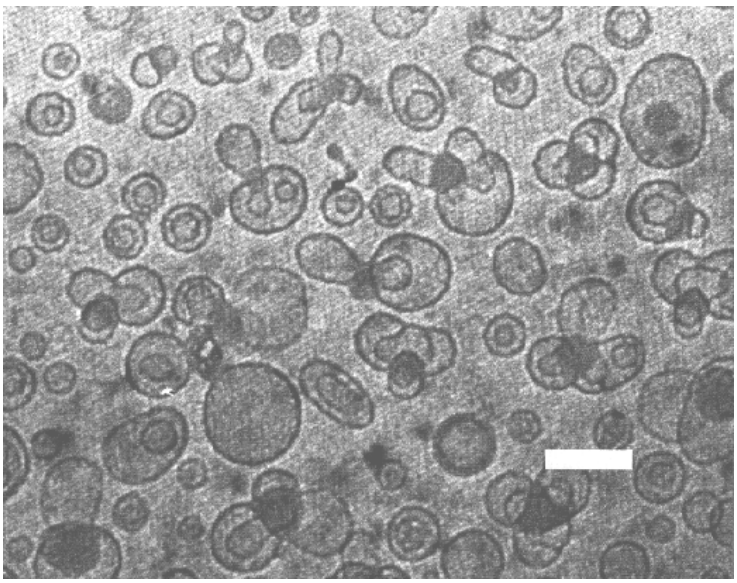

Fig. 146 Cryo-TEM micrograph of oil droplets stabilised by adhering liposomes ('propeller liposomes') (from Nattermann Phospholipid GmbH [1995]) **(bar corresponds to 200 nm)**

It must be emphasised that these observations were made at high lecithin/oil ratios, and similar complete coverage of oil droplets would not be expected for parenteral fat emulsions. It is, however, possible, that the aggregated structures seen in Figs. 142,143+144 contribute to increased stability towards coalescence and may thus help to stabilise parenteral fat emulsions [Groves et al., 1985]. Since 10% O/W-emulsions remain stable when formulated with only half of the emulsifier, and 20% and 30% emulsions can be produced both using 1.2% of lecithin, it seems that the contribution of the liposomal excess lecithin to autoclaving stability is not as pronounced as assumed by these authors.

To clarify whether the interactions of liposomes and emulsion droplets could have an influence on the autoclaving stability of the emulsions (as had been suggested by Groves et al. [1985]), samples of Intralipid 20® were centrifuged and the resultant cream layer redispersed in various media by vortexing. These dispersions were then subjected to 20 min of autoclaving. Control samples, which had been redispersed in the original aqueous phase, possess droplet diameters only slightly different from the original sample (Tab. 28). These are, however, smaller than was determined for the non-centrifuged, re-autoclaved Intralipid® sample. Droplet size distributions still lie well within the range tolerable for i.v. administration. The oil droplets had resisted coalescence during centrifugation and were readily redispersed under these conditions.

Surprisingly, emulsion droplets redispersed in glycerol/water withstood a second autoclaving process although now only 2/3 of the initial lecithin content was present. The stability was, however, also influenced by pH. Judging from the PCS mean diameters, these emulsions appeared only slightly changed. However, Laser Diffractometry data showed that to a limited degree coalescence had occurred. The samples prepared by redispersion of the cream layer in alkaline glycerol/water showed particle size distributions closest to the original and redispersed original sample. Especially the more sensitive LD data revealed that the samples redispersed in neutral glycerol/water exhibited slight increases in droplet diameter during autoclaving. This points to instability caused by insufficient charge stabilisation of the droplets at this pH. The samples redispersed in an SUV dispersion also proved to be less stable than those where pH-adjustment of the aqueous phase was performed. It could, therefore, be concluded that the mere presence of liposomal material in excess cannot stabilise the emulsion droplets.

Emulsion	Z-Av. (nm)	PI	LD $d50_{Vol}$ (nm)	LD $d90_{Vol}$ (nm)
Intralipid 20® original emulsion not re-autoclaved	342.0	0.134	480	880
Intralipid 20® redispersed in original subnatant	347.0	0.109	483	884
Intralipid 20® re-autoclaved	351.1	0.095	480	890
Intralipid 20® redispersed in liposome dispersion (1.2% w/w Lipoid E80®)	359.8	0.092	510	920
Intralipid 20® redispersed in glycerol/water (2.25% w/w), pH 6.8	350.0	0.071	520	940
Intralipid 20® redispersed in glycerol/water (2.25% w/w), pH 10.0	351.4	0.089	485	896

Tab. 28 Particle size distributions of a re-autoclaved commercial parenteral emulsion by PCS (intensity distribution) **(left)** and Laser Diffractometry [Mastersizer Micro, Fraunhofer Mode, 50% and 90% of volume distribution] **(right)** after centrifugation for 4 hrs at 13000 g and subsequent autoclaving (20 min, 121°C) of the cream phase redispersed in various media

This finding can be attributed to the pH of the liposomal dispersion medium, which had not been adjusted to higher values before autoclaving, and thus again demonstrates the importance of controlling surface-charge by pH of the aqueous phase. The Intralipid® sample had certainly undergone hydrolysis during its original manufacturing and storage. Hydrolysis and the formation of FFAs would therefore be expected to be of even greater importance for the freshly produced systems, where an even more pronounced initial drop in pH would be predicted. The contribution of an alkaline pH to autoclaving stability is therefore more effective than the mere presence of liposomal material (contained in excess).

4.5 Conclusions

The results from the structural investigations show that lecithin-stabilised parenteral fat emulsions are composed of oil droplets, small uni- and bi-lamellar liposomes and aggregates of both. The size of the liposomes produced lies in the range 20-100 nm and is not affected by steam-sterilisation. However, aggregation of liposomes and emulsion droplets is greatly promoted by the autoclaving process. This interaction of liposomes and oil droplets was predicted by Groves and Herman [1993], but is not reversible, as implied by these authors. In

contrast to their assumption, the liposomes and oil droplets do not form a bicontinuous or large lamellar mesophase. The two populations coexist, or, if aggregated, largely maintain their initial shape and size. The number of liposomes present and the interactions observed are evidently not responsible for the extraordinary autoclaving stability of the emulsions.

Multilamellar layers of phospholipids covering emulsion droplets, as suggested by Friberg et al. [1976] and Rydhag and Wilton [1981], were never observed. However, their reports were based on studies of emulsions in the µm range, formulated with marked surfactant excess and under milder dispersing conditions. The high-pressure homogenisation used for the production of submicron parenteral emulsions favours the formation of SUVs rather than multilamellar structures.

Determination of the lecithin excess in the emulsions is still not straightforward and remains difficult. Particle sizing equipment is not sensitive enough to determine quantitatively the amount of small liposomes present. This can be explained by the weak scattering signal arising from the liposomes, which becomes easily hidden in the presence of oil droplets. The fractionation of liposomes by AFFF did not overcome this problem, since the amount of free, non-aggregated liposomes present was still too low to be detected in the model emulsions. The fractionation of emulsion samples by centrifugation confirms the presence of excess lecithin, where different amounts of pellet were obtained. This pellet was proved to consist of mainly phospholipids, glycerol and remnant triglycerides. By centrifuging the emulsions, however, artifacts can easily be produced, altering the amount and structure of the excess lecithin. The good stability of the charged emulsion droplets against coalescence under centrifugation conditions was demonstrated. The absence of a continuous lamellar phase in the small continuous interdroplet aqueous film was proven, in contrast to the reports of Groves et al. [1985].

By using ^{31}P-NMR and Cryo-TEM it was also shown that lowering the lecithin/oil ratio is not the only way to reduce excess liposomes. A more effective dispersing at higher homogenisation pressure also yielded a reduction in excess liposomes.

Conventional direct thermal analysis of emulsions is limited to the dispersed phase. For investigation of lecithin by these means, higher concentrations would be required. However, the discrimination between lecithin related to the O/W interface and liposomal material is not possible. Cryo-TEM and ^{31}P-NMR analysis are more suitable for this purpose, since NMR proved to be sensitive to the small liposome and oil droplet populations, which in these emulsions are frequently underestimated by number.

Summary

This work aimed at clarification of the mechanisms responsible for the autoclaving stability of lecithin-stabilised parenteral fat emulsions. The structures formed within these O/W-emulsions were investigated, as well as their influence on stability. Since both are dependent on the composition of the lecithins, a characterisation of various commercial egg lecithins was performed.

Quantitative phospholipid analysis was successfully achieved by combining gradient-HPLC with densitometric HPTLC quantitation of LPC. The results obtained with commercial and model parenteral emulsions showed some variety among different emulsion manufacturers (Intralipid® emulsions showed a lower PC:PE ratio and contained more PE than was reported by Kuksis [1985]). The variability in PC:PE ratios observed does, however, not influence the stability of the emulsions. It was confirmed that pure PC is not useful as a single emulsifier; egg lecithins of more complex composition (Lipoid E80® and E75®) with 78% PC and 73% PC can be used for production of emulsions of similar composition and stability to commercial samples.

Lipoid E80® yields stable emulsions which can be autoclaved provided the pH is adjusted to alkaline beforehand. Obvious differences between the emulsifying properties of DPPC, egg PC (Lipoid EPC®) and the less-pure egg lecithins (Lipoid E80® and E75®) are seen, which cannot be explained by their monolayer film rigidity and compressibility alone. These differences result therefore mainly from the presence of minor components or 'impurities'. Lyso-PC and Na-oleate were shown to reduce droplet-coalescence rates when admixed to the intact lecithins. However, the amounts necessary to observe droplet stabilisation are higher than those typically occurring in the emulsions (up to 18% lyso-PC shortly after the end of the shelf-life of Intralipid 20®). A strong effect was, however, found for changes in Zeta potential. Charged phospholipid components and Na-fatty acid salts contribute to more negative Zeta potentials and thus increase the stability of the emulsions against heat-stress. Phospholipids contained in liposomes hydrolysed faster during heat stress than in association with oil droplets, and hydrolysis of PE is faster than of PC. Since accelerated hydrolysis of the lecithins occurs during autoclaving, and the hydrolysis products do not move from the O/W-interfacial layer, lecithin hydrolysis increases the Zeta potential of the oil droplets. This effect is, however, closely related to the pH of the emulsions during autoclaving. If it falls during autoclaving the Zeta potential is also lowered, which leads to cracking of the emulsions, although at pH 7 even higher Zeta potentials are observed than before autoclaving. The adjustment of pH is therefore a prerequisite to obtain autoclavable emulsions and should best be carried out before

homogenisation of the crude emulsions. Since charge repulsion is regarded as the main stabilising mechanism of these emulsions, measurement of Zeta potential is useful for the prediction of emulsion stability. It is, however, only of value when the emulsions' pH can be controlled.

The predominant structures within parenteral emulsions are oil droplets in the submicron range and small unilamellar vesicles of excess lecithin not related to the O/W-interfacial monolayer. No multilamellar mesophase could be observed, neither before nor after autoclaving of the preparations. Micelles from lecithin hydrolysis products are not formed to any great extent. Phospholipid redistribution from the aqueous to the oil phase of the emulsions during autoclaving, as Groves and Herman [1993] reported, could be confirmed. Since, however, the ratio between the main phospholipids remained unchanged, this phenomenon is caused by enhanced aggregation of liposomes with oil droplets during autoclaving. This may easily be misread as an increase in phospholipid content of the creamed oil phase.

This type of O/W-emulsion is not stabilised by liquid-crystalline mesophases, as has been proposed in the literature. The amount of lecithin not located at the oil/water-interface as a monolayer is too low. Moreover, any excess lecithin forms stable unilamellar liposomes under the typical processing conditions. After autoclaving, aggregation of liposomes and oil droplets is the only structural change detectable by Cryo-TEM and ^{31}P-NMR. An additional stabilising effect of these aggregates is unlikely since 5%, 10%, 20% and 30% emulsions can be produced and autoclaved using the same amount of lecithin. The different amounts of lecithin excess do, however, not lead to differences in autoclaving stability. From the investigation of creamed and redispersed emulsions it is shown that oil droplets covered by only about 2/3 of the initial phospholipid content can be autoclaved a second time, provided pH is slightly alkaline. Neutral or slightly acidic liposome dispersions when used as the redispersion medium destabilise the oil droplets, showing that pH-dependent charge repulsion is more important for autoclaving stability than the presence of additional lecithin in the form of liposomes. Reports from Chiba and Tada [1990] and Krafft et al. [1991] who observed destabilising effects arising from excess lecithin, may also be explained by pH-depression or enhanced droplet aggregation. It is, however, unclear whether excess liposomes act as a 'charge buffer' helping to increase the tolerability of electrolyte addition to the emulsions. This would be expected to affect admixing of drugs to the parenteral emulsions and should be investigated further.

A toxicologically-unfavourable emulsifier excess can be reduced either by decreasing the lecithin:oil ratio or increasing homogenisation pressure. The latter helps additionally to decrease droplet size, which may also be advantageous for keeping within particle size limits for i.v. administration. Only Cryo-TEM allows direct observation of liposomes present beside oil droplets. Quantitation of this liposomal material is, however, difficult. ^{31}P-NMR as a non-

destructive method may be used for this purpose. Further AFFF experiments are necessary to clarify whether liposomes can be detected in commercial parenteral emulsions.

This work shows that the presence of a co-surfactant like Na-oleate, either added or produced in situ by lecithin hydrolysis, helps to avoid concurrent recoalescence and overprocessing of the emulsions at higher homogenisation pressure. Side effects caused by free fatty acids or lyso-phospholipids are, however, probably minimised as long as these remain in association with the oil droplets. Small amounts of liposomes are still present in the smallest emulsions and are, therefore, ubiquitous in parenteral emulsions.

Future work should focus on the detection and evaluation of thermotropic phase transitions according to lecithin composition. More concentrated, water-reduced emulsions should be investigated by FT-IR, ^{31}P-NMR, DSC and Small Angle X-Ray Diffraction. Analysis of emulsions with increased lecithin content is not useful, as additional liposomes are formed and discrimination between lecithin at the O/W-interface and as liposomes is not possible using these techniques.

Zusammenfassung

Die vorliegende Arbeit hatte zum Ziel, die Mechanismen aufzuklären, die für die Autoklavierungsstabilität Lecithin-stabilisierter parenteraler Fettemulsionen verantwortlich sind. Desweiteren wurden die in diesen O/W-Emulsionen vorliegenden Strukturen und deren Einfluß auf die Stabilität der Emulsionen untersucht. Da sowohl die paradoxerweise komplexen Strukturen als auch die Stabilität der scheinbar 'einfachen' Lecithin-stabilisierten Dispersionen von der Zusammensetzung der Lecithine abhängen, wurde zunächst eine Charakterisierung verschiedener kommerzieller Eilecithine durchgeführt.

Quantitative Phospholipid-Analytik konnte erfolgreich durch Kombination eines Gradienten-HPLC-Verfahrens mit densitometrischer HPTLC-Bestimmung von LPC eingesetzt werden. Die Ergebnisse der Phospholipidbestimmung kommerzieller und eigener Emulsionen zeigen einige Abweichungen der Zusammensetzung zwischen verschiedenen Herstellern (Intralipid®-Emulsionen weisen ein niedrigeres PC:PE Verhältnis auf und enthalten mehr PE als von Kuksis [1985] angegeben). Die Variabilität der ermittelten PC:PE Verhältnisse hatte jedoch auf die Stabilität der Emulsionen keinen Einfluss. Die Untersuchungen bestätigten, daß reines Ei-PC als alleiniger Emulgator ungeeignet ist, Eilecithine komplexerer Zusammensetzung (Lipoid E80® and E75®) mit 78% und 73% PC für die Herstellung von Emulsionen ähnlicher Zusammensetzung und Stabilität wie die der Handelspräparate jedoch verwendet werden können.

Mit Lipoid E80® werden stabile, autoklavierbare Emulsionen erhalten, wenn ihr pH-Wert zuvor auf alkalische Werte eingestellt wurde. Es treten deutliche Unterschiede zwischen den Emulgiereigenschaften von DPPC, Ei-PC (Lipoid EPC®) und den weniger aufgereinigten Eilecithinen (Lipoid E80® and E75®) auf, die nicht allein mit ihren Monolayer-Filmeigenschaften (Festigkeit und Komprimierbarkeit) erklärt werden können. Entsprechende Unterschiede sind daher hauptsächlich auf die Anwesenheit von Nebenbestandteilen und 'Verunreinigungen' des Lecithins zurückzuführen. Es konnte gezeigt werden, daß Lyso-PC und Na-Oleat die Tropfen-Koaleszenzrate reduzieren, wenn sie intaktem Lecithin zugemischt werden, allerdings waren hierzu solche Mengen nötig, wie sie normalerweise nicht in den Emulsionen vorkommen (z.B. bis zu 18% Lyso-PC in Intralipid 20® kurz nach dem Verfalldatum). Ein ausgeprägter Effekt kann jedoch für das Zetapotential festgestellt werden. Geladene Phospholipidbestandteile und Na-Fettsäuresalze tragen dazu bei, daß das Zetapotential der Emulsionströpfchen stärker negativ und damit die Stabilität der Emulsionen gegenüber Hitzebehandlung erhöht wird. Phospholipide in Liposomen werden während Hitzeeinwirkung schneller hydrolytisch abgebaut als solche, die sich auf den Öltropfen

befinden. Die Hydrolyse von PE schreitet dabei schneller voran als die von PC. Da die Hydrolyse der Lecithinbestandteile während des Autoklavierens beschleunigt abläuft, und die Hydrolyseprodukte offensichtlich an der O/W-Grenzfläche verbleiben, erhöht diese Hydrolyse des Lecithins sogar das Zetapotential der Öltropfen. Dieser Effekt ist allerdings abhängig vom pH-Wert der Emulsionen während des Autoklavierens. Fällt dieser während des Sterilisationsprozesses ab, erniedrigt sich auch das Zetapotential entsprechend, was schließlich zum Brechen der Emulsion führt, obwohl bei pH 7 sogar ein stärker negatives Zetapotential gemessen werden kann, als vor dem Autoklavieren. Die Einstellung des pH-Wertes stellt somit eine Grundvoraussetzung für die Autoklavierbarkeit dieser Emulsionen dar und sollte am Besten noch vor dem Homogenisierungsschritt erfolgen. Da die beobachtete Ladungsabstossung als Hauptmechanismus der Stabilisierung dieser Emulsionen angesehen werden kann, ermöglichen Zetapotentialmessungen Vorhersagen über die Emulsionsstabilität, sind jedoch nur dann aussagekräftig, wenn der pH-Wert der Emulsionen kontrolliert werden kann.

Die überwiegend vorkommenden Strukturelemente in parenteralen Fettemulsionen sind Öltropfen mit Durchmessern < 1µm sowie kleine unilamellare Vesikel aus überschüssigem Lecithin (Liposomen), welches nicht an den O/W-Grenzflächen-Monolayer gebunden vorliegt. Eine multilamellare Mesophase konnte weder vor noch nach dem Autoklavieren der Proben beobachtet werden. Ebenfalls werden keine Mizellen aus Lecithin-Hydrolyseprodukten in nennenswertem Umfang gebildet. Eine Umverteilung der Phospholipide während der Hitzesterilisation von der wässrigen in die Ölphase (wie von Groves und Herman [1993] beschrieben) kann bestätigt werden. Da aber das Verhältnis zwischen den Hauptphospholipiden PC und PE weitgehend unverändert bleibt, kann dieses Phänomen eher mit der verstärkten Aggregation von Liposomen und Öltropfen auf Grund der Autoklavierung erklärt werden. Dieses kann fälschlicherweise leicht als erhöhter Phospholipidgehalt der aufgerahmten Ölphase interpretiert werden.

Folglich wird dieser Typ von O/W-Emulsion nicht durch flüssig-kristalline Mesophasen stabilisiert, wie es in der Literatur vorgeschlagen worden ist. Für einen solchen Mechanismus ist der vorliegende Gehalt an Emulgator, der nicht als Monolayer an der O/W-Grenzfläche lokalisiert ist, zu gering. Ausserdem bildet überschüssiges Lecithin unter den vorliegenden Herstellungsbedingungen bevorzugt kleine unilamellare Vesikel aus. Der einzige erkennbare strukturelle Unterschied nach dem Autoklavieren stellt die Anhaftung (Aggregation) zwischen diesen Liposomen und den Öltröpfchen dar, was durch Cryo-TEM und ^{31}P-NMR beobachtet werden kann. Ein zusätzlicher stabilisierender Effekt durch solche Aggregation ist allerdings eher unwahrscheinlich, da sowohl 5%, 10%, 20% als auch 30% Emulsionen mit dem gleichen Gehalt an Lecithin hergestellt und autoklaviert werden können. Die dabei entstehenden

verschieden hohen Lecithinüberschüsse führen jedenfalls zu keinem Unterschied in der Autoklavierbarkeit dieser Systeme. Anhand der Untersuchungen mittels Zentrifugation aufgerahmter und redispergierter Proben wird deutlich, daß Öltropfen, die nur von 2/3 des ursprünglichen Gesamt-Lecithingehaltes bedeckt sind, ein weiteres Mal autoklaviert werden können, sofern der pH-Wert der Dispersion erneut auf leicht alkalische Werte eingestellt wird. Neutrale bis leicht sauere Liposomen-Dispersionen als Redispergiermedium destabilisieren die Öltropfen, und zeigen somit, daß der Einfluss der pH-abhängigen Ladungsabstossung für die Autoklavierungsstabilität von größerer Bedeutung ist, als die Anwesenheit von zusätzlichem Lecithin in Form von Liposomen. Berichte von Chiba und Tada [1990] und Krafft et al. [1991], die einen destabilisierenden Effekt für überschüssiges Lecithin festgestellt haben, könnten daher ebenfalls durch einen pH-Abfall oder verstärkte Tropfenaggregation erklärt werden. Es ist dennoch unklar, ob überschüssige Liposomen als 'Ladungspuffer' fungieren und so die Toleranz der Emulsionen gegenüber Elektrolytzusatz erhöhen können. Dieses würde ebenfalls die Inkorporierung von Arzneistoffen in Parenteralemulsionen beeinflussen und sollte daraufhin untersucht werden.

Um toxikologisch unerwünschten Lecithinüberschuss zu vermindern, kann entweder das Lecithin:Öl Verhältnis reduziert, oder erhöhter Homogenisationsdruck verwendet werden. Letzteres führt außerdem dazu, daß die mittleren Tröpfchengrößen weiter verringert werden können, was für die beabsichtigte i.v. Gabe ebenfalls von Vorteil wäre. Nur Cryo-TEM läßt eine direkte Bestimmung von Liposomen neben Öltropfen zu. Die quantitative Bestimmung dieses liposomalen Materials ist trotz allem schwierig. ^{31}P-NMR als nicht-destruktives Verfahren kann zu diesem Zweck herangezogen werden. Weitere AFFF-Versuche sind nötig, um abschliessend zu klären, ob Liposomen mit dieser Methode in Handelspräparaten nachgewiesen werden können.

Die Anwesenheit eines Co-Emulgators wie Na-Oleat (entweder zugesetzt oder in situ durch Hydrolyse entstanden) ermöglicht, unter höherem Homogenisationsdruck Rekoaleszenz und Überbeanspruchung des Systems zu vermeiden. Nebenwirkungen verursacht durch freie Fettsäuren oder Lyso-Phospholipide sind minimal, solange diese an den Öltropfen lokalisiert sind. Dennoch verbleiben auch in den feinsten Emulsionen kleine Anteile an Liposomen, und sind daher als ubiquitär in diesen Emulsionen vorkommend anzusehen.

Zukünftige Forschungsbemühungen sollten auf die Detektion und Auswertung thermotroper Phasenübergänge in Abhängigkeit von der Lecithin-Zusammensetzung abzielen. Mittels FT-IR, ^{31}P-NMR, DSC und Kleinwinkelröntgenbeugung sollten Systeme mit höherem Lecithingehalt (Wasser-reduzierte Emulsionen) analysiert werden. Untersuchungen an Emulsionen mit höherem Gesamt-Lecithinanteil sind nicht sinnvoll, da hierbei vermehrt liposomaler Überschuss entsteht und eine nachfolgende Unterscheidung zwischen Lecithin an der O/W-Grenzfläche und Liposomen mit diesen Methoden nicht möglich ist.

Cited Literature

(1) **Allen, T.** "Particle Size Measurement", Vol. 4, Chapman & Hall, London, (1990)

(2) **Bach, A. C.; Frey, A.; Lutz, O.** "Clinical and Experimental Effects of Medium-Chain-Triglyceride-Based Fat Emulsions - A Review", Clinical Nutrition, (1989), **8**, 223-235

(3) **Bach, A.; Férézou, J.; Frey, A.** "Phospholipid-rich particles in commercial parenteral fat emulsions. An overview", Prog. Lipid Res., (1996), **35**, 2, 133-153

(4) **Balazs, P. E.; Schmit, P. L.; Szuhaj, B. F.** "High-Performance Liquid Chromatographic Separations of Soy Phospholipids", JAOCS, (1996), **73**, 2, 193-197

(5) **Beare-Rogers, J. L.; Bonekamp-Nasner, A.; Dieffenbacher, A.** "Determination of the Phospholipid Profile of Lecithins by High Performance Liquid Chromatography", Pure&Appl. Chem., (1992), **64**, 3, 447-454

(6) **Becher, P.** "Emulsions - Theory and Practice", Reinhold, New York, (1965)

(7) **Becher, P.** (Ed.) "Encyclopedia of Emulsion Technology", Vol. 3, Marcel Dekker Inc., New York, (1988)

(8) **Belitz, H. D.; Grosch, W.** "Lehrbuch der Lebensmittelchemie", Springer Verlag, Heidelberg, (1982)

(9) **Bell, S. J.; Mascioli, E. A.; Bistrian, B. R.; Babayan, V. K.; Blackburn, G. L.** "Alternative lipid sources for enteral and parenteral nutrition: Long and medium-chain triglycerides, structured triglycerides, and fish oils", J. Am. Diet. Soc., (1991), **91**, 74-78

(10) **Blume, A.; Huebner, W.; Messner, G.** "Fourier Transform Infrared Spectroscopy of ^{13}C=O-Labeled Phospholipids Hydrogen Bonding to Carbonyl Groups", Biochemistry, (1988), **27**, 8239-8249

(11) **Boberg, J.; Håkansson, I.** "Physical and biological changes in an artificial fat emulsion during storage", J. Pharm. Pharmacol., (1964), **16**, 641-646

(12) **Bock, T.** "Emulsionen als parenterale Arzneistofftraegersysteme - Herstellung, Charakterisierung und Optimierung", Ph.D. Thesis, Christian-Albrechts-University, Kiel, (1994)

(13) **Bock, T. K.; Lucks, J.-S.; Kleinebudde, P.; Mueller, R. H.; Mueller, B. W.** "High Pressure Homogenisation of Parenteral Fat Emulsions - Influence of Process Parameters on Emulsion Quality", Eur. J. Pharm. Biopharm., (1994), **40**, 3, 157-160

(14) **Bott, S.; Hart, H.** Laboratory Equipment Digest, (1990), **3**

(15) **Bott, S. E.; Hart, W. H.** (Eds.) "Particle Size Distribution II", Vol. 472, American Chemical Society, Washington DC, (1991)

(16) **Boyd, J. V.; Krog, N.; Sherman, P.** in "Theory and Practice of Emulsion Technology", Smith, A. L. (Ed.), Academic Press, London, (1974), 37

(17) **Broesel, S.; Stang, M.; Schubert, H.** "Emulgieren in Hochdruckhomogenisatoren", Hochschulkurs Emulgiertechnik, University of Karlsruhe, (1998)

(18) **Brown, G. H.; Wolker, J. J.** "Liquid Crystals and Biological Structures", Academic Press, London, (1979)

(19) **Burnell, E. E.; Cullis, P. R.; De Kruijff, B.** "Effects of Tumbling and Lateral Diffusion on Phosphatidylcholine Model Membrane ^{31}P-NMR Lineshapes", Biochimica et Biophysica Acta, (1980), **603**, 63-69

(20) **Caldwell, K. D.** "Field-Flow Fractionation of Particles" in "Modern Methods of Particle Size Analysis", Barth, H. (Ed.), John Wiley&Sons, New York, (1984), 211-250

(21) **Carpentier, Y. A.; Simoens, C.; Siderova, V.; El Nakadi, I.; Vanweyenberg, V.; Eggerickx, D.; Deckelbaum, R.** "Recent Developments in Lipid Emulsions: Relevance to Intensive Care", Nutrition, (1997), **13**, 9 (Suppl.), 73S-78S

(22) **Casal, H. L.; Mantsch, H. H.** "Polymorphic Phase Behaviour of Phospholipid Membranes studied by Infrared Spectroscopy", Biochimica et Biophysica Acta, (1984), **779**, 381-401

(23) **Cevc, G.; Marsh, D.** (Eds.) "Phospholipid Bilayers - Physical Principles and Models", Vol. 5, John Wiley&Sons, New York, (1987)

(24) **Chan, S. I.; Bocian, D. F.; Petersen, N. O.** "Nuclear Magnetic Resonance Studies of the Phospholipid Bilayer Membrane" in "Membrane Spectroscopy", Grell, E. (Ed.), Springer Verlag, Heidelberg, (1981)

(25) **Chapman, D.** "Phase transitions and fluidity characteristics of lipids and cell membranes", Quarterly Revision of Biophysics, (1975), **2**, 8, 185-235

(26) **Chaturvedi, D.; Patel, N. M.; Lodhi, S. A.** "Effect of terminal heat sterilization on the stability of phospholipid-stabilized submicron emulsions", Acta Pharm. Nord., (1992), **4**, 1, 51-55

(27) **Chesters, A. K.** "The Modelling of Coalescence Processes in Fluid-Liquid-Dispersions: A Review of Current Understanding", TransIChemE, (1991), **69A**, 259-270

(28) **Chiba, K.; Tada, M.** "Relationship between the Emulsion Stability and Phospholipid Distribution in the Aqueous Phases Inside and Outside of an Emulsion Droplet", Agric. Biol. Chem., (1990), **54**, 4, 907-912

(29) **Cockbain, E. G.; McRoberts, T. S.** J. Colloid. Sci., (1953), **8**, 440, (cited after Hansrani, 1980)

(30) **Cornelus, C.; Giulieri, F.; Krafft, M.-P.; Riess, J. G.** "Impact of the structure of phospholipid dispersions on the stability of fluorocarbon/phospholipid emulsions for biomedical uses", Colloids and Surfaces A:Physicochemical and Engineering Aspects, (1993), **70**, 233-238

(31) **Cortijo, M.; Alonso, A.; Gómez-Fernández, J. C.; Chapman, D.** J. Mol. Biol., (1982), **157**, 597-618

(32) **Cullis, P. R.; De Kruijff, B.** "Polymorphic Phase Behaviour of Lipid Mixtures as Detected by ^{31}P NMR", Biochimica et Biophysica Acta, (1978), **507**, 207-218

(33) **Cullis, P.; Hope, M.; Tilcock, C.** "Lipid Polymorphism" in "Membrane Fusion", Wilschut; Hoekstra (Eds.), Marcel Dekker Inc., New York, (1991), 36-64

(34) **Dahn, M. S.** "Structured Lipids: An Alternative Energy Source", Nutrition in Clinical Practice, (1995), **10**, 89-90

(35) **Darby, T. D.; Wallin, R. F.** "Toxicity of Lipids" in "Advances in Parenteral Nutrition", Johnston (Ed.), MT Press, Lancaster, (1978)

(36) **Das, K. P.; Kinsella, J. E.** "Stability of food emulsions: Physicochemical role of protein and non-protein emulsifiers", Advances in Food and Nutrition Research, (1991), **34**, 81-201

(37) **Davies, D.** "Oil Emulsion Analysis by Fourier Transform Infrared Spectrometry", Chemists' Conference 40th, (1987)

(38) **Davis, S. S.** "Pharmaceutical Aspects of i.v. Fat Emulsions", J. Hosp. Pharm., (1974), **32**, 149-170

(39) **Davis, S. S.; Hadgraft, J.; Palin, K. J.** "Medical and pharmaceutical applications of emulsions" in "Encyclopedia of Emulsion Technology", Becher, P. (Ed.), Vol. 2, Marcel Dekker Inc., New York, (1985), 159-238

(40) **Davis, S. S.; Hansrani, P. K.** "The influence of emulsifying agents on the phagocytosis of lipid emulsions", Int. J. Pharm., (1985), **23**, 69

(41) **Dawes, W. H.; Groves, M. J.** "The Effect of Electrolytes on Phospholipid-Stabilized Soyabean Oil Emulsions", International Journal of Pharmaceutics, (1978), **1**, 141-150

(42) **Derjaguin, B. V.** "Theory of stability of colloids and thin films", Plenum Press, New York, (1989)

(43) **Dickinson, E.; Stainsby, G.** "Emulsion Stability" in "Advances in Food Emulsions and Foams", Dickinson, E.; Stainsby, G. (Eds.), Elsevier Applied Science, London, (1988), 1-44

(44) **Diederichs, J. E.** "Surfactant-Liposome zur Behandlung des IRDS - Charakterisierung und Scaling-Up", Ph.D. Thesis, Christian-Albrechts-University, Kiel, (1993)

(45) **du Plessis, J.; Tiedt, L. R.; van Wyk, C. J.; Ackermann, C.** "A new transmission electron microscope method for the determination of particle size in parenteral fat emulsions", International Journal of Pharmaceutics, (1986), **34**, 173-174

(46) **Eccleston, G. M.** "Emulsions" in "Encyclopedia of Pharmaceutical Technology", Swarbrick, J.; Boylan, J. C. (Eds.), Vol. 5, Marcel Dekker Inc., New York, (1992), 137-188

(47) **Eckart, J.; Adolph, M.; Muehlen, U.; van der Naab, V.** "Fat emulsions containing medium chain triglycerides in parenteral nutrition of intensive care patients", J.Parent.Ent.Nutr., (1980), **4**, 360-366

(48) **Eriksson, P.-O.; Rilfors, L.; Lindblom, G.; Arvidson, G.** "Multicomponent Spectra from 31P-NMR Studies of the Phase Equilibria in the System Dioleoylphosphatidylcholine-Dioleoylphosphatidylethanolamine-Water", Chemistry and Physics of Lipids, (1985), **37**, 357-371

(49) **Ewers, W. E.; Sutherland, K. L.** Australian J. Sci. Res., (1952), **A5**, 697

(50) **Férézou, J.; Lai, N.-T.; Leray, C.; Hajri, T.; Frey, A.; Cabaret, Y.; Courtieu, J.; Lutton, C.; Bach, A.** "Lipid composition and structure of commercial parenteral emulsions", Biochimica et Biophysica Acta, (1994), **1213**, 149-158

(51) **Fiedler, H. P.** "Lexikon der Hilfstoffe fuer Pharmazie, Kosmetik und angrenzende Gebiete", Vol. 4, Editio Cantor, Aulendorf, (1996)

(52) **Fisher, L. R.; Parker, N. S.** "Effect of Surfactants on the Interactions between Emulsion Droplets" in "Advances in Food Emulsions and Foams", Dickinson, E.; Stainsby, G. (Eds.), Elsevier Applied Science, London, (1988), 45-90

(53) **Fookson, J. E.; Wallach, D. F. H.** "Structural Differences among Phosphatidylcholine, Phosphatidylethanolamine and Mixed Phosphatidylcholine / Phosphatidylethanolamine Multilayers: An Infrared Absorption Study", Archives of Biochemistry and Biophysics, (1978), **189**, 1, 195-204

(54) **Friberg, S.; Jansson, P. O.; Cederberg, E.** "Surfactant Association Structure and Emulsion Stability", Journal of Colloid and Interface Science, (1976), **55**, 3, 614-623

(55) **Friberg, S.; Larsson, K.** (Eds.) "Food Emulsions", Vol. 5, Marcel Dekker Inc., New York, (1997)

(56) **Fringeli, U. P.; Guenthard, H. H.** "Infrared Membrane Spectroscopy" in "Membrane Spectroscopy", Grell, E. (Ed.), Springer Verlag, Heidelberg, (1981)

(57) **Gaines, G. L.** "Insoluble Monolayers at Liquid-Gas Interfaces", Interscience Publishers, New York, (1966)

(58) **Gennis, R. B.** "Biomembranes: Molecular Structure and Function", Springer Verlag, Heidelberg, (1989)

(59) **Giddings, J. C.** "Field-Flow Fractionation: Analysis of Macromolecular, Colloidal and Particulate Materials", Science, (1993), **260**, 1456-1465

(60) **Gillespie, T.; Rideal, E. K.** Trans. Faraday Soc., (1954), **52**, 173 (cited after Hansrani, 1980)

(61) **Grit, M.; de Smidt, J. H.; Struijke, A.; Crommelin, D. J. A.** "Hydrolysis of phosphatidylcholine in aqueous liposome dispersions", Int. J. Pharm., (1989), **50**, 1-6

(62) **Grit, M.; Zuidam, N. J.; Crommelin, D. J. A.** "The Effect of Charge on the Hydrolysis Kinetics of Partially Hydrogenated Egg Phosphatidylcholine and Egg Phosphatidylglycerol in Aqueous Liposome Dispersions" Proc. Intern. Symp. Control. Rel. Bioact. Mater., (1991), 483-484

(63) **Groves, M. J.; Yalabik, H. S.** "The Behaviour of Sub-Micrometre Particles in a Centrifugal Field", Powder Technology, (1975), **12**, 233-238

(64) **Groves, M. J.** "The Application of Particle Characterization Methods to Submicron Dispersions and Emulsions" in "Modern Methods of Particle Size Analysis", Barth, H. (Ed.), John Wiley&Sons, New York, (1984), 43-92

(65) **Groves, M. J.; Wineberg, M.; Brain, A. P. R.** "The Presence of Liposomal Material in Phosphatide Stabilized Emulsions", J. Dispersion Science and Technology, (1985), **2**, 6, 237-243

(66) **Groves, M. J.; Herman, C. J.** "The Redistribution of Bulk Aqueous Phase Phospholipids During Thermal Stressing of Phospholipid-stabilized Emulsions", J. Pharm. Pharmacol., (1993), **45**, 592-596

(67) **Guenzler, H.; Boeck, H.** "IR-Spektroskopie", Verlag Chemie GmbH, Weinheim, (1993)

(68) **Guisard, D.; Debry, G.** "Metabolic effects of a medium-chain triglyceride emulsion injected intravenously in man", Horm.Metab.Res., (1972), **509**, 4

(69) **Hadfield, J. I. H.** Clin. Med., (1966), **73**, 25 (cited after Hansrani, 1980)

(70) **Hajri, T.; Férézou, J.; Lutton, C.** "Effects of intravenous infusions of commercial fat emulsions (Intralipid 10 or 20%) on rat plasma lipoproteins: phospholipids in excess are the main precursors of lipoprotein-X-like particles", Biochimica et Biophysica Acta, (1990), **1047**, 121-130

(71) **Hamilton, R. L.; Goerke, J.; Guo, L. S. S.; Williams, M. C.; Havel, R. J.** "Unilamellar liposomes made with the French pressure cell: a simple preparative and semiquantitative technique", Journal of Lipid Research, (1980), **21**, 981-992

(72) **Hamilton, J. A.; Vural, J. M.; Carpentier, Y. A.; Deckelbaum, R. J.** "Incorporation of medium chain triglycerols into phospholipid bilayers: effects of long chain triacylglycerols, cholesterol, and cholesteryl esters", J. Lipid Res., (1996), **37**, 4, 773-782

(73) **Hanahan, D. J.** in "Lipid Chemistry", John Wiley&Sons, New York, (1960), 42-105

(74) **Hansrani, P. K.** "Studies on intravenous fat emulsions", Ph.D. Thesis, University of Nottingham, (1980)

(75) **Harkins, W. D.** "Physical Chemistry of Surface Films", Reinhold, New York, (1952)

(76) **Håkansson, I.** "Physico-chemical changes in artificial fat emulsions during storage: Studies of the hydrolysis and its physiological effects", Acta Chem. Scand., (1966), **30**, 2267-2281

(77) **Herman, C. J.; Groves, M. J.** "Hydrolysis Kinetics of Phospholipids in Thermally Stressed Intravenous Lipid Emulsion Formulations", J. Pharm. Pharmacol., (1992), **44**, 539-542

(78) **Herman, C.** "The Influence of Thermal Stress on the Properties of Phospholipid-Stabilized Emulsions", Ph.D. Thesis, UIC, Chicago, (1992)

(79) **Herman, C. J.; Groves, M. J.** "The Influence of Free Fatty Acid Formation on the pH of Phospholipid-Stabilized Triglyceride Emulsions", Pharmaceutical Research, (1993), **10**, 5, 774-776

(80) **Hiemenz, P. C.** "Principles of Colloid and Surface Chemistry", Marcel Dekker Inc., New York, (1986)

(81) **Hienerwadel, R.** "Ladungstransport in photosynthetischen Reaktionszentren", University of Freiburg, (1993)

(82) **Hunter, R. J.** "Zeta Potential in Colloid Science", Academic Press, London, (1981)

(83) **Huth, K.; Schoenborn, W.; Boerner, J.** "Zur Pathogenese der Unvertraeglichkeitserscheinungen bei parenteraler Fettzufuhr", Med. Ernaehr., (1967), **8**, 146-148

(84) **Hyltander, A.; Sandström, R.; Lundholm, K.** "Metabolic Effects of Structured Triglycerides in Humans", Nutrition in Clinical Practice, (1995), **10**, 91-97

(85) **International Union of Pure and Applied Chemistry** "Manual on Colloid and Surface Science", International Union of Pure and Applied Chemistry, Butterworth, (1972)

(86) **Ishii, F.; Sasaki, I.; Ogata, H.** "Effect of phospholipid emulsifiers on physicochemical properties of intravenous fat emulsions and/or drug carrier emulsions", J. Pharm. Pharmacol., (1990), **42**, 513-515

(87) **Jeppsson, R. I.** "Parenteral administration of lipid-soluble drugs in oil emulsion vehicles", Acta Pharm. Suecica, (1976), **Suppl. 13**, 43

(88) **Karbstein, H.** "Untersuchungen zum Herstellen und Stabilisieren von Oel-in-Wasser-Emulsionen", Ph.D. Thesis, University (TH) of Karlsruhe, (1994)

(89) **Kawilarang, C. R. T.; Georghiou, K.; Groves, M. J.** "The Effect of Additives on the Physical Properties of a Phospholipid-Stabilized Soybean Oil Emulsion", Journal of Clinical and Hospital Pharmacy, (1980), **5**, 151-160

(90) **Kemps, J. M. A.; Crommelin, D. J. A.** "Chemische stabiliteit van fosfolipiden in farmaceutische preparaten: peroxidatie van fosfolipiden in watering milieu", Pharm. Weekblad , (1988), **123**, 457-468

(91) **Kleinberger, G.; Pamperl, H.** "Allgemeine Charakteristika und Fragen zur Galenik von Fettemulsionen", Infusionstherapie und klinische Ernaehrung, (1983), **10**, 108-117

(92) **Kohlrausch, A.; Steffens, K.-J.** "Laserbeugungsspektroskopie zur Partikelgroeßenmessung intravenoes applizierbarer Oel-in-Wasser-Emulsionen", Pharm. Ind., (1997), **59**, 903-910

(93) **Komatsu, H.; Kitajima, A.; Okada, S.** "Pharmaceutical Characterization of Commercially Available Intravenous Fat Emulsions: Estimation of Average Particle Size, Size Distribution and Surface Potential Using Photon Correlation Spectroscopy", Chem. Pharm. Bull., (1995), **43**, 8, 1412-1415

(94) **Krafft, M. P.; Rolland, J. P.; Riess, J. G.** "Detrimental Effect of Excess Lecithin on the Stability of Fluorocarbon/Lecithin Emulsions", J. Phys. Chem., (1991), **95**, 5673-5676

(95) **Kuksis, A.** "Animal Lecithins" in "Lecithins", Szuhaj; List (Eds.), AOCS, (1985), 105-162

(96) **Kumar, V. V.; Malewicz, B.; Baumann, W. J.** "Lysophosphatidylcholine stabilizes small unilamellar phosphatidylcholine vesicles: Phosphorous-31 NMR evidence of the wedge effect", Biophys. J., (1989), **55**, 789-792

(97) **Lance, M. R.; Washington, C.; Davis, S. S.** "Evidence for the Formation of Amphotericin B-phospholipid Complexes in Langmuir Monolayers", Pharmaceutical Research, (1996), **13**, 7, 1008-1014

(98) **Lanza, G. M.; Wallace, K. D.; Scott, M. J.; Cacheris, W. P.; Abendschein, D. R.; Christy, D. H.; Sharkey, A. M.; Miller, J. G.; Gaffney, P. J.; Wickline, S. A.** "A novel site-targeted ultrasonic contrast agent with broad biomedical application", Circulation, (1996), **94**, 12, 3334-3340

(99) **Larsson, K.** "Physical Properties - Structural and Physical Characteristics" in "The lipid handbook", Gundstone, G. D.; Harwood, J. L.; Padley, G. D. (Eds.), Chapman and Hall Ltd., London, (1986), 321-446

(100) **Lauda** "Manual of the Film Balance FW-2", (1987)

(101) **Lee, A. G.** "Lipid Phase Transitions and Phase Diagrams. I. Lipid Phase Transitions", Biochimica et Biophysica Acta, (1977), **472**, 237-281

(102) **Lee, G. W. J.; Groves, M. J.** "A pragmatic approach to the particle sizing of submicrometre emulsions using a laser nephelometer", Powder Technol., (1981), **28**, 49-54

(103) **Lee, G.; Dick, D.; Vasquez, E. M.; Werner, K.** "pH measurements of suspensions" in "Pharmaceutical Technology - Drug Stability", Rubinstein, M. H. (Ed.), E. Horwood, (1989)

(104) **LeNeveu, D. M.; Rand, R. P.; Gingell, D.; Parsegian, V. A.** "Apparent Modifications of Forces between Lecithin Bilayers", Science, (1976), **191**, 399-400

(105) **LeVeen, H. H.; Giordano, P.; Spletzer, J.** "The mechanism of removal of i.v. injected fat", Arch.Surgery, (1961), **83**, 169-179

(106) **Levin, S.; Klausner, E.** "Measurements of Size Distribution and Density of a Pharmaceutical Fat Emulsion, using field-programmed sedimentation field-flow fractionation (SdFFF)", Pharm. Res., (1995), **12**, 1218-1224

(107) **Li, J.; Caldwell, K. D.; Anderson, B. D.** "A method for the early evaluation of the effects of storage and additives on the stability of parenteral fat emulsions", Pharm. Res., (1993), **10**, 535-541

(108) **Lidgate, D. M.; Fu, R. C.; Fleitman, J. S.** "Using a microfluidizer to manufacture parenteral emulsions", BioPharm, (1989), **45**, 28-33

(109) **Lipp, H. P.; Schuler, U.; Saal, J.; Schaaf, D.** "Amphotericin B in Fettemulsionen: Vorteile gegenueber der konventionellen Therapie", Arzneimitteltherapie, (1993), **11**, 10, 319-326

(110) **Lucks, J.-S.** "Parenterale Fettemulsionen als Arzneistofftraeger - Herstellung, Charakterisierung und Stabilitaet", Ph.D. Thesis, Christian-Albrechts-University, Kiel, (1993)

(111) **Lutz, O.; Meraihi, Z.; Férézou, J.; Frey, A.; Lutton, C.; Bach, A. C.** "The Mesophase of Parenteral Fat Emulsion Is Both Substrate and Inhibitor of Lipoprotein Lipase and Hepatic Lipase", Metabolism, (1990), **39**, 12, 1225-1231

(112) **Magdassi, S.; Royz, M.; Shoshan, S.** "Chemical Instability of Phospholipids: A Key Factor in Stabilization of Perfluorocarbon Emulsions", J. Dispersion Science and Technology, (1991), **12**, 1, 69-82

(113) **Marmer, W. N.** "Plant Phospholipid Analysis" in "Lecithins", Szuhaj; List (Eds.), AOCS, (1985), 247-288

(114) **Marsh, D.** "Handbook of Lipid Bilayers", CRC Press, (1990)

(115) **Mayhew, E.; Lazo, R.; Vail, W. J.; King, J.; Green, A. M.** "Characterization of Liposomes Prepared Using a Microemulsifier", Biochimica et Biophysica Acta, (1984), **775**, 169-174

(116) **McCluer, R.; Ullman, M. D.; Jungalwala, F. B.** "HPLC of Glycosphingolipids and Phospholipids" in "Advances in Chromatography", (1986), Vol. 25

(117) **McKibbin, J. M.; Hegsted, D. M.; Stare, F. J.** "Complete Parenteral Nutrition", Fed. Proc., (1943), **2**, 98

(118) **Microfluidics International Corp.** "Microfluidizer Processor User Guide", 1996

(119) **Miyamoto, V. K.; Stoeckenius, W.** "Preparation and characteristics of lipid vesicles", J. Membr. Biol., (1971), **4**, 252-269

(120) **Muchtar, S.; Levy, M. Y.; Sarig, S.; Benita, S.** "Stability assessment of a fat emulsion prepared with an original mixture of purified phospholipids", S.T.P. Pharma Sciences, (1991), **2**, 1, 130-136

(121) **Muehlebach, S.; Graf, R.-B.; Sommermeyer, K.** "Stabilitaetsuntersuchungen an parenteralen Lipidemulsionen nach thermischer und mechanischer Belastung. Der Sudanrot-Test als einfache Testmethode", Pharm. Acta Helv., (1987), **62**, 5-6, 130-133

(122) **Mueller, J. F.; Iacono, J.** "The Effects of Multiple Daily Infusions of a 15% Cottonseed Oil Emulsion in Humans" in "Fette in der Medizin", Vol. 6, Henning, N.; Berg, G. (Eds.), Pallas Verlag, Munich, (1967)

(123) **Mueller, R. H.** "Colloidal Carriers for Controlled Drug Delivery and Targeting", Wissenschaftliche Verlagsgesellschaft, Stuttgart, (1991)

(124) **Mueller, R. H.; Lucks, J. S.; Diederichs, J. E.; Heinemann, S.** "Lecithin Stabilized Emulsions for Parenteral Nutrition, a Three-Year Stability Study", Proceed. 6th Int. Conf. On Technol. (APGI), (1992), **4**, 351-360

(125) **Mueller, R. H.; Heinemann, S.** "Emulsions for Intravenous Application. II. Destabilisation and stabilisation mechanisms in fat emulsions", Pharm. Ind., (1993), **55**, 10, 948-953

(126) **Mueller, R. H.; Heinemann, S.** "Fat emulsions for parenteral nutrition. IV. Lipofundin MCT/LCT regimes for total parenteral nutrition (TPN) with high electrolyte load", International Journal of Pharmaceutics, (1994), **107**, 121-132

(127) **Mueller, R. H.; Mehnert, W.; Lucks, J. S.; Schwarz, C.; zur Muehlen, A.; Weyhers, H.; Freitas, C.; Ruehl, D.** "Solid Lipid Nanoparticles (SLN) - an alternative colloidal drug carrier system for controlled drug delivery", Eur. J. Pharm. Biopharm., (1995), **41**, 62-69

(128) **Mueller, R. H.** "Zetapotential und Partikelladung in der Laborpraxis", Wissenschaftliche Verlagsgesellschaft, Stuttgart, (1996)

(129) **Mueller, R. H.; Schuhmann, R.** "Teilchengroessenmessung in der Laborpraxis", Wissenschaftliche Verlagsgesellschaft, Stuttgart, (1996)

(130) **Napper, D. H.** "Polymeric Stabilization of Colloidal Dispersions", Academic Press, London, (1983)

(131) **Nattermann Phospholipid GmbH** "Nattermann Phospholipid Presentations in Cosmetics 1990-1995", (1995)

(132) **New, R. R. C.** (Ed.) "Liposomes - a practical approach", IRL Press, (1990)

(133) **Ni, Y.; Klein, D. H.; Song, D.** "Recent developments in pharmacokinetic modeling of perfluorocarbon emulsions", Artif. Cells Blood Substit. Immobil. Biotechnol., (1996), **24**, 2, 81-90

(134) **Nicolet Instrument Corporation** "OMNIC V2.0 User's Guide", (1993)

(135) **Nomura, T.** "Experimentelle Studien ueber intravenoese Fettinfusion unter besonderer Beruecksichtigung parenteraler Ernaehrung", J. Exp. Med., (1929), **13**, 51-64

(136) **Pelura, T. J.; Johnson, C. S.; Tarara, T. E.; Weers, J. G.** "Stabilization of Perflubron emulsions with egg yolk phospholipid", Biomat., Art. Cells & Immob. Biotech., (1992), **20**, 2-4, 845-848

(137) **Ph.Eur.1997** "European Pharmacopeia", Vol. 3, (1997)

(138) **Ph.Forum** "Globule Size Distribution in Intravenous Emulsions / Photon Correlation Spectroscopy Method for Determination of Mean Fat Globule Diameters and Distributions in Intravenous Emulsions", Pharmacopeial Forum, (1994), **20**, 2, 7170-7174

(139) **Pharmacia&Upjohn** "Intralipid 10/20/30 - Emulsions for Parenteral Nutrition", Scientific Brochure (German), I0060 Wd4/1 9707 AS, (1997)

(140) **Plantz, P. E.** "Particle Size Measurements From 0.1 to 1000 µm Based on Light Scattering and Diffraction" in "Modern Methods of Particle Size Analysis", Barth, H. (Ed.), John Wiley&Sons, New York, (1984), 173-210

(141) **Prankerd, R. J.; Stella, V. J.** "The Use of Oil-in-Water Emulsions as a Vehicle for Parenteral Drug Administration", Journal of Parenteral Science & Technology, (1990), **44**, 3, 139-149

(142) **Prosise, W. E.** "Commercial Lecithin Products: Food Use of Soybean Lecithin" in "Lecithins", Szuhaj; List (Eds.), AOCS, (1985)

(143) **Pscheidl, E. M.; Wan, J. M.; Blackburn, G. L.; Bistrian, B. R.; Istfan, N. W.** "Influence of ω-3 Fatty Acids on Splanchnic Blood Flow and Lactate Metabolism in an Endotoxemic Rat Model", Metabolism, (1992), **41**, 7, 698-705

(144) **Pscheidl, E.; Hedwig-Geissing, M.; Winzer, C.; Richter, S.; Ruegheimer, E.** "Effects of chemically defined structured lipid emulsions on reticuloendothelial system function and morphology of liver and lung in a continuous low-dose endotoxin rat model", Journal of Parenteral and Enteral Nutrition, (1995), **19**, 1, 33-40

(145) **Pscherer, G.** "Die Herstellung von Fettemulsionen" in "Fette in der parenteralen Ernaehrung", Hempel, V.; Clauberg, G. (Eds.), Bibliomed - Medizinische Verlagsgesellschaft mbH Melsungen, (1981)

(146) **Rabiner, T.; Garti, N.; Aserin, A.** "Intravenous Fat Emulsions for Parenteral Nutrition", Tenside Detergents, (1986), **23**, 6, 342-345

(147) **Repta, A. J.** "Formulation of investigational anticancer drugs" in "Topics in Pharmaceutical Sciences", Breimer, D. D.; Speiser, P. (Eds.), Elsevier, Amsterdam, (1981), 131

(148) **Rotenberg, M.; Rubin, M.; Bor, A.; Meyuhas, D.; Talmon, Y.; Lichtenberg, D.** "Physico-chemical characterization of Intralipid™ emulsions", Biochimica et Biophysica Acta, (1991), **1086**, 265-272

(149) **Rote Liste** (German Drug Reference), Editio Cantor, Aulendorf, (1998)

(150) **Rubino, J. T.** "The Influence of Charged Lipids on the Flocculation and Coalescence of Oil-in-Water Emulsions. I: Kinetic Assessment of Emulsion Stability", Journal of Parenteral Science & Technology, (1990), **44**, 4, 210-215

(151) **Rydhag, L.** "The Importance of the Phase Behaviour of Phospholipids for Emulsion Stability", Fette, Seifen, Anstrichmittel, (1979), **81**, 4, 168-173

(152) **Rydhag, L.; Wilton, I.** "The Function of Phospholipids of Soybean Lecithin in Emulsions", JAOCS, (1981), 830-837

(153) **Sandström, R.; Hyltander, A.; Körner, U.; Lundholm, K.** "Structured Triglycerides to Postoperative Patients: A Safety and Tolerance Study", Journal of Parenteral and Enteral Nutrition, (1993), **17**, 2, 153-157

(154) **Saunders, L.** "Some properties of mixed sols of lecithin and lysolecithin", J. Pharm. Pharmacol., (1957), **9**, 834-839

(155) **Schoeffski, P.; Wunder, R.; Petersen, D.; Koehne, C.-H.; Freund, M.; Ganser, A.** "Intralipid does not decrease the toxicity of Amphotericin B. Results of a randomized Phase II-trial in neutropenic patients with fever of unknown origin or pneumonia", Blood, (1996), **88**, 10, 1995

(156) **Schoefl, G. I.** Proc. Roy. Soc. Biochim., (1968), **169**, 147-152 (cited after Thompson, 1974)

(157) **Schoofs, T.** "Laserpartikelanalyse und hohe Aufloesung im Feinstbereich - ein Widerspruch ?", Chemie-Technik, (1990), **9**, 61-62

(158) **Schubert, H.** "Advances in the mechanical production of food emulsions", Proc. International Congress on Engineering and Food, Brighton, (1997), AA 82-AA 87

(159) **Schuberth, O.; Wretlind, A.** "I.V. infusion of fat emulsions, phosphatides and emulsifying agents", Acta Chir. Scand. Supp., (1961), **278**, 1-21

(160) **Schueckler, F.** "Auswirkungen von Azone und Dodecl-L-Pyroglutamat auf Struktur und Barriereeigenschaften des menschlichen Stratum Corneums", Ph.D. Thesis, Ruprecht-Karls-University, Heidelberg, (1992)

(161) **Schuhmann, R.; Mehnert, W.; Mueller, R. H.** "Coulter Counter Based Coalescence Assay for the Determination of Emulsion Stability after Addition of Electrolyte", Pharm. Ind., (1993), **55**, 7, 701-704

(162) **Schuhmann, R.** "Physikalische Stabilitaet Parenteraler Fettemulsionen - Entwicklung eines Untersuchungsschemas unter besonderem Aspekt analytischer Moeglichkeiten", Ph.D. Thesis, Free University, Berlin, (1995)

(163) **Schuhmann, R.; Mueller, R. H.** "Optimierung der Probenaufbereitung fuer Coulter-Counter-Messungen", Pharm.Ind., (1998), **60**, 2, 157-163

(164) **Schurr, P. E.** "Composition and Preparation of Experimental Intravenous Fat Emulsions", Cancer Research, (1969), **29**, 258-260

(165) **Seelig, J.** "^{31}P Nuclear Magnetic Resonance and the Head Group Structure of Phospholipids in Membranes", Biochimica et Biophysica Acta, (1978), **515**, 105-140

(166) **Shaw, D. J.** "Introduction to Colloid and Surface Chemistry", Vol. 3, Butterworths, (1983)

(167) **Small, D.** "The physical chemistry of lipids: from alkanes to phospholipids", Plenum Press, New York (1986)

(168) **Smith, A. L.; Mitchell, D. P.** "The Centrifuge Technique in the Study of Emulsion Stability" in "Theory and Practice of Emulsion Technology", Smith, A. L. (Ed.), Academic Press, London, (1976), 61-74

(169) **Sotirhos, N.; Herslöf, B.; Kenne, L.** "Quantitative analysis of phospholipids by ^{31}P-NMR", Journal of Lipid Research, (1986a), **27**, 386-392

(170) **Sotirhos, N.; Ho, C.-T.; Chang, S. S.** "High Performance Liquid Chromatographic Analysis of Soybean Phospholipids", Fette Seifen Anstrichmittel, (1986b), **88**, 1, 6-8

(171) **Spector, A.** "Fatty acid binding to plasma albumin", Journal of Lipid Research, (1975), **16**, 165-179

(172) **Spooner, P. J. R.; Gantz, D. L.; Hamilton, J. A.; Small, D. M.** "The Distribution of Oleic Acid between Chylomicron-like Emulsions, Phospholipid Bilayers and Serum Albumin", The Journal of Biological Chemistry, (1990), **265**, 21, 12650-12655

(173) **Stang, M.; Schubert, H.** "Avoidance of coalescence of newly-formed droplets during emulsification processes", Proc. International Congress on Engineering and Food, Brighton, (1997), I13-I16

(174) **Stricker, H. E.** (Ed.) "Physikalische Pharmazie", Wissenschaftliche Verlagsgesellschaft mbH, Stuttgart, (1987)

(175) **Szoka, F. J.; Papahadjopoulos, D.** "Comparative Properties And Methods of Preparation of Lipid Vesicles (Liposomes)", Ann. Rev. Biophys. Bioeng., (1980), **9**, 467-508

(176) **Tank, C.; Antonietti, M.** "Characterization of water-soluble polymers and aqueous colloids with asymmetrical flow field-flow fractionation", Macromol. Chem. Phys., (1996), **197**, 2443

(177) **Thompson, S. W.** "The Pathology of Parenteral Nutrition with Lipids", Charles C. Thomas, Springfield Ill., (1974)

(178) **Ulman, A.** "An introduction to ultrathin organic films - from Langmuir-Blodgett to Self-Assembly", Academic Press, London, (1991)

(179) **USP23/NF18** (The U.S. Pharmacopeia), (1995)

(180) **van den Tempel, M.** Rec. Trav. Chim., (1953), **72**, 433, 442

(181) **van Zanten, J. et al.** "Characterization of Vesicles by Classical Light Scattering", Journal of Colloid and Interface Science, (1991), **146**, 330-336

(182) **Vance, D.; Vance, J.** "Biochemistry of Lipids, Lipoproteins and Membranes", Elsevier, Amsterdam, (1991)

(183) **Vermess, M.; Adamson, R. H.; Doppman, J. L.; Girton, M.** "Computed Tomographic Demonstration of Hepatic Tumor with the Aid of i.v. Iodinated Fat Emulsion", Radiology, (1977), **125**, 711-715

(184) **Verwey, E. J. W.; Overbeek, J. T. G.** "Theory of the stability of lyophobic colloids", Elsevier, Amsterdam, (1948)

(185) **Villalaín, J.; Gómez-Fernández, J. C.** "Fourier transform infrared spectroscopic study of mixtures of palmitic acid with dipalmitoylphosphatidylcholine using isotopic substitution", Chemistry and Physics of Lipids, (1992), **62**, 19-29

(186) **Vold, R. D.; Groot, R. C.** "An Ultracentrifugal Method for the Quantitative Determination of Emulsion Stability", J. Phys. Chem., (1962), **66**, 1969-1975

(187) **Vold, R.; Groot, R.** "The effect of electrolytes on the ultracentrifugal stability of emulsions", Journal of Colloid and Science, (1964), **19**, 384-398

(188) **Wallach, D. F. H.; Verma, S. P.; Fookson, J.** "Application of Laser Raman and Infrared Spectroscopy to the Analysis of Membrane Structure", Biochimica et Biophysica Acta, (1979), **559**, 153-208

(189) **Walstra, P.** "Formation of Emulsions" in "Encyclopedia of Emulsion Technology", Vol. 1, Becher, P. (Ed.), Marcel Dekker Inc., New York, (1983)

(190) **Washington, C.; Davis, S. S.** "Ageing effects in parenteral fat emulsions: the role of fatty acids", International Journal of Pharmaceutics, (1987), **39**, 33-37

(191) **Washington, C.; Davis, S. S.** "The production of parenteral feeding emulsions by Microfluidizer", International Journal of Pharmaceutics, (1988), **44**, 169-176

(192) **Washington, C.; Chawla, A.; Christy, N.; Davis, S. S.** "The electrokinetic properties of phospholipid-stabilized fat emulsions", International Journal of Pharmaceutics, (1989), **54**, 191-197

(193) **Washington, C.; Athersuch, A.; Kynoch, D. J.** "The electrokinetic properties of phospholipid stabilized fat emulsions. IV. The effect of glucose and pH", International Journal of Pharmaceutics, (1990), **64**, 217-222

(194) **Washington, C.; Connolly, M. A.; Manning, R.; Skerratt, M. C. L.** "The electrokinetic properties of phospholipid stabilized fat emulsions. V. The effect of amino acids on emulsion stability", International Journal of Pharmaceutics, (1991), **77**, 57-63

(195) **Washington, C.** "The electrokinetic properties of phospholipid stabilized fat emulsions. VI. Zeta potentials of Intralipid 20% in TPN mixtures", International Journal of Pharmaceutics , (1992), **87**, 167-174

(196) **Washington, C.; Sizer, T.** "Stability of TPN mixtures compounded from Lipofundin S and Aminoplex amino-acid solutions: Comparison of laser diffraction and Coulter counter droplet size analysis", International Journal of Pharmaceutics, (1992), **83**, 227-231

(197) **Weber, E. J.** "Corn Lecithin" in "Lecithins", Szuhaj; List (Eds.), AOCS, (1985), 43

(198) **Weers, J. G.; Scheuing, D. R.** "Micellar Sphere to Rod Transitions" in "Fourier Transform Infrared Spectroscopy in Colloid and Interface Science", Scheuing, D. R. (Ed.), ACS Press, Washington, (1991), 87-122

(199) **Weiner, B. B.** "Particle Sizing Using Photon Correlation Spectroscopy" in "Modern Methods of Particle Size Analysis", Barth, H. (Ed.), John Wiley&Sons, New York, (1984), 93-116

(200) **Weltzien, H. V.** "Cytolytic and membrane-perturbing properties of lysophosphatidylcholine", Biochimica et Biophysica Acta, (1979), **559**, 259-287

(201) **Westesen, K.; Wehler, T.** "Physicochemical Characterization of a Model Intravenous Oil-in-Water Emulsion", Journal of Pharmaceutical Sciences, (1992), **81**, 8, 777-786

(202) **Westesen, K.; Wehler, T.** "Investigation of the Particle Size Distribution of a Model Intravenous Emulsion", Journal of Pharmaceutical Sciences, (1993), **82**, 12, 1237-1244

(203) **Whateley, T. L.; Steele, G.; Urwin, J.; Smail, G. A.** "Particle Size Stability of Intralipid and Mixed Total Parenteral Nutrition Mixtures", Journal of Clinical and Hospital Pharmacy, (1984), **9**, 113-126

(204) **Wretlind, A.** "The pharmacological basis for the use of fat emulsions in intravenous nutrition", Act. Chir. Scand. (Supp.), (1964), **325**, 31-42

(205) **Wretlind, A.** "Current Status of Intralipid and other Fat Emulsions" in "Fat Emulsions in Parenteral Nutrition", Meng, H. C.; Wilmore, D. W. (Eds.), American Medical Association, Chicago, (1976)

(206) **Wyatt, P. J.** "Light scattering and the absolute characterization of macromolecules", Anal. Chim. Acta, (1993), **272**, 1

(207) **Wyatt Technology** "ASTRA for Particles", Wyatt Technology Corp., Santa Barbara, (1998)

(208) **Yamaguchi, T.; Nishizaki, K.; Itai, S.; Hayashi, H.; Ohshima, H.** "Physicochemical Characterization of Parenteral Lipid Emulsion: Influence of Cosurfactants on Flocculation and Coalescence", Pharmaceutical Research, (1995a), **12**, 9, 1273-1278

(209) **Yamaguchi, T.; Nishizaki, K.; Itai, S.; Hayashi, H.; Ohshima, H.** "Physicochemical Characterization of Parenteral Lipid Emulsion: Determination of Hamaker Constants and Activation Energy of Coalescence", Pharmaceutical Research, (1995b), **12**, 3, 342-347

(210) **Yeadon, D. A.; Goldblatt, L. A.; Altschul, A. M.** "Lecithin in oil-in-water emulsions", JAOCS, (1958), **35**, 435-438

CURRICULUM VITAE

Name:	Christoph Tilmann Wabel
Born:	August 1st 1969 in Frankfurt am Main
Parents:	Wilhelm Wabel, Marketing Director Ute Wabel, Grammar School Teacher
Legal status:	Not married
Nationality:	German
School education:	
1975 - 1979	Primary School in Dossenheim, Rhein-Neckar-Kreis
1979 - 1988	Kurfuerst-Friedrich-Gymnasium in Heidelberg
May 19th 1988	School-leaving exam
Professional Career:	
WS 1988/89	Chemistry Studies at the University of Heidelberg
SS 1989 - WS 1992/93	Pharmacy Studies at the University of Heidelberg
April 20th 1993	2nd State Examination
May 1993 - October 1993	Preregistration Pharmacist at the Hof-Apotheke, Heidelberg
November 1993 – April 1994	Preregistration Pharmacist at the Division of Pharmaceutical Development of the Dr. Karl Thomae GmbH, Biberach/Riss
July 1994	3rd State Examination and Registration as Pharmacist
July 1994 - June 1998	Graduate Student at the Department of Pharmaceutics at the University of Erlangen-Nuernberg